Staphylococcal evasion of neutrophil functions

Daphne Stapels

Staphylococcal evasion of neutrophil functions
PhD thesis, Utrecht University, the Netherlands

ISBN: 978-94-6295-131-0
Cover design: Daphne Stapels
Lay-out: Daphne Stapels
Printing: Uitgeverij BOXPress, proefschriftmaken.nl

About the cover: The cover illustration shows the surfaces the serine proteases (neutrophil elastase, proteinase 3, cathepsin G, and mast cell chymase) that are inhibited by the staphylococcal extracellular adherence proteins (Eap, EapH1, EapH2). All individual structures have been aligned with the co-crystal structure of EapH1 bound to neutrophil elastase, which we describe in this thesis.

Printing of this thesis was kindly financially supported by the ABN Amro bank, N.V.; Astellas Pharma B.V.; Elastin Products Company, Inc. (Owensville, Missouri, USA); Infection and Immunity Center Utrecht; the Netherlands Society of Medical Microbiology (NVMM) and the Royal Netherlands Society for Microbiology (KNVM); and Division ‘Laboratorium en Apotheek’, University Medical Center Utrecht.

Staphylococcal evasion of neutrophil functions

Hoe Staphylococcen neutrofielen ontwijken

(met een samenvatting in het Nederlands)

Proefschrift

ter verkrijging van de graad van doctor aan de Universiteit Utrecht op gezag van de rector magnificus, prof.dr. G.J. van der Zwaan, ingevolge het besluit van het college voor promoties in het openbaar te verdedigen op

donderdag 9 april 2015 des middags te 2.30 uur

door

Daphne Alida Cornelia Stapels

geboren op 6 februari 1987
te Gouda

Promotor: Prof. dr. J.A.G. van Strijp

Copromotor: Dr. S.H.M. Rooijakkers

– Hakuna Matata –

Loosely translated:
Don't worry about
the things beyond your
control

Leden van de leescommissie:	Prof. dr. L. Koenderman *(voorzitter)* Prof. dr. W. Bitter Prof. dr. B.V. Geisbrecht Prof. dr. R. Goldschmeding Prof. dr. C.E. Hack
Paranimfen:	Evelien T.M. Berends Steven G.E. Braem

TABLE OF CONTENTS

CHAPTER 1 |	General introduction	9
CHAPTER 2 |	*Staphylococcus aureus* secretes a unique class of neutrophil serine protease inhibitors *PUBLISHED, Proc. Natl. Acad. Sci. USA (2014). 111(36): 13187-13192*	21
CHAPTER 3 |	Molecular insights into the inhibition of neutrophil proteases by extracellular adherence proteins *manuscript in preparation*	39
CHAPTER 4 |	*Staphylococcus aureus* protects its immune-evasion proteins against degradation by neutrophil serine proteases *manuscript under review*	57
CHAPTER 5 |	The extracellular adherence protein from *Staphylococcus aureus* inhibits the classical and lectin pathways of complement by blocking formation of the C3 proconvertase *PUBLISHED, J. Immunol. (2014). 193(12): 6161-6171*	75
CHAPTER 6 |	Immune-modulating properties of staphylococcal extracellular adherence proteins	97
CHAPTER 7 |	General discussion	111
	Part I: Rationale for NSP inhibition by bacteria *PUBLISHED, Curr. Opin Microbiol. (2015). 23:42-48*	113
	Part II: The role of EAPs in *Stapylococcus aureus* defense	121
ADDENDUM |	Nederlandse samenvatting	133
	Dankwoord	
	Curriculum vitae	
	List of publications	

1

General introduction

Innate immune defenses and *Staphylococcus aureus*

LIST OF ABBREVIATIONS

α1-AT	alpha-1-antitrypsin
A2M	alpha-2-macroglobulin
ACT	antichymotrypsin
C5aR	C5a receptor
CG	cathepsin G
CHIPS	chemotaxis-inhibitory protein of *S. aureus*
CR1	complement-receptor 1
CR3	complement-receptor 3
CXCR2	CXC chemokine receptor 2
DPP-I	dipeptyl peptidase-I
Eap	extracellular adherence protein
EapH1	Eap-homologue 1
EapH2	Eap-homologue 2
Ecb	extracellular complement-binding protein
Efb	extracellular fibrinogen-binding protein
FB	factor B
FcαR	Fc receptor for IgA
FD	factor D
fMLF	formylated peptide Met-Leu-Phe
FPR1	formyl-peptide receptor 1
FPR2	formyl-peptide receptor 2
ICAM-1	intercellular adhesion molecule 1
IL-8	interleukin 8
LukED	leukocinin ED
MAMP	microbial-associated molecular pattern
MASP	mannan-binding lectin-associated protease
MBL	mannose-binding lectin
MPO	myeloperoxidase
NE	neutrophil elastase
NETs	neutrophil extracellular traps
NSP	neutrophil serine protease
NSP4	neutrophil serine protease 4
PBMC	peripheral blood mononuclear cell
PI-6	protease inhibitor 6
PR3	proteinase 3
PSGL-1	P-selectin glycoprotein ligand 1
PVL	Panton-Valentine leukocidin
SAK	staphylokinase
Sbi	*S. aureus* binder of IgG
SCIN	staphylococcal inhibitor of complement
SLPI	secretory leukocyte protease inhibitor
SpA	staphylococcal protein A
SSL7	superantigen-like protein 7
TSST-1	toxic-shock syndrome toxin 1

INNATE IMMUNE SYSTEM

The innate immune system forms the first line of defense against all types of microorganisms. It recognizes invading microorganisms via general patterns of non-self molecules (microbial-associated molecular patterns, MAMPs). It can act relatively fast, since it does not require clonal expansion of cells specifically recognizing a particular species. It consists of humoral and cellular components that are functionally intertwined to generate an optimal immune response[1].

Humoral innate immunity

The humoral arm of the innate immune system consists of an abundant collection of plasma proteins. These function individually, like antimicrobial proteins, or in a cascade, like the complement system. These cascades rely on circulating pro-forms of proteins, which become activated mostly via proteolytic cleavage[2]. Thereby they ensure amplification of the initial signal. Naturally, these systems need to be tightly regulated to prevent false, uncontrolled immune activation[2].

Complement

The complement cascade opsonizes invading bacteria to mark them for destruction by immune cells. In addition, the terminal complement complex can directly lyse Gram-negative bacteria[3]. Initiation of the complement cascade can occur via three distinct pathways, of which the classical and lectin pathways are quite similar (Fig. 1). For initiation

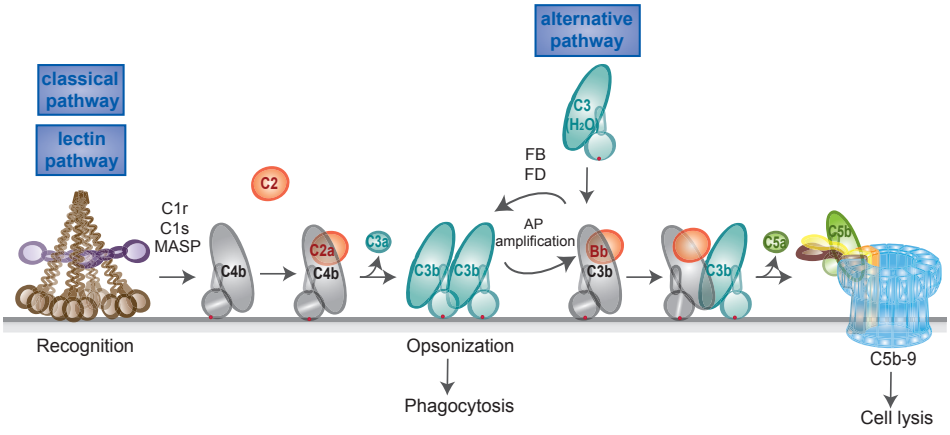

Figure 1. Complement activation on the bacterial surface. The classical and lectin pathways are initiated when recognition molecules (C1q or MBL, brown) bind their associated serine proteases (C1s and MASP-2, purple) that cleave C4 into C4b and C2 into C2a. The C4b2a complex on the bacterial surface is a C3 convertase that cleaves C3 to release the anaphylatoxin C3a and to deposit C3b. The complement reaction is amplified via the alternative pathway, where the deposited C3b molecules initiate formation of another C3 convertase (C3bBb), which associates with the serine proteases FD and FB to convert more C3. Subsequently, C3b molecules also generate C5 convertases by binding onto or near the C3 convertases (forming C4b2aC3b and C3bBbC3b). This initiates a substrate switch, which causes cleavage of C5 into soluble C5a and C5b that forms a complex with C6-9 to generate the terminal complement complex (C5b-9). This figure was partly modified from Berends *et al.*[3].

of the classical pathway C1q recognizes antibody-opsonized bacteria, and for initiation of the lectin pathway mannose-binding lectins (MBL) or ficolins recognize sugar moieties on the bacterial surface. Both processes will activate serine proteases (either C1s or mannan-binding lectin-associated proteases (MASPs)) that cleave C4 into C4b, which is deposited on the bacterial surface via its reactive thioester. Subsequently, C2 is cleaved to generate active C2a, and together with C4b this forms a C3 convertase that can cleave soluble C3 into the anaphylatoxin C3a and the opsonin C3b. The generated reactive thioester of C3b will be employed to opsonize the bacterial surface. Recognition of C3b-opsonized bacteria by the complement-receptor 1 (CR1) and CR3 on immune cells will then induce phagocytosis. The third activation pathway, the alternative pathway, mainly functions as an amplification loop of C3b deposition. In combination with the serine proteases factor B (FB) and factor D (FD) this will lead to increased deposition of C3b. Subsequently, C5 convertases are generated by addition of a C3b molecule to one of the C3 convertases (yielding C4b2aC3b, or C3bBbC3b). These convertases cleave C5 into C5a, which is a potent anaphylatoxin, and C5b, that subsequently associates with C6-9 to form the terminal complement complex[3].

Cellular innate immunity

Whereas the complement system marks invading bacteria for destruction, the cellular arm of the innate immune system is designed to clear them. The cellular innate immune system comprises blood cells of the myeloid lineage, which are divided into mononuclear cells (monocytes and macrophages) and polymorphonuclear cells (neutrophils, mast cells, basophils and eosinophils)[2]. Neutrophils (and to some extent mast cells and basophils) phagocytose invading bacteria. Subsequently, macrophages are attracted to the site of infection to clear these neutrophils[2,4]. Monocytes are classically seen as the blood-circulating precursors of these tissue macrophages. Lastly, mast cells and basophils play important roles in fighting helminthic infections and maintaining homeostasis[2]. Of these innate, myeloid cells, neutrophils are the most abundant, forming 60% of the total amount of white blood cells.

Neutrophils

Neutrophils have a prominent role in antimicrobial defense, which is clearly demonstrated by the numerous recurrent infections in neutropenic patients[5]. Like the other polymorphonuclear cells, neutrophils belong to the granulocytes, indicating that their cytosol contains numerous granules in which various antimicrobial peptides and proteases are stored. Different granules store different proteins: azurophilic (primary) granules contain high amounts of myeloperoxidase and neutrophil serine proteases (NSPs), collagenase (secondary) and gelatinase (tertiary) granules instead contain high amounts of lactoferrin and gelatinase, respectively, and secretory granules mainly contain cell-surface receptors[6]. The antimicrobial contents of these granules play important roles in all mechanisms via which neutrophils can rapidly kill bacteria[6].

Upon bacterial infection, neutrophils are among the first cells of the innate immune

system to migrate towards the infection[7]. Bacterial infection induces local production of chemoattractants, like formylated peptides, C5a, and chemokines (e.g. IL-8). Neutrophils sense these chemoattractants via specific receptors (respectively FPR1 and FPR2, C5aR, and CXCR2). This induces cellular activation and altered receptor expression (e.g. up-regulation of CR3)[8]. In addition, endothelial cells upregulate their receptors (for example PSGL-1 and ICAM-1) that promote rolling of neutrophils over the endothelium and subsequent firm adhesion. In the next step, neutrophils transmigrate over the endothelial cell layer, and terminate their initial interactions with the endothelium via incompletely-defined mechanisms[9]. Whereas the chemotactic gradient of IL-8 had been most potent in guiding the neutrophil toward the activated endothelium, other chemotactic gradients (i.e. fMLF) are now favored to guide the neutrophil from the endothelium to the site of infection[8].

Once at the site of infection, neutrophils have several antimicrobial weapons at their disposal (Fig. 2)[10]. First, neutrophils can engulf bacteria via phagocytosis. This is initiated when CR1 or CR3 recognize the C3b-oponized bacteria, or alternatively when Fc receptors recognize IgG-opsonized bacteria. Subsequently, pseudopods of neutrophilic plasma membrane will extend and surround the bacterium to induce complete uptake of the bacterium into a phagocytic vacuole[11]. Fusion of the azurophilic granules with the formed phagocytic vacuole will deliver antimicrobial proteins to the bacteria. Together with the generated reactive oxygen species, this will induce bacterial killing (Fig. 2A)[11]. Second, neutrophils can directly release their granular content into the extracellular milieu via exocytosis (degranulation)[7]. This is an unfavorable mechanism, since it will also cause bystander damage to neighboring cells (Fig. 2B). Third, neutrophils can release their antimicrobial proteins and restrict bystander damage by secreting neutrophil extracellular traps (NETosis). NET formation requires DNA decondensation, and disintegration of the nuclear and granular membranes. Subsequently, the DNA will mix intracellular with the granular components, upon which this meshwork is excreted. Within NETs, bacteria are entrapped and might be killed by the antimicrobial components (Fig. 2C)[12].

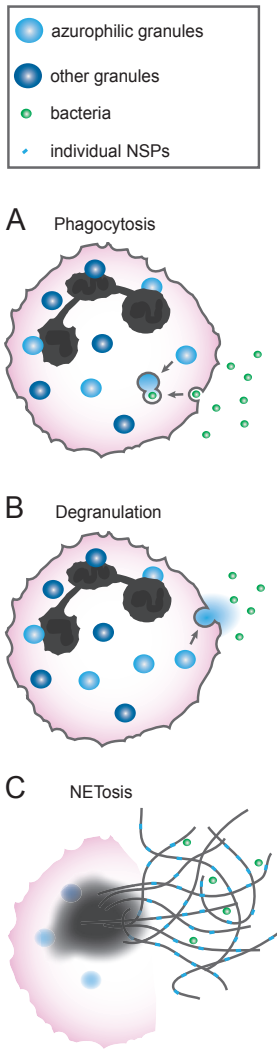

Figure 2. Antimicrobial strategies of neutrophils. (A) Phagocytosis: neutrophils ingest opsonized bacteria, after which the granules fuse with the phagocytic vacuole to release NSPs and antimicrobial components that kill the bacteria. (B) Degranulation: neutrophils release their granule contents into the extracellular space, after which antimicrobial components kill the bacteria in the extracellular milieu. (C) NETosis: neutrophils excrete a mix of granule components and DNA to capture bacteria. This figure was published in Stapels *et al.*[10].

Neutrophil serine proteases

The azurophilic granules contain a family of related neutrophil serine proteases (NSPs)[6], consisting of neutrophil elastase (NE), proteinase 3 (PR3), cathepsin G (CG), and the recently discovered neutrophil serine protease 4 (NSP4)[13]. The genes for NE (*ELANE)*, PR3 (*PRTN*) and NSP4 (*NSP4*) are all located on chromosome 19p13.3. This cluster also contains the proteolytically inactive homologue azurocidin (*AZU1*)[13]. On the other hand, the gene for CG (*CTSG*) is located within the chymase locus on chromosome 14q11.2[14]. Of all leukocytes, neutrophils contain the highest amounts of NSPs per cell, with 1 pg NE[15], 3 pg PR3[16], 0.8 pg CG[15], but only about 0.04 pg NSP4[13]. Since transcription of these genes occurs just before the formation of the azurophilic granules in the promyelocytic stage of neutrophil differentiation[6], lower amounts of NSPs are also found in other innate immune cells[14,17,18].

The NSPs are synthesized with an additional C-terminal peptide with a yet unknown function and an N-terminal inhibitory propeptide. This dipeptide is cleaved off within the post-Golgi organelles by cathepsin C (dipeptidyl peptidase-I; DPP-I) to obtain potentially active proteases[14]. However, within the azurophilic granules the NSPs are kept inactive by tight binding to proteoglycans. Active proteases are only released into the phagocytic vacuole when the altered ion concentrations release the interaction of NSPs with the proteoglycans[6,19,20]. Within the phagocytic vacuole, NSP concentrations are believed to increase to up to 50 mg/ml (based on calculations for MPO[15,16,19]). Upon activation of neutrophils, NSPs are found associated with the neutrophil plasma membrane. NE dissociates from the membrane upon binding its inhibitor alpha-1-antitrypsin (α1-AT), indicating that membrane-associated NE would not be present within serum[21]. The body further protects itself against unwanted proteolytic activity of NSP via other NSP inhibitors[7,13]. For example, plasma also contains high concentrations antichymotrypsin (ACT), and alpha-2-macroglobulin (A2M). Neutrophils and macrophages express serpin B1 in their cytoplasm and all granulocytes and epithelial cells express protease inhibitor 6 (PI-

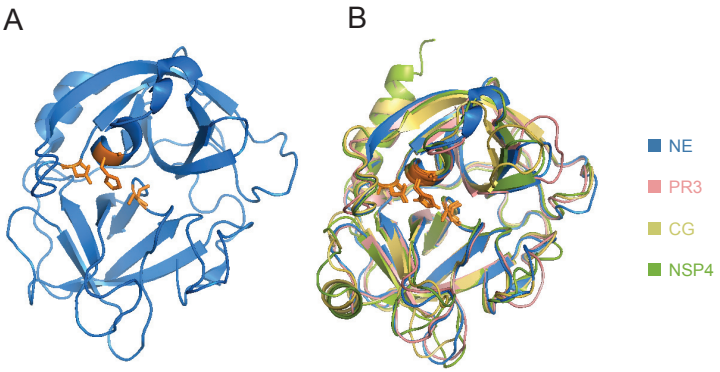

Figure 3. Structural homology amongst the human neutrophil serine proteases. (A) Crystal structure of NE (PDB code 3Q76), displayed in blue, with the catalytic triad His-Asp-Ser in orange. (B) Structural overlay of the four human NSPs. All catalytic triads are depicted in orange. NE (PDB code 3Q76, *in blue*), PR3 (PDB code 1FUJ, *in pink*), CG (PDB code 1CGH, *in yellow*), and NSP4 (PDB code 4Q7X, *in green*).

6), PI-9, secretory leukocyte protease inhibitor (SLPI), and elafin[7].

The catalytic site of NSPs is formed by a charge-relay system of His-Asp-Ser, which is common to all chymotrypsin-like serine proteases[7,22]. These residues are interspersed in the primary sequence, but brought together in the tertiary protein structure[7] (Fig. 3A). The primary sequences of the other NSPs are between 35 and 56 % identical to NE. Even though this results in very similar folding (Fig. 3B), these proteases display different substrate specificities[22]: NE and PR3 prefer to cleave directly after small, hydrophobic residues, like Val and Ala[22]; CG mainly prefers to cleave after large, hydrophobic residues, like Trp, Phe, and Tyr[13,22]; and NSP4 cleaves after the positively charged Arg, and post-translationally modified Arg[13,23]. These differences in substrate specificity ensure that, as a group, the NSPs have the ability to cleave a wide variety of substrates. This enables NSPs to play important roles in all antibacterial functions of neutrophils. However, their broad substrate specificity, the fact that they act at multiple locations (intracellular and extracellular), and the presence of various protease inhibitors, often complicate detailed understanding of NSP contributions to anti-bacterial host defense.

STAPHYLOCOCCUS AUREUS

Staphylococcus aureus is a commensal, Gram-positive bacterium that harmlessly colonizes 20% of the population on the skin and in anterior nares. An additional 60% is intermittent carrier[24]. Even though harmless in itself, carriage is known to predispose to invasive infections, ranging from skin and soft-tissue infections to life-threatening pneumonia and sepsis[25]. Standard treatment occurs via surgical drainage and/or antibiotic treatment, depending on the type of infection[26,27]. Unfortunately, antibiotic resistance is on the rise since the 1990s. And whereas these resistant strains used to occur mainly in health-care settings, currently also community-acquired strains become more prevalent[25,28]. Moreover, an effective vaccine is not available[29]. Together, these factors call for a better understanding of this pathogen so that new types of treatment might be developed.

Immune evasion

S. aureus is a master of immune evasion. This either promotes invasive infections, in which the immune response clearly cannot cope with the infection, or colonization, for which the local immune reactions have to be suppressed in order to prevent clearance[30]. Staphylococcal immune evasion relies upon two dozen small, secreted proteins that, often redundantly, target all processes of the innate immune response[31]. Despite their wide array of immune targets, these proteins show remarkable resemblances. They can roughly be divided in three groups (Fig. 4A). (1) The superantigen-like folded proteins, which adopt a beta-grasp fold, wherein an alpha-helix diagonally spans a five-stranded mixed-beta sheet. (2) The SCIN-like folded proteins, which consist of three alpha-helixes that roughly resemble the letter ‘N’. (3) The pore-forming toxins, which consist of multiple beta sheets, of which one can extend to form a part of a membrane pore. Multiple pore-forming toxins together form a pore that can lyse eukaryotic cells. Apparently, these

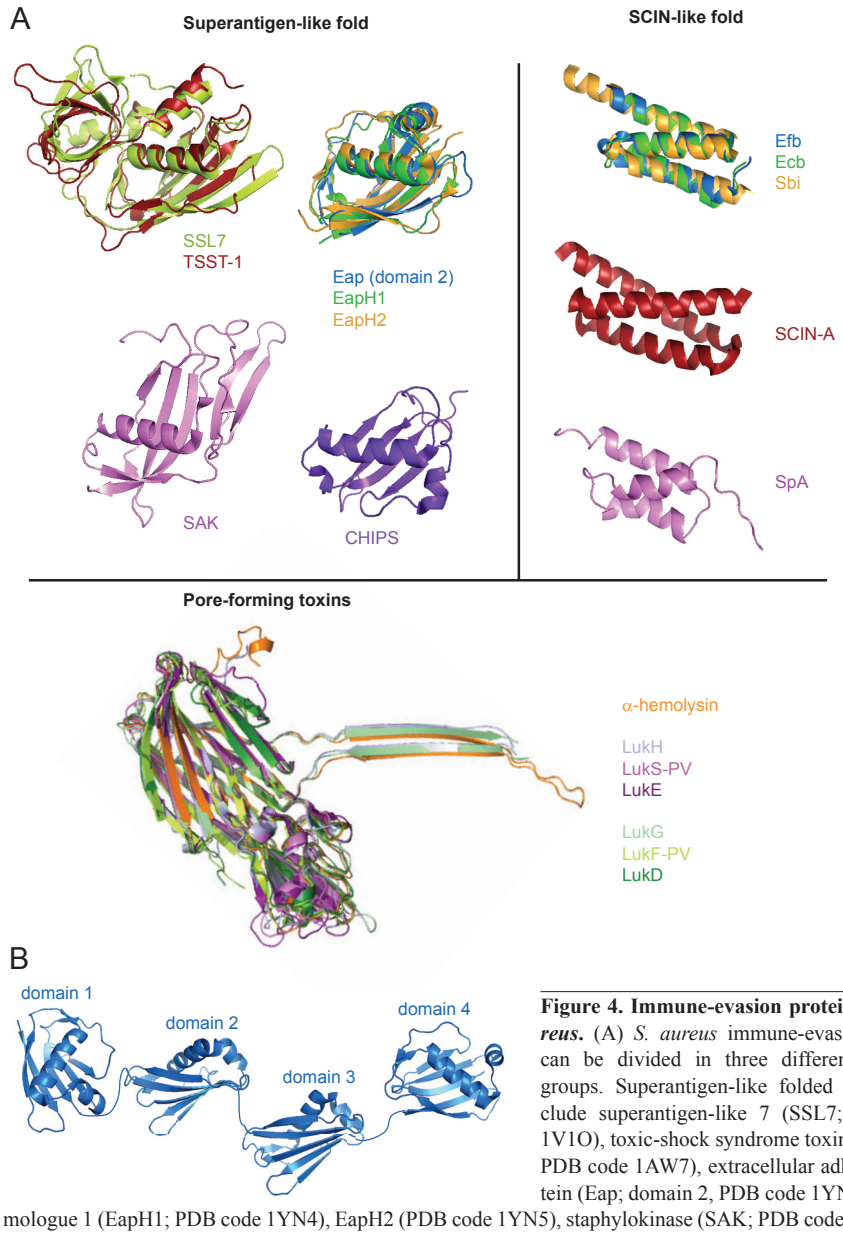

Figure 4. Immune-evasion proteins of *S. aureus*. (A) *S. aureus* immune-evasion proteins can be divided in three different structural groups. Superantigen-like folded proteins include superantigen-like 7 (SSL7; PDB code 1V1O), toxic-shock syndrome toxin 1 (TSST-1; PDB code 1AW7), extracellular adherence protein (Eap; domain 2, PDB code 1YN3), Eap-homologue 1 (EapH1; PDB code 1YN4), EapH2 (PDB code 1YN5), staphylokinase (SAK; PDB code 1C76), chemotaxis inhibitory protein of *S. aureus* (CHIPS; PDB code 1XEE) (*top, left*). SCIN-like folded proteins include extracellular fibrinogen-binding protein (Efb; PDB code 2GOM), extracellular complement-binding protein (Ecb; PDB code 2NOJ), *S. aureus* binder of IgG (Sbi; PDB code 2WY8), staphylococcal complement inhibitor (SCIN; PDB code 2QFF), and staphylococcal protein A (SpA; PDB code 1BDD) (*top, right*). The pore-forming toxins include α-hemolysin (PDB code 7AHL), leukocidin GH (LukGH; PDB code 4TW1), Panton-Valentine leukocydin, S-component (LukS-PV; PDB code 1T5R), LukE (PDB code 3ROH), LukF-PV (PDB code 1PVL), LukD (PDB code 4Q7G) (*bottom*). Note that the structures of α-hemolysin and LukGH depict the molecules in their pore-forming orientation, whereas the other molecules are depicted as in solution. (B) Model of Eap in solution, based on PDB code 1YN3 and the findings by Hammel *et al.*[39].

are energetically-favorable folds that have been optimized during evolution to interact with the diverse array of immune proteins.

The targets of these immune-evasion proteins are for a large part to be found within the complement system and on immune cells. Within the complement system SSL10, SAK, SpA, and Sbi inhibit activation of the classical pathway; SCIN, SCIN-B/C, and Sbi inhibit C3 conversion; and Efb, Ecb, and SSL7 inhibit C5 conversion[32]. Examples of receptor-targeting immune-evasion molecules are CHIPS, which inhibits signaling via the C5aR; TSST-1 and other superantigens, that bind to the T-cell receptor to activate them without the need for a MHC-presented peptide; PVL, which targets the C5aR to form a pore in neutrophils; and LukED which targets multiple chymokine receptors to form a pore in a wide array of immune cells[32–34]. These individual proteins show that functional similarity not necessarily relies on structural similarity (e.g. although both are classical pathway inhibitors, SAK resembles superantigens, whereas Sbi resembles SCIN proteins). Likewise, similarities in structure do not necessarily lead to similar functions (e.g. TSST-1 functions as a superantigen, whereas its structural homologue Eap does not[35]).

Some of these proteins have multiple immune-evasion functions. That is, SSL7 can bind both IgA to inhibit its signaling via the FcαR, and C5 to prevent complement activation at this level[36]. Eap has been shown to inhibit both neutrophil recruitment and influence proliferation of peripheral blood mononuclear cells (PBMCs; consisting for 50-70% of T cells)[37,38]. However, the exact protein targeted to mediate these phenomena have not been identified. Eap is particularly intriguing, since it expresses multiple superantigen-like domains in a row (Fig. 4B)[39], which might enable these multiple functions to be captured in one protein.

AIM OF THIS THESIS

In this thesis we aim to further unravel the intricate balance between *S. aureus* and the innate immune system. Since neutrophil serine proteases (NSPs) are believed to play a crucial role in immunity, but no staphylococcal coping mechanisms for NSPs are known, we here explore how *S. aureus* deals with these proteases. In the past, new immune-evasion molecules have taught us much about *S. aureus* pathogenesis and the host immune response. Knowledge on both is required for adequate therapies against *S. aureus*, but might also increase our understanding of other immunopathologies.

REFERENCES

1. Beutler B: Innate immunity: an overview. *Mol. Immunol.* 2004, 40:845–859.
2. Koenderman L, Buurman W, Daha MR: The innate immune response. Immunol. Lett. 2014, 162:95–102.
3. Berends ETM, Kuipers A, Ravesloot MM, Urbanus RT, Rooijakkers SHM: Bacteria under stress by complement and coagulation. *FEMS Microbiol. Rev.* 2014, 38:1146–1171.
4. Silva MT: Macrophage phagocytosis of neutrophils at inflammatory/infectious foci: a cooperative mechanism in the control of infection and infectious inflammation. *J. Leukoc. Biol.* 2011, 89:675–683.
5. Van de Vosse E, Verhard EM, Tool AJT, de Visser AW, Kuijpers TW, Hiemstra PS, van Dissel JT: Severe congenital neutropenia in a multigenerational family with a novel neutrophil elastase (ELANE) mutation. *Ann. Hematol.* 2011, 90:151–158.
6. Borregaard N, Cowland JB: Granules of the human neutrophilic polymorphonuclear leukocyte. *Blood* 1997, 89:3503–3521.
7. Korkmaz B, Horwitz MS, Jenne DE, Gauthier F: Neutrophil Elastase, Proteinase 3, and Cathepsin G as Therapeutic Targets in Human Diseases. *Pharmacol. Rev.* 2010, 62:726–759.
8. Phillipson M, Kubes P: The neutrophil in vascular inflammation. *Nat. Med.* 2011, 17:1381–1390.
9. Zen K, Guo Y-L, Li L-M, Bian Z, Zhang C-Y, Liu Y: Cleavage of the CD11b extracellular domain by the leukocyte serprocidins is critical for neutrophil detachment during chemotaxis. *Blood* 2011, 117:4885–4894.
10. Stapels DAC, Geisbrecht BV, Rooijakkers SHM: Neutrophil serine proteases in antibacterial defense. *Curr. Opin. Microbiol.* 2015, 23:42–48.
11. van Kessel KPM, Bestebroer J, van Strijp JAG: Neutrophil-Mediated Phagocytosis of Staphylococcus aureus. *Front. Immunol.* 2014, 467: doi:10.3389/fimmu.2014.00467.
12. Fuchs TA, Abed U, Goosmann C, Hurwitz R, Schulze I, Wahn V, Weinrauch Y, Brinkmann V, Zychlinsky A: Novel cell death program leads to neutrophil extracellular traps. J. Cell Biol. 2007, 176:231–241.
13. Perera NC, Schilling O, Kittel H, Back W, Kremmer E, Jenne DE: NSP4, an elastase-related protease in human neutrophils with arginine specificity. *Proc. Natl. Acad. Sci. U. S. A.* 2012, 109:6229–6234.
14. Korkmaz B, Moreau T, Gauthier F: Neutrophil elastase, proteinase 3 and cathepsin G: physicochemical properties, activity and physiopathological functions. *Biochimie* 2008, 90:227–242.
15. Campbell EJ, Silverman EK, Campbell MA: Elastase and cathepsin G of human monocytes. Quantification of Cellular Content, Release in Response to Stimuli, and Heterogeneity in Elastase-Mediated Proteolytic Activity. *J. Immunol.* 1989, 143:2961–2968.
16. Campbell EJ, Campbell MA, Owen CA: Bioactive Proteinase 3 on the Cell Surface of Human Neutrophils: Quantification, Catalytic Activity, and Susceptibility to Inhibition. *J. Immunol.* 2000, 165:3366–3374.
17. Caughey GH: Serine proteinases of mast cell and leukocyte granules. A league of their own. *Am. J. Respir. Crit. Care Med.* 1994, 150:S138–142.
18. Fol M, Iwan-Barańska L, Stączek P, Krupiński M, Różalska S, Kowalewicz-Kulbat M, Druszczyńska M, Madiraju MVVS, Kaczmarczyk D, Rudnicka W: Interactions between an M. tuberculosis strain overexpressing mtrA and mononuclear phagocytes. *Adv. Med. Sci.* 2013, 58:172–183.
19. Reeves EP, Lu H, Jacobs HL, Messina CGM, Bolsover S, Gabella G, Potma EO, Warley A, Roes J, Segal AW: Killing activity of neutrophils is mediated through activation of proteases by K+ flux. *Nature* 2002, 416:291–297.
20. Segal AW: How neutrophils kill microbes. *Annu. Rev. Immunol.* 2005, 23:197–223.
21. Korkmaz B, Attucci S, Jourdan M-L, Juliano L, Gauthier F: Inhibition of Neutrophil Elastase by α1-Protease Inhibitor at the Surface of Human Polymorphonuclear Neutrophils. *J. Immunol.* 2005, 175:3329–3338.
22. Hellman L, Thorpe M: Granule proteases of hematopoietic cells, a family of versatile inflammatory mediators - an update on their cleavage specificity, in vivo substrates, and evolution. *J. Biol. Chem.* 2014, 395:15–49.
23. Lin SJ, Dong KC, Eigenbrot C, van Lookeren Campagne M, Kirchhofer D: Structures of neutrophil serine protease 4 reveal an unusual mechanism of substrate recognition by a trypsin-fold protease. *Structure* 2014, 22:1333–1340.
24. Kluytmans J, Belkum A van, Verbrugh H: Nasal Carriage of Staphylococcus aureus: Epidemiology, Underlying Mechanisms, and Associated Risks. *Clin. Microbiol. Rev.* 1997, 10:505–520.
25. Lowy FD: Staphylococcus aureus infections. *N. Engl. J. Med.* 1998, 339:520–532.
26. Liu C, Bayer A, Cosgrove SE, Daum RS, Fridkin SK, Gorwitz RJ, Kaplan SL, Karchmer AW, Levine DP, Murray BE, et al.: Clinical practice guidelines by the infectious diseases society of America for the treatment of methicillin-resistant Staphylococcus aureus infections in adults and children: executive summary. Clin. Infect.

Dis. 2011, 52:285–292.
27. DeLeo FR, Otto M, Kreiswirth BN, Chambers HF: Community-associated meticillin-resistant Staphylococcus aureus. *Lancet* 2010, 375:1557–1568.
28. Tong SYC, Chen LF, Fowler Jr VG: Colonization, pathogenicity, host susceptibility, and therapeutics for Staphylococcus aureus: what is the clinical relevance? *Semin. Immunopathol.* 2012, 34:185–200.
29. Jansen KU, Girgenti DQ, Scully IL, Anderson AS: Vaccine review: "Staphyloccocus aureus vaccines: Problems and prospects". *Vaccine* 2013, 31:2723–3270.
30. Foster TJ: Colonization and infection of the human host by staphylococci: adhesion, survival and immune evasion. *Vet. Dermatol.* 2009, 20:456–470.
31. Spaan AN, Surewaard BGJ, Nijland R, van Strijp JAG: Neutrophils versus Staphylococcus aureus: a biological tug of war. *Annu. Rev. Microbiol.* 2013, 67:629–650.
32. Serruto D, Rappuoli R, Scarselli M, Gros P, van Strijp JAG: Molecular mechanisms of complement evasion: learning from staphylococci and meningococci. *Nat. Rev. Microbiol.* 2010, 8:393–399.
33. Spaan AN, Henry T, van Rooijen WJM, Perret M, Badiou C, Aerts PC, Kemmink J, de Haas CJC, van Kessel KPM, Vandenesch F, et al.: The staphylococcal toxin Panton-Valentine Leukocidin targets human C5a receptors. *Cell Host Microbe* 2013, 13:584–594.
34. Reyes-Robles T, Alonzo F, Kozhaya L, Lacy DB, Unutmaz D, Torres VJ: Staphylococcus aureus leukotoxin ED targets the chemokine receptors CXCR1 and CXCR2 to kill leukocytes and promote infection. *Cell Host Microbe* 2013, 14:453–459.
35. Haggar A, Flock J-I, Norrby-Teglund A: Extracellular adherence protein (Eap) from Staphylococcus aureus does not function as a superantigen. *Clin. Microbiol. Infect.* 2009, 16:1155–1158.
36. Laursen NS, Gordon N, Hermans S, Lorenz N, Jackson N, Wines B, Spillner E, Christensen JB, Jensen M, Fredslund F, et al.: Structural basis for inhibition of complement C5 by the SSL7 protein from Staphylococcus aureus. *Proc. Natl. Acad. Sci. U. S. A.* 2010, 107:3681–3686.
37. Chavakis T, Hussain M, Kanse SM, Peters G, Bretzel RG, Flock J-I, Herrmann M, Preissner KT: Staphylococcus aureus extracellular adherence protein serves as anti-inflammatory factor by inhibiting the recruitment of host leukocytes. *Nat. Med.* 2002, 8:687–693.
38. Haggar A, Shannon O, Norrby-Teglund A, Flock J-I: Dual effects of extracellular adherence protein from Staphylococcus aureus on peripheral blood mononuclear cells. *J. Infect. Dis.* 2005, 192:210–217.
39. Hammel M, Nemecek D, Keightley JA, Thomas GJJ, Geisbrecht BV: The Staphylococcus aureus extracellular adherence protein (Eap) adopts an elongated but structured conformation in solution. *Protein Sci.* 2007, 16:2605–2617.

2

Staphylococcus aureus secretes a unique class of neutrophil serine protease inhibitors

Daphne A.C. Stapels[1], Kasra X. Ramyar[2], Markus Bischoff[3], Maren von Köckritz-Blickwede[4], Fin J. Milder[1], Maartje Ruyken[1], Janina Eisenbeis[3], William J. McWhorter[5], Mathias Herrmann[3], Kok P.M. van Kessel[1], Brian V. Geisbrecht[2*] and Suzan H.M. Rooijakkers[1*]

[1] *Medical Microbiology, UMC Utrecht, The Netherlands*
[2] *Department of Biochemistry and Molecular Biophysics, Kansas State University, Manhattan, KS, USA*
[3] *Saarland University Faculty of Medicine and Medical Center, Homburg/Saar, Germany*
[4] *Department of Physiological Chemistry, University of Veterinary Medicine Hannover, Germany*
[5] *School of Biological Sciences, University of Missouri–Kansas City, Kansas City, MO, USA*

[*] *B.V.G. and S.H.M.R. contributed equally to this work*

Proc. Natl. Acad. Sci. USA (2014). 111(36): 13187-13192

ABSTRACT

Neutrophils are indispensable for clearing infections with the prominent human pathogen *Staphylococcus aureus*. Here we report that *S. aureus* secretes a family of proteins which potently inhibit the activity of neutrophil serine proteases (NSPs): neutrophil elastase (NE), proteinase 3 (PR3), and cathepsin G (CG). The NSPs, but not related serine proteases, are specifically blocked by the extracellular adherence protein (Eap) and the functionally orphan Eap-homologues EapH1 and EapH2, with inhibitory-constant values in the low-nanomolar range. This EAP family is essential for NSP inhibition by *S. aureus in vitro* and promote staphylococcal infection *in vivo*. The crystal structure of the EapH1/NE complex showed that EAP molecules constitute a unique class of non-covalent protease inhibitors that occlude the catalytic cleft of NSPs. These findings increase our insights into the complex pathogenesis of *S. aureus* infections and create opportunities to design novel treatment strategies for inflammatory conditions related to excessive NSP activity.

SIGNIFICANCE STATEMENT

Neutrophils are among the first immune cells to migrate to the site of infection and clear invading bacteria. They store large amounts of neutrophil serine proteases (NSPs) that play key roles in immune defense. Unfortunately, NSPs also contribute to tissue destruction in a variety of inflammatory disorders. In this study we discover that the pathogenic bacterium *Staphylococcus aureus* secretes a family of highly potent and specific NSP inhibitors that promote the pathogenicity of this bacterium *in vivo*. From crystallography experiments we conclude that these proteins constitute a unique class of NSP inhibitors, which can be used to design novel treatment strategies against excessive NSP activity. Furthermore, this study significantly increases our understanding of the complex nature of *S. aureus* infections.

INTRODUCTION

Infections with the human pathogen *Staphylococcus aureus* constitute a major risk to human health. Although this bacterium harmlessly colonizes over 30% of the population via the nose or skin, it causes severe morbidity and mortality upon invasion of deeper tissues[1]. To avert these serious infections, neutrophils play an indispensable role[2]. Neutrophil serine proteases (NSPs), including neutrophil elastase (NE), proteinase 3 (PR3), and cathepsin G (CG), are important for various neutrophil functions. Active NSPs are stored within the azurophilic granules[3], but upon neutrophil activation they either enter the nucleus to regulate extracellular trap (NET) formation[4], or they are released into the extracellular milieu to kill certain bacteria[5], cleave bacterial virulence factors[5,6] or regulate immune responses by cleaving chemokines and receptors[7]. Recently, a fourth neutrophil serine protease, denoted NSP4, was identified[8].

Given the central role of NSPs in neutrophil function, we wondered whether *S. aureus* had evolved mechanisms to cope with NSPs. In this study we discover that *S. aureus* secretes a family of proteins that specifically and potently block NSPs: Eap and the hitherto functional orphans Eap-homologue 1 (EapH1) and 2 (EapH2). Structural studies presented here show that EAP molecules represent a unique class of non-covalent NSP inhibitors that is distinct from the well-known chelonianin class of inhibitors. These mechanistic insights can initiate development of novel, broad-range NSP inhibitors to be used in various inflammatory conditions. Furthermore, these insights increase our understanding of the pathogenicity of *S. aureus* and underline the exceptional capability of this pathogen to adapt to its host by modulating the immune response.

RESULTS

Extracellular adherence proteins of *S. aureus* inhibit NE

To investigate whether *S. aureus* secretes inhibitors of NSPs, we incubated NE with concentrated culture supernatants of different *S. aureus* strains and quantified residual NE activity toward a fluorescent peptide substrate. Indeed, we found that NE was inhibited by supernatants of all tested *S. aureus* strains (Fig. 1A). Fractionation of the supernatant of *S. aureus* Newman by ion-exchange and size-exclusion chromatography yielded two protein bands that corresponded with the NE inhibitory activity. These bands were identified by mass spectrometry as Eap and immunodominant surface antigen B (IsaB) (Fig. 1B). Further analysis revealed that Eap is the NE inhibitor, since NE activity was not affected by the presence of recombinant IsaB, but fully blocked by the presence of recombinant Eap (Fig. 1C). Eap is a 50-70 kDa protein that consists of multiple (most often 4 or 5) repetitive EAP domains (11 kDa). The short linkers between EAP domains are susceptible to proteolysis[9], which likely explains why the band identified as Eap was only around 25 kDa (Fig. 1B).

Eap has previously been reported to mediate bacterial agglutination, tissue adherence, and to block neutrophil migration. While all of these functions require multiple EAP

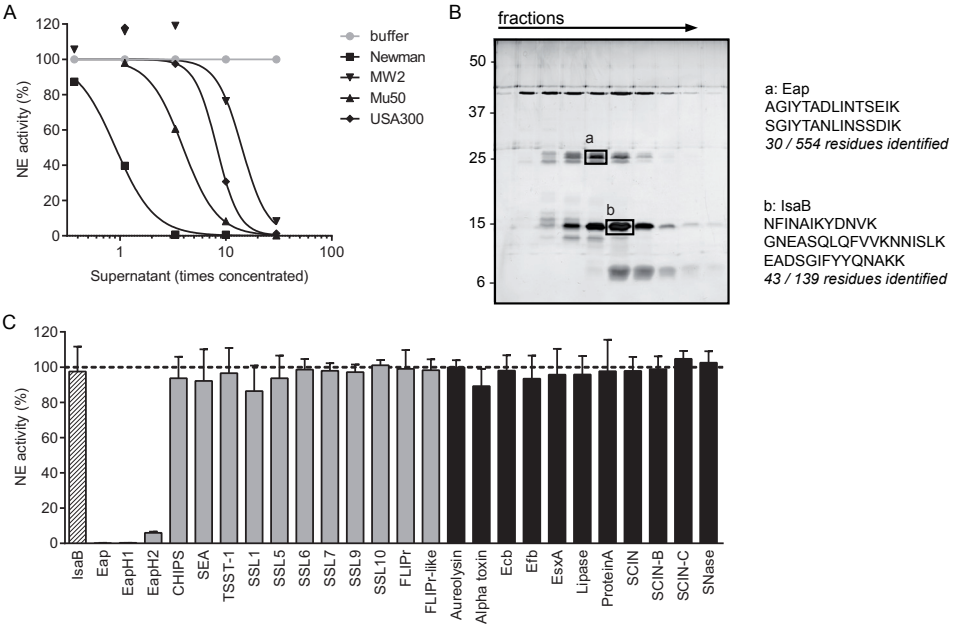

Figure 1. Extracellular adherence protein (EAP) family of *S. aureus* inhibits NE activity. (A) Residual activity of 60 nM NE upon incubation with culture supernatants of multiple *S. aureus* strains. (B) Silver staining analysis of the fractions after gel filtration (*left*). The boxes mark the protein bands analyzed by mass spectrometry and the numbers indicate the sizes of reference proteins (kDa). The identified peptides are depicted next to the gel (*right*). (C) Residual activity of 60 nM NE upon incubation with 100 nM of the mass-spectrometry hits Eap and IsaB (striped bars) and other secreted proteins of *S. aureus*. Proteins containing a similar beta-grasp-type fold as the EAPs are depicted in gray, and with an unrelated structure in black. CHIPS, chemotaxis inhibitory protein of *S. aureus;* SEA, staphylococcal enterotoxin A; TSST-1, toxic shock syndrome toxin-1; SSLs, staphylococcal superantigen-like proteins; FLIPr, formyl peptide receptor-like-1 inhibitory protein; Ecb, extracellular complement binding protein; Efb, extracellular fibrinogen binding protein; EsxA, ESAT-6 secretion system extracellular protein A; SCIN, staphylococcal complement inhibitor; SNase, *S. aureus* nuclease. Data are representative of two independent experiments (A and B) or represent the mean (± SD) of three independent experiments (C). See also Fig. S1.

domains linked in succession[10], we found that NE inhibition is mediated by individual EAP domains (Fig. S1). Each EAP domain is characterized by a beta-grasp fold wherein an alpha-helix is positioned diagonally across a five-stranded, mixed beta-sheet[11]. This fold is also found in the two *S. aureus* proteins that are homologous to Eap but do not share the above described functions: EapH1 (12 kDa) and EapH2 (13 kDa)[11]. Likewise, we found that EapH1 and EapH2 also inhibit NE (Fig. 1C). NE inhibition is specific for the EAP family, since all other tested proteins of *S. aureus* could not inhibit NE (Fig. 1C), including molecules characterized by a similar beta-grasp-type fold as the EAPs (Fig. 1C gray bars)[11,12].

Extracellular adherence proteins specifically inhibit neutrophil serine proteases

NE belongs to the chymotrypsin family of serine proteases and its amino acid sequence is most similar to that of PR3 and CG (55% and 37% amino acid identity, re-

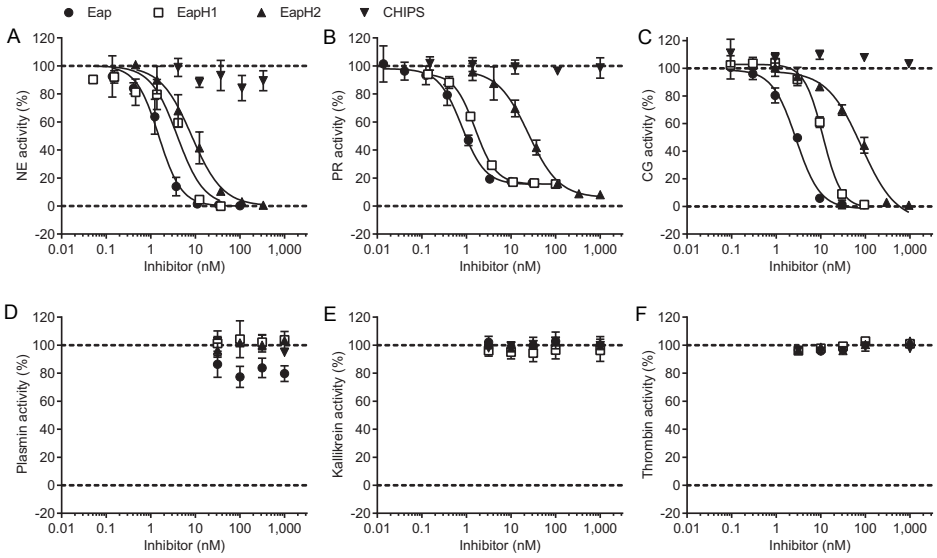

G

Protease	Eap	EapH1	EapH2	SLPI
NE	0.90 (0.51-1.3)	1.9 (0.34-3.4)	4.5 (2.1-6.9)	5.9 (2.2-9.6)
PR3	0.23 (0.052-0.41)	1.0 (0.45-1.6)	21 (5.1-38)	ND
CG	1.5 (0.89-2.2)	4.2 (1.9-6.4)	ND	9.2 (3.8-15)

Figure 2. Extracellular adherence proteins specifically inhibit NSPs. (A) Residual NE activity toward a fluorescent-peptide substrate after incubation of 5 nM NE with variable concentrations of the three EAPs or CHIPS. (B-F) Residual activity of 10 nM PR3 (B), 15 nM CG (C), 10 nM plasmin (D), 1 nM plasma kallikrein (E), and 1 nM thrombin (F), determined as in (A), with substrates specific for each protease. (G) K_i values (nM) according to the competitive inhibition model. An accurate K_i could not be determined for EapH2/CG. ND, not determined. Data represent the mean (± SD) of three independent experiments (A-F) or represent the mean (95% CI) of at least three independent experiments (G).

spectively). More distantly related chymotrypsin-like proteases include plasmin, plasma kallikrein, and thrombin. Of these six proteases, only the three NSPs appeared to be dose-dependently inhibited by the EAPs (Fig. 2A-F).

Next we determined the inhibitory constant (K_i) values of each EAP versus the three NSPs and also measured the K_i values of the endogenous human NE/CG inhibitor SLPI (secreted leukocyte protease inhibitor) as a control. The K_i values observed for all EAP/NSP combinations were in the low-nanomolar range, which is consistent with a very potent inhibition (Fig. 2G). They are also within the same order of magnitude as the K_i of SLPI for both NE and CG. Since previous work has reported a lower K_i for SLPI/NE and SLPI/CG (0.3 nM and 10 nM, respectively)[13], our particular assay system may have even underestimated the inhibitory capacity of the EAPs. Importantly, the experimentally-determined K_i values are all lower than the endogenous expression levels of the EAPs by *S. aureus* in culture (≈ 10 µg/ml or 200 nM)[14], indicating that Eap inhibition of NSPs is physiologically relevant.

EAPs are essential for NSP inhibition and promote staphylococcal infection

The genes for the EAPs lie interspersed throughout the genome and at least two out of three are present in all sequenced *S. aureus* strains. The *eap* gene is located upstream, and therefore outside, of the beta-hemolysin-converting prophage (phiNM3) that contains other immune-evasion proteins like SCIN (*scn*) and CHIPS (*chp*)[15,16] (Fig. 3A). Neither *eapH1*, nor *eapH2* lie in close proximity of phage-associated genes. Using sequential gene deletions by homologous recombination, we constructed a panel of three isogenic *eap* mutants in *S. aureus* strain Newman: Δ*eap*, Δ*eap*Δ*H1* and Δ*eap*Δ*H1*Δ*H2* (*eap*-tri-

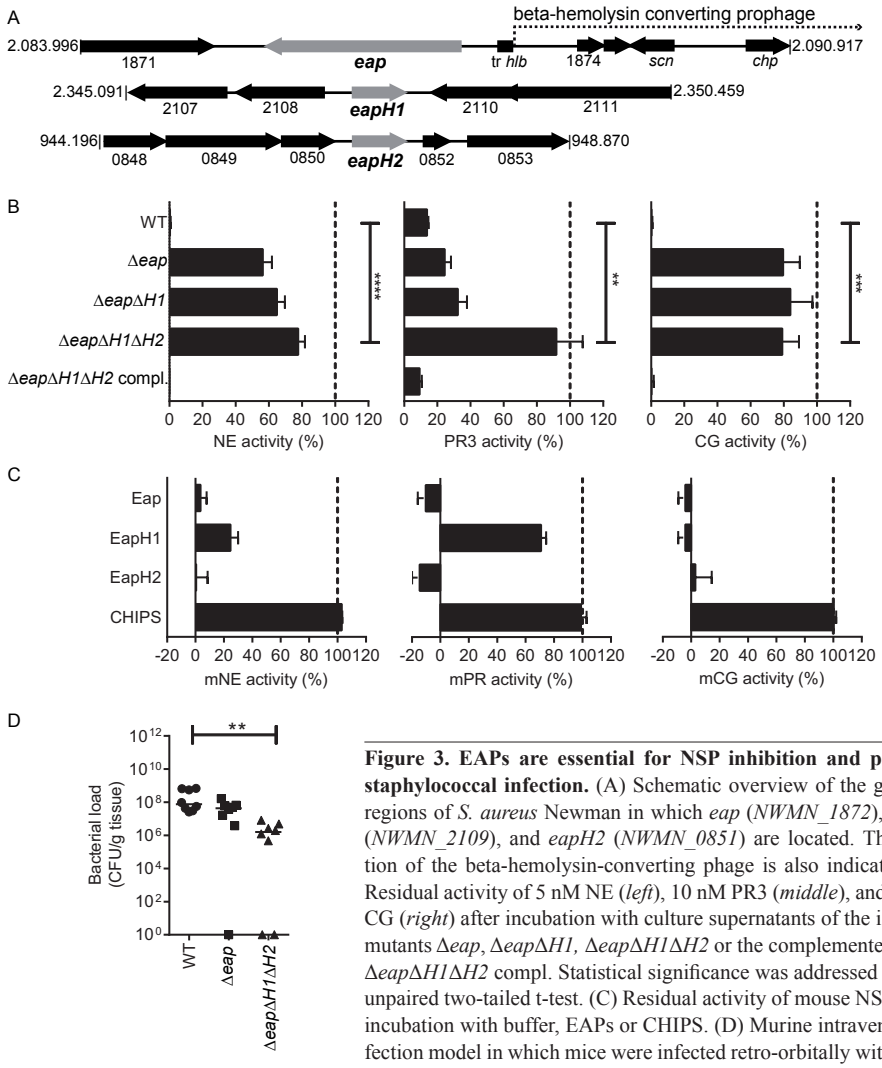

Figure 3. EAPs are essential for NSP inhibition and promote staphylococcal infection. (A) Schematic overview of the genomic regions of *S. aureus* Newman in which *eap* (*NWMN_1872*), *eapH1* (*NWMN_2109*), and *eapH2* (*NWMN_0851*) are located. The location of the beta-hemolysin-converting phage is also indicated. (B) Residual activity of 5 nM NE (*left*), 10 nM PR3 (*middle*), and 15 nM CG (*right*) after incubation with culture supernatants of the isogenic mutants Δ*eap*, Δ*eap*Δ*H1,* Δ*eap*Δ*H1*Δ*H2* or the complemented strain Δ*eap*Δ*H1*Δ*H2* compl. Statistical significance was addressed with an unpaired two-tailed t-test. (C) Residual activity of mouse NSPs after incubation with buffer, EAPs or CHIPS. (D) Murine intravenous infection model in which mice were infected retro-orbitally with $1x10^7$ *S. aureus* Newman WT or isogenic *eap* mutants. Bacterial loads recovered from liver tissues 4 days post infection (n=8). Statistical significance was addressed with a non-parametric Anova test. Data represent the mean (± SD) of three independent experiments (B-C) or horizontal bars indicate the median of all observations (D). See also Fig. S2.

ple mutant). As a control, the *eap*-triple mutant was complemented with the individual genes integrated into their original genomic location (Δ*eap*Δ*H1*Δ*H2* compl.). All isogenic strains showed comparable growth *in vitro*. When incubated with the individual NSPs, stationary-phase supernatant of the WT strain could fully inhibit all three proteases, but supernatant of the *eap*-triple mutant had almost entirely lost this capacity (Fig. 3B). The other mutants showed that Eap is essential for NE and CG inhibition, but that all EAPs together are required for inhibition of PR3. Supernatant of the complemented strain showed restored NSP inhibition to levels equivalent to WT supernatant (Fig. 3B). Although *S. aureus* was found to be resistant to direct killing by NE and CG *in vitro*[17,18], we examined whether the absence of *eap* genes might make *S. aureus* more prone to direct killing by neutrophils *in vitro*. Although there was a tendency towards better killing of the *eap*-triple mutant compared to the WT strain, this difference was not significant (Fig. S2).

To study the role of the EAPs *in vivo*, we compared the pathogenicity of the *eap*-mutant strains in a murine, liver-abscess model[19], since the bacterial burden in the liver is known to be a reliable indicator of staphylococcal virulence[20,21]. First, we confirmed that the purified EAPs also block murine NSPs *in vitro* (Fig. 3C). Then, we injected 1 x 10^7 bacteria retro-orbitally and determined the bacterial loads in the liver tissue after 4 days (Fig. 3D). The bacterial loads in the WT and Δ*eap*-infected animals did not differ significantly. However, the bacterial load in the *eap*-triple mutant infected mice was significantly lower than in WT-infected animals, strongly suggesting that all EAPs together promote *S. aureus* virulence *in vivo*.

EAPs occlude the catalytic site of NSPs

EAP domains inhibit NSPs via a low nanomolar-affinity interaction, as determined by isothermal titration calorimetry (ITC) analysis of EapH1 binding to NE (Fig. S3). This complex was studied in greater detail by determining its co-crystal structure, which was refined to 1.85 Å limiting resolution (Fig. 4A and Table S1). The structure of this inhibitory complex revealed that bound EapH1 lies directly across the Asp^{117}-His^{70}-Ser^{202} active-site triad of NE (Fig. 4B). Given the size of EapH1 and the highly complementary nature of the EapH1/NE interface (surface complementarity value of 0.77 [22]), such an arrangement would be expected to completely impede any protein or peptide-based substrates from accessing the NE active site. Importantly, this interaction is non-covalent since contiguous electron density is not visible between the catalytic Ser^{202} side chain of NE and any of the EapH1 residues in its vicinity (Fig. 4C). The absence of a covalent bond strongly suggests that EapH1, and likely all EAP domains, are mechanistically distinct from a majority of physiological NSP inhibitors (e.g. alpha-1-antitrypsin), which are conventional SERPINs[7].

The EapH1/NE interface buries 830 $Å^2$ of surface area and involves 22 of the 97 EapH1 residues. A large majority of these interfacial residues (16 of 22) are found in two distinct regions of the EapH1 sequence, i.e. residues Val^{53}-Tyr^{63} (hereafter denoted "site 1") and residues Ala^{86}-Gly^{90} (hereafter denoted "site 2"), and they reside in close proxim-

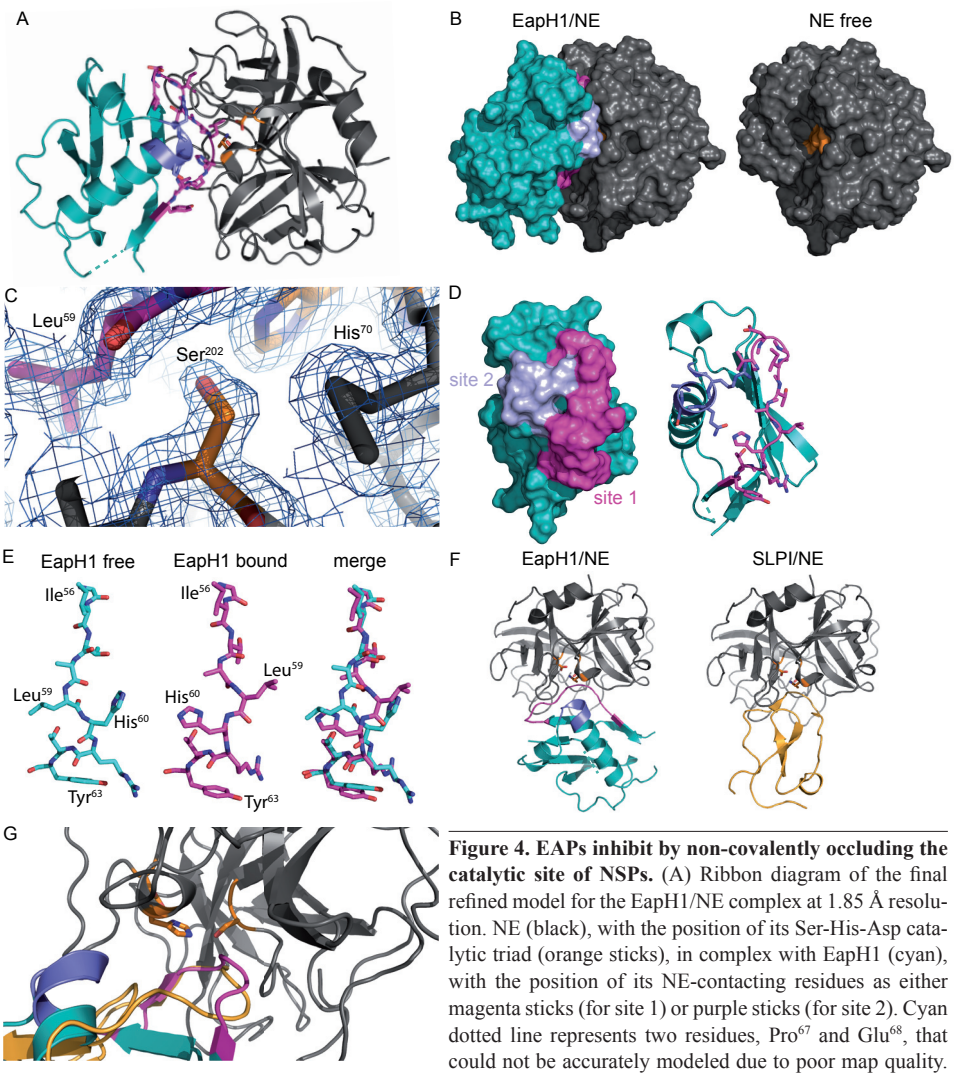

Figure 4. EAPs inhibit by non-covalently occluding the catalytic site of NSPs. (A) Ribbon diagram of the final refined model for the EapH1/NE complex at 1.85 Å resolution. NE (black), with the position of its Ser-His-Asp catalytic triad (orange sticks), in complex with EapH1 (cyan), with the position of its NE-contacting residues as either magenta sticks (for site 1) or purple sticks (for site 2). Cyan dotted line represents two residues, Pro^{67} and Glu^{68}, that could not be accurately modeled due to poor map quality. (B) Comparison of the EapH1/NE complex with NE where both components are shown as molecular surfaces. NE is shown in black with the location of its catalytic triad in orange, while EapH1 is colored as in (A), but depicted as a molecular surface. (C) $2F_o$-F_c electron density map in the region of the NE catalytic site, contoured at 1.5 σ. The locations of the catalytic residue, Ser^{202}, along with His^{60} (a component of the charge-relay system) from NE are marked, as is that of Leu^{59} from EapH1. Proteins are colored as in (A). (D) EapH1 colored as in (A), but depicted as a molecular surface (*left*) or as a cartoon (*right*, for reference). The image has been rotated clockwise in the plane of the page to emphasize the contiguous nature of the NE contact surface, comprised of both site 1 and site 2. (E) Comparison of the loop region comprising EapH1 site 1 in both the free (*left*) and NE-bound (*middle*) states. The image at the right shows a superposition of this region, in both free and bound states. The locations of key residues are indicated. (F) Comparison of the EapH1/NE complex (*left*, for reference) with the SLPI/NE complex (*right*). Proteins are shown as ribbon diagrams with NE in black, EapH1 in cyan, and SLPI in gold. (G) Close-up view of the superposed NE catalytic site (orange sticks) in the presence of inhibitors EapH1 (cyan) and SLPI (gold). PDB deposition 2Z7F was used to render images of the NE/SLPI structure in panels (F) and (G). See also Fig. S3 and Table S1.

ity to one another in the EapH1 tertiary structure (Fig. 4D). While site 1 and site 2 appear to work in concert to form an unbroken, pentagon-shaped surface of EapH1 that interacts with NE, the contacts formed by site 1 (628 Å^2) are significantly more extensive than those formed by site 2 (176 Å^2). Furthermore, the loop that comprises site 1 appears to undergo a substantial conformational rearrangement upon binding (Fig. 4E), as residues Ala^{58}-Arg^{61} rotate nearly 180° in the plane of the prominent beta-sheet when compared to the unbound EapH1 structure[11]. Since this four-residue stretch contributes two of the three hydrogen bonds formed between site 1 and NE, and accounts for almost 70% of the site-1 buried surface area (427 Å^2 of 628 Å^2), EapH1 most likely depends on such conformational change to tightly bind and inhibit NE.

A critical structure/function role for loop regions has also been suggested for other high-affinity protease inhibitors, most notably those of the chelonianin family that includes the endogenous, non-covalent NE inhibitors elafin[23] and SLPI[24]. Besides the insertion of an inhibitory loop region into the NE active site, however, the SLPI/NE complex has little in common with the EapH1/NE complex (Fig. 4F). Furthermore, SLPI and EapH1 share no detectable sequence similarity, nor do the conformations of either inhibitor-derived loop in their NE-bound state share extensive structural identity with one another (Fig. 4G). Based on these sequence and structural differences, we propose that the EAPs constitute a unique class of NSP inhibitors, distinct from that of the well-known SERPINs or chelonianin class of inhibitors.

DISCUSSION

Here we report that the human pathogen *S. aureus* secretes three proteins that form a unique group of NSP inhibitors. These EAPs are very potent, highly specific, and promote *S. aureus* pathogenesis. From previous studies it is clear that all three genes are expressed during *S. aureus* infections *in vivo*, both in mice and humans[25,26]. The fact that *S. aureus* evolved three specific NSP inhibitors strongly indicates that NSPs are critical to host defense against this bacterium. However, due to the manifold physiological substrates of NSPs, the exact function of NSPs in host clearance of *S. aureus* is currently unclear. It is likely that the interpretation of previous animal models trying to address this question[5,18,27] has been confounded by the endogenous production of EAPs. In the future, these conceptual limitations can be overcome by employing the bacterial deletion mutants that are presented here.

A key teleological issue remains as to why *S. aureus* inhibits NSPs by three distinct proteins. We speculate that the *eap* genes are most likely differentially expressed during an infection, creating a broader window of opportunity to block NSPs both at distinct sites of the body and times of infection. In fact, expression of both *eap* and *eapH1* has been reported to be upregulated in presence of azurophilic-granule contents, whereas *eapH2* expression was not affected[28]. In many ways, this redundancy shows striking parallels

with the diverse array of complement-evasion proteins produced by the same organism[29]. The expression of multiple proteins with some level of functional redundancy may be a general principle that underlies *S. aureus* innate immune evasion, regardless of the specific host process that is targeted.

From a broader biological perspective, our work suggests that NSP inhibition by staphylococcal EAP domains has arisen through a distinct evolutionary trajectory from either the SERPIN or chelonianin-class inhibitors found in its human host. In contrast to the SERPINs, EAP domains do not form covalent complexes with their target(s), they do not appear to undergo large conformational changes at sites distal to their inhibitory loop, and they are relatively small (e.g. EAP domains are about one-fourth the molecular weight of the 44 kDa alpha-1-antitrypsin). Furthermore, while EAP domains are more similar in overall size to active fragments of the chelonianin-class inhibitors SLPI and elafin (~6 kDa), their fold is entirely different and, importantly, the *S. aureus* molecules do not require disulfide bonds to constrain their NSP-inhibitory loop into an active conformation.

Despite the many naturally occurring NSP inhibitors found in the human body, NSPs are known to play a significant role in tissue destruction in a variety of inflammatory disorders like cystic fibrosis, chronic obstructive pulmonary disease, emphysema, and rheumatoid arthritis[7]. As a consequence, targeted NSP inhibition has been considered as a plausible treatment in these diseases. But even though substantial work has been done in this area, to date no drug has been registered that targets all NSPs[7]. Here we show that the EAPs have a high inhibitory potency and that, whereas many endogenous NSP inhibitors inhibit only two out of three NSPs, they inhibit all three NSPs. Therefore, EAPs might serve as a template for developing a novel class of synthetic NSP inhibitors. Although drug development is clearly a long-term goal, the results we present here have already increased our understanding of the complex nature of *S. aureus* infections by identifying an effective mechanism through which this devastating pathogen defends itself against human innate immunity.

ACKNOWLEDGEMENTS

We thank Constantin Becker for help with animal experiments; Ted Bae, Niels Bovenschen and Rolf Urbanus for helpful discussions; Kimberly Jefferson (IsaB), Ted Bae (pKOR1), Ian Monk (DC10B) for providing reagents; the Brenkman lab for performing mass spectrometry; Jos van Strijp, Erik Hack, John Lambris, and Daniel Ricklin for critical reading of the manuscript.

This work was supported by a Vidi grant from the Netherlands Organization for Scientific Research (to S.H.M.R.), a Research Fellowship grant from the Federation of European Microbiological Societies (to D.A.C.S.), grant no. 01 KI 07103 Skin Staph from

the German Ministry for Education and Research (to M.H.), and grant AI071028 from the U.S. National Institutes of Health (to B.V.G.). Use of the Advanced Photon Source was supported by the U.S. Department of Energy, Office of Science, Office of Basic Energy Sciences, under Contract No. W-31-109-Eng-38. Data were collected at Southeast Regional Collaborative Access Team (SER-CAT) beamlines at the Advanced Photon Source, Argonne National Laboratory. A list of supporting member institutions may be found online (www.ser-cat.org/members.html).

The authors declare no competing financial interests.

MATERIAL AND METHODS

Screening for NE inhibition

S. aureus strains Newman, MW2, USA300 and Mu50 were cultured for 8 h in Icove's Modified Dulbecco's Medium (Invitrogen). Culture supernatants were concentrated (100x) on a 3 kDa Amicon-Ultra spin column (Merck Millipore). Supernatants were incubated 1:1 with 120 nM NE (Elastin Products Company) in 1 mg/ml BSA-PBS for 60 min at 37 °C. Residual NE activity was determined by the conversion of 230 μM substrate (AAPV-AMC; Calbiochem) for 60 min and fluorescence was measured in a Flexstation fluorometer (Molecular Devices, LLC). AMC: excitation at 360 nm and emission at 460 nm. Final values are expressed as percentage of NE activity in this assay buffer.

Identification of Eap

Supernatant of *S. aureus* Newman was cultured for 18 h in Todd Hewitt broth (THB) and fractionated by using the Äkta system and columns of GE Healthcare. All fractions were analyzed by 15% (wt/vol) SDS-PAGE and silver staining. Activity of the fractionated supernatant, and of the recombinant proteins (100 nM), was tested as during the screening. See Supplemental Materials and Methods for details.

Purified *S. aureus* proteins

TSST-1 (Bioconnect), Protein A (Sigma) and SEA (Sigma) were obtained commercially. All other *S. aureus* proteins were produced recombinantly as His-tagged proteins in *E. coli* and purified using nickel affinity chromatography as described[11,30–33].

Protease activity assays

NE (5 nM), PR3 (10 nM, Elastin Products Company), CG (15 nM, Biocentrum), thrombin (1 nM, Sigma), plasmin (10 nM, Sigma), or plasma kallikrein (1 nM, Innovative Research) were incubated with inhibitors or culture supernatants for 15 min at room temperature in PBS with 0.05% (vol/vol) Igepal-Ca63 (Sigma). Residual protease activity was measured with protease-specific substrates at 37 °C in a Fluostar Omega plate reader (BMG Labtech). Data points showing linear substrate conversion were used to determine relative protease activity. Thereafter, IC_{50} values were determined by plotting a sigmoidal curve without constraints, or the K_i was determined according to the competitive inhibitor model by plotting the protease activity in presence of multiple concentrations of the inhibitors Eap, EapH1, EapH2, or SLPI (R&D systems) against the multiple concentrations of substrate used (all with maximum substrate concentrations higher than the determined K_m). A list of substrates is found in Table S2.

Generation of bacterial mutants

Markerless mutants of *eap* genes in *S. aureus* Newman were generated using the pKOR1 vector[34] with minor modifications. We modified pKOR1 by replacing the lambda recombination cassette and the cat (-) and *ccdB* genes with a conventional multiple cloning site (cloned in ApaI/KpnI, creating the new pKOR1-mcs vector). Subsequently, we ligated the 1000 bp regions immediately upstream and downstream of our gene of interest using PCR overlay and cloned this product into pKOR1-mcs in *E. coli* DC10B[35]. After electroporation

into *S. aureus* Newman, allelic replacement was induced by temperature shift[34]. The mutants were generated in a step-wise fashion: we first deleted the *eap* gene (resulting in MR1811, or Δ*eap*), then *eapH1* (MR1852, or Δ*eap*Δ*H1*) and subsequently *eapH2* (MR1860, or Δ*eap*Δ*H1*Δ*H2*). For complementation of the Δ*eap*Δ*H1*Δ*H2* strain (MR1937, or Δ*eap*Δ*H1*Δ*H2* compl.), we also used the pKOR1 system but now cloned the upstream and downstream regions plus the gene of interest. Homologous recombination restored the presence of the *eap* genes at their original location. All mutants were verified by DNA sequencing and production of secreted Eap was monitored by Western blotting.

Activity of mouse NSPs *in vitro*

Mouse bone-marrow cells were isolated as described before[36]. Erythrocytes were lysed with ACK lysis buffer for 3 min at room temperature. The remaining cells were stimulated with 5 µg/ml cytochalasin B (Sigma) for 10 min at room temperature and degranulated with 1 µM fMLP (Sigma) for 15 min at 37 °C. The supernatant was used as source of murine NSPs. Diluted supernatant (1:8 for NE, 1:16 for PR3, and 1:2 for CG) was incubated with 100 nM of each EAP, or CHIPS. The residual activity was determined with protease-specific substrates[37]. The relative mNSP activity was determined by using the slope of the linear part of the substrate-conversion graph compared to this slope in absence of inhibitors. A list of substrates is found in Table S2.

Animal model

The liver abscess model was performed as described, with minor modifications[19]. Eight-week old female C57/BL6 mice (purchased from Charles River) were infected with 100 µl bacterial suspension (~$1x10^7$ CFU) via retro-orbital injection. Infected mice were treated with a daily dose of caprofen (5 mg/kg; Pfizer), and 4 days post infection, mice were euthanized with pentobarbital (400 mg/kg; Merial GmbH, Hallbergmoos, Germany). Their livers were removed, homogenized in PBS, and viable bacteria therein were quantified by serial dilution. The animal experiments were performed as required by the German regulations of the Society for Laboratory Animal Science (GV-SOLAS) and the European Health Law of the Federation of Laboratory Animal Science Associations (FELASA), and were approved by the local governmental animal care committee (33.9-42502-04-38/2012).

Macromolecular Crystallography

Crystals of EapH1 bound to human NE were obtained from vapor diffusion of hanging drops at 20°C. A sample of the EapH1/NE complex was prepared by mixing a 1:1 molar ratio of each monomer, followed by centrifugal buffer exchange into 10 mM tris (pH 7.4), 50 mM NaCl and concentration to 5 mg/ml total protein (as judged by absorbance at 280 nM). Block-shaped crystals of various sizes appeared within one to three days and grew to their final dimensions over the course of a week from drops consisting of 1 µl complex mixed with 1 µl of reservoir buffer (0.1 M HEPES (pH 7.0), 1.0 M succinic acid, and 1% (w/v) polyethylene glycol-2000) that had been previously diluted with an equal volume of ddH_2O, and that were equilibrated over 500 µl of reservoir buffer. Single crystals were harvested and flash cooled in liquid nitrogen following a brief soak in a cryopreservation solution consisting of the reservoir buffer above supplemented with 20% (w/v) sucrose.

X-ray diffraction data were collected at 1.22 Å wavelength using beamline 22-ID of the Advanced Photon Source, Argonne National Laboratory. Diffraction data were indexed, integrated, and scaled using HKL2000. Crystals of EapH1/NE grew in the space group $P6_1$ and contained a single EapH1/NE complex in the asymmetric unit. Structure solution and refinement were carried out by individual programs as implemented within the PHENIX software package[38]. Initial phases were obtained by molecular replacement using single copies of NE (PDB code 1HNE[39]) and EapH1 (PDB code 1YN4[11]) as sequential search models. The final model was completed after iterative cycles of manual building in COOT[40] followed by refinement using PHENIX.REFINE. In the Ramachandran plot, 97% of the residues modeled occupied favored regions, while the remaining 3% occupied allowed regions. Refined coordinates and structure factors (code 4NZL) have been deposited in the Protein Data Bank, Research Collaboratory for Structural Bioinformatics, Rutgers University, New Brunswick, NJ (http://www.rscb.org/). A more complete description of the crystal properties, diffraction data quality, and characteristics of the final model may be found in Table S1.

Statistics

Statistical analyses were performed using GraphPad Prism 6.0. For determination of residual NSP activity in presence of various bacterial culture supernatants, normality was assumed and an unpaired, two-tailed Stu-

dent's t-test was used. Since the number of data points in the in vivo experiment did not allow for normality testing and we had to correct for multiple comparison, we used a Krusskal-Wallis test. $p < 0.05$ was assumed statistically significant. ****, $p < 0.0001$; ***, $p < 0.001$; **, $p < 0.01$; *, $p < 0.05$.

REFERENCES

1. DeLeo FR, Chambers HF: Reemergence of antibiotic-resistant Staphylococcus aureus in the genomics era. *J. Clin. Invest.* 2009, 119:2464–2474.

2. Miller LS, Cho JS: Immunity against Staphylococcus aureus cutaneous infections. *Nat. Rev. Immunol.* 2011, 11:505–518.

3. Pham CTN: Neutrophil serine proteases: specific regulators of inflammation. *Nat. Rev. Immunol.* 2006, 6:541–550.

4. Papayannopoulos V, Metzler KD, Hakkim A, Zychlinsky A: Neutrophil elastase and myeloperoxidase regulate the formation of neutrophil extracellular traps. *J. Cell Biol.* 2010, 191:677–691.

5. Belaaouaj AA, Kim KS, Shapiro SD: Degradation of Outer Membrane Protein A in Escherichia coli Killing by Neutrophil Elastase. *Science* 2000, 289:1185–1187.

6. Weinrauch Y, Drujan D, Shapiro SD, Weiss J, Zychlinsky A: Neutrophil elastase targets virulence factors of enterobacteria. *Nature* 2002, 417:91–94.

7. Korkmaz B, Horwitz MS, Jenne DE, Gauthier F: Neutrophil Elastase, Proteinase 3, and Cathepsin G as Therapeutic Targets in Human Diseases. *Pharmacol. Rev.* 2010, 62:726–759.

8. Perera NC, Schilling O, Kittel H, Back W, Kremmer E, Jenne DE: NSP4, an elastase-related protease in human neutrophils with arginine specificity. *Proc. Natl. Acad. Sci. U. S. A.* 2012, 109:6229–6234.

9. Hammel M, Nemecek D, Keightley JA, Thomas GJJ, Geisbrecht BV: The Staphylococcus aureus extracellular adherence protein (Eap) adopts an elongated but structured conformation in solution. *Protein Sci.* 2007, 16:2605–2617.

10. Hussain M, Haggar A, Peters G, Chhatwal GS, Herrmann M, Flock J-I, Sinha B: More than one tandem repeat domain of the extracellular adherence protein of Staphylococcus aureus is required for aggregation, adherence, and host cell invasion but not for leukocyte activation. *Infect. Immun.* 2008, 76:5615–5623.

11. Geisbrecht BV., Hamaoka BY, Perman B, Zemla A, Leahy DJ: The crystal structures of EAP domains from Staphylococcus aureus reveal an unexpected homology to bacterial superantigens. *J. Biol. Chem.* 2005, 280:17243–17250.

12. Haas P-J, de Haas CJC, Poppelier MJJ, van Kessel KPM, van Strijp JAG, Dijkstra K, Scheek RM, Fan H, Kruijtzer JAW, Liskamp RMJ, et al.: The structure of the C5a receptor-blocking domain of chemotaxis inhibitory protein of Staphylococcus aureus is related to a group of immune evasive molecules. *J. Mol. Biol.* 2005, 353:859–872.

13. Wright CD, Kennedy JA, Zitnik RJ, Kashem MA: Inhibition of murine neutrophil serine proteinases by human and murine secretory leukocyte protease inhibitor *Biochem. Biophys. Res. Commun.* 1999, 254:614–617.

14. Palma M, Haggar A, Flock J-I: Adherence of Staphylococcus aureus is enhanced by an endogenous secreted protein with broad binding activity *J. Bacteriol.* 1999, 181:2840–2845.

15. Van Wamel WJB, Rooijakkers SHM, Ruyken M, Van Kessel KPM, Van Strijp JAG: The Innate Immune Modulators Staphylococcal Complement Inhibitor and Chemotaxis Inhibitory Protein of Staphylococcus aureus Are Located on β -Hemolysin-Converting Bacteriophages. *J. Bacteriol.* 2006, 188:1310–1315.

16. Bae T, Baba T, Hiramatsu K, Schneewind O: Prophages of Staphylococcus aureus Newman and their contribution to virulence. *Mol. Microbiol.* 2006, 62:1035–1047.

17. Belaaouaj AA, McCarthy R, Baumann M, Gao Z, Ley TJ, Abraham SN, Shapiro SD: Mice lacking neutrophil elastase reveal impaired host defense against gram negative bacterial sepsis. *Nature* 1998, 4:615–618.

18. MacIvor DM, Shapiro SD, Pham CT, Belaaouaj A, Abraham SN, Ley TJ: Normal neutrophil function in cathepsin G-deficient mice. *Blood* 1999, 94:4282–4293.

19. Li C, Sun F, Cho H, Yelavarthi V, Sohn C, He C, Schneewind O, Bae T: CcpA mediates proline auxotrophy and is required for Staphylococcus aureus pathogenesis *J. Bacteriol.* 2010, 192:3883–3892.

20. Xu SX, Gilmore KJ, Szabo PA, Zeppa JJ, Baroja ML, Haeryfar SMM, McCormick JK: Superantigens subvert the neutrophil response to promote abscess formation and enhance Staphylococcus aureus survival in vivo. *Infect. Immun.* 2014, doi:10.1128/IAI.02110-14.

21. Bubeck Wardenburg J, Williams WA, Missiakas D: Host defenses against Staphylococcus aureus infection

require recognition of bacterial lipoproteins. *Proc. Natl. Acad. Sci. U. S. A.* 2006, 103:13831–13836.
22. Lawrence MC, Colman PM: Shape complementarity at protein/protein interfaces. *J. Mol. Biol.* 1993, 234:946–950.
23. Tsunemi M, Matsuura Y, Sakakibara S, Katsube Y: Crystal structure of an elastase-specific inhibitor elafin complexed with porcine pancreatic elastase determined at 1.9 A resolution. *Biochemistry* 1996, 35:11570–11576.
24. Koizumi M, Fujino A, Fukushima K, Kamimura T, Takimoto-Kamimura M: Complex of human neutrophil elastase with 1/2SLPI *J. Synchrotron Radiat.* 2008, 15:308–311.
25. Date SV, Modrusan Z, Lawrence M, Morisaki JH, Toy K, Shah IM, Kim J, Park S, Xu M, Basuino L, et al.: Global gene expression of methicillin-resistant Staphylococcus aureus USA300 during human and mouse infection. *J. Infect. Dis.* 2014, 209:1542–1550.
26. Joost I, Blass D, Burian M, Goerke C, Wolz C, Von Müller L, Becker K, Preissner K, Herrmann M, Bischoff M: Transcription analysis of the extracellular adherence protein from Staphylococcus aureus in authentic human infection and in vitro. *J. Infect. Dis.* 2009, 199:1471–1478.
27. Reeves EP, Lu H, Jacobs HL, Messina CGM, Bolsover S, Gabella G, Potma EO, Warley A, Roes J, Segal AW: Killing activity of neutrophils is mediated through activation of proteases by K+ flux. *Nature* 2002, 416:291–297.
28. Palazzolo-Ballance AM, Reniere ML, Braughton KR, Sturdevant DE, Otto M, Kreiswirth BN, Skaar EP, DeLeo FR: Neutrophil Microbicides Induce a Pathogen Survival Response in Community-Associated Methicillin-Resistant Staphylococcus aureus *J. Immunol.* 2007, 180:500–509.
29. Spaan AN, Surewaard BGJ, Nijland R, van Strijp JAG: Neutrophils versus Staphylococcus aureus: a biological tug of war. *Annu. Rev. Microbiol.* 2013, 67:629–650.
30. Xie C, Alcaide P, Geisbrecht BV., Schneider D, Herrmann M, Preissner KT, Luscinskas FW, Chavakis T: Suppression of experimental autoimmune encephalomyelitis by extracellular adherence protein of Staphylococcus aureus. *J. Exp. Med.* 2006, 203:985–994.
31. Rooijakkers SHM, Milder FJ, Bardoel BW, Ruyken M, van Strijp JAG, Gros P: Staphylococcal complement inhibitor: structure and active sites. *J. Immunol.* 2007, 179:985–994.
32. De Haas CJC, Veldkamp KE, Peschel A, Weerkamp F, Van Wamel WJB, Heezius ECJM, Poppelier MJJG, Van Kessel KPM, Van Strijp JAG: Chemotaxis inhibitory protein of Staphylococcus aureus, a bacterial antiinflammatory agent. *J. Exp. Med.* 2004, 199:687–695.
33. Bestebroer J, Aerts PC, Rooijakkers SHM, Pandey MK, Köhl J, Van Strijp JAG, De Haas CJC: Functional basis for complement evasion by staphylococcal superantigen-like 7. *Cell. Microbiol.* 2010, 12:1506–1516.
34. Bae T, Schneewind O: Allelic replacement in Staphylococcus aureus with inducible counter-selection *Plasmid.* 2006, 55:58–63.
35. Monk IR, Shah IM, Xu M, Tan M-W, Foster TJ: Transforming the untransformable: application of direct transformation to manipulate genetically Staphylococcus aureus and Staphylococcus epidermidis. *MBio* 2012, 3:e00277–11.
36. Siemsen DW, Schepetkin IA, Kirpotina LN, Lei B, Quinn MT: Neutrophil isolation from nonhuman species. In *Neutrophil Methods and Protocols*. Edited by Quinn MT, DeLeo FR, Bokoch GM. Humana Press Inc.; 2007:26–27.
37. Kalupov T, Brillard-Bourdet M, Dadé S, Serrano H, Wartelle J, Guyot N, Juliano L, Moreau T, Belaaouaj A, Gauthier F: Structural characterization of mouse neutrophil serine proteases and identification of their substrate specificities: relevance to mouse models of human inflammatory diseases. *J. Biol. Chem.* 2009, 284:34084–34091.
38. Zwart PH, Afonine PV., Grosse-Kunstleve RW, Hung L, Ioerger TR, McCoy AJ, McKee E, Moriarty NW, Read RJ, Sacchettini JC, et al.: Automated structure solution with the PHENIX Suite. In *Methods Mol Biol vol. 426*. Edited by Kobe B, Guss M, Huber T. Humana Press; 2008:419–435.
39. Navia MA, McKeever BM, Springer JP, Lin T-Y, Williams HR, Fluder EM, Dorn CP, Hoogsteen K: Structure of human neutrophil elastase in complex with a peptide chloromethyl ketone inhibitor at 1.84-A resolution *Proc. Natl. Acad. Sci. U. S. A.* 1989, 86:7–11.
40. Emsley P, Lohkamp B, Scott WG, Cowtan K: Features and development of Coot *Acta Crystallogr. D. Biol. Crystallogr.* 2010, 66:486–501.

SUPPLEMENTAL INFORMATION

Supplemental Figures

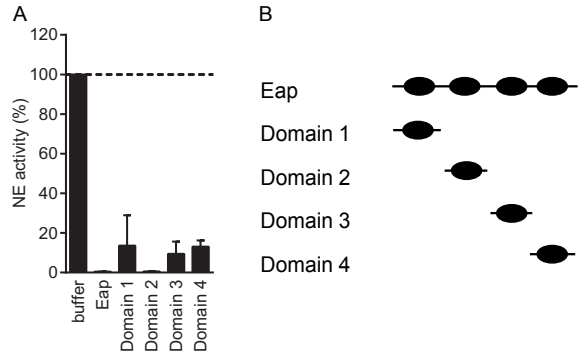

Figure S1. Individual EAP domains inhibit NE. (A) Residual activity of 5 nM NE upon incubation with 30 nM Eap, or its individual domains. (B) Schematic overview of the proteins used in this experiment.

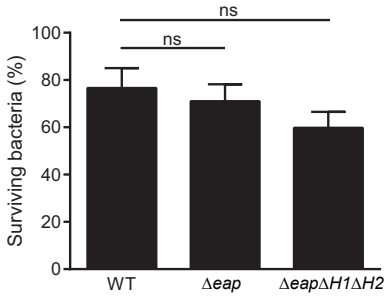

Figure S2. Neutrophil killing assay. Percentage of surviving bacteria compared to growth controls. Serum-opsonized bacteria (5 x 10^4) were incubated with 9 x 10^4 neutrophils. After 30 min. the neutrophils were lysed and the surviving bacteria were enumerated by plating serial dilutions.

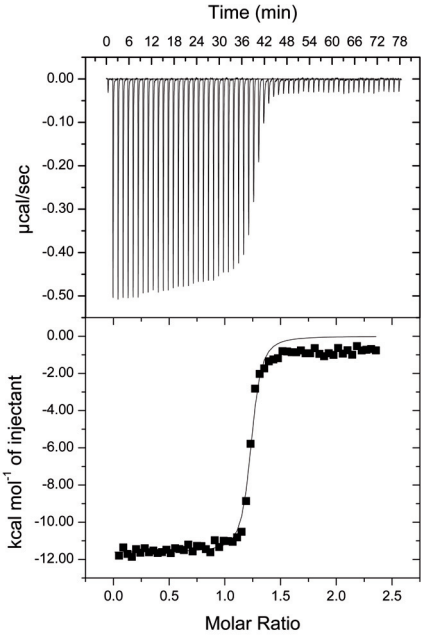

Figure S3. Isothermal titration calorimetry analysis of EapH1 binding to NE. Characterization of NE binding to EapH1 by ITC. Thermogram obtained through the course of one injection series (*top*) and corresponding integrated enthalpy changes following background correction (*bottom*). The solid line indicates the outcome of data fitting according to a single-site binding model. Derivation of the thermodynamic parameters for the EapH1/NE complex revealed a change in enthalpy (ΔH) of -11.2 ± 0.3 kcal/mol, a dissociation constant (K_d) of 25 nM, and a stoichiometry value consistent with a 1:1 interaction (N = 1.2 ± 0.1).

Suplemental Tables

Table S1. Data collection and refinement statistics

	EapH1/NE
Data collection	
Space group	$P6_1$
Cell dimensions	
a, *b*, *c* (Å)	94.95, 94.95, 84.16
α, β, γ (°)	90, 90, 120
Resolution (Å)	50-1.85 (1.86-1.85)[a]
R_{sym} or R_{merge}	13.6 (50.3)
I / σI	24.2 (2.5)
Completeness (%)	99.6 (96.4)
Redundancy	9.4 (3.5)

[a]Values in parentheses are for highest-resolution shell.

	EapH1/NE
Refinement	
Resolution (Å)	49.35-1.85 (1.92-1.85)
No. reflections	35,647
R_{work} / R_{free}	15.7 / 18.8
No. atoms	
Protein	2,402
Ligand/ion	98
Water	279
B-factors	
Protein	33.95
Ligand/ion	36.73
Water	67.67
R.m.s. deviations	
Bond lengths (Å)	0.014
Bond angles (°)	1.47

Table S2. Substrates used to determine protease activity

Protease	Substrate	Company
NE	AAPV-AMC[a] (50 μM)	Calbiochem
PR3	AAPV-AMC[a] (50 μM)	Calbiochem
CG	AAPF-AMC[a] (500 μM)	Genecust, Luxembourg
thrombin	VPR-AMC[a] (100 μM)	Chromogenix
plasmin	VLK-pNA[b] (1 mM)	Oxford Biomedical Research
plasma kallikrein	PFR-pNA[b] (250 μM)	Bachem
mNE	Abz-QPMAVVQSVPQ-EDDnp[c] (20 μM)	Genecust, Luxembourg
mPR3	Abz-VARCADYQ-EDDnp[c] (20 μM)	Genecust, Luxembourg
mCG	Abz-EPFWEDQ-EDDnp[c] (20 μM)	Genecust, Luxembourg

[a] AMC substrates were measured with excitation at 360 nm and emission at 460 nm.
[b] pNA substrates were measured at OD 405 nm.
[c] Abz/EDDnp substrates were measured with excitation at 320 nm and emission at 420 nm[4].

Suplemental Material and Methods

Culture supernatant fractionation

The culture supernatant was 3-times diluted in 50 mM sodium acetate pH 5.0, loaded on a HiTrap SP XL column and eluted with NaCl. All protein-containing fractions were then separated by a Mono S 5/50 GL column in fresh 50 mM sodium acetate pH 5.0 and eluted with a NaCl gradient. The NE-inhibiting fractions were subsequently fractionated with a MonoQ 5/50 GL column in 20 mM ethanolamine pH 10.0 and eluted with a NaCl gradient. The new NE-inhibiting fractions were applied to a Superdex 75 10/300 GL column in PBS and proteins were identified by mass-spectrometry (LC-MS/MS).

Activity of individual EAP domains

Individual EAP domains were cloned and purified as described before[1]. Their NE-inhibiting activity was tested as described under the subheading 'protease activity assays'.

Neutrophil killing assay

Serum and neutrophils were both isolated from blood drawn from healthy adult volunteers after obtaining informed consent. This protocol was approved by the medical-ethical committee of the UMC Utrecht (The Netherlands). Neutrophils were isolated from blood in heparinized vacutainers (Becton Dickinson) and purified over a ficol/histopaque gradient as described previously[2]. Normal human serum (NHS) was isolated as described before[3] and frozen at -80 °C until needed for further use.

Over-night cultures of bacteria in THB were diluted 1:100 in fresh THB and grown to OD_{660} of 0.5. About 10^6 bacteria (5 µl) were opsonized with 10% (vol/vol) NHS, diluted in RPMI-1640 (Invitrogen) supplemented with 0.05% (wt/vol) human serum albumin (HSA; Sanquin), for 15 min at 37 °C. Killing of 5 x 10^4 bacteria by 9 x 10^4 neutrophils was allowed for 30 min in RPMI-HSA, while shaking at 37 °C. The killing was stopped by adding ice-cold water with 1% saponin to lyse the neutrophils. After 15 min incubation on ice, the surviving bacteria were enumerated by plating serial dilutions on THB-agar plates.

Isothermal Titration Calorimetry

ITC experiments were carried out using a VP-ITC instrument (MicroCal) at 25°C and a buffer system of 20 mM tris (pH 8.0) with 200 mM NaCl. To study the interaction between NE and EapH1, 60 injections of 3 µl of EapH1 (350 µM) were titrated into 1.456 ml of NE (19.3 µM). Each set of experiments was performed in triplicate and the final values were derived from the average of all three runs per experiment. A single-site binding model was used to fit the corrected binding isotherm and allowed derivation of thermodynamic parameters using the ORIGIN ITC software (OriginLab).

Supplemental References

1. Geisbrecht BV., Hamaoka BY, Perman B, Zemla A, Leahy DJ: The crystal structures of EAP domains from Staphylococcus aureus reveal an unexpected homology to bacterial superantigens. *J. Biol. Chem.* 2005, 280:17243–17250.

2. Prat C, Bestebroer J, De Haas CJC, Van Strijp JAG, Van Kessel KPM: A New Staphylococcal Anti-Inflammatory Protein That Antagonizes the Formyl Peptide Receptor-Like 1. *J. Immunol.* 2006, 177:8017–8026.

3. Berends ETM, Horswill AR, Haste NM, Monestier M, Nizet V, von Köckritz-Blickwede M: Nuclease expression by Staphylococcus aureus facilitates escape from neutrophil extracellular traps. *J. Innate Immun.* 2010, 2:576–586.

4. Kalupov T, Brillard-Bourdet M, Dadé S, Serrano H, Wartelle J, Guyot N, Juliano L, Moreau T, Belaaouaj A, Gauthier F: Structural characterization of mouse neutrophil serine proteases and identification of their substrate specificities: relevance to mouse models of human inflammatory diseases. *J. Biol. Chem.* 2009, 284:34084–34091.

3

Molecular insights into the inhibition of neutrophil proteases by extracellular adherence proteins

Daphne A.C. Stapels[1], Fin J. Milder[1], Angelino Tromp[1], Aernoud van Batenburg[1], Wilco de Graaf[1], Helmus van de Langemheen[2], Rob Liskamp[2], Suzan H.M. Rooijakkers[1] and Brian V. Geisbrecht[3]

[1] *Medical Microbiology, UMC Utrecht, The Netherlands*
[2] *School of Chemistry, University of Glasgow, United Kingdom*
[3] *Department of Biochemistry & Molecular Biophysics, Kansas State University, Manhattan, KS, USA*

Manuscript in preparation

ABSTRACT

Neutrophils are key players in innate immunity. Within their azurophilic granules, they store neutrophil serine proteases (NSPs) that have a multitude of functions within the immune system, ranging from bacterial killing to fine-tuning the immune response. However, when the immune system is imbalanced, these proteases can also mediate various detrimental effects as seen in inflammatory lung diseases. The Gram-positive bacterium *Staphylococcus aureus* protects itself against NSPs by evolving potent inhibitors. These three extracellular adherence proteins (Eap of 50 kDa, EapH1 of 12 kDa, and EapH2 of 13 kDa) are structural homologues that all contain one or more EAP domains. Recent structural studies indicated that these proteins form a unique class of NSP inhibitors that could potentially serve as templates to develop a novel class of therapeutic NSP inhibitors. Here we further investigated the molecular mechanism of NSP inhibition by EAPs. Led by recent crystal structures and protein-alignment tools, we designed several protein mutants and pinpointed residues in EAPs important for NSP inhibition. Despite the structural homology amongst EAPs, our data indicate that EapH1 and EapH2 might inhibit NSPs via different mechanisms. Furthermore, we explored the range of host proteases that is inhibited by EAPs and determined that mast cell chymase is also targeted. Finally, we identify a molecule homologous to EAPs that lacks NSP inhibitory activity and could serve as a scaffold for future active-site analyses.

INTRODUCTION

Neutrophils are of prime importance in fighting numerous bacterial infections. They are filled with granules that contain antimicrobial peptides and proteins. Their azurophilic granules contain the neutrophil serine proteases (NSPs), comprised of neutrophil elastase (NE), proteinase 3 (PR3), cathepsin G (CG), and neutrophil serine protease 4 (NSP4). These play important roles in all aspects of neutrophilic antibacterial defense. Antibacterial defenses occur in both the extracellular and intracellular environments. For extracellular killing, neutrophils first degranulate, whereby they release the antimicrobial contents of their granules into the extracellular space; or they form neutrophil extracellular traps (NETs), for which they release their DNA coated with granular contents into the extracellular space. For intracellular killing, neutrophils engulf bacteria into a phagosome to which they deliver their granular contents[1]. While these antimicrobial functions of NSPs are believed to contribute directly to the clearance of infections, it is now understood that excessive NSP activity directly correlates with the severity of various inflammatory lung diseases, e.g. chronic obstructive pulmonary disease (COPD), cystic fibrosis (CF), and acute lung injury (ALI)[2]. In these diseases the inflamed lung tissue has attracted a storm of neutrophils, resulting in an uncontrolled release of NSPs via one of the above mechanisms. This creates a positive feed-back loop of proteolytic tissue destruction, inflammation, and increased neutrophil influx. Inhibition of excessive NSP activity has therefore been suggested as a promising treatment option in these diseases[2].

We recently discovered that the opportunistic pathogen *Staphylococcus aureus* has evolved a family of NSP inhibitors, through which it protects itself against the activity of NSPs[3]. The staphylococcal NSP inhibitors include the multi-domain extracellular adherence protein (Eap), and the single-domain Eap homologues (EapH1 and EapH2). Functional studies have shown that all three EAPs can inhibit the best-described NSPs, i.e. NE, PR3, and CG, but not the more distantly-related serine proteases plasmin, thrombin, and plasma kallikrein[3]. Furthermore, structural studies based on a co-crystal structure of EapH1 bound to NE have shown that EAPs inhibit NSPs by binding non-covalently across the catalytic cleft of NSPs, thereby obstructing access for substrates[3]. This mechanism, and the specificity for these three NSPs together, is unprecedented. However, the molecular details of this mechanism have not yet been fully elucidated. Here, we further explore the active sites of the EAPs and the range of serine proteases they can inhibit. This knowledge may help to improve the treatment of *S. aureus* infections, which is needed since the rise of antibiotic resistant strains. Furthermore, these studies provide additional information toward the design of new types of therapeutic protease inhibitors that may be useful in treating human inflammatory diseases.

RESULTS

Mutating contacts within a EapH1/NE co-crystal

Recently, we determined a co-crystal structure of EapH1 bound to NE (Fig. 1A)[3]. This structure highlighted two regions within EapH1 that mediate binding to NE: Val^{53}-Tyr^{63} (Site 1) and Ala^{86}-Gly^{90} (Site 2) (Fig. 1B-C). The most intimate contact seemed to be made by the middle part of Site 1 (Ile^{56}-Arg^{61}), as judged by its contribution to the buried surface area at the EapH1/NE interface. To prove that these residues are crucial for the interaction with NE, we mutated these residues to Ala in both EapH1 and EapH2, yielding H1Δ56-61 and H2Δ56-61 respectively. (For simplicity, we will use the numbering of EapH1 throughout.) In addition, we mutated either the first two or the last three of these residues in EapH1 to Ala (position 58 already is Ala), yielding H1Δ56-57 and H1Δ59-61 respectively (Fig. 1D-F). We measured the circular-dichroism (CD) spectra of all proteins to verify that the induced mutations did not cause complete loss of the tertiary structure. The pattern of the CD spectra of all mutants perfectly resembled that of their corresponding wild-type proteins, showing that all secondary structures were conserved (Fig. 1G-H). Then, we measured the activity of these mutant proteins in an NE activity assay using a fluorescent peptide substrate. Surprisingly, the IC_{50} values of H1Δ56-61 and H2Δ56-61 were comparable to the IC_{50} values of the wild-type proteins (Fig. 1I-J). Also partial mutations of this region did not affect the inhibitory activity (Fig. 1I). Thus, these data indicate that the side chains of residues 56-61 of EapH1 and EapH2 are likely not essential for NE inhibition. Future studies should be directed at mutating the complete Site 1 (Val^{53}-Tyr^{63}) and Site 2.

Two potentially important regions in EapH1 and EapH2

In parallel to the co-crystallography, we analyzed the primary sequences of EapH1 and EapH2 to determine which residues might be important for inhibiting NE. Taken into account that some residues will be conserved in order to preserve the beta-grasp fold, two regions were identified that might be important for function: $Arg^{89}Glu^{94}Lys^{95}$ and Lys^{119}-Ile^{128}. We mutated these residues of EapH1 into Ala, yielding the mutants H1Δ89,94-95 and H1Δ119-128(AA), respectively. Since mutating ten consecutive residues might severely affect protein folding, we also mutated the Lys^{119}-Ile^{128} loop to alternating Gly-Ser residues, yielding H1Δ119-128(GS) (Fig. 2A, *top*; Fig. 2B). In addition, we mutated the corresponding residues in EapH2 (Fig. 2A, *bottom*; Fig. 2C). Then we measured the CD spectra of all generated mutants. Unfortunately, mutants H1Δ119-128(AA), H1Δ119-128(GS), and H2Δ119-128(GS) differed from their corresponding wild-type protein, indicating that these mutants affected the secondary structures within the protein mutants (Fig. 2D-E). Subsequently, we measured the effect of these mutants on NE activity. The results from the protein mutants with deviating CD spectra should be interpreted with caution. Nevertheless, the correctly-folded mutants showed surprising results, since NE inhibition was differently affected by H1Δ89,94-95 compared to H2Δ89,94-95. Compared with EapH1-WT, the IC_{50} of H1Δ89,94-95 increased from 5.7 nM to over 1000 nM.

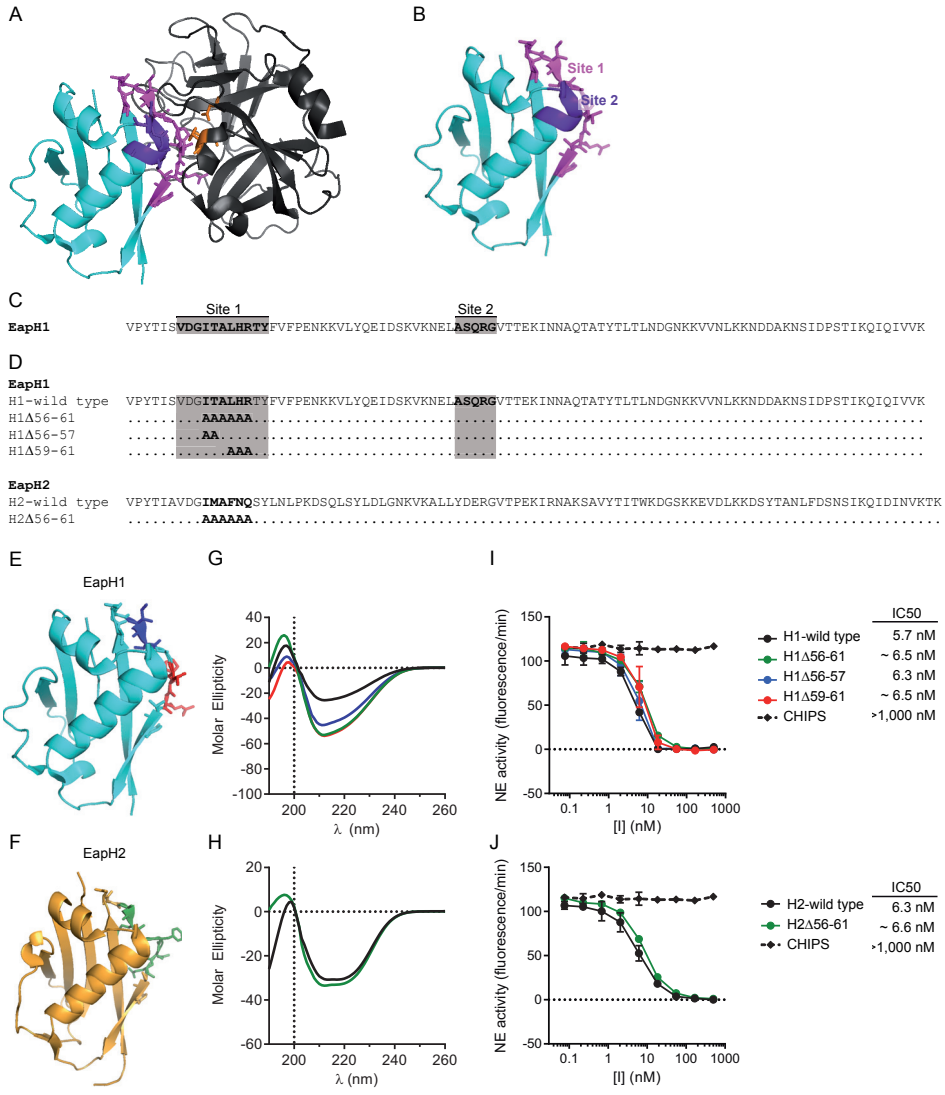

Figure 1. Mutations of co-crystal contacts. (A) Orientation of EapH1 (cyan; PDB code 1YN4), with Site 1 (magenta) and Site 2 (purple) highlighted, when bound to NE (black; PDB code 3Q76), with its catalytic triad (orange) highlighted, for reference. This orientation is modeled to the co-crystal structure of EapH1/NE (PDB code 4NZL)[3]. (B) Two different regions in the primary sequence of EapH1 (Site 1 and Site 2) come together to form the surface that interacts with NE. Site 1 (magenta) and Site 2 (purple) are highlighted. (C) Primary structure of EapH1, with the NE-interacting Site 1 and Site 2 highlighted in gray. (D) Schematic representation of protein mutants made in EapH1 and EapH2. "A" indicates that this residue has been mutated to Ala. "." indicates that this is the same residue as in the WT protein. Site 1 and Site 2 in EapH1 are highlighted in gray. (E-F) Crystal structure of EapH1 (cyan; PDB code 1YN4) (E) and EapH2 (yellow; PDB code 1YN5) (F), with mutated residues highlighted in blue, red, or green. Colors correspond to (I) and (J). (G-H) CD spectra of all generated mutants. The molar ellipticity under 200 λ was less-accurately determined. Colors correspond to (I) and (J). (I-J) Residual NE activity in presence of mutated EapH1 (I) or EapH2 (J). Calculated IC_{50} values are indicated on the right of the graphs.

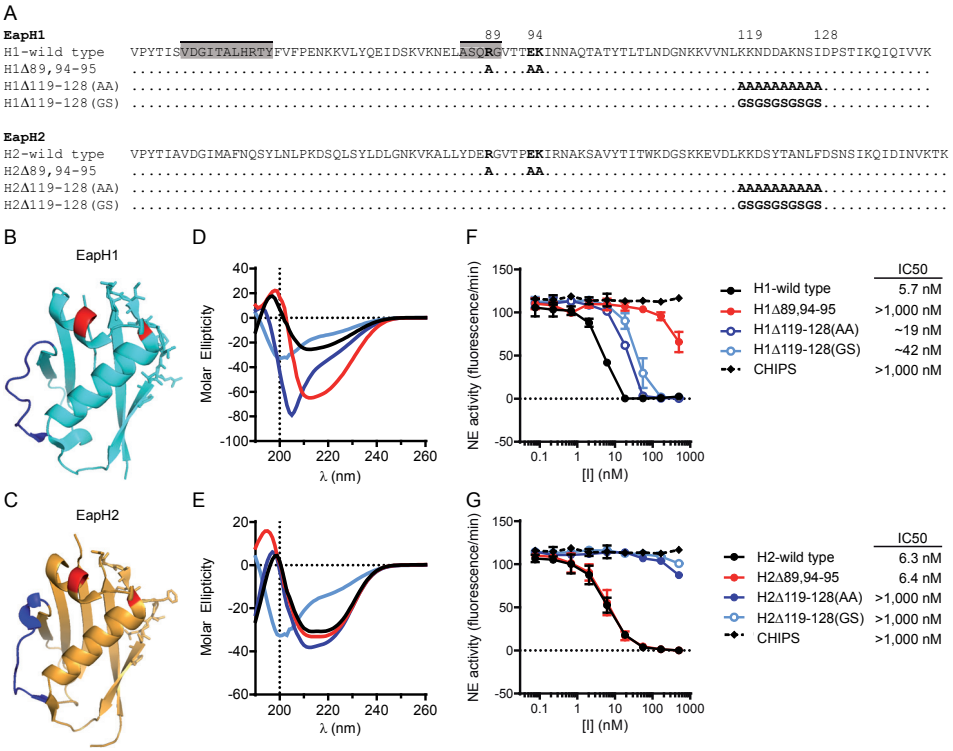

Figure 2. Two differentially important regions in EapH1 and EapH2. (A) Schematic representation of protein mutants made in EapH1 (*top*) and EapH2 (*bottom*). "A", "G", or "S" indicate to what residues the original residues have been changed; "." indicates that this is the same residue as in the WT protein. Site 1 and Site 2 in EapH1 are highlighted in gray. The numbers indicate the position of important residues. (B-C) Crystal structures of EapH1 (PDB code 1YN4) (B) and EapH2 (PBD code 1YN5) (C) with mutated residues in blue and red. Colors correspond to (F) and (G). (D-E) CD spectra of all generated mutants. The molar ellipticity under 200 λ was less-accurately determined. Colors correspond to (F) and (G). (F-G) Residual NE activity in presence of mutated EapH1 (F) or EapH2 (G). Filled symbols represent mutants of which the CD spectra corresponded to the spectrum of the wild-type protein. Clear symbols represent mutants with deviating CD spectra, based on (D) and (E). Calculated IC_{50} values are indicated on the right of the graphs.

Figure 3. SAV1937 as scaffold for active-site studies. (A) Model of Eap in solution, based on PDB code 1YN3 and the findings by Hammel *et al.*[24]. (B) Schematic overview of the EAPs (Eap, EapH1, and EapH2) and the homologous sequence (SAV1937) in the genome of *S. aureus*. (C) Predicted structure of SAV1937, generated with the SWISS-MODEL server, using the Eap-D2 crystal structure (1YN3) as template. (D) Alignment of the crystal structures of the EAPs (EapH1, PDB code 1YN3; EapH2, PDB code 1YN5; and Eap-D2, PDB code 1YN3) and the predicted structure of SAV1937. Colors are inset (*left*). EapH1, with Site 1 and Site 2 highlighted as in Fig. 1 for reference (*right*). (E) Residual NE activity in presence of EapH1, or SAV1937. (F) Alignment of the primary structure of the EAPs (EapH1, EapH2, and individual domains of Eap (D1, D2, D3, and D4)) with SAV1937. Site 1 and Site 2 in EapH1 are highlighted in gray. "EAPs" summarizes the similarity of residues amongst the EAPs and "All" summarizes the similarity of residues amongst all aligned proteins. (*) fully identical residues, (:) residues with strongly similar properties, (.) residues with weakly similar properties (as defined on the ClustalOmega server). Residues possibly important for NE inhibition are indicated in red. The numbers indicate the position of interesting residues.

However, compared with WT-EapH2, the IC_{50} of H2Δ89,94-95 barely increased (from 6.3 nM to 6.4 nM) (Fig. 2F-G, *red lines*). The results for the EapH1 mutant are coherent with the co-crystal structure, since the mutated residues partially overlap with Site 2. However, the results of H2Δ89,94-95 imply that this region is not required for inhibition by EapH2. Moreover, the IC_{50} of H2Δ119-128(AA) increased from 6.3 nM to over 1000 nM, compared to EapH2-WT (Fig. 2G, *dark blue line*). This implies that the Lys^{119}-Ile^{128} loop is important for NE inhibition by EapH2, even though in the EapH1/NE co-crystal structure this loop was positioned opposite of the EapH1/NE interface. All together, these results suggest that EapH1 and EapH2 employ two different mechanisms to inhibit NE, where inhibition would be mediated by $Arg^{89}Glu^{94}Lys^{95}$ in EapH1, and by Lys^{119}-Ile^{128} in EapH2.

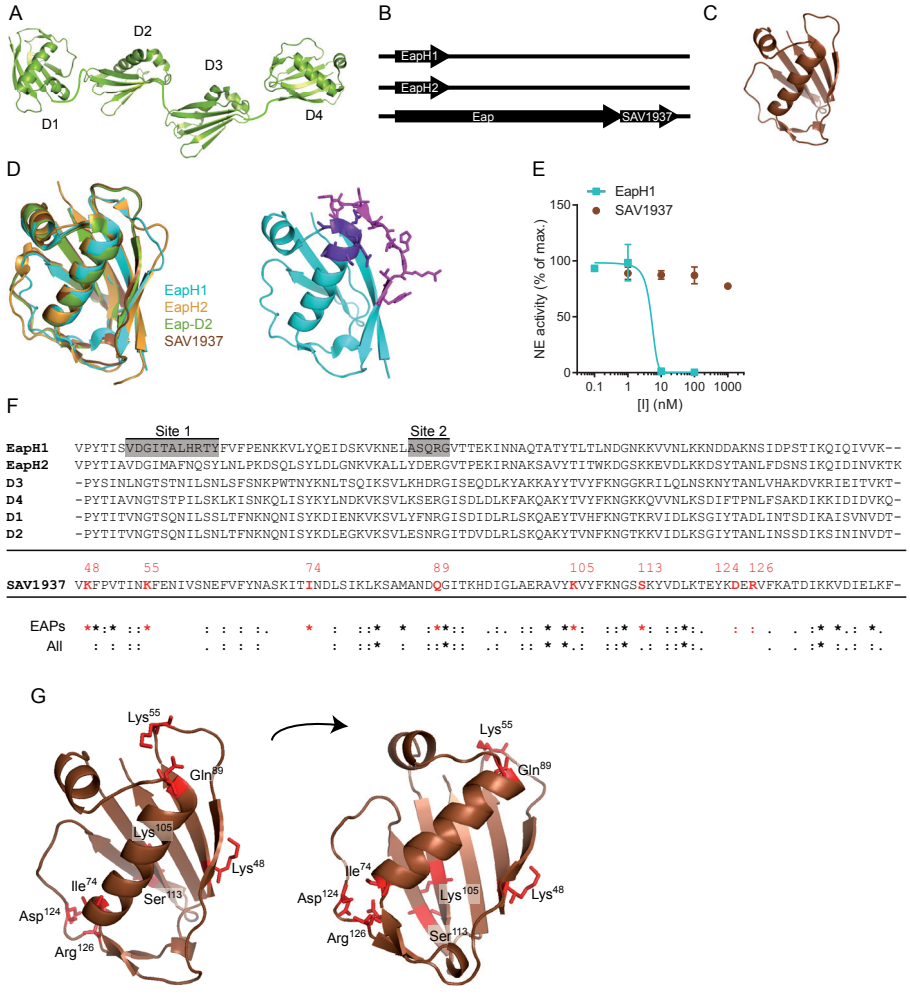

(Figure 3. *continued*) (G) Overview of the position of the highlighted residues in (F) within the predicted structure of SAV1937. The model is depicted in the same orientation as in (D) (*left*), and slightly tilted to better visualize all interesting residues (*right*).

SAV1937 as scaffold for active-site studies

Whereas EapH1 and EapH2 are single-domain proteins, Eap consists of multiple EAP domains, attached to each other via a flexible peptide (Fig. 3A). The individual domains of Eap show about 55% sequence homology amongst each other, and are all potent NSP inhibitors on their own[3]. EapH1 and EapH2 are on average 30% and 40% homologous to these domains, respectively. In addition to these three EAPs, *S. aureus* encodes another homologous DNA sequence directly downstream of Eap (SAV1937, 12 kDa) (Fig. 3B). These nucleotides might be part of the larger Eap protein[4]. They are unlikely to encode for a fourth individual protein, since they do not encode a signal peptide, which is encoded by the other EAPs. SAV1937 is on average 30% homologous to the domains within Eap, corresponding to the level of homology seen for EapH1. Using the SWISS-MODEL server, SAV1937 was predicted to fold as an EAP domain (Fig. 3C), where the crystal structure of domain 2 of Eap (Eap-D2) served as the scaffold to model the folding of SAV1937 on. A structural overlay of the empirically-determined structures of EapH1, EapH2, and Eap-D2 and the predicted structure of SAV1937 showed the striking level of similarity between the folding of these proteins (Fig. 3D). We recombinantly expressed and purified SAV1937 in order to gain insight into its potential function. To our surprise, it did not inhibit NE and other tested NSPs (Fig. 3E), not even at high concentrations. This indicated that we could use this protein to further analyze potential important NSP inhibitory residues in EAPs. We compared the amino-acid sequence of SAV1937 with the sequences of the six EAP domains that inhibit NE (i.e. Eap-D1, Eap-D2, Eap-D3, Eap-D4, EapH1, EapH2). We hypothesized that residues similar within the six EAP domains, but deviating in SAV1937, might contribute to NSP inhibition. Eight residues matched these criteria (Fig. 3F). They are dispersed in the primary structure, but some group together in the tertiary structure. Most notable are residues Lys^{55} and Gln^{89} that lie within Site 1 and Site 2, indicated to be important for contact with NE by the co-crystal structure. In addition, Ile^{74}, $Asp^{124}$and Arg^{126} seem to come together in the tertiary structure. The latter two residues belong to the loop Lys^{119}-Ile^{128}, which seemed important for activity of EapH2 (as judged from the results with the H2Δ119-128(AA) mutant). The absolute importance of these residues for NE inhibition is still to be determined empirically, which is now possible by swapping residues from EapH1 with SAV1937 and vice versa.

Exploring therapeutic inhibitors deducted from EAPs

The mechanism by which the EAP family inhibits NSPs might be translated into the clinic by developing therapeutic NSP inhibitors. Due to high levels of antibodies against all staphylococcal evasion proteins in human serum, EAPs are likely too immunogenic to be used directly as therapeutics. One approach to circumvent this problem is to identify a minimal inhibitory sequence within EAPs that retains NSP inhibitory properties. Therefore, we generated a set of peptides that mimic the active sites deduced from the co-crystal structure (Fig. 4A-B) and measured their capacity to inhibit NE activity. The first set of peptides represents Site 1 in EapH1 (i.e. GITALHRTY) and in EapH2 (i.e. GIMAFNQSY). While the EapH1-derived sequence had no detectable activity (its IC_{50}

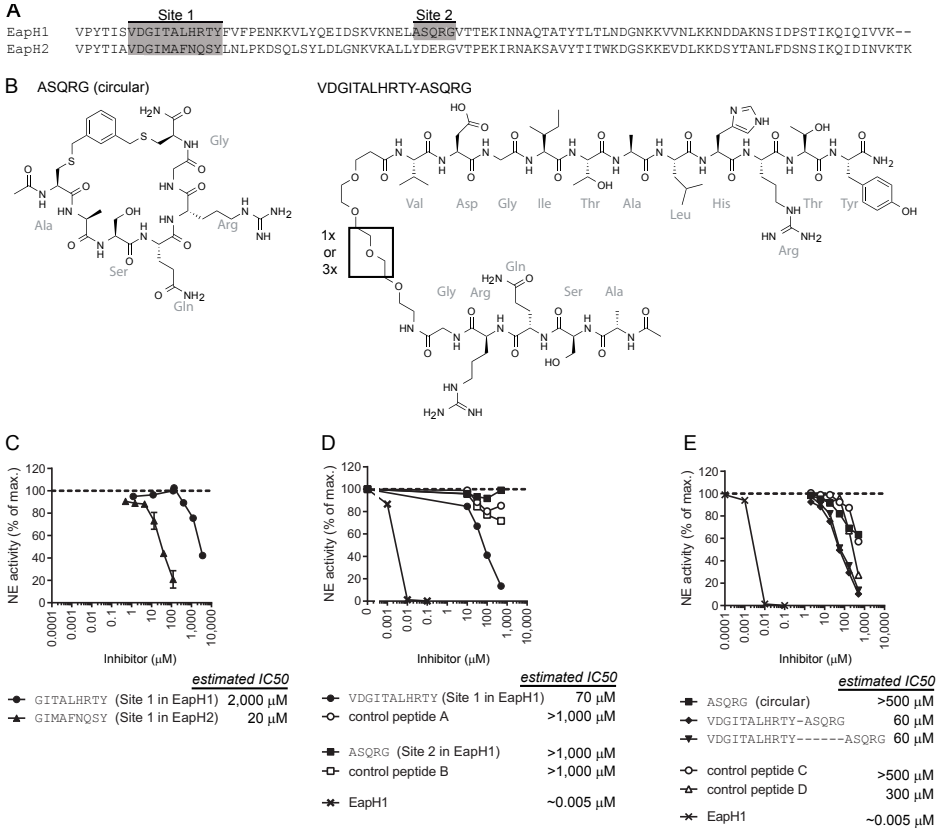

Figure 4. Peptides based on the co-crystal structure of EapH1/NE. (A) Position of the generated peptides within EapH1 and EapH2, corresponding to Site 1 and Site 2. (B) Chemical structures of the circularized peptide of Site 2 in EapH1 (*left*). Chemical structure of the linked peptides of Site 1 and Site 2 in EapH1 (*right*). (C-E) Residual NE activity upon incubation of NE with the generated peptides. (C) Peptides based on Site 1 within EapH1 and EapH2. (D) Peptides based on Site 1 (extended) and Site 2 within EapH1. (E) Modified peptides based on Site 1 and Site 2, as depicted in (B). Estimated IC_{50} values are indicated on the right of the legends. Control peptides consist of different residues, but are matched to the other peptides based on size. EapH1 protein was included for reference of optimal inhibition.

was at least 10^5-fold higher than that of EapH1), the peptide from EapH2 seemed to inhibit NE, albeit at IC_{50} values more than 10^3 fold higher than intact EapH1 (Fig. 4C). In a second approach, we extended the length of the peptide from EapH1 by two residues (i.e. to VDGITALHRTY) and synthesized a peptide deducted from active Site 2 (i.e. ASQRG). The extended peptide based on Site 1 had an increased activity of about 30 fold (IC_{50} of 70 μM), but still was not much more potent than the control peptides, while the peptide based on Site 2 did not inhibit NE at all (IC_{50} > 1000 μM) (Fig. 4D). Neither did these peptides have a synergistic effect, since equimolar addition of both peptides together did not increase the potency of the Site-1-peptide alone (data not shown). Since both sites adopt a three-dimensional structure whilst in the context of EapH1, a third set of peptides was produced that had a more rigid structure. These included a circularized

peptide of Site 2, and both peptides coupled to each other via a variable linker (both short and long) (Fig. 4B). Unfortunately, neither approach decreased the IC_{50} values compared to the IC_{50} values of the corresponding linear peptides (Fig. 4E). Even though the co-crystal provided insights into the mechanism of inhibition, these peptides cannot yet confirm that finding. Most likely, the three-dimensional orientation of these peptides differs from their structure within the EapH1 protein. This emphasizes the need to first conduct additional site-directed mutagenesis studies to decipher the required spatial orientation more precisely.

Specificity of EAPs extends to mast-cell chymase

Previous studies have established that all EAPs inhibit the NSPs NE, PR3, and CG. The related serine proteases thrombin, plasmin, and plasma kallikrein were not inhibited by EAPs[3]. In order to more precisely analyze the specificity of the EAPs, we examined the phylogeny of all human members from the MEROPS S1A class of chymotrypsin-like proteases[5], based on the amino-acid sequence of their protease domain (Fig. S1). To increase clarity, a phylogenetic tree including only important immune proteases was also generated (Fig. 5A). In this phylogenetic tree two NSPs (NE, PR3) are closely related, whereas the two others (CG, NSP4) are more distantly related. The non-neutrophil proteases that cluster most closely to the classical NSPs are mast cell chymase and the family of granzymes (Fig. 5A). We tested the effect of EAPs on two of the interesting proteases:

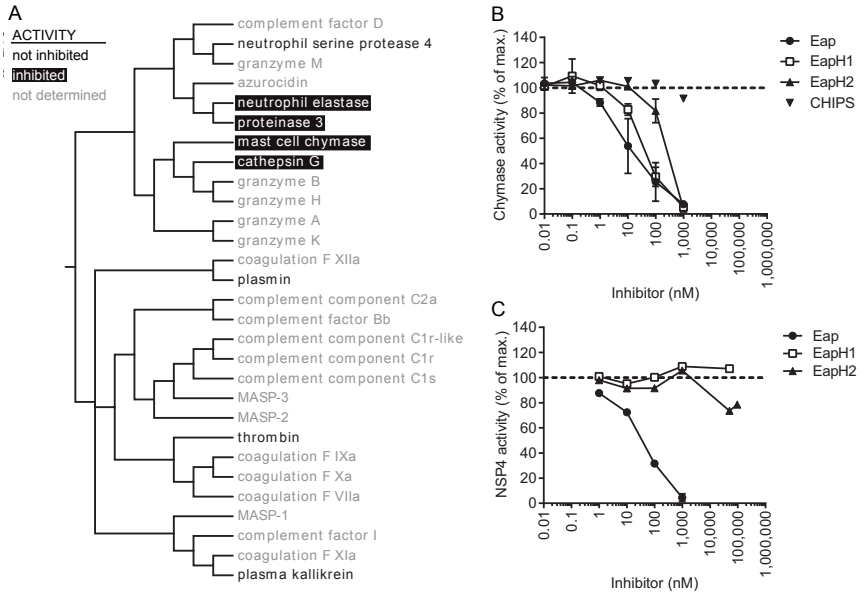

Figure 5. Specificity of EAPs extends to mast-cell chymase. (A) Phylogenetic tree of the human immune proteases of the MEROPS class of serine proteases (S1A), based on the sequence of their protease domains. Color coding: proteases that are inhibited by all EAPs; **proteases** that are not inhibited by all EAPs; proteases of which the activity has not been determined. (B) Residual activity of mast-cell chymase upon incubation with EAPs, and the non-inhibiting CHIPS. (C) Residual activity of NSP4 upon incubation with EAPs.

NSP4 and mast-cell chymase. Mast-cell chymase was inhibited by all three EAPs (Fig. 5B), and the potency of its inhibition was comparable to the inhibition of CG[3]. On the other hand, NSP4 was only inhibited by Eap, and not by EapH1 or EapH2 (Fig. 5C). This is the first serine protease known to be inhibited by only a subset of EAPs. The reason for the observed difference amongst the EAPs might be the slightly different amino acid sequence of the individual domains of Eap compared to EapH1 and EapH2 (only maximal 40% conserved), or by a mechanism in which two domains collaborate to inhibit NSP4. In any case, for both chymase and NSP4 the inhibition pattern nicely reflects the distances in the phylogenetic tree.

DISCUSSION

In this paper we analyzed the molecular mechanism of NE inhibition by EapH1 and EapH2. A co-crystal structure of EapH1 bound to NE indicated some important residues. Mutating a part of these interacting residues did not significantly decrease the inhibitory potency of the EAPs. This suggests that probably all interacting residues are required to inhibit NE. Future mutagenesis studies will be performed to validate this. Since EapH1 and EapH2 have highly similar tertiary structures, we expected them to adopt similar orientations towards NE during inhibition. Interestingly, results of another set of protein mutants suggest that EapH1 and EapH2 employ different mechanisms to inhibit NE: whereas mutating $Arg^{89}Glu^{94}Lys^{95}$ affected the activity of EapH1, mutating the loop Lys^{119}-Ile^{128} affected activity of EapH2. Seen in the light of the co-crystal structure, $Arg^{89}Glu^{94}Lys^{95}$ partly forms active Site 2, which could indeed account for the loss of inhibition by EapH1. However, Lys^{119}-Ile^{128} is positioned on the opposite site of EapH1 in the co-crystal structure, making it unlikely to affect EapH1 activity. Nevertheless, this loop appeared important in the activity of EapH2. It is clear that further studies are required to disclose whether EapH1 and EapH2 indeed bind their NSP targets in different orientations. In addition, since the EAPs seem to employ different mechanism to inhibit NE, we should also consider the possibility that different mechanisms apply to the individual NSPs. Answering both questions could now be facilitated by exchanging residues between the non-inhibiting SAV1937 and EapH1 or EapH2. Only by elucidating the mechanism of inhibition, molecules could be developed to disrupt the binding of EAPs to NSPs. This might ultimately lead to therapies for *S. aureus* infection in which EAPs no longer inhibit NSP, leaving the host immune system better equipped to clear the infection.

In order to develop clinical NSP inhibitors based on the non-covalent EAP / NSP interaction, knowledge about the minimal inhibitory sequence necessary to recapitulate this mechanism is needed. Furthermore, to diminish side effects, a full understanding of the range of inhibited proteases is required. In this paper we showed that, in addition to NE, PR3, and CG, also mast-cell chymase is inhibited by EAPs. Whereas these proteases are named after the cell type in which they are primarily expressed (i.e. neutrophils or mast cells), the proteases themselves are very similar in terms of both their primary and tertiary

structures. Moreover, chymase is encoded by the same gene cluster as CG on chromosome 14. Since this gene cluster also encodes granzymes B and H, which are structurally related to the NSPs and chymase, these proteases might also be inhibited by the EAPs.

Whether *S. aureus* would benefit from inhibiting mast-cell chymase or granzymes is unclear. In general, the role of mast cells during *S. aureus* infection is still debated. *In vitro*, mast-cell extracellular traps (MCETs) entrap *S. aureus*[6]. *In vivo*, mast cells are invaded by *S. aureus* to promote secondary infections[6]. However, another recent study described that although *S. aureus* influences gene expression in mast cells, mice lacking mast cells did not increasingly suffer from *S. aureus*[7]. Therefore, also the importance of mast-cell chymase in *S. aureus* infection is unclear. In addition, granzymes are classically known for their joint effort with perforin to induce apoptosis in virus-infected cells[8]. Lately, evidence accumulates that extracellular granzymes might contribute to immunity by other means, like degrading extracellular matrix proteins to promote immune-cell migration[9]. Moreover, elevated levels of extracellular granzymes were measured during Gram-negative sepsis, hinting towards a role during antibacterial defenses[10]. However, the mechanisms have not yet been identified.

On the contrary, NSP4 was only inhibited by Eap and not by EapH1 or EapH2. If this would be caused by the differences in primary structure of the domains within Eap compared to EapH1 or EapH2, recombinant forms of the single domains from Eap should also inhibit NSP4. If not, two domains within Eap might collaborate to inhibit NSP4, in which one could bind NSP4 so that the second could inhibit NSP4. The discrepancy between inhibition of NSP4 and inhibition of the other NSPs is reflected in the differences of their catalytic site regarding three-dimensional properties[11]. Since the co-crystal structure showed that EapH1 inhibits NE by binding in front of the catalytic cleft, the differences in the catalytic site could cause the different susceptibility to inhibitors. This, together with the relatively large differences in their primary structures as reflected in the phylogenetic tree, makes it plausible that NSP4 is not as potently inhibited by the EAPs as the other NSPs. The finding that NSP4 is less-potently inhibited by EAPs might suggest that it is not crucial in host defense against *S. aureus*.

Altogether, this study provides initial clues into the molecular mechanism by which EAPs inhibit NSPs. It brought about the first suggestions that the functionally and structurally-related proteins EapH1 and EapH2 exhibit different mechanism to achieve their inhibition of NSPs. If so, activity of the other NSPs should definitely be examined too with the various protein mutants to determine whether we righteously used NE as a model for all NSPs. Although this study provides the basis, many avenues still have to be explored to ultimately turn these EAPs into therapies against staphylococcal infections or inflammatory diseases characterized by excessive NSP activity.

ACKNOWLEDGEMENTS

We thank Professor Dieter Jenne for kindly providing NSP4 and it substrate. This work was supported by a Vidi grant from the Netherlands Organization for Scientific Research (to SHMR), and US National Institutes of Health Grant AI071028 (to BVG).

MATERIAL AND METHODS

Constructing EapH1 and EapH2 mutants

The expression vector encoding wild-type EapH1 and EapH2 served as basis for the mutant proteins. Mutations were introduced by overhang-extension PCRs and standard cloning techniques as described before[12]. Introduced mutations were confirmed by sequencing. All EAPs (wild-type and mutants) were expressed with a His-tag as described before[3].

Measuring CD spectra

Samples of purified proteins in PBS (pH 7.4) were passed through a 0.45 µm filter prior to analysis, and diluted to a final concentration where OD_{280nm} was in a linear range (OD_{280} of 0.37 for EapH1, and OD_{280} of 0.40 for EapH2). CD-spectra (260-190 nm) were measured in scanning mode using a Jasco J-815 spectropolarimeter, using a 1 nm bandwidth at a speed of 50 nm/min for a total of 5 replicates. Spectra were averaged prior to mathematical smoothing, using software provided by the manufacturer. Since the spectra were not run on degassed samples, nor under a vacuum, the data of $\lambda < 200$ nm should be considered unreliable.

Constructing peptides

The first set of peptides (Fig. 4C) was ordered at GenScript (NJ, USA) with >95% purity. The peptide from EapH1 (GITALHRTY) was dissolved in double-distilled water (ddH_2O). The peptide from EapH2 (GIMAFNQSY) unfortunately had to be dissolved in the presence of dimethylforamide (DMF). Neat DMF was added dropwise to the peptide in ddH_2O until the solution clarified. The final concentration was ~50% DMF in ddH_2O. Activity of NE in presence of the latter peptide was calculated relatively to the activity of NE without peptide in the corresponding concentration DMF.

The second set of peptides (Fig. 4D) was assembled by solid-phase peptide synthesis on a CS336X peptide synthesizer (CS Bio Company Inc.) using the manufacturer's protocols employing Fmoc-amino acid derivatives. As a coupling reagent a 1:1 mixture of HBTU/HOBt was used. The third set of peptides (Fig. 4E) was assembled in the same manner, but with C-terminal and N-terminal cysteine residues. For these peptides TFA/H_2O/TIS/EDT (90:5:2.5:2.5, v/v/v/v) was used as coupling reagent. The ASQRG-peptide was cyclized using 1,3-Bis(bromomethylene)benzene. The VDGITALHRTY and ASQRG peptides were linked together using oligo-ethylene-glycol linkers of different lengths. After completion of their synthesis, all five peptides were cleaved from the polystyrene Rink Amide AM resin and simultaneously deprotected using a mixture of TFA/TIS/H_2O (95:2.5:2.5, v/v/v). The peptide constructs were purified on a Phenomenex Gemini C18 column (110 Å, 10 µm, 250×22 mm) using an Angilent 1260 infinity preparative HPLC. Purity was established using a Shimadzu analytical HPLC (UV-detector operating at 214 and 254 nm) equipped with a Phenomenex Gemini C18 column (110 Å, 5 µm, 250×4.60 mm) column and was >95%. ESI-MS on a Shimadzu 2010EV apparatus was used for characterization. All these peptides were dissolved in ddH_2O.

The sequences of the used control peptides were: FTFEPFPTNEE (control peptide A), FTFEP (control peptide B), FTFEPFPTNEEIESNK (control peptide C), and FTFEPFPTNEEIESNKKM (control peptide D). These peptides were generated as described before[13].

Modeling overlays

Protein crystal structures were visualized in PyMOL (DeLano Scientific LLC). The structure prediction of SAV1937 was carried out in SWISS-MODEL[14–16]. Sequence alignments were obtained by Clustal Omega[17–19].

Phylogenetic tree

Human serine proteases from the S1A clade of proteases were selected from the MEROPS database[5]. The

proteins were aligned by sequence using Clustal Omega to determine the protease domains (based on the sequence of NE, from Ile[30] to end). The phylogenetic tree of serine proteases was build using these protease-domain sequences in Clustal Omega[20–22] and visualized using Evolview[23].

NE activity

To determine NE inhibition by proteins, NE activity was measured in a total volume of 100 µl Dulbecco's phosphate-buffered saline (PBS) with 0.05% Igepal-CA63 (Sigma). Final concentrations were 5 nM NE (Elastin products company; EPC), indicated concentrations of Eap proteins, and 50 µM substrate (AAPV-AMC, Sigma). The inhibitory capacity of peptides was assessed in the same assay, but the final buffer was 0.5 x PBS with 0.05% Igepal-Ca63. Control peptides were included to estimate the random effect of adding peptides to the NE activity assay. These were as closely matched in size to the tested peptides as possible. Fluorescence was measured in a FluoStar Omega with excitation at 360 nm and emission at 460 nm. IC_{50} values were calculated in GraphPad Prism 6.0 by plotting a curve-fit model with restrictions to maximum (100%) and minimum (0%). The IC_{50} values for the peptides were estimated, since too little data was available for proper calculations.

Chymase activity

Activity of indicated concentrations EAPs was tested as described for NE, with final concentrations of 6.3 nM chymase (Sigma-Aldrich) and 500 µM substrate (AAPF-AMC, Genecust, Luxembourg).

NSP4 activity

NSP4 and its substrate were a kind gift of professor Dieter Jenne. Activity of indicated concentrations of EAPs was tested in 100 µl, with final concentrations of 10 nM NSP4, and 5 µM substrate (Mca-GIKPRSRP-Lys(Dnp)-rr (r = D-Arg)). Assay buffer was Tris-buffered saline (TBS; 20 mM Tris with 150 mM NaCl, pH7.5) with 0.05 % Igepal-Ca63, or PBS with 0.05 % Igepal-Ca63. Fluorescence was measured in a FluoStar Omega with excitation at 320 nm and emission at 420 nm.

REFERENCES

1. Bardoel BW, Kenny EF, Sollberger G, Zychlinsky A: The Balancing Act of Neutrophils. *Cell Host Microbe* 2014, 15:526–536.
2. Korkmaz B, Horwitz MS, Jenne DE, Gauthier F: Neutrophil Elastase, Proteinase 3, and Cathepsin G as Therapeutic Targets in Human Diseases. *Pharmacol. Rev.* 2010, 62:726–759.
3. Stapels DAC, Ramyar KX, Bischoff M, von Köckritz-Blickwede M, Milder FJ, Ruyken M, Eisenbeis J, McWhorter WJ, Herrmann M, van Kessel KPM, et al.: Staphylococcus aureus secretes a unique class of neutrophil serine protease inhibitors. *Proc. Natl. Acad. Sci. U. S. A.* 2014, 111:13187–13192.
4. Buckling A, Neilson J, Lindsay J, Enright M, Day N, Massey RC: Clonal Distribution and Phase-Variable Expression of a Major Histocompatibility Complex Analogue Protein in Staphylococcus aureus. *J. Bacteriol.* 2005, 187:2917–2919.
5. Rawlings ND, Barrett AJ, Bateman A: MEROPS: the database of proteolytic enzymes, their substrates and inhibitors. *Nucleic Acids Res.* 2012, 40:D343–350.
6. Abel J, Goldmann O, Ziegler C, Höltje C, Smeltzer MS, Cheung AL, Bruhn D, Rohde M, Medina E: Staphylococcus aureus evades the extracellular antimicrobial activity of mast cells by promoting its own uptake. *J. Innate Immun.* 2011, 3:495–507.
7. Rönnberg E, Johnzon C-F, Calounova G, Garcia Faroldi G, Grujic M, Hartmann K, Roers A, Guss B, Lundequist A, Pejler G: Mast cells are activated by Staphylococcus aureus in vitro but do not influence the outcome of intraperitoneal S. aureus infection in vivo. *Immunology* 2014, 143:155–163.
8. Buzza MS, Bird PI: Extracellular granzymes: current perspectives. *J. Biol. Chem.* 2006, 387:827–837.
9. Buzza MS, Zamurs L, Sun J, Bird CH, Smith a I, Trapani JA, Froelich CJ, Nice EC, Bird PI: Extracellular matrix remodeling by human granzyme B via cleavage of vitronectin, fibronectin, and laminin. *J. Biol. Chem.* 2005, 280:23549–23558.
10. Lauw FN, Simpson A, Hack CE, Prins JM, Wolbink AM, van Deventer SJ, Chaowagul W, White NJ, van Der Poll T: Soluble granzymes are released during human endotoxemia and in patients with severe infection due to Gram-negative bacteria. *J. Infect. Dis.* 2000, 182:206–213.
11. Lin SJ, Dong KC, Eigenbrot C, van Lookeren Campagne M, Kirchhofer D: Structures of neutrophil serine

protease 4 reveal an unusual mechanism of substrate recognition by a trypsin-fold protease. *Structure* 2014, 22:1333–1340.
12. Rooijakkers SHM, Milder FJ, Bardoel BW, Ruyken M, van Strijp JAG, Gros P: Staphylococcal complement inhibitor: structure and active sites *J. Immunol.* 2007, 179:985–994.
13. Haas P, Haas CJC De, Kleibeuker W, Poppelier MJJG, van Kessel KPM, John AW, Liskamp RMJ, van Strijp JAG: N-terminal residues of the Chemotaxis Inhibitory Protein of Staphylococcus aureus are essential for blocking Formylated Peptide Receptor but not C5a Receptor. *J. Immunol.* 2004, 173:5704–5711.
14. Bordoli L, Kiefer F, Arnold K, Benkert P, Battey J, Schwede T: Protein structure homology modeling using SWISS-MODEL workspace. *Nat. Protoc.* 2009, 4:1–13.
15. Arnold K, Bordoli L, Kopp J, Schwede T: The SWISS-MODEL workspace: a web-based environment for protein structure homology modelling. *Bioinformatics* 2006, 22:195–201.
16. Biasini M, Bienert S, Waterhouse A, Arnold K, Studer G, Schmidt T, Kiefer F, Cassarino TG, Bertoni M, Bordoli L, et al.: SWISS-MODEL: modelling protein tertiary and quaternary structure using evolutionary information. *Nucleic Acids Res.* 2014, 42:W252–258.
17. McWilliam H, Li W, Uludag M, Squizzato S, Park YM, Buso N, Cowley AP, Lopez R: Analysis Tool Web Services from the EMBL-EBI. *Nucleic Acids Res.* 2013, 41:W597–600.
18. Goujon M, McWilliam H, Li W, Valentin F, Squizzato S, Paern J, Lopez R: A new bioinformatics analysis tools framework at EMBL-EBI. *Nucleic Acids Res.* 2010, 38:W695–699.
19. Sievers F, Wilm A, Dineen D, Gibson TJ, Karplus K, Li W, Lopez R, McWilliam H, Remmert M, Söding J, et al.: Fast, scalable generation of high-quality protein multiple sequence alignments using Clustal Omega. *Mol. Syst. Biol.* 2011, 7. doi:01.1038/msb.2011.75.
20. Larkin MA, Blackshields G, Brown NP, Chenna R, McGettigan PA, McWilliam H, Valentin F, Wallace IM, Wilm A, Lopez R, et al.: Clustal W and Clustal X version 2.0. *Bioinformatics* 2007, 23:2947–2948.
21. Saitou N, Nei M: The Neighbor-joining Method: A New Method for Reconstructing Phylogenetic Trees. *Mol. Biol. Evol.* 1987, 4:406–425.
22. Kimura M: A simple method for estimating evolutionary rates of base substitutions through comparative studies of nucleotide sequences. *J. Mol. Evol.* 1980, 16:111–120.
23. Zhang H, Gao S, Lercher MJ, Hu S, Chen W-H: EvolView, an online tool for visualizing, annotating and managing phylogenetic trees. *Nucleic Acids Res.* 2012, 40:W569–572.
24. Hammel M, Nemecek D, Keightley JA, Thomas GJJ, Geisbrecht BV: The Staphylococcus aureus extracellular adherence protein (Eap) adopts an elongated but structured conformation in solution. *Protein Sci.* 2007, 16:2605–2617.

SUPPLEMENTAL INFORMATION

(see next page)

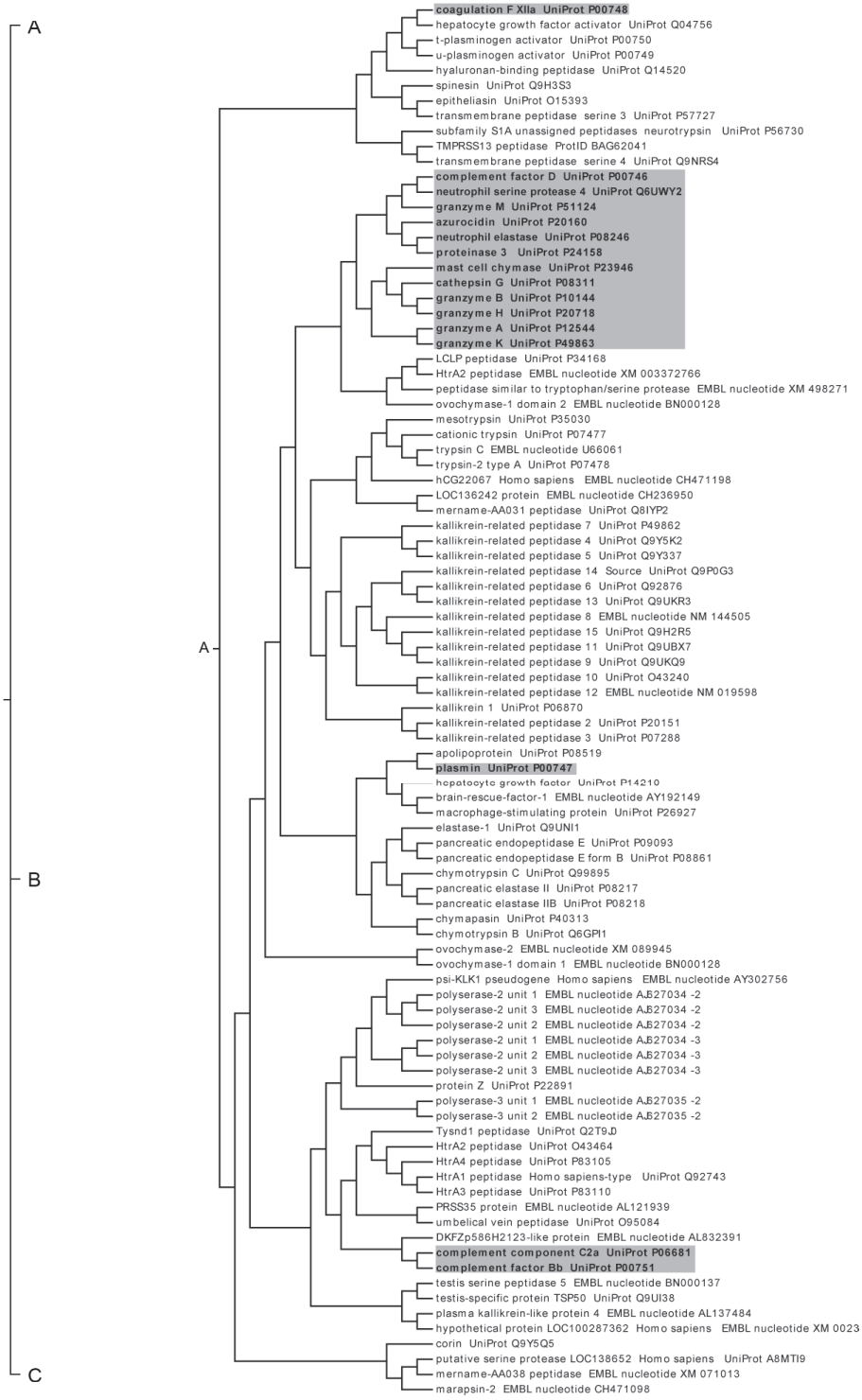
A
B
C
A
coagulation F XIIa UniProt P00748
hepatocyte growth factor activator UniProt Q04756
t-plasminogen activator UniProt P00750
u-plasminogen activator UniProt P00749
hyaluronan-binding peptidase UniProt Q14520
spinesin UniProt Q9H3S3
epitheliasin UniProt O15393
transmembrane peptidase serine 3 UniProt P57727
subfamily S1A unassigned peptidases neurotrypsin UniProt P56730
TMPRSS13 peptidase ProtID BAG62041
transmembrane peptidase serine 4 UniProt Q9NRS4
complement factor D UniProt P00746
neutrophil serine protease 4 UniProt Q6UWY2
granzyme M UniProt P51124
azurocidin UniProt P20160
neutrophil elastase UniProt P08246
proteinase 3 UniProt P24158
mast cell chymase UniProt P23946
cathepsin G UniProt P08311
granzyme B UniProt P10144
granzyme H UniProt P20718
granzyme A UniProt P12544
granzyme K UniProt P49863
LCLP peptidase UniProt P34168
HtrA2 peptidase EMBL nucleotide XM 003372766
peptidase similar to tryptophan/serine protease EMBL nucleotide XM 498271
ovochymase-1 domain 2 EMBL nucleotide BN000128
mesotrypsin UniProt P35030
cationic trypsin UniProt P07477
trypsin C EMBL nucleotide U66061
trypsin-2 type A UniProt P07478
hCG22067 Homo sapiens EMBL nucleotide CH471198
LOC136242 protein EMBL nucleotide CH236950
mername-AA031 peptidase UniProt Q8IYP2
kallikrein-related peptidase 7 UniProt P49862
kallikrein-related peptidase 4 UniProt Q9Y5K2
kallikrein-related peptidase 5 UniProt Q9Y337
kallikrein-related peptidase 14 Source UniProt Q9P0G3
kallikrein-related peptidase 6 UniProt Q92876
kallikrein-related peptidase 13 UniProt Q9UKR3
kallikrein-related peptidase 8 EMBL nucleotide NM 144505
kallikrein-related peptidase 15 UniProt Q9H2R5
kallikrein-related peptidase 11 UniProt Q9UBX7
kallikrein-related peptidase 9 UniProt Q9UKQ9
kallikrein-related peptidase 10 UniProt O43240
kallikrein-related peptidase 12 EMBL nucleotide NM 019598
kallikrein 1 UniProt P06870
kallikrein-related peptidase 2 UniProt P20151
kallikrein-related peptidase 3 UniProt P07288
apolipoprotein UniProt P08519
plasmin UniProt P00747
hepatocyte growth factor UniProt P14210
brain-rescue-factor-1 EMBL nucleotide AY192149
macrophage-stimulating protein UniProt P26927
elastase-1 UniProt Q9UNI1
pancreatic endopeptidase E UniProt P09093
pancreatic endopeptidase E form B UniProt P08861
chymotrypsin C UniProt Q99895
pancreatic elastase II UniProt P08217
pancreatic elastase IIB UniProt P08218
chymapasin UniProt P40313
chymotrypsin B UniProt Q6GPI1
ovochymase-2 EMBL nucleotide XM 089945
ovochymase-1 domain 1 EMBL nucleotide BN000128
psi-KLK1 pseudogene Homo sapiens EMBL nucleotide AY302756
polyserase-2 unit 1 EMBL nucleotide AJ527034 -2
polyserase-2 unit 3 EMBL nucleotide AJ527034 -2
polyserase-2 unit 2 EMBL nucleotide AJ527034 -2
polyserase-2 unit 1 EMBL nucleotide AJ527034 -3
polyserase-2 unit 2 EMBL nucleotide AJ527034 -3
polyserase-2 unit 3 EMBL nucleotide AJ527034 -3
protein Z UniProt P22891
polyserase-3 unit 1 EMBL nucleotide AJ527035 -2
polyserase-3 unit 2 EMBL nucleotide AJ527035 -2
Tysnd1 peptidase UniProt Q2T9J0
HtrA2 peptidase UniProt O43464
HtrA4 peptidase UniProt P83105
HtrA1 peptidase Homo sapiens-type UniProt Q92743
HtrA3 peptidase UniProt P83110
PRSS35 protein EMBL nucleotide AL121939
umbelical vein peptidase UniProt O95084
DKFZp586H2123-like protein EMBL nucleotide AL832391
complement component C2a UniProt P06681
complement factor Bb UniProt P00751
testis serine peptidase 5 EMBL nucleotide BN000137
testis-specific protein TSP50 UniProt Q9UI38
plasma kallikrein-like protein 4 EMBL nucleotide AL137484
hypothetical protein LOC100287362 Homo sapiens EMBL nucleotide XM 0023
corin UniProt Q9Y5Q5
putative serine protease LOC138652 Homo sapiens UniProt A8MTI9
mername-AA038 peptidase EMBL nucleotide XM 071013
marapsin-2 EMBL nucleotide CH471098

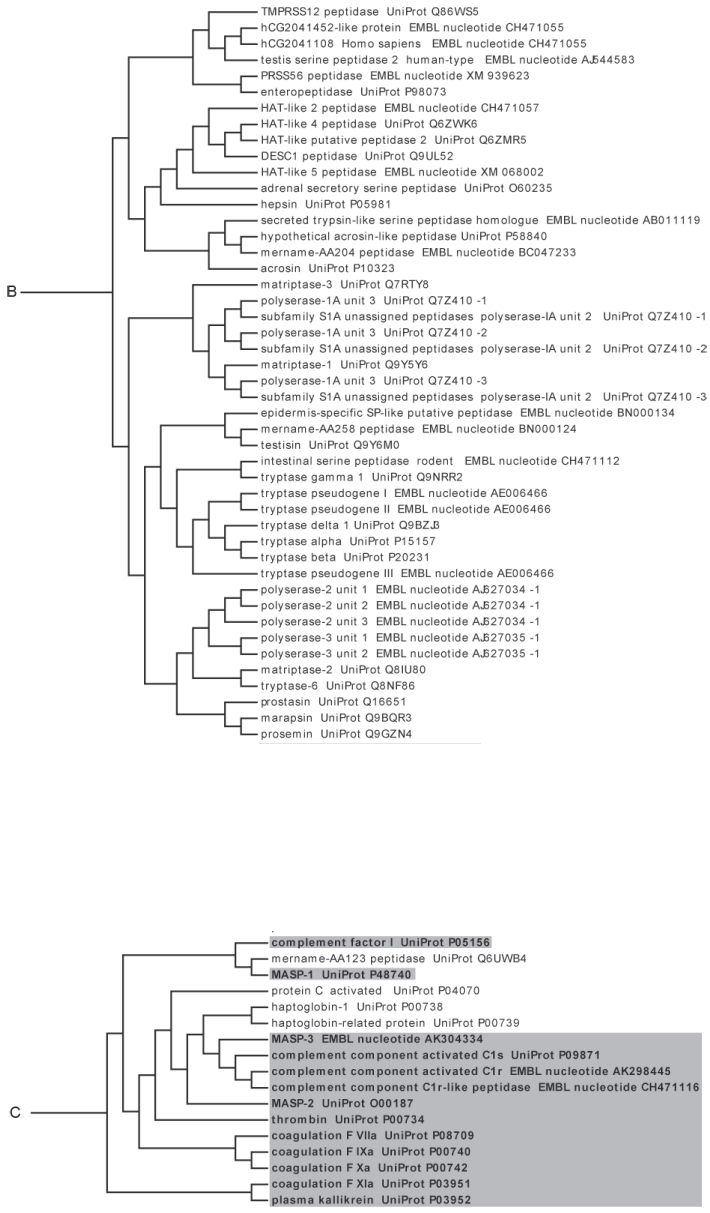

Figure S1. Phylogenetic tree of all human proteases of the MEROPS class of serine proteases (S1A), based on their protease domains. Overview of the complete tree, with the three clades (A-B-C) indicated (*left*) and the proteases that belong to these tree clades (*right*). Gray, immune proteases included in the more concise phylogenetic tree of Fig. 6A.

4

Staphylococcus aureus protects its immune-evasion proteins against degradation by neutrophil serine proteases

Daphne A.C. Stapels[1*], Annemarie Kuipers[1*], Maren von Köckritz-Blickwede[2], Maartje Ruyken[1], Angelino Tromp[1], Mal J. Horsburgh[3], Carla J.C. de Haas[1], Jos A.G. van Strijp[1], Kok P.M. van Kessel[1#] and Suzan H.M. Rooijakkers[1#]

[1] *Medical Microbiology, UMC Utrecht, The Netherlands*
[2] *Department of Physiological Chemistry, University of Veterinary Medicine Hannover, Germany*
[3] *Institute of Integrative Biology, University of Liverpool, United Kingdom*

[*] *These authors contributed equally to this work*
[#] *These authors are joint senior authors*

Manuscript under review

ABSTRACT

Neutrophils store large quantities of neutrophil serine proteases (NSPs) that contribute to antibacterial immune defenses. Even though neutrophils are indispensable in fighting *Staphylococcus aureus* infections, the importance of these NSPs in anti-staphylococcal defense is yet unknown. We recently discovered that *S. aureus* produces three highly specific inhibitors for NSPs (the extracellular adherence proteins (EAPs): Eap, EapH1 and EapH2), emphasizing the importance of NSPs in staphylococcal defense. In this study we demonstrate that NSPs can functionally inactivate secreted virulence factors of *S. aureus*. In return, *S. aureus* uses its EAPs to effectively protect other secreted proteins from NSP degradation. Specifically, we find that a large group of *S. aureus* immune-evasion proteins is vulnerable to proteolytic inactivation by neutrophil elastase and/or cathepsin G *in vitro*. Interestingly, proteins with similar immune-escape functions appeared to have differential cleavage sensitivity towards NSPs. By using targeted *eap* mutants of *S. aureus*, we found that the secreted virulence factors are also degraded *in vivo*. Eap-dependent protection against NSP cleavage was demonstrated both in complex bacterial supernatants *in vitro* and during an infection *in vivo*. These findings show that NSPs target *S. aureus* during infection and can explain why this role of NSPs was masked in previous studies. Furthermore, these studies indicate that therapeutic inactivation of EAPs can help to restore the natural host immune defenses against *S. aureus*.

AUTHOR SUMMARY

Staphylococcus aureus infections form an increasing problem in healthcare settings and the community. The emergence of multi-resistant strains and failure of current vaccination trials, calls for new angles of therapeutic development. The success of this bacterial pathogen highly depends on its large array of virulence factors that enable it to cause disease in the human host. Whereas it is long known that neutrophils are essential for fighting staphylococcal infections, the role of their neutrophil serine proteases (NSPs) was believed to be trivial. Nevertheless, *S. aureus* does secrete a family of extracellular adherence proteins (EAPs) that are potent NSP inhibitors. Here we describe that NSPs are definitely important in fighting *S. aureus* infections, since they can degrade and inactivate many secreted *S. aureus* virulence factors. At the same time, however, *S. aureus* has evolved the EAPs to protect its virulence factors from NSP degradation. Therefore, any new therapeutic strategy would likely be more effective if the EAPs are inactivated, so that the other staphylococcal virulence factors can be dismantled by the immune system itself.

INTRODUCTION

Staphylococcus aureus is an opportunistic pathogen that constitutes a major risk to human health, especially due to the growing prevalence of antibiotic resistant strains[1]. This Gram-positive bacterium harmlessly colonizes over 30% of the population in the anterior nares or on the skin. Nevertheless, when the mechanical barriers of the immune system are breached, it can invade deeper tissues and cause severe diseases such as endocarditis, pneumonia and sepsis[2]. Bacterial clearance requires an efficient innate immune response in which the neutrophil population is of utmost importance[3]. Neutrophils kill bacteria via multiple mechanisms that can be divided in intracellular and extracellular killing. Intracellular killing occurs after the neutrophil engulfed the bacterium via phagocytosis. Extracellular killing occurs after bacterial entrapment in neutrophil extracellular traps (NETs) (which consist of DNA decorated with granular contents) or after degranulation that results in the extracellular release of the granular contents. Within the azurophilic granules, neutrophils store large quantities of active neutrophil serine proteases (NSPs): neutrophil elastase (NE), cathepsin G (CG), proteinase 3 (PR3), and NSP4[4,5]. Each protease displays its own substrate specificity, and together they target a wide range of proteins, varying from host-immune factors to bacterial proteins. Despite the large body of evidence describing the antimicrobial nature of NSPs[6–8], the exact role of these proteases in the defense against *S. aureus* infections is still ambiguous[9,10].

Interestingly, we recently reported that *S. aureus* evolved mechanisms to specifically counteract NSPs[11]. We discovered that the family of extracellular adherence proteins (Eap, and its two structural homologues EapH1 and EapH2) are highly specific NSP inhibitors that potently block NE, CG and PR3[11]. Structural studies demonstrated that EAPs bind the catalytic cleft of NSPs and thereby prevent accessibility for substrates[11]. In an infection model these three proteins together proved to be important for bacterial virulence. The fact that *S. aureus* evolved these NSP inhibitors suggests importance of NSPs in the defense against *S. aureus*. Moreover, the expression of these inhibitors might have complicated previous studies trying to address the role of NSPs in defense against *S. aureus*. Using *S. aureus* mutants that lack EAPs, we can now study the role of NSPs during *S. aureus* infection. Interestingly, we find that NSPs can degrade and inactivate secreted virulence factors of *S. aureus*. However, by the expression of EAPs, *S. aureus* effectively protects its virulence factors against NSP inactivation *in vitro* and *in vivo*.

RESULTS

NE and CG target secreted staphylococcal virulence factors

In order to study the role of NSPs in defense against *S. aureus*, we first analyzed their activity against staphylococcal virulence factors *in vitro*. Since our laboratory specializes in bacterial immune-evasion mechanisms we focused on the activity of NSPs against well-characterized *S. aureus* immune-evasion proteins. These include the chemotaxis

inhibitory protein of *S. aureus* (CHIPS), the formyl peptide receptor-like 1 inhibitory proteins (FLIPr and FLIPr-like), the staphylococcal complement inhibitor (SCIN) family and the staphylococcal superantigen-like proteins (SSLs)[12]. To study whether these immune-evasion proteins are degraded by NSPs, we incubated their recombinant forms with purified NE or CG (see Table S1 for an overview of the used proteins). Upon incubation, most tested immune-evasion proteins of *S. aureus* were degraded by NE (Fig. 1). For instance, during incubation with 100 U/ml NE for 30 min, NE cleaved off a small part of CHIPS (Fig. 1A). This degradation was both dose- and time-dependent (Fig. 1A, 1B). On the contrary, CHIPS was insensitive to degradation by CG (Fig. 1A). The FLIPr molecule was cleaved by both proteases resulting in fragments undetectable by SDS-PAGE, but the 70% homologous protein FLIPr-like was only partially cleaved under these conditions (Fig. 1C). All tested SSLs (SSL5, 6, 7, 10, and 11) seemed resistant to CG-mediated cleavage, but SSL5, SSL7, and SSL11 were susceptible to NE (Fig. 1D). These differences in susceptibility also appeared in the SCIN family of proteins. SCIN-A only decreased a little in size upon cleavage by NE, SCIN-C was completely cleaved to undetectable fragments, but SCIN-B remained completely intact. None of the SCIN proteins were susceptible to CG-mediated cleavage (Fig. 1E). As apparent from these results, some immune-evasion proteins are completely degraded by NE, whereas five molecules (CHIPS, SCIN-A, SSL5, SSL7 and SSL11) seemed to be cleaved at a specific site (Fig. 1F). We identified these cleavage sites by comparing the molecular masses of the proteins before and after cleavage using surface-enhanced laser desorption/ionization coupled to a time-of-flight mass spectrometer (SELDI-TOF) (Fig. 1G, Fig. S1) in combination with N-terminal sequencing (for CHIPS and SCIN-A) and immunoblotting (for CHIPS) (Fig. S1). Interestingly, the cleavage sites were all near the N-terminus and in complete agreement with the known preferred cleavage sites for NE behind small, hydrophobic residues[13]. Taken together, the immune-evasion proteins of *S. aureus* can be degraded by NSPs *in vitro*, albeit there are profound differences in susceptibility.

NSPs inactivate immune-evasion proteins

Next, we analyzed whether the immune-evasion proteins would lose their function upon NSP cleavage. CHIPS binds to the formyl peptide receptor 1 (FPR1) and C5a receptor (C5aR1) on innate immune cells. The activation of these two G protein-coupled receptors can be measured by the release of intracellular calcium[14]. To prevent direct activation of neutrophils by NE or CG[15,16], we added the protease inhibitor alpha-1-antitrypsin (α1-AT) to these samples before measuring the calcium flux and verified that mixtures of only NE or CG with α1-AT did not influence the calcium flux. As expected, CHIPS blocked the intracellular calcium response elicited via the FPR1 and C5aR1 (Fig. 2A). However, when CHIPS was cleaved with NE, it could no longer inhibit FPR1 (Fig. 2A). In concordance, a CHIPS mutant lacking the first 30 amino acids (CHIPSΔ30) could not inhibit FPR1 activation either. In contrast, C5aR inhibition was not abrogated after incubation with NE (Fig. 2A). These findings correspond to previously published data showing that the N-terminal phenylalanine residue of CHIPS is essential for blocking

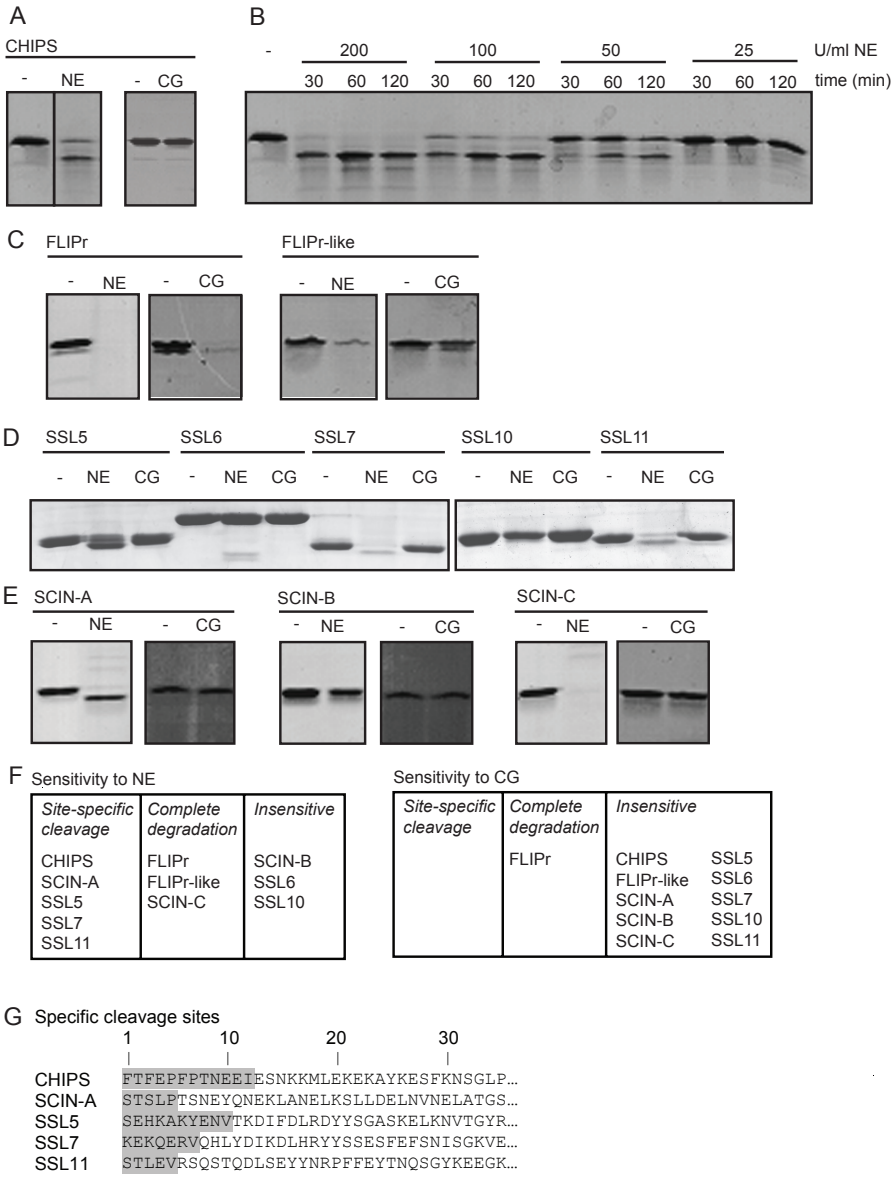

Figure 1. *S. aureus* immune-evasion proteins are cleaved by NE and CG. (A) 200 µg/ml CHIPS was incubated 1:1 (v/v) with 100 U/ml NE or 20 mU/ml CG for 30 min at room temperature. (B) Time-dependent (30, 60, 120 min) and concentration-dependent (200, 100, 50, 25 U/ml NE) cleavage of CHIPS at room temperature. (C-E) Degradation of FLIPr and FLIPr-like (C), SSL proteins (D), and SCIN proteins (E) as described in (A). (F) Overview of the cleavage patterns of the staphylococcal immune-evasion proteins. Site-specific cleavage, one specific cleavage site has been identified; complete degradation, individual degradation products were no longer detectable on SDS-PAGE; insensitive, not cleaved by NE or CG. (G) Site-specific cleavage sites as identified by SELDI-TOF and N-terminal sequencing. Results are representatives of three independent experiments.

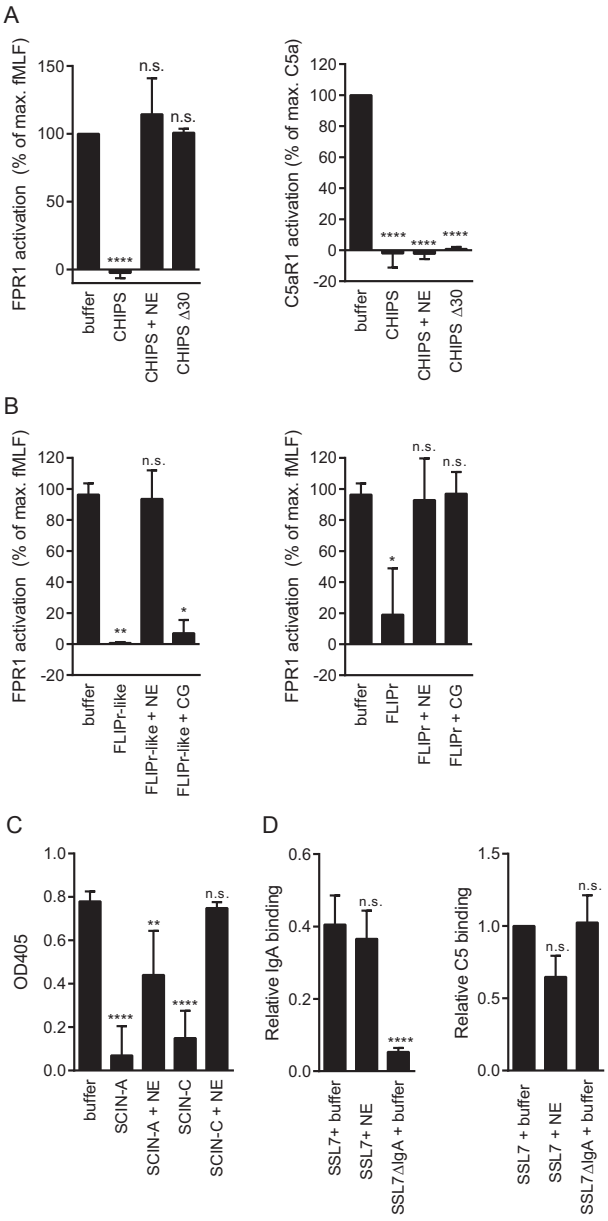

Figure 2. Cleaved immune-evasion proteins are partially inactive. (A) Calcium mobilization via FPR1 (*left*) or C5aR1 (*right*) in neutrophils pre-incubated with CHIPS, CHIPSΔ30, or purified NE-treated His-CHIPS. Cleavage: 200 U/ml NE for 60 min at room temperature. Signals are expressed relative to buffer-treated cells. (B) Calcium mobilization via FPR1 in neutrophils pre-incubated with FLIPr-like and its NE and CG-treated forms (*left*) or FLIPr and its NE and CG-treated forms (*right*). Cleavage: 100 U/ml NE or 20 mU/ml CG for 60 min at room temperature. The reaction was stopped with 100 μg/ml α1-antitrypsin before adding it to the neutrophils. Signals are expressed relative to buffer-treated cells. (C) Alternative complement pathway-dependent lysis of rabbit erythrocytes in 10% serum, pre-incubated with buffer or NE-treated SCIN-A, SCIN-B, or SCIN-C. Cleavage: 100 U/ml NE for 30 min at room temperature. (D) Binding of IgA and C5 to SSL7, a mutant of SSL7 defective in IgA binding (SSL7ΔIgA), or NE-treated SSL7 proteins. The reaction was stopped with α-1-antitrypsin. Cleavage: 100 U/ml NE for 30 min at room temperature. All bars represent the mean ± SD of at least three independent experiments. Significance is addressed with a one-sample t-test with 100% as reference value (A, B), or with a one-way ANOVA, adjusted for multiple comparison (C, D).

FPR1, whereas amino acids 31-133 are needed for inhibition of C5aR1[17–19].

FLIPr-like is another potent inhibitor of neutrophil activation via FPR1 (Fig. 2B). When FLIPr-like was cleaved by NE, the stimulation of FPR1 was restored and thus FLIPr-like had lost its function (Fig. 2B). CG-treated FLIPr-like could still inhibit neutrophil activation. This reflects the previously observed lack of FLIPr-like cleavage by CG (Fig. 1). Moreover, the homologous protein FLIPr can also inhibit neutrophil activation

via FPR1. This function was abrogated both by NE- and CG-cleavage (Fig. 2B). All observations for FPR1 also held true for the related G protein-coupled receptor FPR2 (data not shown).

The SCIN family of proteins is known to inhibit the C3 convertases of the complement system, thereby blocking all downstream effectors of complement such as formation of the terminal pathway membrane attack complex[20]. This can be measured *in vitro* using a hemolytic assay in which erythrocytes are lysed by human complement. In this assay complement activation was still inhibited by NE-cleaved SCIN-A, confirming that the first 5 N-terminal residues are not crucial for the function of SCIN-A[20]. NE-cleaved SCIN-C had lost all ability to inhibit complement, which reflects the SDS-PAGE results that show total degradation (Fig. 2C). Interestingly, within this family of evasion proteins with a similar function there are differences in susceptibility.

SSL7 binds both IgA, to diminish immune-cell activation via the FcαR, and C5, to diminish complement activation. In an ELISA setup, we found that NE-cleaved SSL7 could still bind IgA, whereas it was compromised in its C5 binding capacity (Fig. 2D). Taken together, while some functions remain preserved, most immune-evasion proteins are functionally inactivated by NSP cleavage.

Staphylococcal EAPs protect immune-evasion proteins from degradation

To examine whether the EAPs could protect immune-evasion proteins from degradation by NSPs, we first incubated purified CHIPS or SCIN-A with 100 U/ml NE in the presence or absence of purified EAPs. As a control, we included the human NSP inhibitor α1-AT. As shown by immunoblot, all three EAPs inhibited the cleavage of CHIPS and SCIN-A (Fig. 3A). To study this in a more physiological condition we analyzed the degradation of CHIPS and SCIN-A within a complex mixture of bacterial supernatants. To study the contribution of EAPs, we included our recently constructed isogenic mutants that lack one or more EAPs: Δ*eap*, Δ*eap*Δ*H1*, Δ*H1*Δ*H2,* and Δ*eap*Δ*H1*Δ*H2*. In addition we took along the complemented strain Δ*eap*Δ*H1*Δ*H2*compl.[11]. Interestingly, we observed that endogenously produced CHIPS and SCIN-A are degraded by NE, but only in supernatants that lack Eap (Δ*eap*, Δ*eap*Δ*H1*, and Δ*eap*Δ*H1*Δ*H2*) (Fig. 3B). This suggests that naturally produced Eap can protect other proteins in the supernatant from NE degradation. To better mimic the NSP concentration *in vivo*, we also used supernatants of fMLF-degranulated neutrophils as a source of NSPs[21]. The protease levels within cell-free supernatant ($5x10^6$ neutrophils per mL) were equivalent to 43 ± 5 U/mL NE and 45 ± 27 mU/mL CG (n=5). When these degranulated neutrophils were incubated with the bacterial supernatants, the endogenous CHIPS and SCIN-A proteins in bacterial supernatants were fully degraded, which is likely caused by the presence of multiple NSPs (Fig. 3C). Again, we found that the presence of Eap (i.e. WT, Δ*H1*Δ*H2,* and Δ*eap*Δ*H1*Δ*H2*compl.) in the supernatant protects CHIPS and SCIN-A against NSP degradation.

Eap protects immune-evasion proteins from NSP degradation *in vivo*

Finally, we studied whether NSP degradation of staphylococcal virulence factors, and

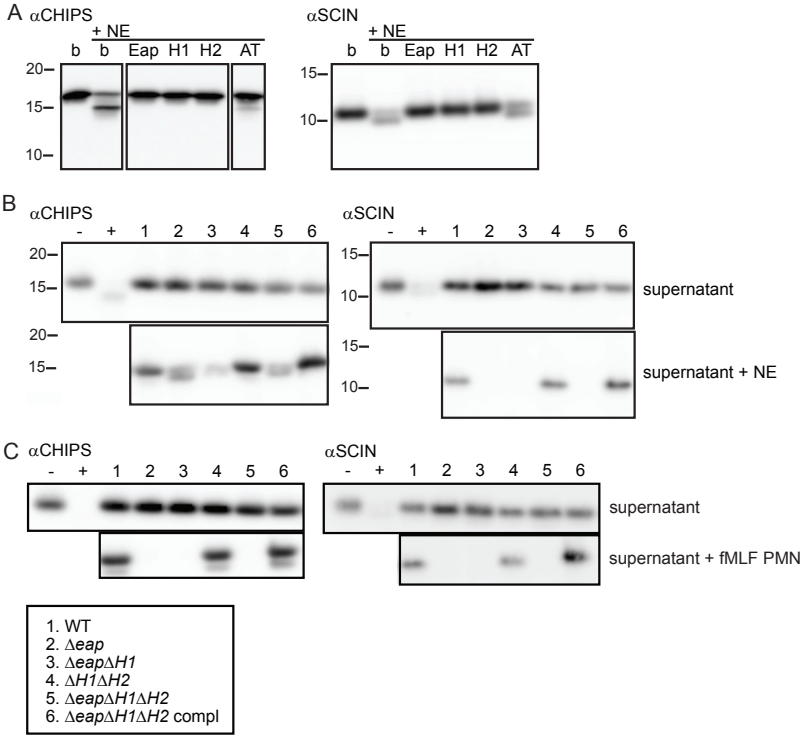

Figure 3. Cleavage of immune-evasion proteins is rescued by the staphylococcal EAP family. (A) Eap, EapH1, and EapH2 (75 µg/ml) inhibit the cleavage of 100 µg/ml immune-evasion proteins CHIPS (*left*), or SCIN-A (*right*) by 100 U/ml NE when incubated for 30 min at room temperature. (B) Cleavage of the immune-evasion proteins CHIPS (*left*) and SCIN-A (*right*) by 35 U/ml NE in supernatant of *S. aureus* WT and mutant strains for 45 min at 37°C. (C) Cleavage of the immune-evasion proteins CHIPS and SCIN-A by fMLP-stimulated PMN in supernatant of *S. aureus* WT and mutant strains for 45 min at 37°C. The concentrations of proteases used for incubation with bacterial supernatants during this incubation was ~ 40 U/ml NE and ~ 45 mU/ml CG. Results represent three independent experiments. Sizes of marker bands (kDa) are indicated on the left.

protection by EAPs, also occurs during an infection *in vivo*. To address this, we performed a murine pneumonia model with the isogenic *eap*-mutant strains. The bacteria were inoculated via the nostrils and after 6 or 24 h bronchoalveolar lavage fluid (BALF) and lungs were harvested to determine the number of surviving bacteria[22]. In addition, the amount of myeloperoxidase (MPO) activity in the lungs was quantified as a measure of the number of intrapulmonary neutrophils. Already after 6 h of infection the WT bacteria seemed to survive better than both mutant strains. After 24 h this difference was even more pronounced, comprising a factor 10 or 100 (for Δ*eap*, or Δ*eap*Δ*H1*Δ*H2* respectively), although only the difference between the WT and Δ*eap*Δ*H1*Δ*H2* infection was statistically significant. Of note, the difference between WT and Δ*eap*Δ*H1*Δ*H2* infection might be even bigger, since two out of nine WT-infected mice succumbed to their infection before the 24-h time point (Fig. 4A). These results confirm our previously reported findings in an intravenous infection model showing the contribution of all EAPs to viru-

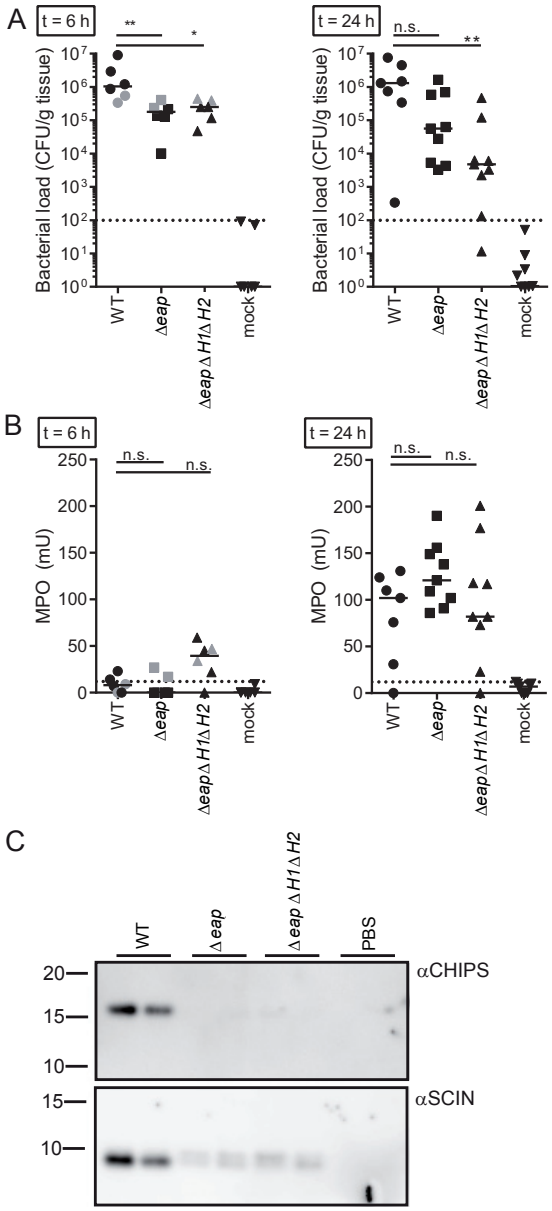

Figure 4. *S. aureus* protects its immune-evasion proteins from cleavage *in vivo*. (A) Surviving bacteria during pneumonia in mice. Mice were infected intranasally with 4 x 10^8 *S. aureus* Newman WT or isogenic *eap* mutants and bacterial loads were recovered from the right lungs at 6 h (*left*) or 24 h (*right*) post infection. Dotted line indicates detection limit as apparent from the mock-infected mice. Gray symbols indicate the mice analyzed in (C). (B) Quantification of the MPO activity in the BALF at 6 h (*left*) or 24 h (*right*) post infection. Dotted line indicates detection limit as apparent from the mock-infected mice. Gray symbols indicate the mice analyzed in (C). (C) Immunoblot for CHIPS (*top*) and SCIN-A (*bottom*) of BALF of mice at 6 h post infection. Samples are from the mice that are highlighted in gray in panels (A) and (B). Each symbol represents a sample from an individual mouse. Horizontal bars indicate the median of all observations. Statistical significance was addressed with a non-parametric one-way ANOVA, corrected for multiple testing with a Tukey's multiple comparison test. Sizes of marker bands (kDa) are indicated on the left.

lence. The neutrophil recruitment in all three infections was similar, albeit there is a trend towards more pulmonary neutrophils at 6 h in the Δ*eap*Δ*H1*Δ*H2*-infected mice. After 24 h all bacterial strains had induced a pronounced neutrophil recruitment (Fig. 4B). To determine whether the immune-evasion proteins would be degraded *in vivo* as well, we compared the levels of the immune-evasion proteins in the BALF at 6 h after infection. To enable a fair comparison, we exclusively analyzed BALF of mice (two per group) that had similar bacterial loads (both in lung homogenate and BALF). Intriguingly, CHIPS

and SCIN-A could be clearly detected in the BALF of WT-infected mice, but were undetectable in the mice infected with either mutant strain (Fig. 4C). Since the isogenic mutant strains produce normal levels of immune-evasion proteins in liquid culture, the absence of immune-evasion proteins during infection is most likely caused by enhanced breakdown. In conclusion, the degradation of CHIPS and SCIN-A proteins also occurs *in vivo* during an infection with *S. aureus*, but only in absence of Eap, which normally protects these immune-evasion proteins from degradation by NSPs.

DISCUSSION

The work presented here is a compelling demonstration of the continuous battle between pathogenic bacteria and host immune components. Many groups have previously illustrated how *S. aureus* evolved a plethora of secreted virulence factors to specifically down-modulate effective inflammatory responses. These mechanisms include effective complement inhibitors (Efb/Ehp, SCIN proteins, Sbi), phagocytosis blockers (Efb, FLIPr/FLIPr-like) and neutrophil toxins[23–28]. And although we find that neutrophil proteases are capable of inactivating these immune-evasion proteins, we also demonstrate the counteracting mechanism of *S. aureus* to evolve NSP inhibitors to protect its other secreted proteins[11]. This way, the bacterium keeps it virulence arsenal intact allowing a successful infection of the human host.

Interestingly, we observed a differential activity of NSPs versus homologous immune-evasion factors with similar functions. For long it was not well understood why *S. aureus* expresses such a redundant arsenal of immune-escape factors. For instance, the family of SCIN proteins (SCIN-A, B and C) all block C3 convertase enzymes with similar activity. The fact that SCIN-C is fully inactivated by NE, while the function of SCIN-A remained intact, may explain for the first time why *S. aureus* secretes so many different proteins that exert the same function. In addition, *S. aureus* relies on a family of NSP inhibitors to allow full and effective protection against NSP inactivation. Interestingly, expression of *eap* is regulated by the Sae two-component system, which also regulates expression of many immune-evasion proteins such as CHIPS and SCIN-A[29]. This coordinated expression of the immune-evasion proteins and the NSP inhibitor assures timely inhibition of NSPs by Eap to protect these immune-evasion proteins. The exact contribution of EapH1 and EapH2 to the protection of immune-evasion proteins was not clear from our *in vivo* studies, but their contribution is likely underestimated in our experiments by the use of strain Newman, that is known to over-express Sae-regulated genes like *eap*.

Although it is clear from this study that NSPs and *S. aureus* immune-evasion proteins encounter each other during an infection, the exact circumstances are yet unclear. NSPs are known to function both inside neutrophil phagosomes and extracellular after neutrophil degranulation or NETosis. The cleavage of CHIPS and SCIN-A that we observed *in vivo* could therefore have taken place at multiple sub-cellular locations. However, since these proteins have their functions outside the neutrophil, we anticipate that this is also the site where they are expressed. Furthermore, the location at which NSP inhibition by

EAPs is most important will depend on which virulence factor is analyzed. Here we show that extracellular immune-evasion proteins are protected.

Even though we now focused on immune-evasion proteins, we presume that all extracellular proteins (both surface-bound and secreted) of *S. aureus* can be targeted by NSPs. Other reports already indicated that the cleavage of virulence factors is a common function of NSPs. For example, NE and CG both cleave *Pseudomonas aeruginosa* flagellin, which yields it unable to activate epithelial cells[30]. Furthermore, NE degrades the Shigella virulence factors IpaA-C and IcsA, to inhibit bacterial escape from the phagosome[31]. Also *in vitro* studies indicated that the *S. aureus* α-toxin and ClfA are subject to degradation by NE or CG, respectively[32,33]. We now show for the first time that the degradation of bacterial virulence factors occurs during an *S. aureus* infection *in vivo*. Previous studies could not unanimously prove the importance of NSPs in defense against *S. aureus*. For example, NE-knockout mice[34] and CG-knockout mice[10] survived intraperitoneal challenge equally well as compared to WT mice. During intravenous challenge only CG-knockout mice showed decreased survival compared to both NE-knockout and WT mice[9]. The function of NSPs was likely underestimated in these studies because of the use of wild-type bacteria expressing EAPs. Using the *eap* deletion mutants, we could now demonstrate that NSPs are indeed important in intravenous[11] and pneumonia infections (this study).

Altogether, we show that the degradation of bacterial virulence factors occurs both *in vitro* and *in vivo* during an *S. aureus* infection. As a countermeasure, *S. aureus* has evolved its own defense against this degradation in the form of EAPs. This finding perfectly illustrates that *S. aureus* and its hosts have evolved a delicate balance requiring defense mechanisms from both sides. Furthermore, these studies indicate that therapeutic inactivation of EAPs can restore the natural host defenses against *S. aureus*.

ACKNOWLEDGEMENTS

We would like to thank Friederike Reuner and Sandra Pfeifer for help with the animal experiments. The authors declare no compete of interest.

MATERIAL AND METHODS

Ethics statement

All blood donors provided written informed consent in accordance with the Declaration of Helsinki. The medical ethics committee of the University Medical Center Utrecht (Utrecht, The Netherlands) approved the used protocol. Animal experiments were performed as required by the German regulations of the Society for Laboratory Animal Science (GV-SOLAS) and the European Health Law of the Federation of Laboratory Animal Science Associations (FELASA), and were approved by the local governmental animal care committee (Lower Saxony, 33.9-42502-04-12/0855).

Human materials

Normal human serum (NHS) was isolated as described before[35] and frozen at -80 °C until further use. Neutrophils were isolated over a Ficoll/Histopaque gradient from blood from heparinized vacutainers (Becton Dickinson), as described before[26]. Neutrophils were degranulated by stimulation at 37°C with cytochalasin B,

TNF-α and fMLF as described before[21].

Staphylococcal proteins

Proteins were recombinantly expressed with a cleavable His-tag as described before for CHIPS[19], CHIPSΔ30 (truncated CHIPS, lacking the first 30 amino acids)[19], FLIPr[26], FLIPr-like[27], SCIN-A[28], SCIN-B, SCIN-C[20], SSL-5, -6, -7, -10, and -11[36,37], and Eap, EapH1 and EapH2[38,39]. See Table S1, which summarizes the used proteins with their calculated theoretical mass value (MW) and the mass value obtained by SELDI-TOF.

Degradation of staphylococcal proteins by NSPs

Purified staphylococcal proteins (200 µg/ml) were incubated 1:1 (v/v) with PBS or PBS- Ipegal-CA630 (Sigma Aldrich), NE (Elastin Products Company), or CG (Calbiochem, Merck) at room temperature. Protease concentration and incubation times are indicated in the Fig. legends. Where indicated, proteases were pre-incubated for 1 min with inhibitors (EAPs or α-1-antitrypsin (Sigma Aldrich)) before the staphylococcal proteins were added. Reactions were stopped with Laemmli sample buffer and analyzed by SDS-PAGE.

SDS-PAGE and immunoblotting

Samples were heated for 5 min at 90°C. Proteins were separated by electrophoresis on a 15% (w/v) SDS-PAGE and visualized by Coomassie Brilliant Blue staining (Merck). Proteins in samples for immunoblotting were separated by 4-12% NuPAGE (Life technologies) and transferred onto polyvinylidenedifluoride (PVDF) membranes (Millipore, Merck) in Tris-glycine buffer containing 20% (v/v) methanol and 0.03% (w/v) SDS. The membranes were blocked with 4% (w/v) non-fat dry milk in PBS-T (PBS containing 0.05% (v/v) Tween-20) for at least 1 h. Membranes were incubated with specific, polyclonal antibodies (rabbit-α-CHIPS (0.1 µg/ml), or rabbit-α-SCIN-A (1 µg/ml) in 1% (w/v) non-fat dry milk in PBS-T) for 1 h at 37°C. After 3 washes, the primary antibodies were detected with peroxidase-conjugated goat antibodies (Southern Biotechnologies, UK), diluted 1:15,000 for one hour at 37°C. Finally, the blots were washed with PBS-T and bands were visualized by enhanced chemiluminescence (ECL, Amersham), or ECL-prime (for the mouse samples).

Identification of cleaved peptides

Cleavage products were analyzed by SELDI-TOF and N-terminal sequencing. SELDI analysis was performed using a normal phase NP20 ProteinChip® array that contains silicon-oxide groups to bind proteins through hydrophilic and charged residues. Products in PBS were applied, 2 µl per spot, air dryed and washed with 5 µl water. To the dry spot, 1 µl of a saturated solution of sinapinic acid (Ciphergen) in 50% acetonitrile and 0.5% trifluoracetic acid was added and air dried. The arrays were transferred to the Ciphergen SELDI reader (model 4000) and analyzed following desorption of bound proteins by short intense pulses from a UV laser.

For N-terminal sequencing the proteins were transferred to a PVDF membrane after electrophoresis using CAPS (10 mM)/methanol (40%) buffer. The membranes were washed with distilled water, stained with Coomassie Brillant Blue R-250 in 40% methanol and washed again. The protein bands of interest were excised from the dried membrane and used for N-terminal sequencing by the Edman procedure at Alphalyse (Odense, Denmark).

Purification of cleaved fragments

For purification of protease-derived fragments from CHIPS and SCIN-A, His-tagged proteins (100 µg) were incubated with 200 U/ml NE or PBS buffer in a volume of 100 µl for 1 h at room temperature. The reaction was stopped by adding the NE inhibitor MeOSuc-AAPV-CMK (Sigma Aldrich) to a final concentration of 1 mM. To separate the cleavage fragment from the unmodified protein, the sample was run over a His-select™ Spin column (Sigma-Aldrich) by centrifugation for 5 min at 10,000 rpm in an Eppendorf minifuge. The column was washed once with 100 µl PBS and combined with the first retentate. Specific CHIPS or SCIN-A content was determined by specific capture ELISA using monoclonal and polyclonal antibodies as previously described[40]. The presence of residual His-tagged protein was verified by a capture ELISA onto Ni-NTA HisSorb™ plates (Qiagen). Bound His-tagged protein was detected with a specific rabbit anti-CHIPS or anti-SCIN-A IgG and peroxidase-conjugated goat anti-rabbit IgG.

Neutrophil calcium mobilization

Neutrophils were loaded with 2 µM Fluo-3-AM (acetomethyl ester) for 20 min at room temperature under

constant agitation and washed once. Cells were resuspended in RPMI-1640 with 0.05% (w/v) human serum albumin (HSA) at 5 x 10^6 cells/ml and incubated for 5 min with 1 µg/ml inhibitory protein, fragments, or buffer only, at room temperature. Prior to stimulation, cells were diluted 5-fold and transferred to Falcon tubes with a volume of 180 µl. The basal fluorescence was determined by flow cytometry (FACSCalibur, BD Biosciences) for 10 seconds, the tube was withdrawn from the sample holder, and 10-fold concentrated stimulus was added. Cells were activated with 30 nM MMK-1 (Sigma Aldrich), 3 nM fMLF (Sigma Aldrich) in assays with CHIPS, 1 nM fMLF in assays with FLIPr(-like), or 0.1 nM C5a (Calbiochem, Merck). The tube was rapidly placed back to continue the fluorescence readings until 52 seconds. The difference in mean fluorescence intensity (MFI) before and after stimulation was used as a measure of neutrophil activation. Data are expressed as percentage stimulation as compared to the positive control (stimulus without inhibitor).

Alternative complement pathway assay (AP50)

Rabbit red-blood cells (from Alsever rabbit blood, Biotrading Benelux B.V.) were washed with PBS and adjusted to a concentration of 1.5 x 10^8/ml in VBS-MgEGTA (veronal-buffered saline with 5 mM $MgCl_2$ and 10 mM EGTA). In a U-shaped microplate, 2-fold serial dilutions of SCIN proteins, fragments or buffer were mixed with 10% NHS in VBS-MgEGTA and incubated for 15 min at room temperature in a volume of 100 µl. Subsequently, 50 µl red-blood cells were added and incubated for 1 h at 37°C. The plate was centrifuged and 100 µl supernatant was transferred to a new flat-bottom microplate to measure the red-blood cell lysis at OD_{405nm}.

IgA and C5 ELISA

Greiner high-bound microtiter plates were coated with 1 µg/ml SSL7, or NE-treated SSL7. After blocking with 4% BSA in PBS-T, a serial dilution of purified human IgA or C5 (Calbiochem) was added. Bound proteins were detected with peroxidase-labeled anti-HuIgA or monoclonal anti-C5 (Quidel) antibody. Coated SSL7 was also directly detected by a serial dilution of rabbit anti-SSL7. Primary antibodies were detected with the appropriate peroxidase-labeled secondary antibodies.

Isogenic bacterial mutants

The markerless mutants *S. aureus* Newman Δ*eap*Δ*H1* (MR1852) and Δ*H1*Δ*H2* (MR1912) were generated as described previously for Δ*eap* (MR1811) and Δ*eap*Δ*H1*Δ*H2* (MR1860)[11].

Degradation of virulence factors within supernatants

Bacterial strains were grown overnight in Todd-Hewitt broth (THB). This culture was diluted 1:100 in Iscove's modified Dulbecco's medium (IMDM; Gibco, Invitrogen) and grown for 8 h at 37°C while shaking. Supernatants were collected after centrifugation for 15 min at 2,660 x *g*. Before storage at -20°C, supernatants were sterile filtered and concentrated ten times with 3-kDa Amicon spin columns (Millipore). Degradation of virulence factors by NSPs was assessed by incubating concentrated bacterial supernatants 1:1 (v/v) with 40 µg/ml NE (~35 U/ml) or fMLF-stimulated neutrophil supernatants for 45 min at 37°C. Cleavage products were analyzed by immunoblotting.

Quantification of released NE and CG

The amount of human NE and CG released by degranulated neutrophils was quantified with specific substrates (MeOSuc-AAPV-pNA for NE and Suc-AAPF-pNA for CG (Calbiochem)). The substrates were dissolved in DMSO and diluted with PBS to 1 mM (for NE) and 10 mM (for CG). Substrate solutions were mixed 1:1 (v/v) with samples, incubated for 30 min at 37°C and OD_{405nm} was measured in a BioRad microplate reader. Purified enzymes served as standards to calculate the sample concentrations.

Murine pneumonia model

The pneumonia model was performed as previously described[22], with minor modifications. Female C57/BL6 mice (purchased from Harlan-Winkelmann, Germany) were bred in the animal facility at University of Veterinary Medicine Hannover, Germany and kept under specific pathogen free (SPF)-conditions. They were infected when they were 9, 10 or 17 weeks old (equally distributed amongst the different treatment groups). Overnight cultures of *S. aureus* were diluted 1:100 in fresh THB and grown to OD_{660nm} 0.8. Bacteria were centrifuged for 10 min at 3500 x *g* and resuspended in PBS to contain 2 x 10^{10} CFU/ml. Mice were anesthetized with 75 mg/kg ketamine (WDT) and 5 mg/kg xylazine (Serumwerk Bernburg AG) in PBS. They were infected

with 10 µl bacteria in each nostril. Mice were held upright after infection and recovery from anesthesia was monitored. Either 6 or 24 h after inoculation the mice were sacrificed with isofluorane (Baxter, Germany). The lungs were flushed with 1 ml sterile PBS to obtain the BALF. CFU were enumerated by plating serial dilutions on sheep-blood agar (SBA; Becton-Dickinson). The right lung was excised and homogenized for 30 s in PBS to enumerate CFU in the tissue. The left lung was excised and homogenized for 30 s in 50 mM phosphate buffer with 1% (w/v) hexadecyltrimethylammonium bromide (HTAB; Sigma-Aldrich) to determine enzyme activity. MPO activity was determined as a measure for the neutrophil influx[41]. Therefore, homogenized left lungs and the MPO reference (Calbiochem) were diluted 1:10 with o-dianisidine dichloride (DDC; Sigma-Aldrich) and 0.05% (v/v) H_2O_2 in 50 mM phosphate buffer. After 1 h the OD_{450nm} was measured.

Statistical analysis

Statistical analyses were performed by using GraphPad Prism 6.0. $P < 0.05$ was assumed to be statistically significant. ****$P < 0.0001$; ***$P < 0.001$; **$P < 0.01$; *$P < 0.05$.

REFERENCES

1. Chua K, Laurent F, Coombs G, Grayson ML, Howden BP: Antimicrobial resistance: Not community-associated methicillin-resistant Staphylococcus aureus (CA-MRSA): A clinician's guide to community MRSA - its evolving antimicrobial resistance and implications for therapy. *Clin. Infect. Dis.* 2011, 52:99–114.
2. Lowy FD: Staphylococcus aureus infections. *N. Engl. J. Med.* 1998, 339:520–532.
3. Miller LS, Cho JS: Immunity against Staphylococcus aureus cutaneous infections. *Nat. Rev. Immunol.* 2011, 11:505–518.
4. Perera NC, Schilling O, Kittel H, Back W, Kremmer E, Jenne DE: NSP4, an elastase-related protease in human neutrophils with arginine specificity. *Proc. Natl. Acad. Sci. U. S. A.* 2012, 109:6229–6234.
5. Faurschou M, Borregaard N: Neutrophil granules and secretory vesicles in inflammation. *Microbes Infect.* 2003, 5:1317–1327.
6. Belaaouaj AA, Kim KS, Shapiro SD: Degradation of Outer Membrane Protein A in Escherichia coli Killing by Neutrophil Elastase *Science* 2000, 289:1185–1187.
7. Hirche TO, Benabid R, Deslee G, Achilefu S, Guenounou M, Hancock RE, Belaaouaj A, Gangloff S: Neutrophil Elastase Mediates Innate Host Protection against Pseudomonas aeruginosa. *J. Immunol.* 2008, 181:4945–4954.
8. Standish AJ, Weiser JN: Human neutrophils kill Streptococcus pneumoniae via serine proteases. *J. Immunol.* 2009, 183:2602–2609.
9. Reeves EP, Lu H, Jacobs HL, Messina CGM, Bolsover S, Gabella G, Potma EO, Warley A, Roes J, Segal AW: Killing activity of neutrophils is mediated through activation of proteases by K+ flux. *Nature* 2002, 416:291–297.
10. MacIvor DM, Shapiro SD, Pham CT, Belaaouaj A, Abraham SN, Ley TJ: Normal neutrophil function in cathepsin G-deficient mice. *Blood* 1999, 94:4282–4293.
11. Stapels DAC, Ramyar KX, Bischoff M, von Köckritz-Blickwede M, Milder FJ, Ruyken M, Eisenbeis J, McWhorter WJ, Herrmann M, van Kessel KPM, et al.: Staphylococcus aureus secretes a unique class of neutrophil serine protease inhibitors. *Proc. Natl. Acad. Sci. U. S. A.* 2014, 111:13187–13192.
12. Spaan AN, Surewaard BGJ, Nijland R, van Strijp JAG: Neutrophils versus Staphylococcus aureus: a biological tug of war *Annu. Rev. Microbiol.* 2013, 67:629–650.
13. Korkmaz B, Horwitz MS, Jenne DE, Gauthier F: Neutrophil Elastase, Proteinase 3, and Cathepsin G as Therapeutic Targets in Human Diseases. *Pharmacol. Rev.* 2010, 62:726–759.
14. Postma B, Poppelier MJ, van Galen JC, Prossnitz ER, van Strijp JAG, de Haas CJC, van Kessel KPM: Chemotaxis inhibitory protein of Staphylococcus aureus binds specifically to the C5a and formylated peptide receptor. *J. Immunol.* 2004, 172:6994–7001.
15. Brozna JP, Senior RM, Kreutzer DL, Ward PA: Chemotactic factor inactivators of human granulocytes *J. Clin. Invest.* 1977, 60:1280–1288.
16. Tralau T, Meyer-Hoffert U, Schröder J-M, Wiedow O: Human leukocyte elastase and cathepsin G are specific inhibitors of C5a-dependent neutrophil enzyme release and chemotaxis. *Exp. Dermatol.* 2004, 13:316–325.
17. Haas P, de Haas CJC, Kleibeuker W, Poppelier MJJG, van Kessel KPM, John AW, Liskamp RMJ, van Strijp JAG: N-terminal residues of the Chemotaxis Inhibitory Protein of Staphylococcus aureus are essential for

blocking Formylated Peptide Receptor but not C5a Receptor. *J. Immunol.* 2004, 173:5704–5711.
18. Gustafsson E, Forsberg C, Haraldsson K, Lindman S, Ljung L, Furebring C: Purification of truncated and mutated Chemotaxis Inhibitory Protein of Staphylococcus aureus--an anti-inflammatory protein. *Protein Expr. Purif.* 2009, 63:95–101.
19. Haas P-J, de Haas CJC, Poppelier MJJ, van Kessel KPM, van Strijp JAG, Dijkstra K, Scheek RM, Fan H, Kruijtzer JAW, Liskamp RMJ, et al.: The structure of the C5a receptor-blocking domain of chemotaxis inhibitory protein of Staphylococcus aureus is related to a group of immune evasive molecules. *J. Mol. Biol.* 2005, 353:859–872.
20. Rooijakkers SHM, Milder FJ, Bardoel BW, Ruyken M, van Strijp JAG, Gros P: Staphylococcal complement inhibitor: structure and active sites *J. Immunol.* 2007, 179:985–994.
21. van Kessel KPM, van Strijp JAG, Verhoef J: Inactivation of recombinant human tumor necrosis factor-a by proteolytic enzymes released from stimulated human neutreophils. *J. Immunol.* 1991, 147:3862–3868.
22. Bubeck Wardenburg J, Patel RJ, Schneewind O: Surface proteins and exotoxins are required for the pathogenesis of Staphylococcus aureus pneumonia. *Infect. Immun.* 2007, 75:1040–1044.
23. Koch TK, Reuter M, Barthel D, Böhm S, van den Elsen J, Kraiczy P, Zipfel PF, Skerka C: Staphylococcus aureus Proteins Sbi and Efb Recruit Human Plasmin to Degrade Complement C3 and C3b. *PLoS One* 2012, 7:e47638.
24. Jongerius I, Köhl J, Pandey MK, Ruyken M, van Kessel KPM, van Strijp JAG, Rooijakkers SHM: Staphylococcal complement evasion by various convertase-blocking molecules. *J. Exp. Med.* 2007, 204:2461–2471.
25. Spaan AN, Henry T, van Rooijen WJM, Perret M, Badiou C, Aerts PC, Kemmink J, de Haas CJC, van Kessel KPM, Vandenesch F, et al.: The staphylococcal toxin Panton-Valentine Leukocidin targets human C5a receptors. *Cell Host Microbe* 2013, 13:584–594.
26. Prat C, Bestebroer J, de Haas CJC, van Strijp JAG, van Kessel KPM: A New Staphylococcal Anti-Inflammatory Protein That Antagonizes the Formyl Peptide Receptor-Like 1. *J. Immunol.* 2006, 177:8017–8026.
27. Prat C, Haas P-J, Bestebroer J, de Haas CJC, van Strijp JAG, van Kessel KPM: A homolog of formyl peptide receptor-like 1 (FPRL1) inhibitor from Staphylococcus aureus (FPRL1 inhibitory protein) that inhibits FPRL1 and FPR. *J. Immunol.* 2009, 183:6569–6578.
28. Rooijakkers SHM, Ruyken M, Roos A, Daha MR, Presanis JS, Sim RB, van Wamel WJB, van Kessel KPM, van Strijp JAG: Immune evasion by a staphylococcal complement inhibitor that acts on C3 convertases. *Nat. Immunol.* 2005, 6:920–927.
29. Rooijakkers SHM, Ruyken M, van Roon J, van Kessel KPM, van Strijp JAG, van Wamel WJB: Early expression of SCIN and CHIPS drives instant immune evasion by Staphylococcus aureus. *Cell. Microbiol.* 2006, 8:1282–1293.
30. López-Boado YS, Espinola M, Bahr S, Belaaouaj A: Neutrophil serine proteinases cleave bacterial flagellin, abrogating its host response-inducing activity. *J. Immunol.* 2004, 172:509–515.
31. Weinrauch Y, Drujan D, Shapiro SD, Weiss J, Zychlinsky A: Neutrophil elastase targets virulence factors of enterobacteria *Nature* 2002, 417:91–94.
32. Worlitzsch D, Kaygin H, Steinhuber A, Dalhoff A, Botzenhart K, Döring G: Effects of Amoxicillin, Gentamicin, and Moxifloxacin on the Hemolytic Activity of Staphylococcus aureus In Vitro and In Vivo. *Antimicrob. Agents Chemother.* 2001, 45:196–202.
33. Brinkmann V, Reichard U, Goosmann C, Fauler B, Uhlemann Y, Weiss DS, Weinrauch Y, Zychlinsky A: Neutrophil extracellular traps kill bacteria. *Science* 2004, 303:1532–1535.
34. Belaaouaj AA, McCarthy R, Baumann M, Gao Z, Ley TJ, Abraham SN, Shapiro SD: Mice lacking neutrophil elastase reveal impaired host defense against gram negative bacterial sepsis. *Nature* 1998, 4:615–618.
35. Berends ETM, Dekkers JF, Nijland R, Kuipers A, Soppe JA, van Strijp JAG, Rooijakkers SHM: Distinct localization of the complement C5b-9 complex on Gram-positive bacteria. *Cell. Microbiol.* 2013, 15:1955–1968.
36. Bestebroer J, Aerts PC, Rooijakkers SHM, Pandey MK, Köhl J, van Strijp JAG, de Haas CJC: Functional basis for complement evasion by staphylococcal superantigen-like 7 *Cell. Microbiol.* 2010, 12:1506–1516.
37. Bestebroer J, Poppelier MJJG, Ulfman LH, Lenting PJ, Denis C V, van Kessel KPM, van Strijp JAG, de Haas CJC: Staphylococcal superantigen-like 5 binds PSGL-1 and inhibits P-selectin-mediated neutrophil rolling. *Blood* 2007, 109:2936–2943.
38. Xie C, Alcaide P, Geisbrecht BV., Schneider D, Herrmann M, Preissner KT, Luscinskas FW, Chavakis T: Suppression of experimental autoimmune encephalomyelitis by extracellular adherence protein of Staphylococcus aureus. *J. Exp. Med.* 2006, 203:985–994.
39. Geisbrecht BV., Hamaoka BY, Perman B, Zemla A, Leahy DJ: The crystal structures of EAP domains

from Staphylococcus aureus reveal an unexpected homology to bacterial superantigens. *J. Biol. Chem.* 2005, 280:17243–17250.
40. Gustafsson E, Haas P-J, Walse B, Hijnen M, Furebring C, Ohlin M, van Strijp JAG, van Kessel KPM: Identification of conformational epitopes for human IgG on Chemotaxis inhibitory protein of Staphylococcus aureus. *BMC Immunol.* 2009, 10. doi: 10.1186/1471-2172-10-13.
41. Bradley PP, Priebat DA, Chritensen RD, Rothstein G: Measurement of cutaneous inflammation: estimation of neutrophil content with an enzyme marker. *J. Invest. Dermatol.* 1982, 78:206–209.
42. Gasteiger E, Hoogland C, Gattiker A, Duvaud S, Wilkins MR, Appel RD, Bairoch A: Protein Identification and Analysis Tools on the ExPASy Server. In *The Proteomics Protocols Handbook*. Edited by Walker JM. Humana Press; 2005:571–608.
43. se Haas CJC, Veldkamp KE, Peschel A, Weerkamp F, van Wamel WJB, Heezius ECJM, Poppelier MJJG, van Kessel KPM, van Strijp JAG: Chemotaxis inhibitory protein of Staphylococcus aureus, a bacterial antiinflammatory agent. *J. Exp. Med.* 2004, 199:687–695.
44. Bestebroer J, van Kessel KPM, Azouagh H, Walenkamp AM, Boer IGJ, Romijn RA, van Strijp JAG, de Haas CJC: Staphylococcal SSL5 inhibits leukocyte activation by chemokines and anaphylatoxins. *Blood* 2009, 113:328–337.
45. Fevre C, Bestebroer J, Mebius MM, de Haas CJC, van Strijp JAG, Fitzgerald JR, Haas P-JA: Staphylococcus aureus proteins SSL6 and SElX interact with neutrophil receptors as identified using secretome phage display. *Cell. Microbiol.* 2014, 16:1646–1665.
46. Langley R, Wines B, Willoughby N, Basu I, Proft T, Fraser JD: The Staphylococcal Superantigen-Like Protein 7 Binds IgA and Complement C5 and Inhibits IgA-Fc RI Binding and Serum Killing of Bacteria *J. Immunol.* 2005, 174:2926–2933.
47. Walenkamp AME, Boer IGJ, Bestebroer J, Rozeveld D, Timmer-Bosscha H, Hemrika W, van Strijp JAG, de Haas CJC: Staphylococcal Superantigen-like 10 Inhibits CXCL12-Induced Human Tumor Cell Migration. *Neoplasia* 2009, 11:333–344.
48. Patel D, Wines BD, Langley RJ, Fraser JD: Specificity of staphylococcal superantigen-like protein 10 toward the human IgG1 Fc domain. *J. Immunol.* 2010, 184:6283–6292.
49. Chung MC, Wines BD, Baker H, Langley RJ, Baker EN, Fraser JD: The crystal structure of staphylococcal superantigen-like protein 11 in complex with sialyl Lewis X reveals the mechanism for cell binding and immune inhibition. *Mol. Microbiol.* 2007, 66:1342–1355.

SUPPLEMENTAL INFORMATION

Supplemental Figure

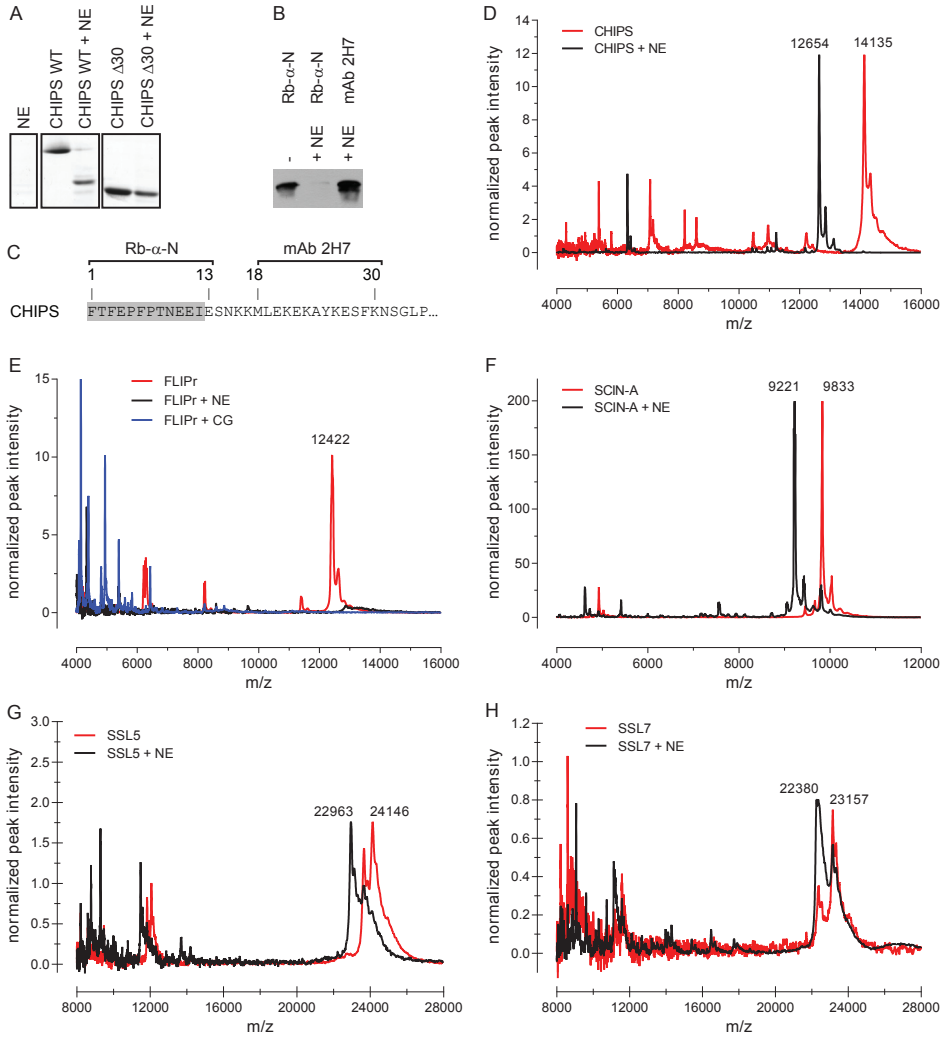

Figure S1. Identification of the NE-cleavage sites within the immune-evasion proteins. (A) Susceptibility to cleavage by 100 U/ml elastase for 30 min at room temperature of CHIPS and its N-terminal deletion mutant CHIPSΔ30. The cleavage reaction was analyzed on SDS-PAGE. (B) NE-treated CHIPS was blotted with rabbit anti-N-terminal peptide (Rbα-N) to detect the amino-terminal domain of CHIPS, or with mouse mAb 2H7 that recognizes a region within amino acids 18-31. (C) Schematic overview of the antibodies (Rb-α-N and mAb 2H7) used to identify the NE-cleavage site within CHIPS. (D-H) SELDI-TOF analysis of immune-evasion proteins before and after cleavage by 100 U/ml NE or 20 mU/ml CG for 30 min at room temperature on a NP20 protein chip. (D) CHIPS treated with NE. (E) FLIPr treated with NE or CG. (F) SCIN-A treated with NE. (G) SSL5 treated with NE. (H) SSL7 treated with NE. Relevant mass regions are shown and the peaks are labeled with the exact mass.

Supplemental table

Table S1. Staphylococcal immune-evasion proteins used.

Protein	Gene	Immune-evasion function	Ref.	MW[42]	SELDI-TOF
CHIPS	NWMN_1877	blocks FPR1 and C5aR1	[43]	14112	14124
FLIPr	SA1001	blocks FPR2	[26]	12318	12431
FLIPr-like	MW1038	blocks FPR1and FPR2	[27]	12011	11904
SCIN-A	NWMN_1876	inhibits C3 convertases	[28]	9805	9824
SCIN-B	SA1004	idem	[20]	9862	9899
SCIN-C	SAR1131	idem	[20]	9878	9897
SSL5	SAOUHSC_00390	blocks PSGL-1 and GPCRs	[37,44]	24161	24129
SSL6	SAOUHSC_00391	binds CD47	[45]	23573	23584
SSL7	SAOUHSC_00392	binds C5 and IgA	[36,46]	23157	23149
SSL10	SAOUHSC_00395	binds CXCR4 and IgG	[47,48]	23074	23065
SSL11	SAOUHSC_00399	binds sialyl Lewis X	[49]	22298	22320

List of recombinantly made staphylococcal proteins, with their source gene, immune-evasion function, and molecular weight (predicted based on amino-acid sequence, and determined by SELDI-TOF).

5

The extracellular adherence protein from Staphylococcus aureus inhibits the classical and lectin pathways of complement by blocking formation of the C3 proconvertase

Jordan L. Woehl[1*], Daphne A.C. Stapels[2*], Brandon L. Garcia[3], Kasra X. Ramyar[1], Andrew Keightley[3], Maartje Ruyken[2], Maria Syriga[4], Georgia Sfyroera[4], Alexander B. Weber[3], Michal Zolkiewski[1], Daniel Ricklin[4], John D. Lambris[4], Suzan H.M. Rooijakkers[2#] and Brian V. Geisbrecht[1,3#]

[1] *Department of Biochemistry & Molecular Biophysics, Kansas State University, Manhattan, KS, USA*
[2] *Medical Microbiology, UMC Utrecht, The Netherlands*
[3] *School of Biological Sciences, University of Missouri-Kansas City, Kansas City, MO, USA*
[4] *Department of Pathology & Laboratory Medicine, University of Pennsylvania, Philadelphia, PA, USA*

[*] *Equal contribution*
[#] *These authors shared supervision of this study*

J. Immunol. (2014). 193(12): 6161-6171

ABSTRACT

The pathogenic bacterium *Staphylococcus aureus* actively evades many aspects of human innate immunity by expressing a series of small inhibitory proteins. A number of these proteins inhibit the complement system, which labels bacteria for phagocytosis and generates inflammatory chemoattractants. Although the majority of staphylococcal complement inhibitors act on the alternative pathway to block the amplification loop, only a few proteins act on the initial recognition cascades that constitute the classical pathway (CP) and lectin pathway (LP). We screened a collection of recombinant, secreted staphylococcal proteins to determine whether *S. aureus* produces other molecules that inhibit either the CP and/or LP. Using this approach, we identified the extracellular adherence protein (Eap) as a potent, specific inhibitor of both the CP and LP. We found that Eap blocked CP/LP-dependent activation of C3, but not C4, and that Eap likewise inhibited deposition of C3b on the surface of *S. aureus* cells. In turn, this significantly diminished the extent of *S. aureus* opsonophagocytosis and killing by neutrophils. This combination of functional properties suggested that Eap acts specifically at the level of the CP/LP C3 convertase (C4b2a). Indeed, we demonstrated a direct, nanomolar-affinity interaction of Eap with C4b. Eap binding to C4b inhibited binding of both full-length C2 and its C2b fragment, which indicated that Eap disrupts formation of the CP/LP C3 pro-convertase (C4b2). As a whole, our results demonstrate that *S. aureus* inhibits the two initiation routes of complement by expression of the Eap protein, and thereby define a novel mechanism of immune evasion.

INTRODUCTION

The complement system serves as a critical hub in the human innate immune and inflammatory system, and fulfills numerous roles in homeostasis, defense, repair, and disease[1]. Despite its diverse list of functions, complement remains best known for its ability to opsonize and eliminate invading microorganisms. To achieve this most efficiently, the microbial surface must first be recognized by one of a series of pattern-recognition proteins[1]. These ligand-bound 'sensors' can then trigger one of three canonical activation routes, (the classical (CP), lectin (LP), and alternative (AP) pathways), which all result in cleavage of the abundant plasma protein C3 into its bioactive C3a (chemoattractant) and C3b (covalent opsonin) fragments. Although such activation of C3 may occur at a low level spontaneously, this central process is catalyzed at the bacterial surface through the function of two transiently-stable, multi-subunit proteolytic complexes known as C3 convertases. In the case of the CP or LP, the initiating complexes of surface Ig-bound C1 or carbohydrate-bound MBL/MASPs trigger proteolytic activation of C4 to produce C4b. Surface-bound C4b then binds C2 to form the CP/LP C3 pro-convertase which, when proteolytically-activated by the same initiation complexes named above, gives rise to the fully-active CP/LP C3 convertase, C4b2a. C4b2a converts native C3 into C3b, and ultimately gives rise to the AP C3 convertase (C3bBb). In this scenario surface deposed C3b, along with the pro-enzyme factor B (FB) and factor D (FD), cooperate to generate the C3bBb complex. It is this surface-bound AP C3 convertase that activates massive amounts of C3 into C3b, thereby being responsible for the self-amplifying nature of the complement response, and which stimulates efficient opsonization of bacteria and production of powerful inflammatory mediators like C3a and C5a[2]. Furthermore, deposited C3b molecules also activate the terminal pathway of complement that results in the formation of the membrane attack complex (C5b-9) that can directly kill Gram-negative bacteria.

The pathogenic bacterium *Staphylococcus aureus* has evolved a diverse and multifaceted approach to successfully evade the human innate immune response3–5. Central to this global strategy is its ability to manipulate the human complement system to a greater extent than perhaps any other pathogen studied thus far3,4,6. While studies from the last decade have revealed much on the diverse nature of *S. aureus* complement evasion, the large number of C3 convertase inhibitors that act on the AP suggests that conceptually similar mechanism(s) that affect the CP and/or LP might be manifested by a component of the *S. aureus* immune evasion arsenal. In this regard, the fact that CP and LP share the same C3 convertase, C4b2a, raises the intriguing possibility that a single inhibitor might effectively block C3b deposition and downstream anaphylatoxin production via both of these pathways simultaneously. While staphylococcal complement inhibitor (SCIN) proteins have been reported to inhibit the CP and LP at the level of C3b deposition, their activities against these pathways are only partial and are substantially weaker than they are against the AP7,8. Thus, we hypothesized that *S. aureus* might express and secrete an as yet unidentified inhibitor of CP and LP C3 convertase formation and/or activity.

To this end, we screened a collection of recombinant secreted *S. aureus* proteins to

examine whether any of these molecules had inhibitory activities on the CP/LP. In doing so, we identified the staphylococcal extracellular adherence protein (Eap) as a potent, specific inhibitor of both the CP and LP. We found that Eap, but not its structural homologs EapH1 and EapH29, inhibits the CP/LP in a dose-dependent manner by forming a nanomolar affinity complex with C4b. This C4b/Eap complex inhibits binding of C2 to C4b, and therefore impedes formation of the CP/LP C3 pro-convertase. From a broader perspective, the studies we present here suggest that the effects of Eap on the CP/LP in many respects mirror those of the staphylococcal complement inhibitor Efb-C, which inhibits AP C3 pro-convertase formation by binding C3b10. In sum, this work provides new insight into staphylococcal immune evasion, and also describes an entirely novel mechanism of CP/LP regulation that may hold significant implications for future design of therapeutic CP/LP inhibitors.

RESULTS

Identification of Eap as an inhibitor of the CP and LP of complement

We screened a library of approximately 30 secreted staphylococcal proteins to test if any of these molecules were capable of inhibiting the CP and LP on the surface of pathway-specific activator/acceptor coated ELISA plates11. In doing so, we discovered that a recombinant form of Eap inhibited both pathways at the level of terminal complement complex (C5b-9) deposition (Fig. 1A). This effect was specific for the CP and LP, since Eap did not block the AP (*Data Not Shown*). A gene encoding Eap is found in 98% of all clinical isolates of *S. aureus*12. Although there is some variability in the molecular weight of Eap protein produced by different strains, characterization of Eap from *S. aureus* strain Mu50 (~50 kDa) and Newman (~63 kDa) in various assays suggests that these two isoforms retain similar functions13,14. Consistent with this, Eap proteins from both *S. aureus* Mu50 and Newman are equally potent in their ability to inhibit the CP and LP (*Data Not Shown*). Eap from *S. aureus* strain Mu50 is comprised of four tandem repeats of an ~100 residue motif known as the EAP domain9. These repeats share between 40-80% identity with one another, and show approximately 25-50% identity to the structurally related *S. aureus* proteins, EapH1 and EapH2, which themselves consist of little more than a single EAP domain9. While Eap potently inhibited the CP and LP at the level of C5b-9, neither EapH1 nor EapH2 had any significant impact on either pathway. Thus, the inhibitory effect on the CP and LP is specific to Eap, and not a general feature of EAP domain-containing proteins. To determine the specific steps in the CP and LP that are inhibited by Eap, we investigated whether Eap could block C4b or C3b deposition. We found that Eap inhibited C3b deposition by the CP and LP both in human and mouse serum (Fig. 1B, Fig. S1A), but Eap failed to block C4b deposition (Fig. 1C). Together, these results indicate that Eap blocks activation of C3, but not C4, via both the CP and LP of complement.

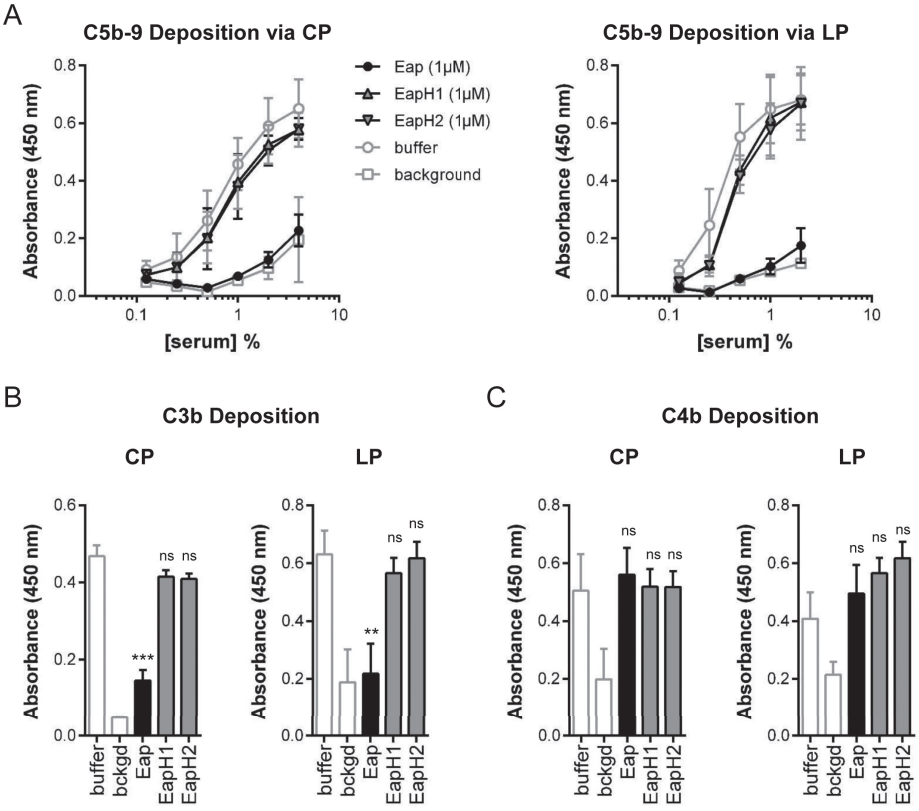

Figure 1. Eap inhibits complement activation via the classical and lectin pathways. The effect of Eap on distinct routes of complement activation was assessed via ELISA-based methods. (A) The effect of 1 μM Eap, EapH1, or EapH2 on CP (*left*) and LP-mediated (*right*) complement activation was measured across a dilution series of NHS. Activation was detected as C5b-9 deposition on an ELISA plate surface. (B) The effect of 1 μM Eap, EapH1, or EapH2 on CP and LP-mediated complement activation in 1% (v/v) NHS. Activation was detected as C3b deposition on an ELISA plate surface. (C) The same experiment as in (B), except that activation was detected as C4b deposition on an ELISA plate surface. Error bars represent the mean ± SD of three independent experiments. Measures of statistical significance in (B) and (C) were determined by an unpaired t-test of each experimental series versus buffer control. **, $p \leq 0.01$; ***, $p \leq 0.001$; ns, not significant.

Eap inhibits deposition of C3b at the *S. aureus* surface and blocks phagocytosis and killing

The results described above revealed that Eap specifically inhibits C3 activation via the CP and LP. Nevertheless, one limitation of these experiments is that they employed artificial activator and acceptor surfaces to study the complement response. To test whether Eap could impact an experimental system that more closely reflects the situation found *in vivo*, we examined the effect of Eap on C3b opsonization of the *S. aureus* cell surface. Although Eap is a secreted protein, approximately 30% of Eap rebinds the bacterial surface after secretion[15]. To address the role of surface-bound Eap in complement inhibition, we analyzed C3b deposition and subsequent phagocytosis for both the *S. aureus* Newman

WT strain and an isogenic *eap*-mutant strain (Δ*eap*) in parallel[14] (Fig. S1B). Neither assay revealed any difference in the level of C3b deposition or phagocytosis between the WT and mutant strain in the absence of exogenous Eap, suggesting that surface-retained Eap does not contribute significantly to *S. aureus* complement evasion (Fig. 2A, B). However, exogenously added Eap (1 μM) blocked deposition of C3b on both strains by nearly 50% across four different serum concentrations that ranged from 1% to 8% (v/v) (Fig. 2A). As expected, this diminished level of C3b opsonization in the presence of Eap significantly inhibited the efficiency with which neutrophils phagocytosed both strains (Fig. 2B).

We then used the Δ*eap* strain to conduct several additional experiments aimed at assessing the significance of Eap's effects on phagocytosis and its impact on bacterial sur-

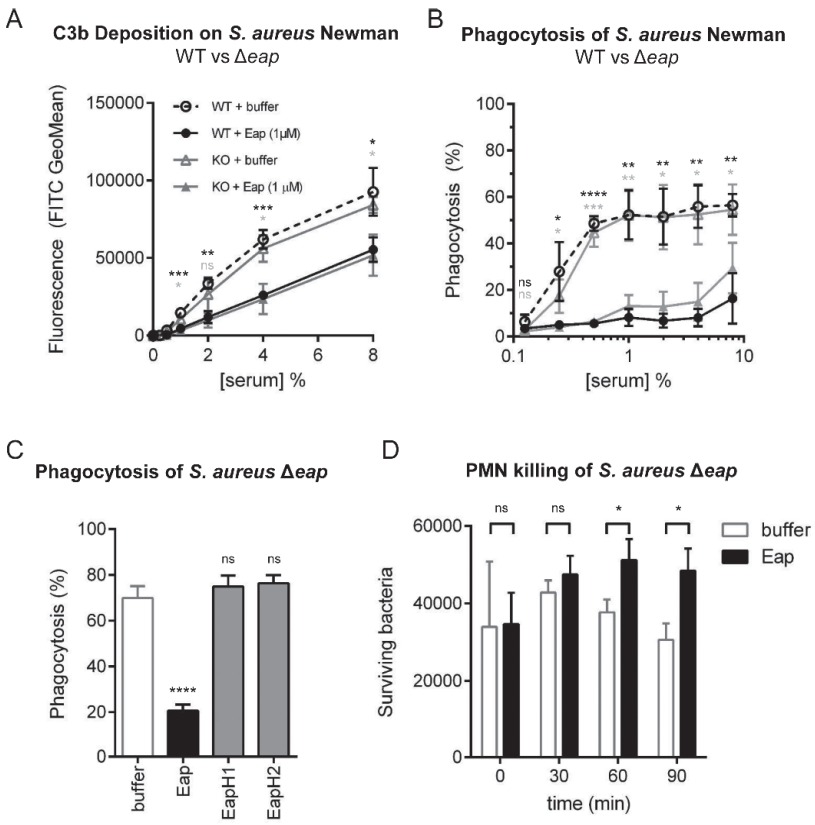

Figure 2. Eap inhibits opsonization, phagocytosis, and killing of *S. aureus*. The impact of recombinant Eap on complement deposition and phagocytosis of *S. aureus* Newman strains was assessed using flow cytometry. (A) C3b deposition on the surface of *S. aureus* Newman WT or Δ*eap* in the presence of 1 μM Eap or a buffer control. (B) Phagocytosis of *S. aureus* Newman WT or Δ*eap* in the presence of 1 μM Eap or a buffer control; legend as in (A). (C) Extent of phagocytosis of *S. aureus* Newman Δ*eap* using 1% (v/v) NHS in the presence of 1 μM Eap, EapH1, or EapH2, or a buffer control. (D) Neutrophil-mediated killing of *S. aureus* Newman Δ*eap* opsonized in the presence of 1 μM Eap or a buffer control. Error bars represent the mean ± SD of three independent experiments and at least two different donors. Measures of statistical significance were determined by an unpaired t-test of each experimental series versus the corresponding buffer control for each strain and serum concentration as appropriate. *, p≤0.05; **, p≤0.01; ***, p≤0.001; ****, p≤0.0001; ns, not significant.

vival. To begin, we found that inhibition of phagocytosis by increasing concentrations of Eap was both dose-dependent and saturable (Fig. S1C). Importantly, the concentration of Eap found in stationary liquid cultures of *S. aureus* (up to 10 μg/ml, or ~ 200 nM16) resulted in greater than 50% inhibition of phagocytosis by human neutrophils. While the concentration of Eap secreted into the human body during *S. aureus* infections remains uncertain, these data suggest that Eap-dependent inhibition of the CP/LP, and subsequently of phagocytosis, is likely physiologically relevant. Along these lines, and in concordance with the ELISA data presented above, this anti-phagocytic effect was not observed when either control protein EapH1 or EapH2 was added at the same exogenous concentration that resulted in potent inhibition of phagocytosis by Eap (Fig. 2C). Finally, we observed that diminished levels of phagocytosis likewise resulted in significantly diminished killing of *S. aureus* by human neutrophils (Fig. 2D). Together, these results indicate that secreted Eap specifically blocks CP/LP-mediated opsonization of *S. aureus* with C3b and subsequent phagocytosis and killing of *S. aureus* by neutrophils.

Eap binds with nanomolar affinity to complement component C4b

We observed that Eap bound an approximately 200 kDa protein present in EDTA-treated human serum but not in C4-depleted serum (Fig. S2A). While this result provided evidence that Eap binds to native C4, the functional studies presented above indicated that Eap inhibits an event within the CP and LP that mediates activation of C3 but leaves C4 activation intact. We therefore predicted that Eap must act on either the fully assembled CP/LP C3 convertase (C4b2a) or an isolated component thereof. As a first test of this hypothesis, we examined the behavior of purified C4b and a mixture of C4b and Eap by analytical size-exclusion chromatography (Fig. 3A, *left panel*). Inclusion of equimolar amounts of Eap in the C4b sample resulted in a pronounced shift of the peak to a larger apparent molecular weight that eluted as a single species. Indeed, bands corresponding to both Eap and C4b were present when the peak fractions were analyzed by Coomassie-stained SDS-PAGE (Fig. 3A, *right panel*). Due to potential inaccuracy of molecular weight estimates obtained from size-exclusion chromatography, we also used analytical ultracentrifugation to provide further characterization of the C4b/Eap complex. Sedimentation equilibrium data for both C4b/Eap and C4b alone were obtained at one concentration and were well-described by a single particle model (Fig. S2C). Whereas the molecular weight for C4b itself was estimated at 268 kDa, the apparent molecular weight C4b/Eap was estimated at 308 kDa. Since previous sedimentation equilibrium studies of Eap yielded an apparent molecular weight of 51 kDa for this protein[17], these data strongly suggest that Eap forms a 1:1 complex with C4b.

We next utilized a bead-based AlphaScreen assay to explore both the affinity and specificity of the C4b/Eap interaction in greater detail[18,19]. Whereas untagged Eap itself could diminish the luminescence signal generated by interaction between myc-tagged Eap and C4b-biotin in a dose-dependent manner, neither EapH1 nor EapH2 had any competitive effect even at the highest concentrations tested (Fig. 3B). Non-linear curve fitting of the C4b/Eap competition data revealed an apparent *K*d of 185 ± 14 nM for this

complex. Saturable binding of similar affinity was also observed when either native C4 or C4c was used as the competitor, and fit to apparent *K*d values of 45 ± 2 and 138 ± 16 nM, respectively (Fig. S2B). To study the C4b/Eap interaction through an independent approach, we constructed an SPR biosensor wherein C4b-biotin was uniformly immobilized on a streptavidin-coated surface similarly to what we have previously reported for C3b-biotin[10,18–20]. Significantly, neither EapH1 nor EapH2 bound the C4b surface even at concentrations 10-fold higher than those which showed clear evidence of C4b binding by Eap (Fig. 3C). Thus, the ability of Eap to bind C4b and the lack of C4b binding by EapH1 and EapH2 is in agreement with the inhibition of CP/LP function by Eap and the lack thereof by its homologues.

Eap binding to C4b and inhibition of the CP/LP requires the third domain of Eap

The modular architecture of the Eap protein raised questions as to whether a discrete combination of these domains is responsible for binding to C4b and, furthermore, wheth-

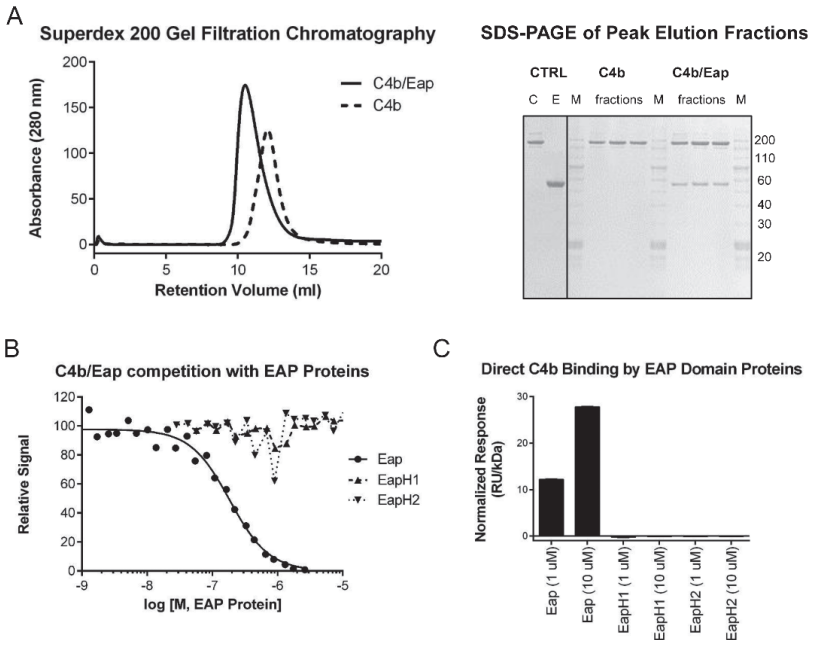

Figure 3. Eap forms a nanomolar affinity complex with complement component C4b. (A) Analysis of the C4b/Eap complex by analytical gel-filtration chromatography. Chromatograms for C4b and C4b/Eap (*left*) and Coomassie-stained SDS-PAGE analysis of the peak fractions from each injection (*right*). C, C4b; E, Eap; M, molecular weight marker. (B) The ability of untagged Eap, EapH1, and EapH2 to compete the AlphaScreen signal generated by myc-Eap and C4b-biotin was assessed over a logarithmic dilution series. While three independent trials were carried out, the data presented here are from single representative titrations. The smooth line indicates the outcome of fitting all points to a dose-response curve when competition was observed. (C) Binding of Eap, EapH1, and EapH2 to an oriented C4b-biosensor surface. The peak signals achieved following injection stop for samples at 1 and 10 μM, done in triplicate, were normalized to the molecular weight of their respective analyte proteins. Note that error bars are shown, but represent comparatively small variations due to the high precision of the assay system.

er that domain drives inhibition of CP/LP activity. To address these issues simultaneously, we overexpressed and purified a series of Eap fragments consisting of adjacent pairs of domains (i.e. Eap12, Eap23, and Eap34) as well as the individual Eap repeats themselves (i.e. Eap1, Eap2, Eap3, and Eap4) (Fig. 4A). Like EapH1 and EapH2, an equimolar mixture of the individual Eap repeats did not compete the luminescence signal generated by myc-Eap binding to C4b-biotin at concentrations up to 10 μM (Fig. 4B). Similarly, competition by Eap12 was detected only at the highest concentrations examined. By contrast, saturable binding of nearly equivalent affinity to Eap was observed in the same assay system for both Eap23 (*K*d = 293 ± 38 nM) and Eap34 (*K*d = 525 ± 65 nM) (Fig. 4B). Consistent with this, Eap23 and Eap34 both inhibited C5b-9 deposition via the CP and LP, though Eap34 did so at levels closer to Eap in both assays (Fig. 4C). In summary, the facts that (i) none of the individual Eap domains manifested clear C4b-binding or inhibitory properties against either the CP or LP, (ii) Eap12 bound C4b nearly 100-fold more weakly

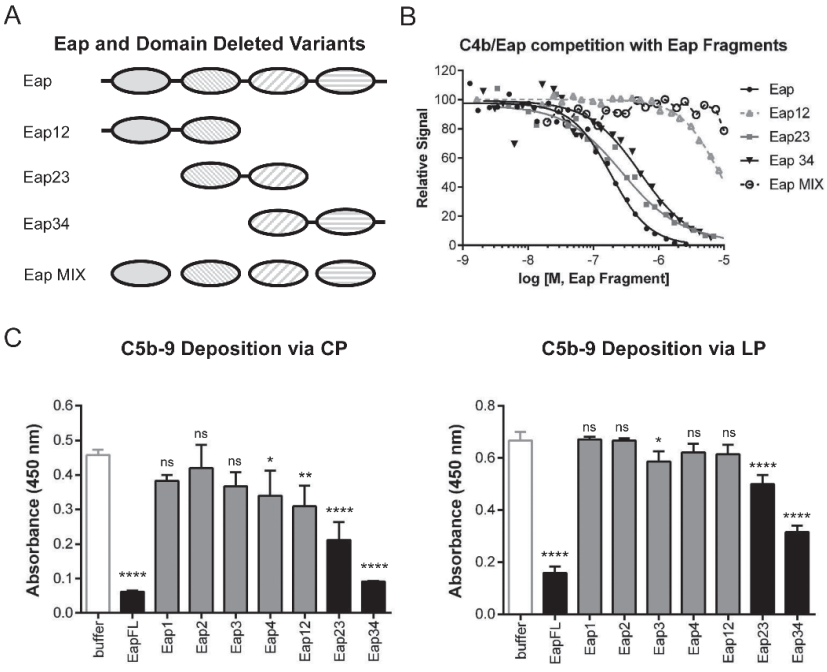

Figure 4. The third domain of Eap is necessary for C4b binding and inhibition of the CP/LP. (A) Diagram of full-length and domain-deleted forms of Eap used to map functional sites within Eap. (B) The ability of untagged Eap, Eap12, Eap23, Eap34, and an equimolar mixture of individual Eap domains (Eap MIX) to compete the AlphaScreen signal generated by myc-Eap and C4b-biotin was assessed over a logarithmic dilution series. While three independent trials were carried out, the data presented here are from a single representative titrations. The smooth line indicates the outcome of fitting all points to a dose-response curve when competition was observed. Legend is inset. (C) The effect of including 1 μM Eap, or various truncations thereof, on C5b-9 deposition on ELISA plates coated with either CP- (*left*) or LP-specific (*right*) activators. 1% (v/v) NHS was used as a source of complement components. Error bars represent the mean ± standard deviation of three independent experiments. Measures of statistical significance were determined by one-way ANOVA for the various Eap truncations versus buffer control alone. *, p≤0.05; **, p≤0.01; ****, p≤0.0001; ns, not significant.

than Eap itself and failed to inhibit both the CP and LP on its own, and (iii) Eap23 and Eap34 both bind C4b and inhibit the CP and LP indicate that domain Eap3 is necessary, but not sufficient for Eap binding to C4b and inhibition of the CP and LP.

Eap blocks binding of C2 to C4b by interfering with the initial C4b2 interaction

Formation of the CP/LP C3 convertase is a stepwise process that starts with the deposition of surface-bound C4b. Though C4b has no enzymatic activity of its own, it serves as a molecular platform first for binding of C2 to yield the C4b2 pro-convertase and then for C1s/MASP-dependent cleavage of C2 to generate a fully-active C4b2a convertase[1]. We examined whether Eap binding to C4b would inhibit binding of C2 to C4b, and thus disrupt formation of the C4b2 pro-convertase. Indeed, C2 efficiently diminished the luminescence signal in the AlphaScreen assay generated by myc-Eap and C4b-biotin with an apparent IC_{50} of 460 ± 32 nM (Fig. 5A). The C2 pro-protease is comprised of two

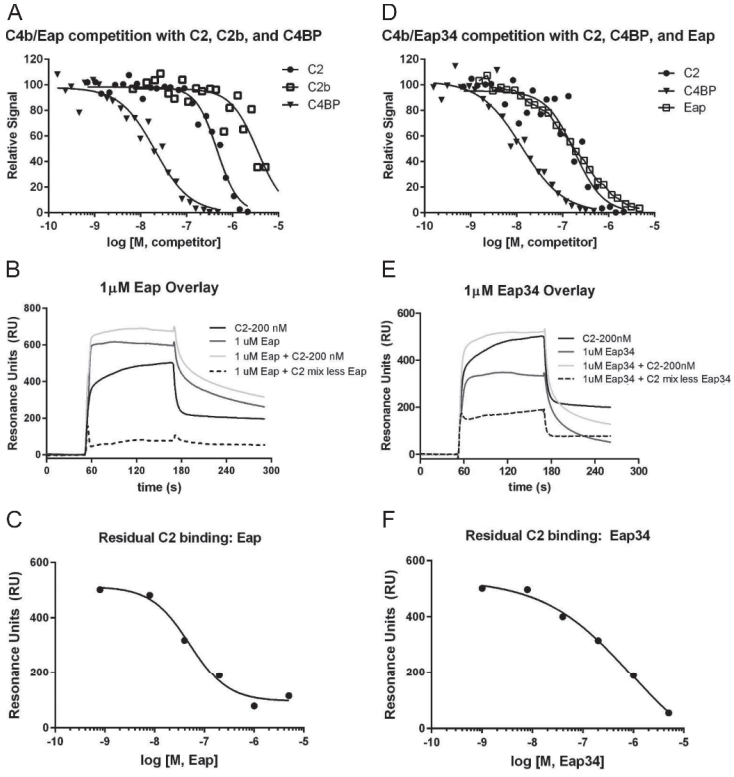

Figure 5. Eap binding inhibits the interaction of C2 with C4b. (A) The ability of recombinant human C2, C2b, and C4BP to compete the AlphaScreen signal generated by myc-Eap and C4b-biotin was assessed over a logarithmic dilution series. While three independent trials were carried out, the data presented here are from a single representative titration. The smooth line indicates the outcome of fitting all points to a dose-response curve. (B) Representative data from an SPR competition experiment where the effect of 1 μM Eap on the interaction of 200 nM C2 with a C4b-biotin surface was examined. The residual C2 binding in the presence of Eap is shown as a dashed line, while the sensorgram for the same concentration of C2 in the absence of any Eap is shown as the darkest black line. (C) Residual C2 binding in the presence of various concentrations of Eap fit to a dose-response curve (IC_{50} = 50 nM). (D) Identical experiment to (A), with the exception that the ability of recombinant human C2, C4BP, and Eap to compete the AlphaScreen signal generated by myc-Eap34 and C4b-biotin was assessed. (E) Identical experiment to (B), with the exception that Eap34 was used as the competitor instead of Eap. The residual C2 binding in the presence of Eap34 is shown as a dashed line, while the sensorgram for the same concentration of C2 is shown as the darkest black line. (F) Residual C2 binding in the presence of various concentrations of Eap34 fit to a dose-response curve (IC_{50} = 870 nM).

functionally discrete regions. Whereas the larger C2a region houses its serine protease module, the smaller C2b fragment provides the molecular basis for its initial interaction with C4b[21,22]. We therefore tested whether Eap inhibition of C2 binding to C4b might arise from disrupting the C4b2b interaction using the same AlphaScreen assay system described above. Although C2b bound to C4b with approximately 7.6-fold lower affinity than full-length C2 (IC_{50} = 3.5 ± 0.6 μM), it still effectively competed with Eap for C4b binding (Fig. 5A). Together, these data show that Eap shares a common binding site on C4b with C2 and, further, that this C4b site is also important for forming the initial interaction that gives rise to the CP/LP C3 pro-convertase, C4b2.

To test this inhibitory mechanism through an alternative approach, we devised an SPR strategy to investigate the outcome of increasing Eap concentrations on the ability of a C4b-biotin surface to bind C2 (Fig. 5B). In this experiment, if C4b were capable of binding Eap and C2 independently of one another, then the sensorgrams characteristic of the specific concentrations for each analyte alone would be strictly additive. Injection of 200 nM C2 in the presence of Eap resulted in a diminished response from what would be expected from two independent analytes, however. When the residual C2 contribution to the SPR signal from six different observations was fit to a dose-response curve as a function of Eap concentration, we obtained an IC_{50} value of approximately 50 nM (Fig. 5C). Since this figure is in reasonably good agreement with the *K*d of the C4b/Eap interaction (185 nM, as determined by AlphaScreen (Fig. 3B)), the outcome of this set of experiments provided an independent confirmation of the results presented in Fig. 5A above.

The requirement of Eap3 for both C4b binding (Fig. 4B) and inhibition of CP/LP activity (Fig. 4C) suggested that the ability to inhibit C4b2 binding should also be intrinsic to a minimal functional region of the Eap protein. To test this hypothesis, we established another AlphaScreen assay system where the ability of various ligands to inhibit the luminescence signal generated by myc-Eap34 binding to C4b-biotin could be assessed quantitatively. Using this approach, we determined that full-length C2 likewise competed with Eap34 for a binding site on C4b with an apparent IC_{50} of 180 ± 31 nM (Fig. 5D). While this apparent IC_{50} represents somewhat tighter binding than was observed for C2 competing the myc-Eap C4b-biotin pair (460 ± 32 nM), the higher noise level inherent to this latter assay may have affected the accuracy of fitting these data. Nevertheless, a repeat of the SPR competition assay, this time using Eap34 instead of full-length Eap, yielded similar results to those obtained previously (Fig. 5E). When the residual C2 contribution to the SPR signal from six different observations was fit to a dose-response curve as a function of Eap34 concentration, we obtained an IC_{50} value of approximately 870 nM (Fig. 5F). Again, this value is in good agreement with the *K*d of the C4b/Eap34 interaction (525 nM, as determined by AlphaScreen (Fig. 4B)). Thus, the observation that Eap34 on its own competes with C2 for C4b binding demonstrates that disruption of the initial pro-convertase assembly event is necessary for Eap-mediated inhibition of the CP/LP.

The Eap binding site on C4b represents a functional hotspot within the CP/LP

The CP/LP C3 convertase is only transiently stable when formed and decays with

a half-life of approximately 60 s at 37 °C23. This rate of spontaneous decay is greatly enhanced in the presence C4BP, which irreversibly dissociates C2a from its C4b scaffold and in addition serves as a cofactor for FI-mediated degradation of C4b to iC4b and C4c. Since the results presented here demonstrated that Eap effectively inhibits C4b2 binding, we examined whether Eap might also disrupt the interaction of C4BP with C4b. Through use of the AlphaScreen assay, we found that C4BP also competed with Eap for binding to C4b (Fig. 5A). Non-linear curve fitting of the competition data revealed an apparent IC_{50} of 21 ± 3 nM for the C4b/C4BP interaction, which represents approximately 9-fold tighter binding when compared to the C4b/Eap interaction (Fig. 3B). This suggests that Eap would not disrupt the inhibitory function of C4BP when both are present in equimolar concentrations. We obtained a similar result when C4BP was used to compete the luminescence signal generated by myc-Eap34 binding C4b-biotin (Fig. 5B), where non-linear curve fitting revealed an apparent IC_{50} of 13 ± 2 nM. It has to be noted, however, that this IC_{50} value reflects only the apparent affinity, and does not represent that of the individual C4b binding sites present within the polyvalent C4BP assembly[24].

Since Eap binds C4b at a similar site as C4BP, we tested whether Eap itself might display intrinsic cofactor activity to stimulate FI-mediated proteolysis of C4b. When purified C4b was incubated with both C4BP and FI, we were able to show rapid degradation of C4b into iC4b and then C4c, as judged by SDS-PAGE and LC-MS/MS of tryptic peptides derived from various bands on gel (Fig. S3A, *top panel, left*). However, substitution of Eap for C4BP in an otherwise identical assay provided no evidence for proteolysis of C4b by FI (Fig. S3A, top panel, right). Thus, while Eap has no intrinsic FI co-factor activity, it shares a C4b binding site with multiple factors critical to the function and regulation of the CP/LP. We therefore propose that the Eap binding site on C4b represents a functional hotspot within the CP/LP, and that this hotspot is analogous to what we previously described for the binding site of the SCIN family of AP inhibitors on C3b[6,18,20,25].

DISCUSSION

Although a number of recent studies have described unique mechanisms deployed by *S. aureus* to disrupt and evade human immunity, a large majority of these have focused on strategies that specifically target components within the complement AP (e.g. C3b). In this study, however, we used a biochemical screening strategy to identify *S. aureus* Eap as an inhibitor of both the CP and LP. Inhibition of the CP/LP is specific to Eap, since this activity is not found in either of its closest structural homologs, EapH1 and EapH2, that also adopt the β-grasp fold characteristic of EAP domains[9,26]. Eap-mediated inhibition of the CP and LP occurs directly, since it arises from Eap forming a nanomolar affinity complex with a shared component of both pathways, C4b. Thus, instead of expressing specific inhibitors for the CP and LP separately, our results show that *S. aureus* simultaneously disrupts the two most potent complement initiation routes via a single protein, Eap. On this basis, we believe that Eap defines both a novel mechanism of staphylococcal immune evasion and a new class of complement regulatory proteins.

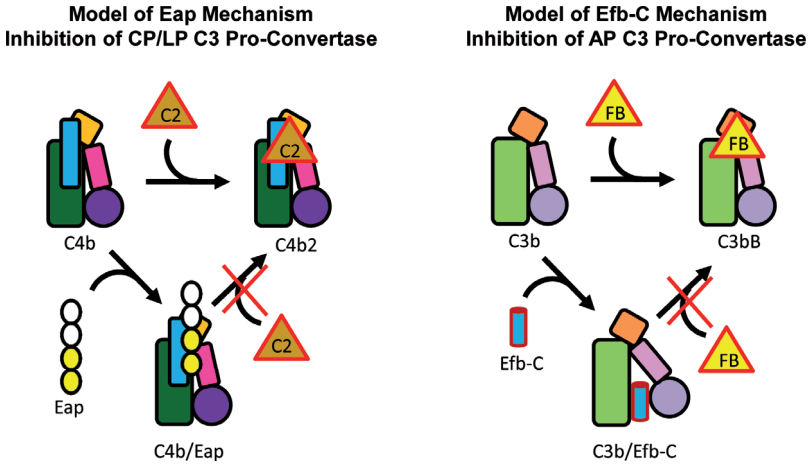

Figure 6. Proposed mechanism for Eap-mediated inhibition of the CP/LP C3 and its similarities to the *S. aureus* AP inhibitor, Efb-C. The overall structural similarities between C4b and C3b are represented by the similar shapes of their cartoon representations. The shaded green rectangle represents the macroglobulin-like core, the orange square the C345C domain, the small pink rectangle the CUB domain, and filled circle the thioester-containing domain (i.e. C4d and C3d). The thin blue rectangle represents the γ-chain unique to C4/b. (A) The inhibitor Eap is shown with two domains filled in yellow to represent the domains 3 and 4 'active site', as described in Figs. 4 and 5. (B) The inhibitor Efb-C is shown as a blue cylinder. Efb-C binding to the C3d domain[45] and stabilization of an open, inactive conformation of C3b that is unable to bind FB[10] is depicted by reorientation of the CUB-TED region relative to the macroglobulin-like core of C3b.

A number of other significant bacterial and fungal pathogens have also been shown to subvert the activity of CP and LP (Reviewed in[3,27]). However, nearly all of these organisms evade the CP and LP via adsorption of the naturally occurring CP/LP regulator, C4BP, to their surface via expression of specific C4BP binding proteins. This is conceptually similar to evasion of the AP through cell-surface adsorption of FH via FH-binding proteins, which is very likely the single most widely distributed complement evasion strategy among pathogens[3,27]. Interestingly, the fact that Eap functions not by binding to a naturally occurring regulator (i.e. C4BP), but through the altogether distinct mechanism of blocking initial stages of CP/LP C3 pro-convertase assembly mirrors what we have previously described for *S. aureus* evasion of the AP (Reviewed in[6]). Here, expression and secretion of factors such as SCIN-A, SCIN-B/-C, Efb, and Ehp/Ecb has been demonstrated to interfere with one or more of the molecular events required to assemble and/or regulate the fully active AP C3 convertase, C3bBb. For whatever reason, it seems that *S. aureus* has taken a unique evolutionary path that has led it to produce multiple inhibitors that act by binding directly to either C3b or C4b, which themselves serve as essential scaffolds for assembly of all C3 and C5 convertases. Although the possibility that *S. aureus* also absorbs native host regulators FH[28] and C4BP[29] cannot be discounted, an overwhelming amount of structural, biochemical, functional, and immunological evidence in the literature strongly suggests that direct inhibition of convertase assembly, dynamics, and function, rather than indirect disruption via adsorption of fluid-phase regulators, is of paramount importance to *S. aureus* pathogenesis.

Our functional data demonstrate that Eap blocks both the CP and LP at the level of C3 activation. This inhibition arises from impaired formation of the CP/LP C3 pro-convertase, C4b2, which would subsequently reduce formation of the active CP/LP C3 convertase, C4b2a. The mechanistic basis of CP/LP inhibition by Eap therefore appears very similar to AP inhibition by Efb-C, which itself binds to C3b and reduces formation of the AP C3 pro-convertase, C3bB, by nearly 80%[10] (Fig. 6). An important distinction between Eap and Efb-C, however, is that the latter has been shown to act in an allosteric manner[10]. Our observation of direct competition for C4b binding between Eap and both C2 and C2b seems to favor a purely steric mechanism for Eap inhibition of CP/LP C3 convertase formation, although the possibility of Eap-dependent 'action-at-a-distance' type effects on C4b cannot be dismissed without significantly more structural insights into these interactions. Still, the fact that Eap also blocks the C4b/C4BP interaction strongly suggests that the Eap binding site on C4b constitutes a functional 'hotspot' for CP/LP C3 convertase formation, dynamics, and function. This raises some attractive conceptual analogies between Eap and the SCIN family of C3b-binding AP C3 convertase inhibitors[6,18,20]. Furthermore, it also suggests that effective targeting of these functional 'hotspots' that exist in various host response pathways might be a central theme behind pathogen-specific evolution of innate immune evasion mechanisms.

Given its potent effects on the CP and LP, it is perhaps not surprising that Eap has been shown to promote staphylococcal virulence in rodent models of both acute peritonitis[30], as well as chronic arthritis, osteomyelitis, and abscess formation[31]. Though the precise contributions of the CP and LP remain to be fully evaluated in each of these experimental systems, the consistent requirement of Eap for maximal levels of staphylococcal virulence in such studies is difficult to ignore. Moreover, the discovery that patients with demonstrated *S. aureus* infections present with high titers of anti-Eap antibodies[32], and that their titers of anti-Eap IgG correlate with the severity of infection[32], strongly suggests that Eap inhibition of the CP/LP is relevant to human disease as well. Along these lines, we have recently made the unexpected observation that all staphylococcal EAP domain-containing proteins (i.e. Eap, EapH1, and EapH2) are capable of high-affinity, non-covalent inhibition the innate immune serine proteases neutrophil elastase, cathepsin G, and proteinase-3[14]. These so-called 'neutrophil serine proteases' (NSPs), which are stored in azurophilic granules and released upon neutrophil activation, serve a number of crucial roles in both neutrophil effector functions and in the innate cellular response against invading microorganisms such as *S. aureus*[33]. The fact that complement activity is based upon a series of site-specific proteolyses seems to suggest that EAP domain-mediated inhibition of NSPs must share basic molecular-level features with inhibition of the CP/LP by Eap. However, our observations that (i) CP/LP inhibition is specific to Eap, and not intrinsic to all EAP domains (Figs. 1 and 2), (ii) this inhibition is based upon the unique ability of Eap to bind C4b (Figs. 3 and 4), and (iii) Eap blocks, rather than promotes recruitment of the C2 pro-protease to C4b (Fig. 5), as might otherwise be expected for a high-affinity protease inhibitor14, argue that the structural basis for Eap's effects on the CP/LP must be altogether distinct from EAP domain inhibition of NSPs. Understand-

ing the nature of these distinctions at the structural level should therefore prove to be a very informative endeavor.

Though much remains to be learned in that regard, it is already abundantly clear that a number of debilitating and potentially lethal human diseases have been linked to either acute or chronic overactivation of the complement CP and/or LP[34–36]. Among these are ischemia/reperfusion injuries, rheumatoid arthritis, systemic lupus erythematosus, multiple sclerosis, and even Alzheimer's disease. Since many of these diseases are only poorly managed by current therapeutic regimens, our discovery of Eap as a potent CP/LP inhibitor raises the possibility that improved treatment of these conditions might come through further detailed study of Eap, its molecular interactions, and its ability to specifically attenuate CP/LP activity *in vivo*. Since high levels of anti-Eap antibodies are found in even healthy persons[32], direct use of Eap as a therapeutic is unlikely, due to greatly increased risk of immune complex disease. Thus, future work aimed at discovering either non-immunogenic peptides, peptidomimetics, or even small molecules that retain Eap-like inhibitory activities on the CP/LP will be necessary to exploit Eap's promise within these areas.

ACKNOWLEDGEMENTS

We thank Dr. Edimara S. Reis, Dr. Apostolia Tzekou and Ms. Antigonia Ulndreaj for their assistance in the functional analysis of Eap. We also thank Prof. Matthias Herrmann and Dr. Markus Bischoff for providing samples of Eap from *S. aureus* strain Newman.

This work was supported by U.S. National Institutes of Health grants AI071028 and AI113552 to B.V.G., and AI068730, AI030040, and AI097805 to J.D.L, and by a Vidi grant from the Netherlands Organization for Scientific Research (NWO-Vidi, #91711379) to S.H.M.R.

MATERIALS AND METHODS

Preparation of Native and Recombinant Proteins

Human serum proteins C3, C3b, C4, C4b, C1s, C4b-binding protein (C4BP), and factor I (FI) were obtained in purified form from Complement Technologies (Tyler, TX). Recombinant forms of C2 and C2b were expressed and purified from the conditioned culture medium of transiently transfected human embryonic kidney (HEK)-293 cells according to the general methods described previously[37]. All recombinant *S. aureus* proteins were overexpressed and purified according to the general methods described previously[38], with the exception that recombinant, full-length Eap was prepared according to the published protocol of Xie *et al.*[13].

Human Derived Materials

Blood was drawn from healthy adult volunteers after obtaining informed consent and approval of the protocol by the medical-ethical committee of the University Medical Center Utrecht (Utrecht, The Netherlands). Normal human serum (NHS) was isolated as described before[39] and frozen at -80 °C until needed for further use. For neutrophil preparation, heparinized vacutainers (Becton Dickinson) were used and neutrophils were isolated over a ficol/histopaque gradient as described previously[40].

Complement Pathway Activity on an Artificial Surface

Functional activity of the CP, LP and AP was determined essentially as described[11]. In short, Nunc-Maxisorb ELISA plates were coated overnight to specifically activate the CP (coated with 3 µg/ml human IgM (Calbiochem)), LP (coated with 20 µg/ml *Saccharomyces cerevisiae* mannan (Sigma)), or AP (coated with 20 µg/ml *Salmonella enteriditis* LPS (Sigma)). Plates were blocked with 1% (w/v) BSA in PBS with 0.05% (v/v) Tween 20 (Merck). The indicated percentages of NHS or mouse serum (Innovative Research) were incubated with 1 µM of recombinant *S. aureus* proteins in the appropriate assay buffers for a maximum of 5 min at 25 °C (veronal-buffered saline (VBS) at pH 7.5 with 0.1% (w/v) gelatin, 500 µM CaCl2, and 250 µM MgCl2 for CP and LP; VBS at pH 7.5 with 0.1% (w/v) gelatin, 5 mM MgCl2, and 10 mM EGTA for AP). Deposited C3b, C4b, and C5b-9 were detected with specific antibodies (0.1 µg/ml α-human C3c WM-1 clone digoxigenin (DIG) labeled or 1 µg/ml rat-α-mouse C3 (Hycult, HM1078), American Type Culture Collection; 1 µg/ml αC4d, Quidel; 1 µg/ml αC5b-9 aE11, Santa Cruz respectively). Secondary, HRP-labeled antibodies were detected with 100 µg/ml tetramethylbenzidine and 60 µg/ml ureum peroxide in 100 mM sodium acetate buffer at pH 6.0. The reaction was stopped by adding an equal volume of 2 M H2SO4, and the absorbance at 450 nm was measured using a BioRad microplate reader.

Complement Deposition on S. aureus

S. aureus Newman WT or Δ*eap* (MR1811)[14] were grown on a blood-agar plate overnight at 37 °C. Bacteria were resuspended in assay buffer (20 mM HEPES (pH 7.4) with 140 mM NaCl, 0.5 mM CaCl2, 0.25 mM MgCl2, and 0.1% (w/v) BSA). Eap (1 µM) was added to the indicated concentrations of NHS and this mixture was added directly to the bacteria (8×10^6 CFU) in a total volume of 100 µl and incubated at 37 °C with shaking for 10 min. Unbound components were washed away with assay buffer and deposited C3b was quantified by flow cytometry (FACS Verse, BD) by using the specific FITC-conjugated goat $F(ab')_2$ anti-human-C3 (Protos Immunoresearch, Burlingame, CA).

Phagocytosis Assays

S. aureus Newman WT or Δ*eap* transformed with pCM2941, a vector inducing constitutive expression of superfolded GFP (sGFP) under the *sarA* promotor, was grown in Todd-Hewitt broth (THB) until an OD_{600} of 0.5. Bacteria were washed with RPMI-1640 (Invitrogen) supplemented with 0.05% (w/v) human serum albumin (HSA; Sanquin), aliquoted, and stored at -80 °C until use. Eap, EapH1 or EapH2 (1 µM) was added to the indicated concentrations of NHS in RPMI/HSA and directly added to the thawed bacteria (2.5×10^6 CFU) Then, 2.5×10^5 isolated neutrophils were added to obtain a total volume of 250 µl and incubated at 37 °C with shaking at 600 rpm for 15 min. The reaction was stopped by adding 100 µl ice-cold 2% (v/v) paraformaldehyde. Phagocytosis was assessed by flow cytometry (FACS Verse, BD). Graphs show the percentage of GFP-positive neutrophils. The fluorescent signal exclusively originated from intracellular bacteria, as verified by confocal microscopy.

Neutrophil-mediated Killing

S. aureus Newman WT or Δ*eap* were grown in THB to OD_{660} of 0.5 (corresponding to 2×10^8 CFU/ml). Eap was added in 1 µM and 10 % NHS was added for 15 min at 25 °C in RPMI/HSA to allow for opsonization. Opsonized bacteria (5×10^4 CFU) were incubated with 9×10^4 neutrophils in 100 µl RPMI/HSA. The reaction was stopped at the indicated time points with 900 µl ice-cold 0.1% saponin (w/v). After 15 min. the samples were resuspended via a 25-Gauge needle, to assure lysis of the neutrophils[42]. Surviving bacteria were enumerated by plating serial dilutions on Luria broth-agar plates.

Eap Affinity Isolation of Human Serum Proteins

A recombinant form of Eap that harbored a single, N-terminal cysteine was expressed and purified from *E. coli* similarly to wild-type Eap[13]. Eap produced in this manner was site-specifically biotinylated using EZ-link Maleimide-PEG2-Biotin reagent according to manufacturer's suggestions (ThermoFisher, Inc.). Following derivatization, 2 µg of Eap-biotin were added to samples containing either 20 µl EDTA serum or C4-depleted serum (Complement Technologies), and an appropriate quantity of PBS to give a final volume of 100 µl. The samples were incubated for 1 h at room temperature, after which time 30 µl of 50% (v/v) slurry of magnetic streptavidin-coated Dynabeads were added (Invitrogen, Inc.). Following an additional 15 min incubation, the beads were isolated via a magnet, washed three times with 100 µl of PBS, and all remaining liquid was removed

by aspiration. 15 µl of non-reducing Laemmli buffer were added to each sample, and 5 µl of each sample were analyzed by SDS-PAGE followed by staining with Coomassie Brilliant Blue.

Stoichiometry and Molecular Weight Estimations

The apparent molecular weight and stoichiometry of the C4b/Eap complex was determined by a combination of size-exclusion chromatography and sedimentation equilibrium analytical ultracentrifugation. For chromatographic analysis, samples consisting of either C4b or C4b/Eap (20 µM final concentration) were prepared and 100 µl were injected at 0.75 ml/min onto a Superdex S200 Increase 10/30 column that had been previously equilibrated at 4 °C in a buffer of PBS. The contents of peak fractions were analyzed by Coomassie-stained SDS-PAGE of samples that had been prepared under non-reducing conditions. For sedimentation equilibrium analysis, all experiments were performed using a Beckman XL-I ultracentrifuge with a four-position analytical, titanium (AN-Ti) rotor. Protein solutions (1.6 µM C4b or C4b/Eap complex in PBS; 110 µl) and dialysate buffer (PBS; 120 µl) were placed in the double-sector centrifuge cells. The samples were equilibrated at 4 °C at 6,000 rpm and the approach to equilibrium was monitored by repetitive absorption scans at 280 nm every 6 h. The apparent equilibrium was reached after ~ 60 h. After the final data collection, the rotor was accelerated to 42,000 rpm for ~ 2 h and the cells were scanned to obtain the baseline absorption value. Data were analyzed with the software supplied with the instrument (Beckman-Coulter, Inc.). Both the protein partial specific volume and buffer density were calculated using Sednterp software (http://bitcwiki.sr.unh.edu/index.php/Main_Page).

Biotinylation of C4b

Biotinylated C4b was prepared by overnight, room-temperature incubation of native C4 (1 mg/ml final concentration) with C1s (5 µg/ml final concentration) in the presence of EZ-link Maleimide-PEG2-Biotin reagent according to manufacturer's suggestions (ThermoFisher, Inc.). The reaction mixture (250 µl in PBS (pH 7.0)) was buffer exchanged into 20 mM tris (pH 8.0), applied to a 1 ml Resource Q anion exchange column (GE LifeSciences), and the bound proteins eluted with a gradient to 1 M NaCl over 10 column volumes. Fractions containing biotinylated-C4b were identified and characterized by a combination of SDS-PAGE and Western blotting using streptavidin-conjugated HRP (ThermoFisher, Inc.). Purified C4b-biotin was pooled, quantified spectrophotometry, and stored at 4 °C in the existing buffer until further use.

AlphaScreen Binding Assays

An AlphaScreen equilibrium competition assay was used to derive both positional information and apparent dissociation constants for C4b binding to various complement components and staphylococcal inhibitors. This assay system is based upon modification of a previously published protocol[18] and is established via the following principle: a luminescence signal is generated by laser excitation of a streptavidin-coated donor bead, which recognizes C4b-biotin that binds directly to a second target protein (in this case myc-Eap), which itself can be adsorbed to an acceptor bead coated with anti-c-myc monoclonal IgG. C4b/Eap competition binding assays were carried out in a total volume of 25 µl by adding each assay component to the following final concentrations: 50 nM myc-Eap, 5 nM C4b-biotin, 20 µg/µl anti-c-myc AlphaScreen acceptor beads, and 20 µg/µl AlphaScreen donor beads. A dilution series was prepared for each unlabeled competitor protein of interest. Reactions were performed over 2.5 h and were begun by incubating the C4b-biotin, myc-Eap, and a given concentration of each competitor protein for 1 h. Following this, the acceptor beads were added, incubated for an hour, then the donor beads were added and incubated for an additional 0.5 h. At that point, the donor beads were excited at 680 nm and the evolving AlphaScreen signal (photon counts/s at 630 nm) for each data point was measured using an EnSpire multimode plate reader (Perkin Elmer Life Sciences). Data analysis and curve fitting was carried out as previously described[18].

Surface Plasmon Resonance Experiments

Interactions between C4b-biotin and the *S. aureus* proteins Eap, EapH1, and EapH2 were measured by surface plasmon resonance (SPR) using either a BiaCore X or BiaCore 3000 instrument (GE Life Sciences) at room temperature. PBS-T (i.e. PBS (pH 7.0) with 0.005% (v/v) Tween-20) was used as the running buffer throughout the entire set of experiments. C4b-biotin was captured on a streptavidin sensor chip (GE Life Sciences) to a density of approximately 5,000 resonance units (RU). Ligands were diluted to their working concentrations in PBS-T. For comparison of EAP-domain proteins' binding to C4b, samples were prepared at 1 and 10 µM and injected for 1 min at a flow rate of 20 µl/min, followed by a dissociation phase of 2 min. Signals were normalized

to the molecular weight of each respective analyte to allow for a ranking of Eap, EapH1, and EapH2 relative affinities for C4b. Surface regeneration was achieved by injecting a solution of 1 M NaCl. Data analyses were carried out using the BiaEvaluation software suite (GE Life Sciences).

An SPR assay was also used to assess the competition between Eap and C2 for binding to C4b[20]. Briefly, a C4b-biotin surface was prepared as described above and a room temperature running buffer of HBS-CMT (20 mM HEPES (pH 7.4), 150 mM NaCl, 5 mM CaCl2, 5 mM MgCl2, and 0.005% (v/v) Tween-20) with a flow rate of 20 µl/min was used for all injections. C2 was injected in triplicate at a concentration of 200 nM to establish a basal level of C2 binding. This concentration was held constant for the competition experiments, which were carried out by varying either the Eap or Eap34 concentration over six points from 5000 nM to 8 nM. To calculate residual C2 binding, the sensorgram of the corresponding Eap/Eap34 injection alone was subtracted from the Eap/Eap34+C2 injection series. The averaged response for the 5 s preceding the injection stop was plotted against the concentration of Eap/Eap34 and fit to a dose-response inhibition curve by non-linear regression as previously described18. Regeneration of the surface was carried out with 2 M NaCl for 2 min followed by 0.2 M sodium citrate for 2 min.

FI Proteolysis Assay

Sequential FI-dependent proteolysis of C4b to iC4b and C4c was monitored by an SDS-PAGE based method. A sample of C4b (0.4 µg/µl in PBS) was incubated with purified FI (0.01 µg/µl) either in the presence or absence of C4BP (0.09 µg/µl), and/or various concentrations of Eap (0, 0.01, 0.06, and 0.6 µg/µl, respectively). Aliquots reflecting the time-course of proteolysis were withdrawn at 0, 2, 5, 10, and 20 min, and the reaction was quenched by addition of Laemmli sample buffer with β-mercaptoethanol to reduce disulfide bonds. Samples were separated on a 10% (w/v) tris-tricine polyacrylamide gel and stained with Coomassie blue. Excised gel bands were reduced, alkylated and subjected to in-gel trypsin digestion by standard methods, and extracted peptides were analyzed by tandem MS as described previously[43]. Identification of activated C4 fragments was accomplished using Mascot 2.4 (Matrix Science, Ltd.) with semi-trypsin specificity. Individual band staining intensities and ratios were quantified by ImageJ[44].

Statistics

All analyses were performed in GraphPad Prism 6.0.

REFERENCES

1. Ricklin D, Hajishengallis G, Yang K, Lambris JD: Complement: a key system for immune surveillance and homeostasis. *Nat. Immunol.* 2010, 11:785–797.
2. Harboe M, Ulvund G, Vien L, Fung M, Mollnes TE: The quantitative role of alternative pathway amplification in classical pathway induced terminal complement activation. *Clin. Exp. Immunol.* 2004, 138:439–446.
3. Lambris JD, Ricklin D, Geisbrecht BV: Complement evasion by human pathogens. *Nat. Rev. Microbiol.* 2008, 6:132–142.
4. Laarman A, Milder F, van Strijp J, Rooijakkers S: Complement inhibition by gram-positive pathogens: molecular mechanisms and therapeutic implications. *J. Mol. Med.* 2010, 88:115–120.
5. Zecconi A, Scali F: Staphylococcus aureus virulence factors in evasion from innate immune defenses in human and animal diseases. *Immunol. Lett.* 2013, 150:12–22.
6. Garcia BL, Ramyar KX, Ricklin D, Lambris JD, Geisbrecht BV: Advances in understanding the structure, function, and mechanisms of the SCIN and Efb families of Staphylococcal immune evasion proteins. *Adv. Exp. Med. Biol.* 2012, 946:113–133.
7. Rooijakkers SHM, Ruyken M, Roos A, Daha MR, Presanis JS, Sim RB, Van Wamel WJB, Van Kessel KPM, van Strijp JAG: Immune evasion by a staphylococcal complement inhibitor that acts on C3 convertases. *Nat. Immunol.* 2005, 6:920–927.
8. Jongerius I, Köhl J, Pandey MK, Ruyken M, van Kessel KPM, van Strijp JAG, Rooijakkers SHM: Staphylococcal complement evasion by various convertase-blocking molecules. *J. Exp. Med.* 2007, 204:2461–2471.
9. Geisbrecht BV., Hamaoka BY, Perman B, Zemla A, Leahy DJ: The crystal structures of EAP domains from Staphylococcus aureus reveal an unexpected homology to bacterial superantigens. *J. Biol. Chem.* 2005, 280:17243–17250.
10. Chen H, Ricklin D, Hammel M, Garcia BL, McWhorter WJ, Sfyroera G, Wu Y-Q, Tzekou A, Li S, Geis-

brecht BV, et al.: Allosteric inhibition of complement function by a staphylococcal immune evasion protein. *Proc. Natl. Acad. Sci. U. S. A.* 2010, 107:17621–17626.
11. Roos A, Bouwman LH, Munoz J, Zuiverloon T, Faber-Krol MC, Fallaux-van den Houten FC, Klar-Mohamad N, Hack CE, Tilanus MG, Daha MR: Functional characterization of the lectin pathway of complement in human serum. *Mol. Immunol.* 2003, 39:655–668.
12. Hussain M, Becker K, Von Eiff C, Peters G, Herrmann M: Analogs of Eap Protein Are Conserved and Prevalent in Clinical Staphylococcus aureus Isolates. *Clin. Diagn. Lab. Immunol.* 2001, 8:1271–1276.
13. Xie C, Alcaide P, Geisbrecht BV., Schneider D, Herrmann M, Preissner KT, Luscinskas FW, Chavakis T: Suppression of experimental autoimmune encephalomyelitis by extracellular adherence protein of Staphylococcus aureus *J. Exp. Med.* 2006, 203:985–994.
14. Stapels DAC, Ramyar KX, Bischoff M, von Köckritz-Blickwede M, Milder FJ, Ruyken M, Eisenbeis J, McWhorter WJ, Herrmann M, van Kessel KPM, et al.: Staphylococcus aureus secretes a unique class of neutrophil serine protease inhibitors. *Proc. Natl. Acad. Sci. U. S. A.* 2014, 111:13187–13192.
15. Flock M, Flock J: Rebinding of Extracellular Adherence Protein Eap to Staphylococcus aureus Can Occur through a Surface-Bound Neutral Phosphatase. *J. Bacteriol.* 2001, 183:3999–4003.
16. Palma M, Haggar A, Flock J-I: Adherence of Staphylococcus aureus is enhanced by an endogenous secreted protein with broad binding activity *J. Bacteriol.* 1999, 181:2840–2845.
17. Hammel M, Nemecek D, Keightley JA, Thomas GJJ, Geisbrecht BV: The Staphylococcus aureus extracellular adherence protein (Eap) adopts an elongated but structured conformation in solution. *Protein Sci.* 2007, 16:2605–2617.
18. Garcia BL, Summers BJ, Lin Z, Ramyar KX, Ricklin D, Kamath DV, Fu Z-Q, Lambris JD, Geisbrecht BV: Diversity in the C3b convertase contact residues and tertiary structures of the staphylococcal complement inhibitor (SCIN) protein family. *J. Biol. Chem.* 2012, 287:628–640.
19. Garcia BL, Summers BJ, Ramyar KX, Tzekou A, Lin Z, Ricklin D, Lambris JD, Laity JH, Geisbrecht BV: A Structurally Dynamic N-terminal Helix Is a Key Functional Determinant in Staphylococcal Complement Inhibitor (SCIN) Proteins. *J. Biol. Chem.* 2013, 288:2870–2881.
20. Ricklin D, Tzekou A, Garcia BL, Hammel M, McWhorter WJ, Sfyroera G, Wu Y-Q, Holers VM, Herbert AP, Barlow PN, et al.: A molecular insight into complement evasion by the staphylococcal complement inhibitor protein family. *J. Immunol.* 2009, 183:2565–2574.
21. Kerr MA, Parkes C: The effects of iodine and thiol-blocking reagents on complement component C2 and on the assembly of the classical-pathway C3 convertase. *Biochem J.* 1984, 219:391–399.
22. Milder FJ, Raaijmakers HCA, Vandeputte MDAA, Schouten A, Huizinga EG, Romijn RA, Hemrika W, Roos A, Daha MR, Gros P: Structure of complement component C2A: implications for convertase formation and substrate binding. *Structure* 2006, 14:1587–1597.
23. Kerr MA: The human complement system: assembly of the classical pathway C3 convertase. *Biochem J.* 1980, 189:173–181.
24. Blom AM, Villoutreix BO, Bahlbäck B: Complement inhibitor C4b-binding protein - friend or foe in the innate immune system? *Mol. Immunol.* 2004, 40:1333–1346.
25. Garcia BL, Ramyar KX, Tzekou A, Ricklin D, McWhorter WJ, Lambris JD, Geisbrecht BV: Molecular basis for complement recognition and inhibition determined by crystallographic studies of the staphylococcal complement inhibitor (SCIN) bound to C3c and C3b. *J. Mol. Biol.* 2010, 402:17–29.
26. Papageorgiou AC, Acharya KR: Microbial superantigens : from structure to function. *Trends Microbiol.* 2000, 8:369–375.
27. Blom AM, Hallström T, Riesbeck K: Complement evasion strategies of pathogens - Acquisition of inhibitors and beyond. *Mol. Immunol.* 2009, 46:2808–2817.
28. Sharp JA, Cunnion KM: Disruption of the alternative pathway convertase occurs at the staphylococcal surface via the acquisition of factor H by Staphylococcus aureus. *Mol. Immunol.* 2011, 48:683–690.
29. Hair PS, Wagner SM, Friederich PT, Drake RR, Nyalwidhe JO, Cunnion KM: Complement regulator C4BP binds to Staphylococcus aureus and decreases opsonization. *Mol. Immunol.* 2012, 50:253–261.
30. Chavakis T, Hussain M, Kanse SM, Peters G, Bretzel RG, Flock J-I, Herrmann M, Preissner KT: Staphylococcus aureus extracellular adherence protein serves as anti-inflammatory factor by inhibiting the recruitment of host leukocytes. *Nat. Med.* 2002, 8:687–693.
31. Lee LY, Miyamoto YJ, Mcintyre BW, Höök M, Mccrea KW, Mcdevitt D, Brown EL: The Staphylococcus aureus Map protein is an immunomodulator that interferes with T cell – mediated responses. *J. Clin. Invest.* 2002, 110:1461–1471.

32. Joost I, Jacob S, Utermöhlen O, Schubert U, Patti JM, Ong M-F, Gross J, Justinger C, Renno JH, Preissner KT, et al.: Antibody response to the extracellular adherence protein (Eap) of Staphylococcus aureus in healthy and infected individuals. *FEMS Immunol. Med. Microbiol.* 2011, 62:23–31.
33. Amulic B, Cazalet C, Hayes GL, Metzler KD, Zychlinsky A: Neutrophil function: from mechanisms to disease. *Annu. Rev. Immunol.* 2012, 30:459–489.
34. Ricklin D, Lambris JD: Complement in immune and inflammatory disorders: therapeutic interventions. *J. Immunol.* 2013, 190:3839–3847.
35. Ricklin D, Lambris JD: Complement in immune and inflammatory disorders: pathophysiological mechanisms. *J. Immunol.* 2013, 190:3831–3838.
36. Ricklin D, Lambris JD: Progress and Trends in Complement Therapeutics *Adv. Exp. Med. Biol.* 2013, 735:1–22.
37. Bouyain S, Watkins DJ: The protein tyrosine phosphatases PTPRZ and PTPRG bind to distinct members of the contactin family of neural recognition molecules. *Proc. Natl. Acad. Sci. U. S. A.* 2010, 107:2443–2448.
38. Geisbrecht BV, Bouyain S, Pop M: An optimized system for expression and purification of secreted bacterial proteins. *Protein Expr. Purif.* 2006, 46:23–32.
39. Berends ETM, Dekkers JF, Nijland R, Kuipers A, Soppe JA, van Strijp JAG, Rooijakkers SHM: Distinct localization of the complement C5b-9 complex on Gram-positive bacteria. *Cell. Microbiol.* 2013, 15:1955–1968.
40. Prat C, Bestebroer J, de Haas CJC, van Strijp JAG, van Kessel KPM: A New Staphylococcal Anti-Inflammatory Protein That Antagonizes the Formyl Peptide Receptor-Like 1. *J. Immunol.* 2006, 177:8017–8026.
41. Pang YY, Schwartz J, Thoendel M, Ackermann LW, Horswill AR, Nauseef WM: agr-Dependent interactions of Staphylococcus aureus USA300 with human polymorphonuclear neutrophils. *J. Innate Immun.* 2010, 2:546–559.
42. Lu T, Porter AR, Kennedy AD, Kobayashi SD, Deleo FR: Phagocytosis and Killing of Staphylococcus aureus by Human Neutrophils. *J. Innate Immun.* 2014, doi:10.1159/000360478.
43. Keightley JA, Shang L, Kinter M: Proteomic analysis of oxidative stress-resistant cells. *Mol. Cell. proteomics* 2004, 3:167–175.
44. Abràmoff MD, Magalhães PJ, Ram SJ: Image Processing with ImageJ. *Biophotonics Int.* 2004, 11:36–42.
45. Hammel M, Sfyroera G, Ricklin D, Magotti P, Lambris JD, Geisbrecht BV: A structural basis for complement inhibition by Staphylococcus aureus. *Nat. Immunol.* 2007, 8:430–437.

SUPPLEMENTAL INFORMATION

Accompanying text for Figure S3

Addition of equimolar concentrations of both C4BP and Eap to this assay appeared to slow the rate of FI proteolysis (Fig. S3A, *bottom panel left*). This likely resulted from competition between Eap and C4BP for the same binding site on C4b, which consequently reduced the effective concentration of substrate available to FI since Eap does not have intrinsic cofactor activity (Fig. S3A, *top panel right*). To explore the functional consequences of Eap competition with C4BP in more detail, we carried out a set of studies wherein the molar ratio of Eap to C4BP was varied between 0, 0.1, 1.0, and 10 (Fig. S3B, *top panel*). Significant inhibition of FI-mediated proteolysis appeared to occur only when Eap was present at 10-fold higher concentration than C4BP (Fig. S3B, *bottom panel*). The requirement of such a high level of Eap to disrupt C4BP activity was most likely due to the weaker affinity of Eap for C4b and its lack of polyvalency, as it forms equimolar complexes with C4b. Thus, while Eap competes with C4BP for the same recognition site on C4b, it has no cofactor activity of its own, nor does competition with C4BP appear to be essential to its effects on the CP/LP of complement.

Supplemental figures

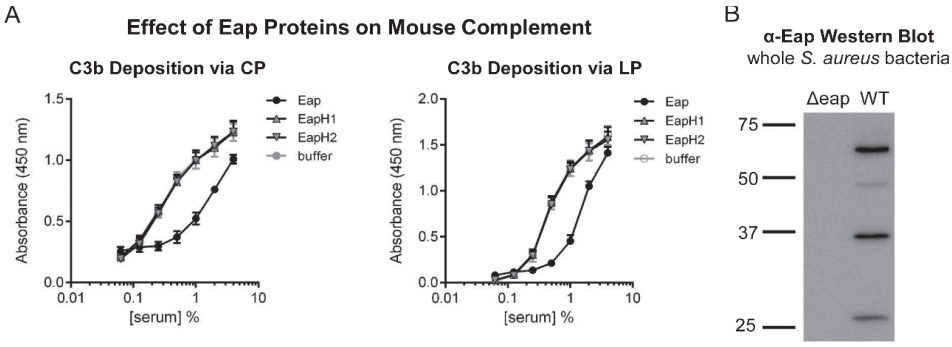

Figure S1. Supporting information on Eap inhibition of CP/LP and phagocytosis. (A) Eap inhibits the murine CP and LP. The effect of 1 μM Eap, EapH1, or EapH2 on CP (*left*) and LP-mediated (*right*) complement activation was measured across a dilution series of serum concentrations. Activation was detected as C3b deposition on an ELISA plate surface. (B) Eap is present on the surface of cells of a WT but not a Δ*eap S. aureus* strain. Bacteria were grown to stationary phase in liquid culture and harvested by centrifugation. After washing, Laemmli sample buffer with DTT was added to an equal volume of cell suspension and the samples were analyzed on a 12.5% (w/v) glycine polyacrylamide gel. Eap was detected by Western blot with 1:20.000 diluted rabbit-α-Eap serum and an HRP-labeled secondary antibody. A control experiment was performed to ensure that the same amount of bacteria were present in each sample by plating serial dilutions of each sample immediately prior to adding the Laemmli buffer. Note that proteolytic degradation of Eap into various combinations of adjacent subdomains has been reporter elsewhere, and is due to protease sensitivity of the interdomain linkers[27]. (C) Phagocytosis of *S. aureus* Newman Δ*eap* using 1% (v/v) NHS as a source of complement components and the indicated concentrations of Eap.

(on next page) Figure S2. Supporting information on Eap binding to C4 and its derivatives. (A) Affinity isolation of C4 from human serum. Biotinylated Eap was used as an affinity reagent to identify potential binding partners in both normal and C4-depleted human serum. Following capture of Eap-biotin by magnetic streptavidin beads and a series of washes, the bound proteins in both samples were separated by SDS-PAGE under non-reducing conditions. A band of approximately 200 kDa was found in the lane corresponding to normal but no C4-depeleted serum, strongly suggesting that Eap binds to native C4. (B) The ability of C4, C4b, and C4c to compete the AlphaScreen signal generated by myc-Eap and C4b-biotin was assessed over a logarithmic dilution series. While three independent trials were carried out, the data presented here are from a single representative titration. The smooth line indicates the outcome of fitting all points to a dose-response curve. (C) Sedimentation equilibrium analytical ultracentrifugation analysis of C4b and C4b/Eap.Experimental data were obtained as described in *Materials & Methods* for C4b (*left*) and an equimolar mixture of C4b/Eap (*right*). Equilibrium profiles were fit to a single particle model to yield the observed molecular weight for both C4b (268 kDa) and C4b/Eap (308 kDa). The top plots in both panels show the random residuals for the respective fits.

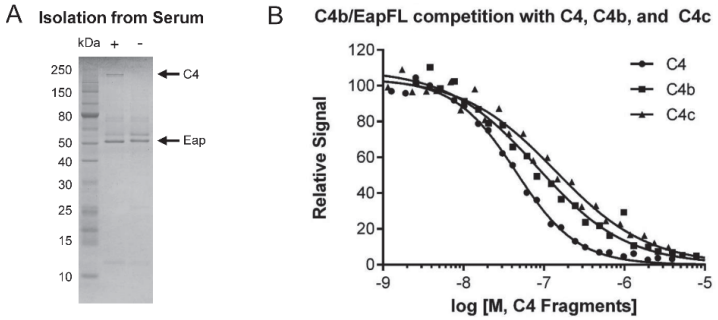

Figure S2.
(legend on previous page)

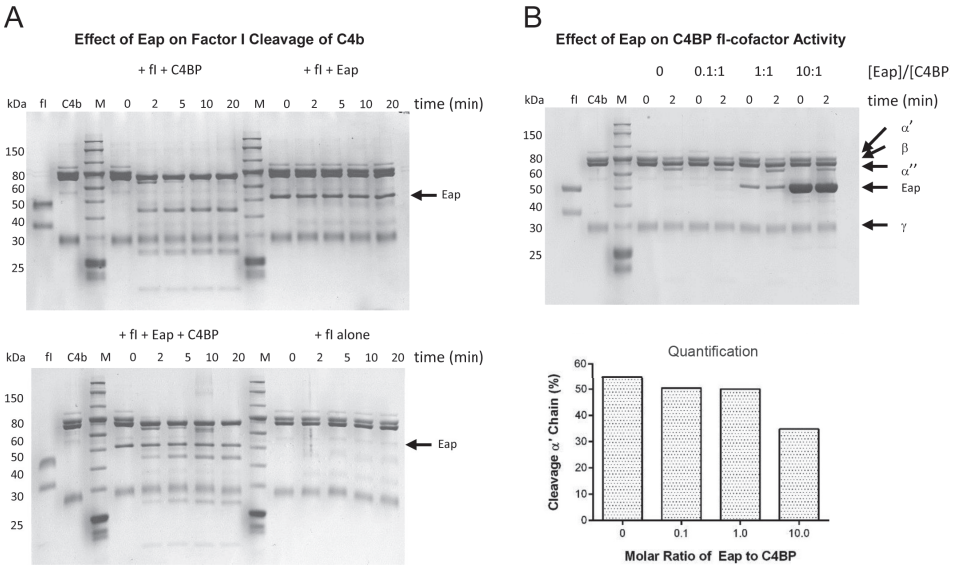

Figure S3. Eap lacks FI-cofactor activity and only weakly impacts C4BP cofactor activity. (A) The effect(s) of including C4BP (*top, left*), Eap (*top, right*), both (*bottom, left*), or neither (*bottom, right*) on FI-mediated proteolysis of C4b. Aliquots of each reaction series (indicated) were withdrawn over the course of 20 min and the proteins were analyzed by SDS-PAGE. (B) The effect of varying the molar ratio of Eap to C4BP on FI-mediated proteolysis of C4b. Aliquots of each reaction series (indicated) were withdrawn at 0 and 2 min, and the proteins were analyzed by SDS-PAGE. The identity of various bands, as determined by mass-spectrometry, is indicated (*top*). The ability of Eap to inhibit C4BP-dependent cleavage of C4b by FI was quantified by densitometry of the α' chain bands before and after the reaction (*bottom*). Additional interpretation is provided in the Accompanying Text above.

6

Immune-modulating properties of staphylococcal extracellular adherence proteins

Daphne A.C. Stapels[1], Lisette Scheepmaker[1], Maartje Ruyken[1], Brian V. Geisbrecht[2], Maren von Köckritz-Blickwede[3] and Suzan H.M. Rooijakkers[1]

[1] Medical Microbiology, UMC Utrecht, The Netherlands
[2] Department of Biochemistry and Molecular Biophysics, Kansas State University, Manhattan, KS, USA
[3] Department of Physiological Chemistry, University of Veterinary Medicine, Hannover, Germany

ABSTRACT

Infections with the human pathogen *Staphylococcus aureus* can only be overcome with the help of neutrophils. Even though neutrophils heavily rely on their neutrophil serine proteases (NSPs) to execute their antimicrobial functions, the direct role of these NSPs in defense against *S. aureus* has never been unambiguously determined. Recent work has established that *S. aureus* secretes a family of NSP inhibitors, consisting of the extracellular adherence protein (EAP)-domain proteins Eap (50 kDa), EapH1 (12 kDa), and EapH2 (13 kDa). With these, the bacterium can prevent degradation of its secreted virulence factors. Since NSPs are also involved in other neutrophil functions, we further evaluated the effect of EAPs on two functions of neutrophil elastase (NE), as best-characterized NSP. First, NE is indispensable in the formation of neutrophil extracellular traps (NETs), which can prevent bacteria from spreading. Here we show that both recombinant Eap, and endogenously expressed EAPs slow down the formation of NETs. Second, NE influences the migration of neutrophils towards the site of infection. Here we show, as a proof of principle, that NE cleaves one of the involved endothelial receptors (ICAM-1) and that this cleavage is inhibited by all three EAPs *in vitro*. *In vivo*, we confirmed that endogenous Eap inhibits neutrophil migration. However, additionally knocking out EapH1 and EapH2 from bacteria did not further affect the levels of neutrophil migration. Altogether, the two processes we examined here, i.e. NET formation and neutrophil migration, might be inhibited by one or more of the EAPs, promoting virulence of *S. aureus*.

INTRODUCTION

Infections with the opportunistic pathogen *Staphylococcus aureus* are an increasingly common burden both in health-care facilities and in the community due to the raise of antibiotic resistant strains[1]. Whereas this Gram-positive bacterium harmlessly colonizes over 30% of the population, it can cause serious diseases like pneumonia and sepsis after breaching the mechanical barriers of the immune system[2]. Neutrophils are indispensable in fighting these beginning infections, for which they rely on the antimicrobial molecules stored in their numerous granules. The azurophilic granules contain the neutrophil serine proteases (NSPs) that include neutrophil elastase (NE), proteinase 3 (PR3), and cathepsin (CG). These NSPs play important roles in the multiple antibacterial strategies of neutrophils. For example, NE degrades the *E. coli* outer membrane protein (OmpA), which induces loss of membrane integrity and bacterial disintegration[3]. NSPs can also indirectly target bacteria by breaking down their virulence factors[4]. The resulting reduced virulence enables other arms of the immune system to clear the bacteria. In addition to these microbial substrates, NSPs cleave targets within the immune system itself to orchestrate the immune response towards more efficient bacterial clearance[5].

As opposed to *E. coli*, direct killing of *S. aureus* by NSPs has never been demonstrated[3,6]. Nevertheless, recent work indicates that *S. aureus* protects itself from NSPs by secreting a family of potent NSP inhibitors. This family of extracellular adherence protein (EAP)-domain proteins consists of Eap and its two homologues (EapH1 and EapH2)[7]. In order to pinpoint the contribution of these EAPs to *S. aureus* virulence, we constructed two markerless mutant strains (i.e. *S. aureus* Δ*eap* and *S. aureus* Δ*eap*Δ*H1*Δ*H2*). By using these strains, we showed that Eap protects staphylococcal virulence factors against degradation by NSPs (CHAPTER 4, this thesis). Moreover, both strains showed diminished virulence in two different animal infection models[7] (CHAPTER 4, this thesis). Obviously, degrading virulence factors is not the only antimicrobial function of NSPs. Therefore, we now examine the effect of EAPs on two other immune processes that are mediated by neutrophil elastase (NE), as prototype NSP.

One important role of NE in immune defense is the initiation of neutrophil extracellular trap (NET) formation. NETs are the neutrophil's last resort to disarm bacteria[8]. Their formation, NETosis, is initiated by a stimulus that induces nuclear decondensation. Subsequent disintegration of the nuclear and granular membranes ensures intracellular mixing of DNA with granular, antimicrobial molecules. Finally, the plasma membrane is disrupted and this meshwork of DNA is excreted to entrap invading bacteria[8]. Recent insights reveal that proper NET formation requires translocation of NE from the granules to the nucleus, where it cleaves histones to promote nuclear decondensation[9]. Since NETs are believed to aid in the immune response by entrapping, or even killing, bacteria, we wondered whether the EAPs would influence NET formation.

The second immune process regulated by NSPs is transmigration of neutrophils[10]. Upon infection, neutrophils need to migrate towards the site of infection in order to kill bacteria. Therefore, they first roll over the activated endothelium, firmly attach to the

endothelial cells, transmigrate over the endothelial cell layer and then detach to proceed to the actual site of infection[11]. Firm attachment of neutrophils to the endothelium is, amongst others, mediated by the interaction of neutrophilic complement-receptor 3 (CR3) with the endothelial intercellular adhesion molecule-1 (ICAM-1). Previous studies have suggested that Eap binds ICAM-1, which would prevent neutrophils to firmly attach to the endothelium, and that it would thereby inhibit neutrophil recruitment[12]. Interestingly, other reports have shown that ICAM-1 is cleaved by NE, presumably after the transmigration of neutrophils. This would allow the detachment of neutrophils and enable them to proceed towards the site of infection[13,14]. We here explore the possibility that the previously observed effect of Eap on neutrophil migration might depend on the inhibition of NE.

RESULTS

EAPs inhibit NET formation

Since NE was recently shown to be required for NET formation, and since Eap inhibits NE, we tested the influence of Eap on NETosis. We stimulated purified, human neutrophils with phorbol myristate acetate (PMA) in the presence or absence of recombinant Eap. The NETs were visualized at various time points by staining the extracellular DNA with both DAPI and histone-DNA-complex antibodies[15]. During normal NETosis, five stages can be discriminated, characterized by the appearance of the neutrophils' nuclei when stained with DAPI and histone-DNA-complex antibodies: (1) unstimulated neutrophils show a lobed nucleus; (2) upon PMA stimulation, these nuclei condense and lose their lobed appearance; (3) the nucleus further decondenses and swells to form a puffy nucleus; (4) the neutrophils form small NETs, in which the extracellular DNA is still in close proximity of the original nucleus; (5) the extracellular DNA stretches further out and forms elongated NETs. In the third stage, the plasma membrane loses its integrity, which allows the histone-DNA antibody to gain access to the DNA. This is the first stage recognized as NET formation (Fig. 1A). In the presence of Eap, the number of nuclei that formed NETs was not affected. However, the area covered with the extracellular DNA did seem to decrease in the presence of Eap (Fig. 1B). Comparison of the microscopy pictures used for these quantifications shows that Eap seemed to halt neutrophils halfway in their process of NET formation; i.e. the image of NETs with Eap after 4 h resembles the small NETs already visible after 2 h in the samples without Eap (Fig. 1C).

Figure 1. EAPs alter NET formation. (A) Examples from the different stages of NET formation, used to quantify NET formation. Unstimulated, decondensed (both counted as no NET), "puffy" cells, small NETs, wide NETs (all counted as NET-forming nuclei). (B) Quantification of nuclei that formed NETs after 4 h of incubation (*left*) and the area covered by these NETs over time (*right*). (C) NET formation in presence or absence of recombinant Eap over time. These are representative pictures of the experiment in (B). (D) Quantification of NET formation induced by WT or *eap*-mutant bacteria. (E) LDH release by neutrophils when NET-formation was induced; same samples as in (D). (F) NET formation induced by WT or *eap*-mutant bacteria. These are representative pictures of two of the experiments in (E). Results represent data of three independent experiments. Groups are compared with a two-tailed Student's t-test in (B) and (D).

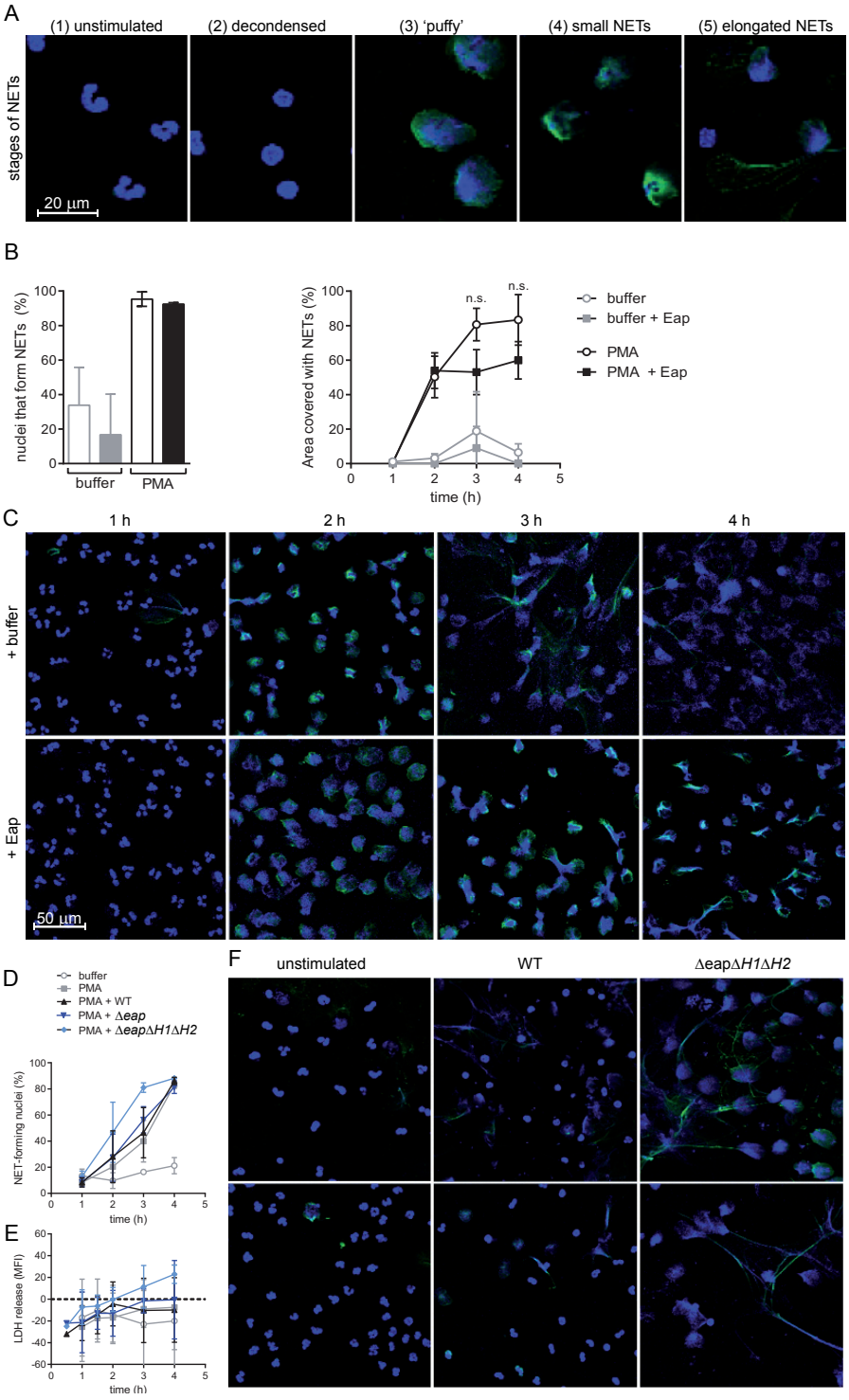
A
(1) unstimulated
(2) decondensed
(3) 'puffy'
(4) small NETs
(5) elongated NETs
stages of NETs
20 µm
B
nuclei that form NETs (%)
buffer
PMA
Area covered with NETs (%)
n.s.
n.s.
time (h)
buffer
buffer + Eap
PMA
PMA + Eap
C
1 h
2 h
3 h
4 h
+ buffer
+ Eap
50 µm
D
buffer
PMA
PMA + WT
PMA + Δeap
PMA + ΔeapΔH1ΔH2
NET-forming nuclei (%)
time (h)
E
LDH release (MFI)
time (h)
F
unstimulated
WT
ΔeapΔH1ΔH2

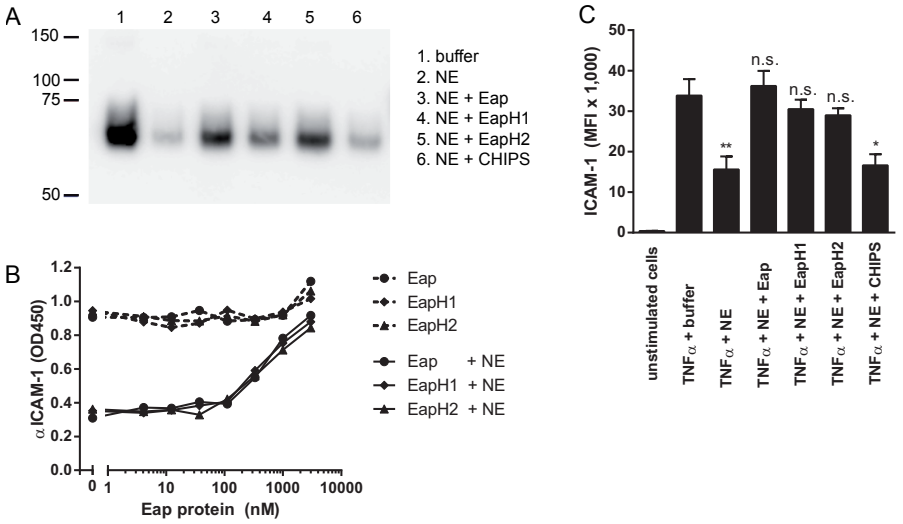

Figure 2. ICAM-1 cleavage by NE is inhibited by the EAPs. (A) Immunoblot analysis of ICAM-1, cleaved by NE in absence or presence of EAPs. (B) Detection of ICAM-1 coated on ELISA-plate wells after incubation with NE in absence or presence of EAPs. (C) Flow-cytometric analysis of surface-expressed ICAM-1 on epithelial EA.hy926 cells. Cells were incubated with NE, with or without EAPs. Results are representatives of three independent experiments (A-B), or reflect the mean of five independent experiments (C). Statistical significance was tested with a non-parametric one-way ANOVA, in which all columns were compared to the buffer column (C).

Since PMA is a very artificial stimulus for NET formation, we also evaluated the influence of EAPs on NETosis induced by bacteria. We compared the amount of NETs induced by WT bacteria (expressing all EAPs), with Δ*eap* bacteria (expressing only EapH1 and EapH2), and with Δ*eap*Δ*H1*Δ*H2* bacteria (expressing no EAPs)[7]. Interestingly, under these conditions the EAPs appeared to inhibit the number of nuclei that form NETs, as seen by the increased number of NET-forming nuclei induced by the Δ*eap*Δ*H1*Δ*H2*-mutant bacteria compared to the WT bacteria (Fig. 1D). This increased proportion of NET-forming nuclei was not caused by higher bystander cell death, as seen from the levels of released lactate dehydrogenase (LDH) during the incubation (Fig. 1E). Examination of the microscopy images illustrated that in the presence of EAPs (WT bacteria) some nuclei formed NETs, but many adjacent nuclei seemed only decondensed. In the absence of EAPs (Δ*eap*Δ*H1*Δ*H2*), however, all nuclei formed NETs, or at least had a puffy appearance (Fig. 1F). Altogether, these results show that NET formation appears to be slowed down or inhibited by the EAPs, though the exact mechanism through which this occurs remains unclear.

EAPs inhibit the cleavage of ICAM-1

Previous studies showed that ICAM-1 is a substrate for NE[14]. To address whether the EAPs might affect neutrophil migration by inhibiting NE activity, we first determined whether they could inhibit ICAM-1 cleavage *in vitro*. We incubated recombinant ectodomain of ICAM-1 with purified NE and analyzed the cleavage on immunoblot. This

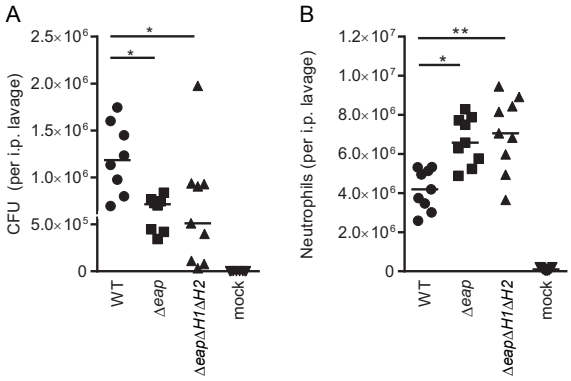

Figure 3. Eap homologues do not contribute to virulence during intraperitoneal infection. (A) Number of recovered CFU after 5 h intraperitoneal infection of mice with WT or *eap*-mutant strains. (B) Number of neutrophils recovered from the peritoneal lavage of infected mice. Each symbol represents an individual mouse and horizontal lines indicate the median values. Statistical significance was tested with a non-parametric one-way ANOVA, in which both mutant strains were compared to the WT strain.

showed that ICAM-1 was cleaved by NE in solution. Furthermore, addition of the recombinant EAPs inhibited the cleavage (Fig. 2A). To determine whether cleavage of surface-bound ICAM-1 could also be inhibited by the EAPs, we studied cleavage of ICAM-1 in an ELISA-based approach. We immobilized the ectodomain of ICAM-1 and subsequently incubated this with NE, in presence or absence of EAPs. Remaining ICAM-1 was detected with a monoclonal antibody against CD54. NE-cleaved ICAM-1 could no longer be detected, whereas the EAPs restored the detection. This indicated that also surface-immobilized ICAM-1 cleavage is inhibited by the EAPs (Fig. 2B). Lastly, to more closely mimic the physiological situation, we induced ICAM-1 expression on epithelial EA.hy926 cells. Incubation with NE induced loss of ICAM-1 staining, whereas the addition of the EAPs restored the ICAM-1 signal as measured by flow cytometry (Fig. 2C). In conclusion, these results clearly demonstrate that cleavage of ICAM-1 *in vitro* is inhibited by Eap, EapH1, and EapH2.

Eap blocks neutrophil recruitment *in vivo*

To explore whether the inhibition of ICAM-1 cleavage would be important *in vivo*, we repeated a previously reported murine, intraperitoneal (i.p.) infection model[12]. In this model, Chavakis *et al.* found that Eap inhibits neutrophil recruitment after 5 hours of infection. These investigators quantified the number of neutrophils recovered from the peritoneum during infection with WT bacteria vs. an *eap*-insertion mutant strain. We extended this model by using our markerless *eap*-mutant strains (Δ*eap* and Δ*eap*Δ*H1*Δ*H2*). Since we previously observed that the Eap homologues contributed to virulence, and since their only known function involves NSP inhibition, we hypothesized that the Δ*eap*Δ*H1*Δ*H2* strain would increase the neutrophil influx even further than the Δ*eap* strain. With our Δ*eap* strain, we observed the same increase in neutrophil numbers as described by Chavakis *et al*. (Fig. 3A). However, we also measured the same amount of neutrophils migrating to the peritoneum during an Δ*eap*Δ*H1*Δ*H2*-infection (Fig. 3A). The observed elevation of neutrophil influx in the mutant strains coincided with a 2-fold increase in bacterial load (Fig. 3B). Thus while the three EAPs inhibited the cleavage of ICAM-1 *in vitro*, only Eap inhibited neutrophil migration *in vivo*. It is yet unclear whether the latter process depends on the inhibition of NE, or whether as yet unappreciated mechanisms also contribute.

DISCUSSION

NSPs are reported to execute many different cleavage reactions important for neutrophil functioning. A recent addition to the wide range of functions for one of the NSPs, NE, is its requirement for NET formation[16]. The most-widely used stimulus to induce NET formation is PMA. This induces generation of reactive oxygen species, upon which NSPs detach from the azurophilic granular membrane[9,17]. The triad of detached NE, CG, and their catalytic-inactive homologue azurocidin, translocates to the cytosol, upon which enzymatic activity of NE is required to reach the nuclear membrane. On the contrary, detached PR3 remains localized in the azurophilic granules. At the nuclear membrane, NE gains access to the nucleus via an unknown process, after which it will cleave histones to promote nuclear decondensation needed for NET formation[9].

Since it is now known that *S. aureus* expresses three inhibitors of NSPs, we examined the influence of the staphylococcal EAPs on NETosis. Interestingly, recombinant, exogenously added Eap slowed down the process of NET formation, whereas endogenously expressed EAPs diminished the number of nuclei that formed NETs. Perhaps these differences in phenotype are induced by different cellular localizations of the proteins in both situations. For exogenously added Eap to affect NETosis via the inhibition of NE, it has to acquire access to the neutrophilic cytosol, or even to the neutrophilic nucleus, since the NE substrates for NETosis are localized there. This might occur in the latter stages of NET formation, since then also the DNA-histone antibody is able to cross the disintegrated plasma membrane. This hypothesis is in line with the finding that exogenous Eap only affects NET formation in the latter stages. However, it also implies that proteolytic degradation of intracellular targets by NE is still required in these latter stages of NETosis. To demonstrate that the effect of Eap can really be traced to inhibition of NE, additional experiments are required to show that the other NSP inhibitors EapH1 and EapH2 evoke the same, or possibly even additive effects. Moreover, if we would succeed in designing an Eap-mutant protein that no longer inhibits NE, one would predict that this protein would also no longer inhibit NET formation. Since neither proteolytic activity of CG or PR3 are required for NET formation, it is unlikely that Eap affects NETosis by interacting with these NSPs.

On the other hand, endogenous EAPs will not only be expressed by extracellular bacteria, but also by phagocytosed bacteria from within the phagocytic vacuole. Moreover, expression of both Eap and EapH1 is upregulated by the contents of azurophilic granules[18], making vacuolar expression of EAPs highly likely. Thus, in addition to the effects shown for exogenous Eap, endogenous EAPs might function from inside the neutrophil. Our experiments with the WT and mutant bacteria show that EAPs influence the number of nuclei that form NETs. The fact that NETosis in presence of the single *eap*-mutant (Δ*eap*) vs. the WT bacteria did not differ, suggests a redundant role for the EAPs. Furthermore, it remains to be determined why only NET formation of some neutrophils was affected. Perhaps only the affected neutrophils had phagocytosed bacteria. Alternatively, differences in maturation status of these neutrophils might have influenced their sensitivity to form NETs[19].

One completely unexplored possibility is that EAPs interfere with the antibacterial properties of NETs after they have formed. Within the NETs, NSPs are proteolytically active, and are hypothesized to contribute to antibacterial defense[20]. Whereas direct bacterial killing within NETs is unlikely[21], NSPs might still contribute to antibacterial defense by degrading virulence factors of the trapped bacteria[20]. This degradation within NETs might be inhibited by the EAPs, as previously shown (CHAPTER 4, this thesis).

Previous studies have indicated a role for NSPs in the migration of neutrophils towards the site of infection[22,23]. Nevertheless, the exact mechanism is not defined since the process is hard to capture *in vitro* and there are multiple potential targets for NE. For example, numerous basal membrane constituents could be targeted to create a passageway for neutrophils[24], or after transmigration either the endothelial ICAM-1[13] or the neutrophilic CR3[23,25] could be cleaved to promote neutrophil migration to more distal sites. Here we confirmed, as a proof of principle, that NE cleaves ICAM-1 and showed that this can be inhibited by all EAPs. Whether this process is important *in vivo* for neutrophil migration remains to be determined. Previous studies showed a redundant role for proteases in promoting neutrophil recruitment[10]. Therefore, in theory EAPs would be efficient inhibitors of neutrophil recruitment *in vivo*, since they inhibit multiple NSPs.

An *in vivo* pilot experiment confirmed that Eap inhibits neutrophil recruitment, as previously reported by Chavakis *et al.*[12]. Contrary to our predictions, this phenotype was not aggravated by additionally knocking out EapH1 and EapH2. The reason for the observed phenotype might be twofold. First, EapH1 and EapH2 might not be expressed in this infection model and in this time frame, or might be expressed in a much lower amount than Eap. If so, abolishing EapH1 and EapH2 would not induce a (measurable) change. Second, the observed phenotype for Eap might not rely on the inhibition of NSPs, but on another aspect of neutrophil recruitment. For example, Chavakis *et al.* hypothesized that Eap inhibits neutrophil recruitment via direct binding to ICAM-1. In that scenario, Eap should bind ICAM-1 within the blood vessel to prevent firm attachment of neutrophils and thereby inhibit intraperitoneal neutrophil recruitment. However, during intraperitoneal infection the bacteria reside outside of the blood vessels, which is also where Eap would be produced. Therefore interference with neutrophil extravasation after transmigration, when both Eap and the neutrophil reached the same side of the vessel wall, seems more feasible; either by inhibiting cleavage of ICAM-1, or by inhibiting cleavage of CR3. Moreover, since we only observed an effect of Eap on neutrophil recruitment, and not of the homologous proteins, the role of Eap on neutrophil recruitment might also be influenced by its ability to inhibit complement activation (CHAPTER 5, this thesis)[26]. To provide insights into the actual mechanism by which Eap inhibits neutrophil recruitment, additional experiments should be performed. To determine whether Eap blocks binding to ICAM-1, or blocks detachment from ICAM-1, the number of intravascular vs. extravascular ICAM-1-binding neutrophils could be quantified. Ideally, we would express an EAP-protein mutant that no longer inhibits NE in bacteria to see if this would yield the same phenotype as the Δ*eap* strain. In that way we could discriminate the NSP-inhibitory

function of Eap from its ability to inhibit complement.

Altogether these data provide additional insights into the possible immune processes that *S. aureus* protects itself from by secreting three NSP inhibitors. Even though we only highlight two functions here, NSPs have a much broader function in antibacterial defense. Other NSP-mediated processes that might influence the course of *S. aureus* infection is the activation and inhibition of certain cytokines and cytokine-receptors[5]. For example, classical activation of IL-1β via caspase-3 within the inflammasome is important in immune defense against *S. aureus*[27]. However, also all NSPs can generate bioactive IL-1β via an alternative pathway, that might affect the course of infection as well[28]. This study shows that by secreting inhibitors of NSPs, *S. aureus* benefits in multiple ways, since all these processes are inhibited at once. Unfortunately, the details of the mechanisms contributing to enhanced *S. aureus* virulence are still unclear. Nevertheless, these pieces of information form initial leads that might someday help to develop additional therapies against *S. aureus* infections.

ACKNOWLEDGEMENTS

We would like to thank Sandra Pfeifer for help with the animal experiments and Friederike Reuner for help with imaging and quantification of the NET formation. We would also like to thank Marc Monestier (Temple University School of Medicine, Philadelphia, USA) for kindly providing the #PL2-6 antibody.

MATERIAL AND METHODS

Ethics statement

All blood donors provided informed consent after full explanation of the purpose, nature and risk of all procedures used, in accordance with the Declaration of Helsinki. The used protocol was approved by the ethics committee of the University of Veterinary Medicine Hannover (Hannover, Germany). Animal experiments were performed as required by the German regulations of the Society for Laboratory Animal Science (GV-SOLAS) and the European Health Law of the Federation of Laboratory Animal Science Associations (FELASA), and were approved by the local governmental animal care committee (Lower Saxony, 33.9-42502-04-12/0855).

Bacteria

S. aureus Newman strains (WT, Δ*eap*, or Δ*eap*Δ*H1*Δ*H2*)[7] were grown in Todd-Hewitt broth (THB). Subsequently they were diluted 1:100 to fresh THB and grown to OD_{660} of 0.4 (*in vitro*), or OD_{660} 0.8 (*in vivo*).

Recombinant proteins

Recombinant Eap (SA1751) was expressed and purified as described before[29]. A recombinant form of the extracellular region of human ICAM-1 was expressed and purified from the conditioned culture medium of transiently transfected HEK293 cells. Briefly, a gene fragment encoding the portion of human ICAM-1 from the predicted mature N-terminus to the residue immediately preceding the single transmembrane domain was amplified by PCR and subcloned into the expression plasmid pSGHV1. This plasmid allows for constitutive expression and secretion of a fusion protein consisting of human growth hormone (hGH), followed by an octahistidine tag, a TEV-protease cleavage site, and the region of ICAM-1 described above. Actively growing HEK293 cells (~70% confluency in ~1500 cm^2 of culture area) were transfected with the pSGHV1-derived vector de-

scribed above using complexes with linear polyethyleneimine. Cells were cultured in DMEM high-glucose supplemented with 1% feutal calf serum (FCS). Conditioned medium was collected every 3 days for a total of 9 days, and clarified by high-speed centrifugation. Approximately 600 ml of medium was buffer exchanged into 20 mM Tris (pH 8.0) with 500 mM NaCl and 10 mM imidazole, and applied to a NiNTA sepharose resin. The bound protein was eluted with a linear gradient to 500 mM imidazole in the same buffer, and digested overnight with TEV protease according to standard protocols. The ICAM-1 fragment was isolated from the digest by re-application to the NiNTA column, except that the unbound fraction was retained in this case. The ICAM-1 containing sample was purified further by anion-exchange and superdex-200 column chromatographies. The final sample contained about 8 mg purified ICAM-1 ectodomain and was stored in aliquots at -80°C until further use.

In vitro NET formation

Protein: neutrophils were isolated from fresh blood of healthy donors by density gradient centrifugation using PolymorphprepTM (ProgenBiotechnik, Germany), as described previously[30]. NETs were induced in 2 x 10^5 neutrophils with 25 nM PMA in presence or absence of 1 µM Eap, in duplo. After 4 h, NETs were fixed with 4% paraformaldehyde and stained for histones (mouse-anti-H1A-H2B-DNA complex, #PL2-6), kindly provided by Marc Monestier, Temple University School of Medicine, Philadelphia, PA7. After washing, slides were mounted in ProlongGold® antifade with DAPI (Invitrogen, Germany) and analyzed by a Leica DMI6000CS confocal fluorescence microscope with a HCXPLAPO 40 x 0.75-1.25 oil immersion objective. Settings were adjusted with control preparations using an isotype control antibody. For each preparation, three randomly selected images were acquired and used for quantification. Data were expressed as percentages of NET-forming cells in relation to the total number of cells or as area covered with NETs. The mean value derived from n = 6 images for each condition per experiment was used for statistical analysis.

Bacteria: neutrophils ($2x10^5$) were stimulated with 25 nM PMA for 20 min. Bacteria ($4x10^5$) were added for 3 h (assuming OD_{660} 0.4 = 4.8 x 10^7 CFU/ml). NET were quantified as described above.

ICAM-1 cleavage

ELISA: Maxisorb ELISA-plate wells (Thermo Scientific) were coated with 5 µg/ml ICAM-1 ectodomain in 50 µl of 100 mM $NaCO_3$ with pH 9.6 o/n at 4 °C. Wells were washed 3 x with PBST (phosphate-buffered saline with 0.05 % Tween-20) and blocked with 4 % (w/v) bovine-serum albumin (BSA)-PBST, for 1 h at 37°C. The wells were incubated with indicated concentrations EAPs, with or without 6.25 µg/ml NE (Elastin Products Company) in 1 % (w/v) BSA-PBST for 1 h at 37 °C. After washing 3 x with PBST, the remaining ICAM-1 was detected with mouse-anti-hCD54-PE (BD Biosciences; 1:3000 diluted in 1 % (w/v) BSA-PBST) for 1 h at 37 °C. After washing 3 x with PBST, this was labeled with a secondary, peroxidase-labeled goat-anti-mouse (Bio-Rad; 1:5000 diluted in 1% BSA-PBST) for 1 h at 37°C and detected with substrate solution, containing 100 µg/ml tetramethylbenzidine and 60 µg/ml ureum peroxide in 100 mM sodium acetate buffer at pH 6.0. The reaction was stopped by adding an equal volume of 2 M H_2SO_4, and the absorbance at 450 nm was measured using a Bio-Rad microplate reader.

Immunoblot: In a total volume of 60 µl PBS, 25 µg/ml ectodomain of ICAM-1, 20 µg/ml NE, and 10 µg/ml inhibitor (EAPs or CHIPS) were incubated for 60 min at 37°C. The reaction was stopped by adding 60 µl of 2 x sample buffer. Per slot of a 12.5% SDS-PAGE 10 µl sample was run and immunoblotted as described before (CHAPTER 4, this thesis). ICAM-1 was detected with mouse-anti-hCD54-PE (1 µg/ml) in 1 % (w/v) non-fat dry milk in PBST and secondary, peroxidase-labeled goat-anti-mouse (1:15.000 diluted) in 1 % (w/v) non-fat dry milk in PBST. Bands were visualized with enhanced chemiluminescence (ECL, Amersham).

Cells: Epithelial cells (EA.hy.926) were cultured in DMEM (Invitrogen) with 10% FCS. One day before the experiment cells were harvested (detached with 3 mM EDTA for 5 min at 37 °C) and 5 x 10^6 cells were stimulated with 1 ng/ml TNFα (Sigma-Aldrich) for 18 h. Cells were washed with RPMI-1640 with 0.05 % HSA (Sanquin) and 50 µl cells were incubated for 60 min at 37 °C with 40 µg/ml NE and 1 µM inhibitor in a total volume of 100 µl RPMI-1640/HSA. The cells were washed with 1 ml RPMI-1640 and the remaining ICAM-1 was stained with mouse-anti-hCD54-PE (1:25 diluted) for 30 min at 4°C and measured by flow cytometry (FACS Verse, BD).

Intraperitoneal infection model

Female C57BL6/J RccHsd mice of 8-16 week old were purchased from Harlan-Winkelmann, Germany or

bred in-house. Bacteria were diluted to OD_{660} 0.4 in THB. Mice were infected with 1x 10^9 CFU i.p. (assuming OD_{660} 0.4 = 1.5 x 10^8 CFU/ml) and sacrificed after 5 h by inhaling isofluoran. The peritoneum was flushed with 5 ml sterile PBS. The peritoneal lavage was spun down with 500x *g* to harvest the immune cells. Neutrophils were stained with anti-Ly6G-FITC and quantified by flow cytometry. Bacteria in the supernatant of the lavage were enumerated by plating serial dilutions on blood-agar plates.

Statistical analysis

Statistical analyses were performed by using GraphPad Prism 6.0. Used tests are indicated in the figure legends. $P < 0.05$ was assumed to be statistically significant. ****, $P < 0.0001$; ***, $P < 0.001$; **, $P < 0.01$; *, $P < 0.05$.

REFERENCES

1. DeLeo FR, Chambers HF: Reemergence of antibiotic-resistant Staphylococcus aureus in the genomics era. *J. Clin. Invest.* 2009, 119:2464–2474.
2. Lowy FD: Staphylococcus aureus infections. *N. Engl. J. Med.* 1998, 339:520–532.
3. Belaaouaj AA, Kim KS, Shapiro SD: Degradation of Outer Membrane Protein A in Escherichia coli Killing by Neutrophil Elastase. *Science* 2000, 289:1185–1187.
4. Weinrauch Y, Drujan D, Shapiro SD, Weiss J, Zychlinsky A: Neutrophil elastase targets virulence factors of enterobacteria. *Nature* 2002, 417:91–94.
5. Korkmaz B, Horwitz MS, Jenne DE, Gauthier F: Neutrophil Elastase, Proteinase 3, and Cathepsin G as Therapeutic Targets in Human Diseases. *Pharmacol. Rev.* 2010, 62:726–759.
6. MacIvor DM, Shapiro SD, Pham CT, Belaaouaj A, Abraham SN, Ley TJ: Normal neutrophil function in cathepsin G-deficient mice. *Blood* 1999, 94:4282–4293.
7. Stapels DAC, Ramyar KX, Bischoff M, von Köckritz-Blickwede M, Milder FJ, Ruyken M, Eisenbeis J, McWhorter WJ, Herrmann M, van Kessel KPM, et al.: Staphylococcus aureus secretes a unique class of neutrophil serine protease inhibitors. *Proc. Natl. Acad. Sci. U. S. A.* 2014, 111:13187–13192.
8. Papayannopoulos V, Zychlinsky A: NETs: a new strategy for using old weapons. *Trends Immunol.* 2009, 30:513–521.
9. Metzler KD, Goosmann C, Lubojemska A, Zychlinsky A, Papayannopoulos V: A Myeloperoxidase-Containing Complex Regulates Neutrophil Elastase Release and Actin Dynamics during NETosis. *Cell Rep.* 2014, 8:883–896.
10. Young RE, Voisin M-B, Wang S, Dangerfield J, Nourshargh S: Role of neutrophil elastase in LTB4-induced neutrophil transmigration in vivo assessed with a specific inhibitor and neutrophil elastase deficient mice. *Br. J. Pharmacol.* 2007, 151:628–637.
11. Spaan AN, Surewaard BGJ, Nijland R, van Strijp JAG: Neutrophils versus Staphylococcus aureus: a biological tug of war. *Annu. Rev. Microbiol.* 2013, 67:629–650.
12. Chavakis T, Hussain M, Kanse SM, Peters G, Bretzel RG, Flock J-I, Herrmann M, Preissner KT: Staphylococcus aureus extracellular adherence protein serves as anti-inflammatory factor by inhibiting the recruitment of host leukocytes. *Nat. Med.* 2002, 8:687–693.
13. Champagne B, Tremblay P, Cantin A, St Pierre Y: Proteolytic cleavage of ICAM-1 by human neutrophil elastase. *J. Immunol.* 1998, 161:6398–6405.
14. Kaynar MA, Houghton MA, Lum EH, Pitt BR, Shapiro SD: Neutrophil elastase is needed for neutrophil emigration into lungs in ventilator-induced lung injury. *Am. J. Respir. Cell Mol. Biol.* 2008, 39:53–60.
15. Neumann A, Völlger L, Berends ETM, Molhoek EM, Stapels DAC, Midon M, Friães A, Pingoud A, Rooijakkers SHM, Gallo RL, et al.: Novel Role of the Antimicrobial Peptide LL-37 in the Protection of Neutrophil Extracellular Traps against Degradation by Bacterial Nucleases. *J. Innate Immun.* 2014, 6:860–868.
16. Papayannopoulos V, Metzler KD, Hakkim A, Zychlinsky A: Neutrophil elastase and myeloperoxidase regulate the formation of neutrophil extracellular traps. *J. Cell Biol.* 2010, 191:677–691.
17. Reeves EP, Lu H, Jacobs HL, Messina CGM, Bolsover S, Gabella G, Potma EO, Warley A, Roes J, Segal AW: Killing activity of neutrophils is mediated through activation of proteases by K+ flux. *Nature* 2002, 416:291–297.
18. Palazzolo-Ballance AM, Reniere ML, Braughton KR, Sturdevant DE, Otto M, Kreiswirth BN, Skaar EP, DeLeo FR: Neutrophil Microbicides Induce a Pathogen Survival Response in Community-Associated Methicil-

lin-Resistant Staphylococcus aureus. *J. Immunol.* 2007, 180:500–509.
19. Martinelli S, Urosevic M, Daryadel A, Oberholzer PA, Baumann C, Fey MF, Dummer R, Simon H-U, Yousefi S: Induction of genes mediating interferon-dependent extracellular trap formation during neutrophil differentiation. *J. Biol. Chem.* 2004, 279:44123–44132.
20. Brinkmann V, Reichard U, Goosmann C, Fauler B, Uhlemann Y, Weiss DS, Weinrauch Y, Zychlinsky A: Neutrophil extracellular traps kill bacteria. *Science* 2004, 303:1532–1535.
21. Menegazzi R, Decleva E, Dri P: Killing by neutrophil extracellular traps: fact or folklore? *Blood* 2012, 119:1214–1216.
22. Woodman RC, Reinhardt PH, Kanwar S, Johnston FL, Kubes P: Effects of human neutrophil elastase (HNE) on neutrophil function in vitro and in inflamed microvessels. *Blood* 1993, 82:2188–2195.
23. Zen K, Guo Y-L, Li L-M, Bian Z, Zhang C-Y, Liu Y: Cleavage of the CD11b extracellular domain by the leukocyte serprocidins is critical for neutrophil detachment during chemotaxis. *Blood* 2011, 117:4885–4894.
24. Heck LW, Blackburn WD, Irwin MH, Abrahamson DR: Degradation of Basement Membrane Laminin by Human Neutrophil Elastase and Cathepsin G. *Am. J. pahhology* 1990, 136:1267–1274.
25. Cai TQ, Wright SD: Human leukocyte elastase is an endogenous ligand for the integrin CR3 (CD11b/CD18, Mac-1, alpha M beta 2) and modulates polymorphonuclear leukocyte adhesion. *J. Exp. Med.* 1996, 184:1213–1223.
26. Woehl JL, Stapels DAC, Garcia BL, Ramyar KX, Keightley A, Ruyken M, Syriga M, Sfyroera G, Weber AB, Zolkiewski M, et al.: The Extracellular Adherence Protein from Staphylococcus aureus Inhibits the Classical and Lectin Pathways of Complement by Blocking Formation of the C3 Proconvertase. *J. Immunol.* 2014, 193:6161–6171.
27. Miller LS, Pietras EM, Uricchio LH, Hirano K, Rao S, Lin H, O'Connell RM, Iwakura Y, Cheung AL, Cheng G, et al.: Inflammasome-Mediated Production of IL-1ß Is Required for Neutrophil Recruitment against Staphylococcus aureus In Vivo. *J. Immunol.* 2007, 179:804–811.
28. Netea MG, van de Veerdonk FL, van der Meer JWM, Dinarello CA, Joosten LAB: Inflammasome-Independent Regulation of IL-1-Family Cytokines. *Annu. Rev. Immunol.* 2015, 33. doi: 10.1146/annurev-immunol-032414-112306.
29. Hussain M, Haggar A, Peters G, Chhatwal GS, Herrmann M, Flock J-I, Sinha B: More than one tandem repeat domain of the extracellular adherence protein of Staphylococcus aureus is required for aggregation, adherence, and host cell invasion but not for leukocyte activation. *Infect. Immun.* 2008, 76:5615–5623.
30. Köckritz-Blickwede M, Chow O: 7-Visualization and Functional Evaluation of Phagocyte Extracellular Traps. *Methods Microbiol.* 2010, 37:139–160.

7

General discussion

Part I: Rationale for neutrophil serine protease inhibition by bacteria

Daphne A.C. Stapels[1], Brian V. Geisbrecht[2] and Suzan H.M. Rooijakkers[1]

[1] Medical Microbiology, UMC Utrecht, The Netherlands
[2] Department of Biochemistry and Molecular Biophysics, Kansas State University, Manhattan, KS, USA

Curr. Opin. Microbiol. (2015). 23:42-48.

Part II: The role of extracellular adherence proteins in *S. aureus* defense

SUMMARY OF THIS THESIS

In this thesis we describe the first-known coping mechanism of the Gram-positive *Staphylococcus aureus* with neutrophil serine proteases (NSPs). In **CHAPTER 2** we identified a family of three secreted *S. aureus* proteins that are potent NSP inhibitors. These extracellular adherence proteins (EAPs) are highly homologous and can all inhibit the NSPs neutrophil elastase (NE), proteinase 3 (PR3), and cathepsin G (CG). The EAP family consists of Eap (53 kDa) and its smaller homologues EapH1 (12 kDa) and EapH2 (13 kDa) (Fig. 1A). A co-crystal structure of EapH1 bound to NE revealed that this inhibition is governed by non-covalent obstruction of the catalytic cleft. Since both the EAPs and the NSPs show high structural homology amongst each other, we hypothesize that the mechanism of inhibition is the same for all interactions (Fig. 1B-C). In **CHAPTER 3** we tried to unravel the molecular mechanism of inhibition in more detail. Despite the high homology amongst the EAPs, we found some indications that the mechanism of inhibition might differ per protein. In addition, studies with other serine proteases in this chapter revealed that mast-cell chymase is the fourth serine protease to be inhibited, whereas neutrophil serine protease 4 (NSP4) is exclusively inhibited by Eap. In addition to unraveling the molecular mechanism, we questioned why *S. aureus* would benefit from inhibiting NSPs. In particular, since the antimicrobial character of NSPs has been extensively described, but the exact role of NSPs during *S. aureus* infections is still debated. By constructing *eap*-mutant strains, we showed in **CHAPTER 4** that *S. aureus* secretes the EAPs to protects its other virulence factors against degradation by NSPs. In **CHAPTER 5** we revealed that Eap also affects innate-immune responses by inhibiting complement activation. This is an entirely different process, not depending on the inhibition of serine proteases, but on the binding of Eap to C4b. Lastly, in **CHAPTER 6** we explore two other processes in which EAPs might influence immune responses against staphylococci: the formation of neutrophil extracellular traps, and neutrophil recruitment. Both are affected by EAPs, but the mechanism is not yet unraveled. Altogether, this thesis evoked many new questions. However, with the finding of three conserved, specific staphylococcal inhibitors of NSPs, this thesis showed us that NSPs are more important in defense against *S. aureus* than previously thought.

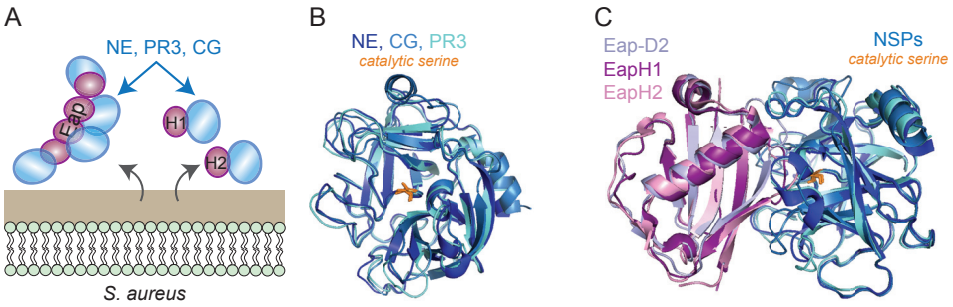

PART I:
RATIONALE FOR NSP INHIBITION BY BACTERIA

Neutrophil serine proteases (NSPs) are long known for their antibacterial properties. We set out to identify how *S. aureus* shields itself from these NSPs and we identified a family of highly specific, secreted NSP inhibitors. Even though the identification of these NSP inhibitors underlines the antibacterial potency of NSPs, the exact role against *S. aureus* is still debated. Therefore, we examine in PART I which antibacterial functions of NSPs are known and in which situations *S. aureus* might encounter them. In addition, we assembled an overview of other bacterial mechanisms to disarm NSPs.

NSP functions in antibacterial defense

NSPs can end up in various immune compartments: intra- and extracellular, and intra- and extravascular (see introduction of this thesis). Thereby, they encounter numerous substrates, which could affect numerous immune processes. For instance, they can cleave chemokines, cytokines, and receptors to either activate or inactivate them, but also function as chemoattractants independently from their proteolytic activity, which has recently been reviewed[1–3]. Here, we will focus on the more direct interactions of NSPs with bacteria (Fig. 2).

Direct killing

The best-known antibacterial function of NSPs is direct killing of bacterial cells. While NE has been shown to directly kill the Gram-negative bacteria *Klebsiella pneumoniae* and *Escherichia coli*, only for the latter it has been shown to depend on cleavage of its outer membrane protein A (OmpA), resulting in loss of membrane integrity and cell death[4,5] (Fig. 2A). Separately, the Gram-positive *Streptococcus pneumoniae* is known to be killed by the concerted action of NE, CG, and PR3 within the phagocytic vacuole, which was also demonstrated *in vivo*[6,7]. This process requires the presence of pneumococcal capsule, although the mechanism is yet unknown[8] (Fig. 2B). Surprisingly, NE seems trivial for killing of the closely related organism, *Staphylococcus aureus*, nor has the role of CG been well established[5,9,10]. Experiments with our bacterial mutant strains (lacking either Eap, or all three EAPs) also indicated little influence of the NSPs in killing of *S. aureus* after phagocytosis *in vitro* (CHAPTER 2)[11]. Neither did NE or CG directly kill *S. aureus* in buffers a range of different pH values (Stapels and Rooijakkers, unpublished results). Taken together, direct anti-microbial activity of NSPs is only demonstrated for

Figure 1. *S. aureus* EAPs inhibit NSPs. (A) *S. aureus* secretes the EAP family of proteins, consisting of Eap, EapH1, and EapH2, that specifically inhibits NSPs. Full-length Eap consists of multiple domains (resembling EapH1 and EapH2) that each bind one NSP molecule. (B) The NSPs NE (PDB code 3Q76), PR3 (PDB code 1FUJ), and CG (PDB code 1CGH) show high structural homology. The catalytic serine residue of all three proteins is depicted in orange. (C) Model of NE, CG, and PR3 binding to different EAPs (EapH1, EapH2, and the second domain of Eap (Eap-D2)), inferred from the co-crystal structure of NE with EapH1 (PDB code 4NZL).

a very limited amount of bacterial species and unlikely to play an important role in *S. aureus* defenses.

Generation of antimicrobial peptides

More indirectly, NSPs can cleave host proteins to generate antimicrobial peptides. The best-known example is the extracellular cleavage of hCAP-18 by PR3 to generate the antimicrobial peptide LL-37[12], which can potently kill *S. aureus*[13]. Separately from this, extracellular NSPs can also cleave serum proteins of the complement and coagulation systems to generate distinct antimicrobial peptides. For example, NE cleaves the central complement protein C3 to generate a peptide that mimics the natural C3a anaphylatoxin. As with C3a, this NE-derived peptide of C3 shows antimicrobial activity against *Enterococcus faecalis* and *Pseudomonas aeruginosa*[14] (Fig. 2C). NE and CG can also cleave thrombin and release peptides that are antimicrobial to *E. coli*[15]. Lastly, NE cleaves the tissue-factor pathway inhibitors (TFPI-1 and TFPI-2) into peptides that kill a wide range of bacteria, or bind *E. coli*, respectively[16,17].

Virulence attenuation

Furthermore, NSPs may attenuate bacterial virulence by inactivating factors required for pathogenesis. For example, NE, but not CG, cleaves the invasins IpaA-C and the mobility protein IcsA of *Shigella flexneri* to prevent bacterial dissemination into the cytoplasm of neutrophils[18] (Fig. 2D). Virulence factors of the related enterobacteria *Salmonella Typhimurium* and *Yersinia enterocolitica* were also cleaved[18]. Such effects are not limited to Gram-negatives, however, as CG cleaves the *S. aureus* adhesin clumping factor A (ClfA) and removes its active domain (Fig. 2E)[19]. Moreover, in CHAPTER 4 we show that also a wide range of secreted virulence factors of *S. aureus* can be degraded. Some of the tested virulence factors had the same immune-evasion functions (i.e. staphylococcal inhibitor of complement (SCIN), and SCIN-B/C). Interestingly, these proteins showed differential susceptibility to degradation by NE, which might partly explain the seemingly redundant arsenal of virulence factors produced by *S. aureus*. In addition, CHAPTER 4 provides the first evidence that degradation of virulence factors really occurs *in vivo,* which was facilitated by the generation of an *eap*-mutant strain. In WT bacteria, expression of Eap would normally protected these virulence factors against degradation. The observed degradation of virulence factors might either occur upon degranulation of neutrophils, or within NETs[20]. Judging from the broad substrate specificity of NSPs and the relatively low concentrations needed to target virulence factors[18], we anticipated that also membrane-bound virulence factors of *S. aureus* are inactivated by NSPs.

NET formation

The role of NSPs during NET formation is perhaps best illustrated by the absolute requirement of active NE to form NETs. Upon NET induction, NE translocates to the nucleus, where it cleaves histones to facilitate the DNA decondensation central to NETosis[21,22]. In addition, all NSPs are found within NETs[23]. Three functions have been ascribed

to NETs. First, they catch the extracellular NSPs, and other antimicrobial agents released from neutrophils, to prevent host damage at distal sites[24]. Second, they ensnare bacteria to prevent them from disseminating to other body sites[25]. Third, they might kill the captured bacteria via the antimicrobial agents attached to the NET-DNA[20].

Besides the large debate about the direct bacterial killing by NETs in general[26], it is unlikely that the NSPs contribute to killing within NETs since even *S. pneumonia* survived entrapment[25], despite its sensitivity to NSPs within the phagocytic vacuole. Moreover, activities of NSPs within NETs are decreased due to their binding to DNA[27]. The high concentrations of NSPs required for bacterial killing are therefore likely not reached within the NETs. In addition, NET-bound NSPs may also be inactivated by high concentration of NSP inhibitors in serum[28]. Altogether, the main role for NSPs probably lies in the induction of NETs, so that they can confine the bacterial infection.

In CHAPTER 6 we explored whether the NE-inhibiting EAPs could affect NET formation. Endogenous, recombinant Eap halted NET formation and prevented the formation of long, extended NETs. Although the effect of recombinant EapH1 and EapH2 is yet unknown, one or both of these proteins influenced NET formation in the context of bacteria, since triple *eap*-mutant bacteria (lacking Eap, EapH1, and EapH2) induced more NETs than WT bacteria. All data together suggest that multiple EAPs can inhibit NET formation, but the observed phenotypes probably largely depended on the expression levels of the individual proteins. Since the only known function of EapH1 and EapH2 is NSP inhibition, the inhibition of NET formation is most likely induced by NE inhibition. Interestingly, *S. aureus* evades NETs by secreting a nuclease that breaks down NETs[29]. The finding that EAPs slow down NET formation, might help *S. aureus* to break down NETs.

Lessons from patients and *in vivo* studies

The recurrent infections in patients with neutrophil deficiencies, including many *S. aureus* infections, show that neutrophils are crucial in human antimicrobial defense[30,31]. This defense was for long believed to completely rely on the reactive oxygen species (ROS), generated in the phagocytic vacuole by NADPH oxidase and myeloperoxidase. However, the direct antibacterial effects of ROS seem to be overstated and it is currently believed that a concerted action of NADPH oxidase and NSPs is necessary for effective eradication of bacteria[32]. This is demonstrated by studies with $NE^{-/-}$ and $CG^{-/-}$ mice that showed that NSPs are crucial for clearance of *E. coli*, *K. pneumoniae* and *S. pneumoniae*[4,5,7]. Now we have identified three staphylococcal inhibitors of NSPs, also a crucial role for NSPs during *S. aureus* infections seems inevitable. EAPs were shown to affect the outcome of murine infection models[11] (CHAPTER 2, 4, and 6). Moreover, Eap is highly expressed in deep human wounds[33]. It remains unknown by which specific component expression is induced, and whether expression inside phagocytic vacuoles or rather extracellular expression yields the most effective NSP inhibition.

Mechanisms of bacteria to block NSPs

In addition to the NSP inhibitors produced by *S. aureus*, other bacterial pathogens

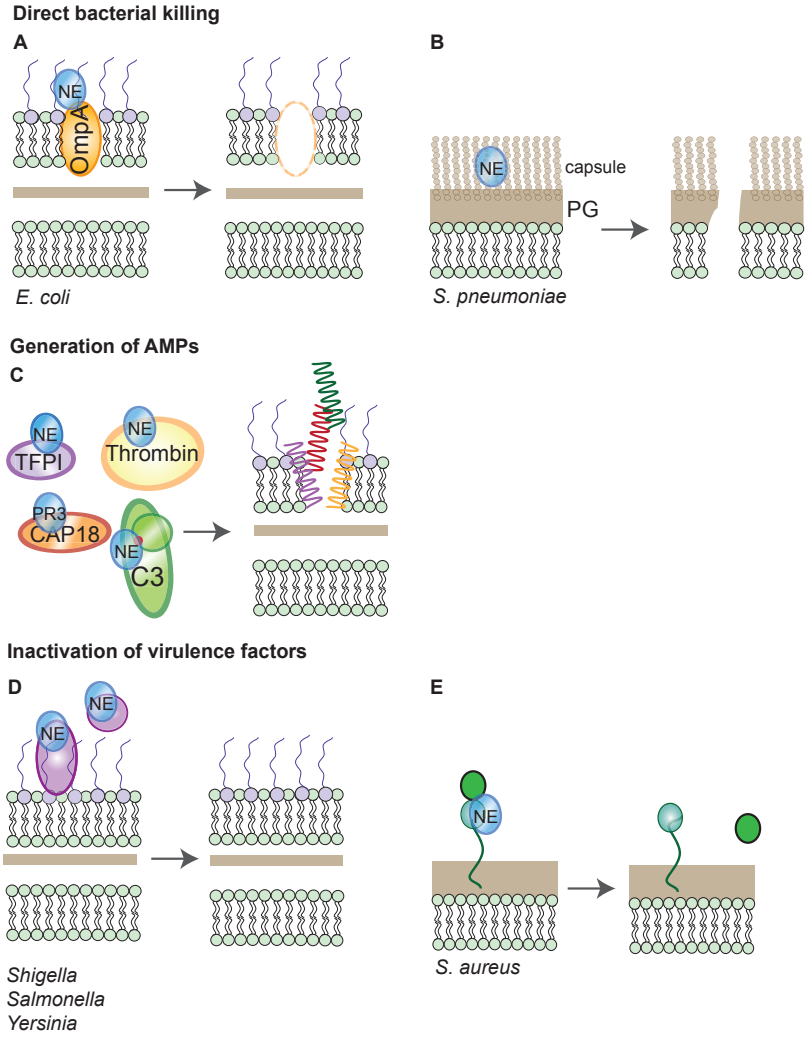

Figure 2. Antimicrobial functions of NSPs. (A-B) NSPs can directly kill bacteria by attacking membrane-associated (*E. coli*) (A), or capsule proteins (*S. pneumoniae*) (B), which leads to loss of membrane integrity. (C) NSPs can cleave host immune proteins to generate antimicrobial peptides. (D-E) NSPs can target and inactivate bacterial virulence factors, shown for Gram-negative (D), and Gram-positive (E) bacteria, resulting in attenuated virulence of bacteria.

evolved strategies to counteract human NSPs too. The mechanisms identified thus far range from protecting bacterial substrates against proteolytic cleavage to the production of protease inhibitors that directly block NSPs. We will here give an overview of the mechanism evolved by different bacteria to cope with the actions of NSPs (Fig. 3).

Modifications of bacterial NSP substrates

Some bacteria protect itself against the detrimental actions of NSPs by modifying

their substrates. For example, *S. epidermidis* and *S. aureus* express glycosyltransferases (SdgA and SdgB) that decorate cell surface-bound proteins with N-acetylglucosamine (GlcNAc) moieties on their serine-aspartate dipeptide (SDR) repeats[19]. These SDR repeats are, among others, found in the virulence factors ClfA and ClfB, SdrC, SdrD, SdrE (*S. aureus*) and SrdF, SdrG and SdrH (*S. epidermidis*). The GlcNAc modification protects them from proteolytic degradation by CG (Fig. 3A). Another mechanism is used by the Gram-negative human pathogen *Neisseria meningitidis*. Like all Gram-negatives, the outer membrane of *N. meningitidis* contains LPS molecules that are anchored to the membrane via lipid A. This can be modified by neisserial phosphoethanolamine transferase (lptA) with phosphoethanolamine to prevent proteolysis-independent killing by CG[34] (Fig. 3A).

Bacterial protease inhibitors

The mechanism by which the EAPs inhibit NSPs is largely unraveled by solving a co-crystal structure of EapH1 bound to NE. This showed that EapH1 forms a non-covalent, 1:1 complex with NE, occluding the NE active site and thereby preventing substrate cleavage (CHAPTER 2)[11]. Based on the high sequence and structural homology amongst the EAPs, we predicted that all EAPs would inhibit NSPs via the same mechanism. Surprisingly, whereas site-directed mutagenesis of NE-interacting residues in EapH1 decreased the amount of inhibition, mutating homologous residues in EapH2 had no effect. On the contrary, mutations in a different loop of EapH2 abolished all NE inhibition (CHAPTER 3). Future mutagenesis studies will have to confirm whether both mechanisms differ. If the mechanism of NSP inhibition varies amongst EAPs, we should consider the possibility that also the mechanism by which individual NSPs are inhibited might differ. Studies with other serine proteases revealed that the EAPs are really specific inhibitors of NSPs, with mast-cell chymase as only exception. That is, the closely related serine proteases thrombin, plasmin and plasma kallikrein are not inhibited by EAPs, and even NSP4, the most-recent identified NSP, is only inhibited by Eap, and not by EapH1 or EapH2 (CHAPTER 3). The question remains why *S. aureus* would encode three proteins with the same function. Perhaps they complement each other in expression pattern. Whereas expression of Eap and EapH1 is upregulated in the presence of components from the azurophilic granules, expression of EapH2 seems to be regulated differently[35]. Nevertheless, this functional redundancy is a recurrent theme in *S. aureus* immune evasion.

Comparable to the EAPs, many Gram-negative bacteria express high-affinity protease inhibitors. The dimeric, periplasmic protein ecotin (16 kDa) inhibits NSPs by forming heterotetrameric complexes[36]. The ecotin orthologues of pathogenic *E. coli*, *Yersinia pestis* and *P. aeruginosa* all potently block NE and CG (Fig. 3B). However, ecotin is not a specific NSP inhibitor, since it also potently inhibits a wide range of other chymotrypsin-like proteases, like trypsin and chymotrypsin[36].

Another interesting group of protease inhibitors is formed by the Gram-negative homologues of the mammalian alpha-macroglobulin (MG) family. MGs are large (>170

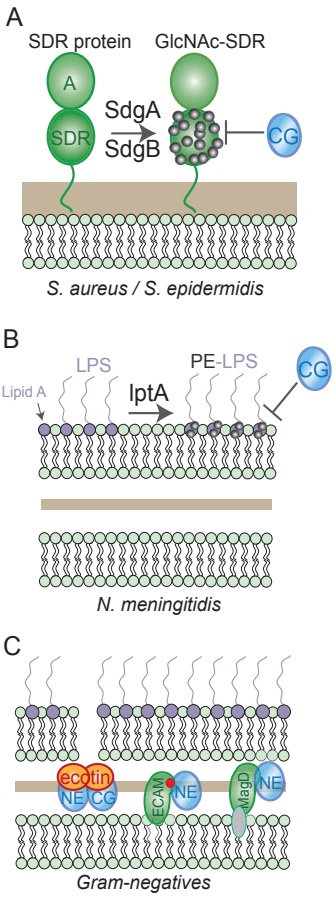

Figure 3. Bacterial mechanisms to block NSPs. (A-B) Modification of bacterial substrates. (A) Glycosyltransferases SdgA and SdgB modify staphylococcal virulence factors with N-acetylglucosamine (GlcNAc) to prevent them being cleaved by CG. (B) LptA modifies neisserial lipid A to prevent killing by CG. (C) In addition to *S. aureus* which secretes the EAPs as inhibitors of NSPs, Gram-negative bacteria express inhibitors of chymotrypsin-like serine proteases in their periplasmic space to prevent activity of a broad range of serine proteases, including NSPs. These inhibitors include ecotin, and the bMG proteins ECAM (*E. coli*) and MagD (*P. aeruginosa*).

kDa) glycoproteins that inactivate a wide variety of proteases[37,38] (Fig. 3C). These bacterial MG-like proteins (bMGs), supposedly acquired via horizontal gene transfer from their metazoan hosts[39], display remarkable structural and functional homology to human α2-MGs. Like αMG, proteolytic cleavage of a 'bait' region in bMGs results in a conformational change that allows the inhibitor to covalently capture the protease. The *E. coli* protein ECAM has a similar secondary structure to human plasma α_2-MG and likewise contains an internal thioester to form covalent complexes with NE, trypsin and chymotrypsin[40].

Intriguingly, both ecotin and bMGs are expressed in the periplasmic space of Gram-negative bacteria. Thus, they can only function against proteases that can breach the bacterial outer cell membrane. Since ecotin was found to protect *E. coli* from killing by purified NE[36], this suggests that NE gains access to the periplasm following degradation of OmpA and disrupts the membrane integrity. Still, these broad-range protease inhibitors might not have evolved to specifically protect bacteria from NE, but might mainly serve to block pancreatic digestive proteases in the mammalian gut or bacterial aggressors that inject proteases in the periplasm[40].

Conclusions

Recent advances in understanding the molecular interplay between NSPs and bacteria now indicate that the role of NSPs in antibacterial host defense is much more diverse than simply directly killing of bacteria. Considering the few species it this has been proven for, a directly bactericidal activity of NSPs seems very much overstated. On the contrary, a large body of evidence shows that these proteases can diminish bacterial virulence in many ways and their specific activities may even differ depending on the exact location where they encounter bacteria (within the phagocytic vacuole or in the extracellular space). Our studies on the interaction of NSPs with *S. aureus* in particular, showed that NSPs could not even kill *eap*-mutant bacteria after phagocytosis. Therefore it seems more

likely that *S. aureus* benefits from inhibiting NSPs in the extracellular space. For example by protecting its virulence factors against degradation, by preventing the generation of antimicrobial peptides, like LL-37, that might kill *S. aureus*, or by delaying NET formation so that the *S. aureus* nuclease can mediate escape. In our opinion, future work should also address whether NSPs collaborate with other antibacterial host defense components such as membrane-perturbing granular components. Still, the fact that bacteria evolved inhibitors of NSPs, which are highly specific in case of *S. aureus*, indicates that their role in anti-bacterial defense is indispensable. The endogenous production of these inhibitors has probably complicated previous studies analyzing the role of NSPs in defense *in vivo* and we feel that future work on NSP host defense functions should take these evasion strategies into account. Overall, these insights will contribute to a better understanding of the roles of NSPs in host defense against bacteria, and against *S. aureus* in particular.

.

PART II:
THE ROLE OF EAPS IN STAPHYLOCOCCAL DEFENSE

In this thesis we described the generation of *eap*-mutant strains of *S. aureus* and used them to investigate the role of NSPs in the defense against this bacterium (CHAPTER 2, 4, AND 6). Although this method is optimal to circumvent the natural inhibition of NSPs during infections, the results might be biased by other functions of the knocked-out proteins. Even though for EapH1 and EapH2 no other functions are known than the inhibition of NSPs, previous studies have shown additional immune-evasion functions for Eap. These studies used independently-generated *eap*-mutant strains of *S. aureus* Newman[41,42]. In PART II, we integrate the results from these previous murine infection models with our *in vivo* results, which compared virulence of the WT, *eap*-mutant (Δ*eap*) and triple *eap*-mutant (Δ*eap*Δ*H1*Δ*H2*) stains. This might provide better insights into the role of EAPs in *S. aureus* infections.

The role of EAPs in murine infection models

Even though the various research groups all explained their *in vivo* findings via different molecular mechanisms, the results of the *in vivo* studies show remarkable similarities. For instance, in CHAPTER 5 we found the same 2-fold increase in peritoneal neutrophil recruitment in an short-term (5 h) infection model with *eap*-mutant bacteria as published earlier[43]. In addition, two groups examined the bacterial survival in the kidneys in an intermediate (4 or 5 days) intravenous (i.v.) infection model, and neither found differences between the WT and *eap*-mutant strains[41,43]. In addition to these similarities, all findings complement each other and give a hint into the virulence mechanism of EAP-domain proteins (Table I).

Bacterial survival

Bacterial survival was quantified in several models at time points ranging from a few hours (5 or 6 h) to a few days (4 or 5 d). These models always compared survival of WT and *eap*-mutant bacteria, and sometimes included the triple *eap*-mutant bacteria. These models showed that Eap is important for bacterial survival in the first few hours upon intraperitoneal (i.p), or intranasal infection[43] (CHAPTER 4 and 6). Upon i.v. infection, Eap did not contribute to survival in several organs (kidney, heart, blood, or joints)[41]. A few hours later (at 1 day), the three EAPs together contributed to bacterial survival, but the sole effect of Eap was no longer obvious (CHAPTER 4). Neither did Eap at this time point contribute to bacterial survival in several organs (kidney, heart, blood, or joints) upon i.v. infection[41]. However, after a few days Eap had contributed to survival in the joints[41]. Only the three EAPs together promoted survival in a retro-orbital i.v. infection model in this timeframe. Thus, Eap promotes bacterial survival directly upon infection via the peritoneum or lung, but upon i.v. infection only after a few days, and in a specific organ. A contribution of either or both EapH1 and EapH2 was only measured after a few more hours in the lung, and after a few days of i.v. infection.

Table I. Outcomes of *in vivo* studies with *eap*-mutant *S. aureus* strains

		outcome				
infection route[a]	**time point**[b]	bacterial survival	lymphocyte recruitment	abscess formation	other	ref.
i.p.	5 h		2-fold more PMN[e] recruited in Δ*eap* vs. WT infection			42
i.p.	5 h	2-fold fewer Δ*eap*[c] and Δ*triple*[d] vs. WT bacteria recovered	2-fold more PMN recruited in Δ*eap* and Δ*triple* vs. WT infection			CH6
lung	6 h	10-fold fewer Δ*eap* and Δ*triple* vs. WT bacteria recovered	trend to more PMN recruited in Δ*triple* vs. WT infection (not in Δ*eap*)			CH4
lung	24 h	100-fold fewer Δ*triple* vs. WT bacteria recovered	no differences (Δ*eap*, Δ*triple*, WT)			CH4
i.v.	6h/24h	equal bacterial counts in the joints, kidney, heart, blood (WT and Δ*eap*)				41
subcutaneous	4 d	equal bacterial counts (WT and Δ*eap*)		equal abscess size (WT and Δ*eap*)		42
i.v.	5 d	equal bacterial counts in the kidney (WT and Δ*eap*)				42
i.v.	4 d	fewer Δ*eap* vs. WT bacteria recovered from the joints (equal in heart, kidney, blood)				41
retro-orbital	4 d	100-fold fewer Δ*triple* vs. WT bacteria recovered				11
wound	10-13 d		(PMN and Mφ[f] recruitment inhibited by rEap)[g]		accelerated wound healing in Δ*eap* vs. WT infection	44

i.v.	3-4 weeks				full recovery of weight loss in Δ*eap*, but not in WT infection	41
i.v.	8 weeks			milder and less frequent arthritis and osteomyelitis; lower frequency of abscesses in heart and kidneys		41

[a] Infection routes: i.p. (intraperitoneal), lung (intranasal), i.v. (intravenous)
[b] h (hours), d (days)
[c] Δ*eap* (either *eap*-mutant strain. Made by Hussain *et al.*, Lee *et al.*, or Stapels *et al.*)
[d] Δ*triple* (triple *eap*-mutant strain (Δ*eap*Δ*H1*Δ*H2*). Made by Stapels *et al.*)
[e] PMN (polymorphonuclear cells, neutrophils)
[f] Mφ (macrophages)
[g] rEap (recombinant Eap)
[h] CH4 and CH6 (CHAPTER 4) and (CHAPTER 6)

Leukocyte recruitment and wound healing

Lowering the number of neutrophils recruited to the site of infection is paramount to bacterial survival in the first few hours. Upon i.p. infection, Eap diminished neutrophil recruitment, which could explain the aforementioned increased bacterial survival[43] (CHAPTER 6). Upon pulmonary infection, neutrophil recruitment was not diminished by Eap alone (CHAPTER 4), yet the three EAPs together seemed (though statistically not significant) to limit neutrophil recruitment (CHAPTER 4). This does not fully explain the decreased survival of the *eap*-mutant at 6 h, but it does match the decreased survival of the triple *eap*-mutant at 24 h. In addition, in a sterile wound model, recombinant Eap inhibited the recruitment of neutrophils and macrophages after one day of infection[44]. Moreover, when these pre-formed wounds were infected with *S. aureus*, endogenously expressed Eap increased the time needed for wound healing (from 10 to 13 days)[44]. Since leukocytes fulfill important roles in wound healing, this might have been a result of the initial diminished leukocyte recruitment[45]. Thus, Eap clearly inhibits neutrophil recruitment, and EapH1 and/or EapH2 have this tendency too. However, it is not the only parameter explaining decreased survival of *eap*-mutant bacteria in the first few hours of infection.

Abscess formation

The long-term contribution of Eap to infection is best illustrated by the weight loss of mice upon 4 weeks of i.v. infection. Whereas the *eap*-mutant-infected mice had restored their original weight loss after 4 weeks, the WT-infected mice still suffered from weight loss compared to day 0[41]. This is the first indication that the reach of Eap extends beyond the first few days. Amongst the long-term complications of *S. aureus* infections are abscess formation, arthritis and osteomyelitis[46]. After a few days, Eap did not (yet) influence the size of the formed skin abscesses in a subcutaneous infection model[43]. However, in the long term (8 weeks) Eap increased the frequency in which mice formed abscesses in the heart and kidneys. In addition, the severity and frequency of both arthritis and osteomyelitis were increased[41]. These differences between the WT and *eap*-mutant strain were abrogated in T-cell deficient nude mice, stressing a role for the adaptive immune response at this time point[41].

Together, these models clearly show that bacterial infection in different organs depends on different virulence factors. This will most likely be caused by the differences in resting cell populations, and the slightly different mechanisms of neutrophil recruitment towards different organs[47]. In addition, by examining various time points, these models assess various aspects of the immune response. In the shorter models innate immune processes like leukocyte recruitment will play an extensive role, whereas in the longer models also the importance of adaptive immunity is highlighted. To understand the molecular mechanisms evoking these phenotypes, we will now integrate these with the *ex-vivo* reported functions for Eap, EapH1, and EapH2.

Molecular mechanisms for EAPs to enhance virulence

Whereas NSP inhibition is the only known function for EapH1 and EapH2, multiple functions of Eap have been described in the past. However, the molecular mechanisms have not always been unraveled. Since these functions may have determined the outcomes of the *in vivo* studies in concert, we will here give an overview of the possible molecular interactions in place (Fig. 4A).

Adherence

Eap obtained its name, extracellular adherence protein, from its affinity for multiple extracellular matrix proteins, including bone sialoprotein, fibronectin (Fn), thrombospondin, vitronectin (Vn) and fibrinogen (FBG)[48]. Some of these proteins also occur in plasma. Indeed, Eap has been shown to bind at least seven plasma proteins, including fibrinogen (Fg), prothrombin, and Fn[49]. The inhibitory constant (K_i) of an enzyme-inhibitor complex

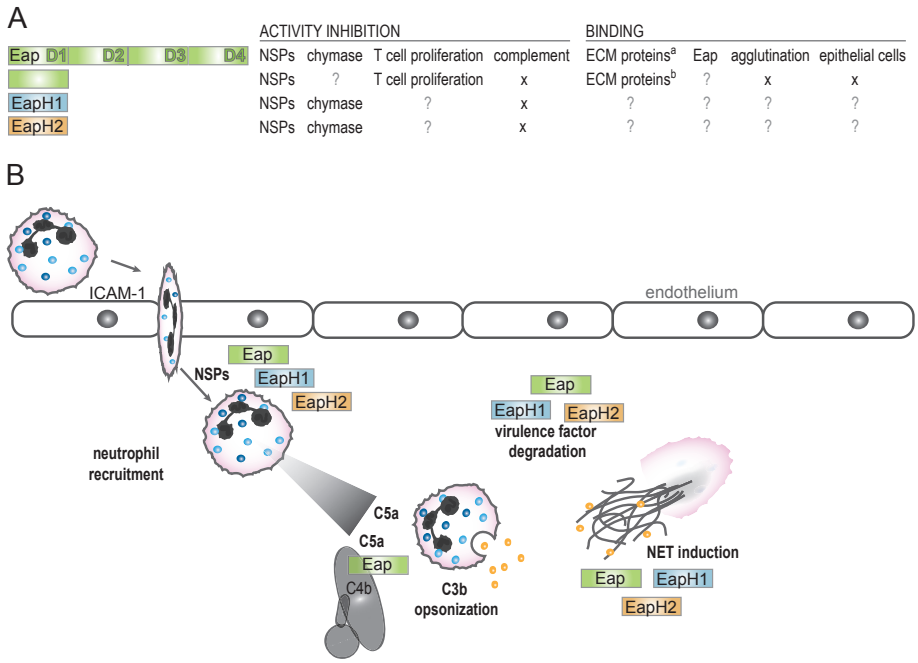

Figure 4. Mechanisms of EAPs to enhance *S. aureus* virulence. (A) Overview of the molecular interactions known for EAPs. Some functions are specific to Eap (containing four domains, depicted in green), and some functions are already present within all individual domains from Eap (in green), or within EapH1 (blue) and EapH2 (yellow). [a]Determined for fibrinogen, fibronectin, thrombospondin, and bone sialoprotein. [b]Some individual domains bind some ECM proteins (e.g. D3 binds fibrinogen, but D5 does not)[51]. "?" unknown. "x" this protein does not have this function. (B) Effects of EAPs on neutrophil functions. Neutrophil recruitment is inhibited by all three EAPs. All of them might inhibit the detachment of neutrophils from the endothelial cells by inhibiting NSP activity. Only Eap inhibits complement activation, thus further inhibiting neutrophil recruitment by diminishing the generation of the chemotactic factor C5a. The complement inhibition by Eap also hampers C3b opsonization of bacteria, leading to diminished phagocytosis. The degradation of *S. aureus* virulence factors by NSPs is prevented by all three EAPs, as is the induction of neutrophil extracellular traps.

denotes the dissociation constant (K_d) for this complex in equilibrium[50]. This shows that the strength of the interaction between EAPs and NSPs (K_i values of 1 nM (Eap), 2 nM (EapH1), and 5 nM (EapH2) for NE) is in the same range as the binding of Eap to FBG, Vn and thrombospondin (K_d values of 2 nM, 3 nM, and 0.5 nM respectively with rEap)[51]. However, in an *in vitro* binding assay with the WT and *eap*-mutant strains, binding to immobilized FBG and Fn was not altered[42]. On the contrary, adherence to fibroblasts and epithelial cells was promoted by endogenous Eap[42,52].

These adherence properties of recombinant Eap promote uptake in keratinocytes[53], although no difference was detected between WT and *eap*-mutant strains[53]. Moreover, Eap promotes bacterial clumping, since it binds both to the *S. aureus* surface and to other Eap molecules[49]. Enhanced agglutination might play a role in the observed increase in biofilm formation in presence of Eap[54]. Unfortunately, the mechanism of binding to this range of targets is unknown. A part of the interactions might be mediated by electrostatic interactions, since Eap is highly cationic[55].

Regardless of the mechanism, the interactions of Eap with these proteins might have increased the adherence of *S. aureus* cells to host tissue and its internalizations in the above-mentioned infection models. If a higher portion of *S. aureus* cells is internalized, these can hide better from the innate immune response and might increase the detrimental effects of infection on the long term. This might partially play a role in the observed enhancement of abscess formation, arthritis, and osteomyelitis[41].

Adherence of Eap to ICAM-1 is believed to cause the inhibition of neutrophil recruitment[43]. Even though proven *in vitro*, the proposed *in-vivo* mechanism is counter intuitive. For Eap to inhibit neutrophil recruitment by binding ICAM-1, it should be expressed on the luminal side of the vasculature. However, in the peritoneal infection model, *S. aureus* resides on the opposite side of the vessel wall. This yields the unsatisfying situation that Eap should first cross the endothelium to be able to inhibit neutrophil recruitment. Moreover, the finding that i.v. ICAM-1 antibodies could inhibit neutrophil recruitment does not prove that Eap functions via the same mechanism. An alternative explanation for the observed inhibition of neutrophil recruitment by intraperitoneal Eap is its inhibition of NE that might cleave ICAM-1, or CD11b (within CR3) to release neutrophils from the endothelium after they have transmigrated[56] (CHAPTER 6).

Inhibition of complement

In CHAPTER 5, we identified Eap as a complement inhibitor. In contrast to the ill-defined interaction of Eap with plasma proteins, we could unravel the mechanism by which Eap inhibits complement activation: Eap binds C4b, which hinders binding of C2, and thereby prevents formation of the C3 convertase (C4b2a). In this way, activation of the complement cascade via the classical and lectin pathways is inhibited[57]. As seen for other functions of Eap, this inhibition requires multiple EAP domains, which explains why EapH1 and EapH2 cannot inhibit complement. Although the K_d of Eap for C4b (185 nM) and C4 (45 nM) is higher than for other proteins, we could show that inhibition of C3

conversion by Eap in serum diminishes the C3b deposition on *S. aureus*, resulting in diminished phagocytosis by neutrophils[57] (CHAPTER 5). This process might contribute to the observed increase in bacterial load in the peritoneum and lungs during the first few hours of infection (CHAPTER 4 and 6). Simultaneously, the inhibition of complement activation at this level will diminish the generation of C3a and C5a. This might contribute to the impaired neutrophil recruitment to the peritoneum[43] (CHAPTER 6), since both molecules are chemotactic factors, and especially C5a promotes the recruitment of neutrophils[58]. Altogether, by inhibiting the cleavage of C3, Eap might both block the generation of chemoattractants (i.e. C3a and C5a) and the opsonizaton of *S. aureus*, which will independently result in a diminished clearance of *S. aureus*.

With this finding, Eap fills a previously empty niche within the redundant arsenal of *S. aureus* complement-evasion proteins. The previously identified proteins covered almost all important processes within the complement system: classical pathway activation (inhibited by superantigen-like protein 10, staphylokinase, staphylococcal protein A, *S. aureus* binder of IgG (Sbi)), C3 conversion (inhitited by staphylococcal complement inhibitor (SCIN), SCIN-B/C, Sbi), C5 conversion (inhibited by extracellular fibrinogen binding protein, extracellular complement binding protein, superantigen-like protein 7), and C5a receptor activation (inhibited by chemotaxis inhibitory protein of *S. aureus*)[59], but not yet the formation of the classical and lectin-pathway C3 convertases. It remains curious why *S. aureus* so redundantly targets the complement system. Most likely, this facilitates most potent protection of *S. aureus*, even if the individual processes are a little leaky.

Chymase inhibition

In CHAPTER 4 we identified mast-cell chymase as the fourth target of the EAPs. Unfortunately, the human chymase does not have one clear-cut orthologue in mice[60]. First of all, mice express multiple chymases (mMCP-1 to -10). Secondly, whereas mMCP-5 shows the highest structure similarity to human chymase, mMCP-4 shows the most similar substrate specificity[60]. Whether these murine chymases are also inhibited by EAP-domain proteins is yet to be determined.

If the mouse chymases would be inhibited, their inhibition could have contributed to the observed *in vivo* phenotypes of the *eap*-mutant bacteria. Interestingly, mMCPs have been shown to promote wound healing[60] and neutrophil recruitment[61], which are both also affected by EAPs. In general, the role of mast cells during *S. aureus* infection is still debated. *In vitro*, mast cell extracellular traps (MCETs) entrap and kill *S. aureus*[62]. Furthermore, during infection, *S. aureus* was shown to invade mast cells to promote secondary infections[62] and it altered gene expression in mast cells[63]. However, mice lacking mast cells, due to mast-cell specific expression of diphtheria toxin, did not increasingly suffer from *S. aureus* infection after a few hours up to 3 days of peritoneal infection[63].

Interfering with T-cell response

Around the time that Eap was first identified, it had also received an alternative name: MHC-II analog protein (Map), inspired by its similarity with the MHC-II peptide-bind-

ing groove[41]. Therefore, Eap was long time expected to affect T-cell activities, which was underlined by the loss of Eap-promoted abscess formation in T-cell deficient nude mice[41]. Unfortunately, the molecular mechanisms have never been pinpointed. The facts that other infection models also showed differences at earlier time points, that neutrophil recruitment was diminished, and that neutrophils influence the responses of all immune cells[64], make it possible that the altered effectivity of T cells *in vivo* might be a secondary effect of the suboptimal initial neutrophil recruitment.

Nevertheless, *in vitro* Eap also directly affected proliferation of peripheral blood mononuclear cells (PBMC; consisting for about 50-70% of T cells)[65]. Low doses decreased proliferation, whereas high doses increased proliferation. Besides the inhibition of NSPs/chymase, this is the only process also influenced by the single domains of Eap[51]. It would not be surprising if EapH1 and EapH2 would show the same effects, since they much resemble the individual domains of Eap. If so, the mechanism cannot be mediated by NSPs, nor chymase, because they were absent in this assay. Therefore, the observed effect could be caused by an entirely different mechanism. Alternatively, possible inhibition of the homologous granzymes, which are present within PBMCs, might have influenced the PBMC proliferation.

Role of EAPs in human infections

Even though it is well-known that mice are not an optimal model system for *S. aureus* infection[66,67], hitherto, all observations of Eap virulence comes from mouse infection models. The evidence for Eap functions in human infections is scarce. However, we expect an important role in infection, since about 98% of all clinical isolates encodes Eap[68], and 100% of the sequenced strains encodes two or more EAPs (NCBI, BLAST). Moreover, expression of Eap was detected in human wounds, with higher expression in deep vs. superficial wounds[33], which increases the likelihood of an important function in that niche. Furthermore, antibodies against all three EAPs were detected in normal human serum (Stapels and Rooijakkers, unpublished results), suggesting that at any stage of colonization or infection these immunogenic proteins are expressed.

Conclusions

Our identification of EAPs as NSP inhibitors shows a new reason for why the EAPs might be so well-conserved amongst *S. aureus* strains. Although inhibition of NSPs will have influenced the outcome of previous *in vivo* studies, the relative role of all the functions described for Eap should still be addressed. Altogether, the various phenotypes observed in the different infection models (bacterial survival, abscess formation, wound healing, and T-cell activity) might for a large part be evoked by Eap's initial inhibition of neutrophil recruitment and its inhibition of neutrophil activities (phagocytosis and NSP activity). Moreover, NSP inhibition is the first known function for the two Eap-homologous proteins, EapH1 and EapH2. Therefore, these proteins might be used in future studies to dissect which functions of Eap influence outcome of infection most: adherence and complement inhibition (only inhibited by Eap), or NSP and chymase inhibition (also

inhibited by EapH1 and EapH2). The fact that also EapH1 and EapH2 are so well-conserved, underlines the hitherto debatable function of NSPs in staphylococcal infections. Blocking the detrimental effects of EAPs during *S. aureus* infection might restore the natural role of NSPs, by which the immune system will be better equipped to fight this bacterium. Moreover, immune diseases that are exaggerated by uncontrolled activity of NSPs (for example, chronic obstructive pulmonary disease, cystic fibrosis, acute lung injury), might benefit from specific NSP inhibition. Direct use of EAPs in the treatment of these lung diseases will be impossible due to the pre-existing high titers of antibodies in all humans. However, the EAPs do highlight a new mechanism of inhibition for NSPs, which might be employed to design new therapeutic NSP inhibitors.

REFERENCES

1. Meyer-Hoffert U, Wiedow O: Neutrophil serine proteases: mediators of innate immune responses. *Curr. Opin. Hematol.* 2011, 18:19–24.
2. Kessenbrock K, Dau T, Jenne DE: Tailor-made inflammation: how neutrophil serine proteases modulate the inflammatory response. *J. Mol. Med.* 2011, 89:23–28.
3. Nauseef WM, Borregaard N: Neutrophils at work. *Nat. Immunol.* 2014, 15:602–611.
4. Belaaouaj AA, McCarthy R, Baumann M, Gao Z, Ley TJ, Abraham SN, Shapiro SD: Mice lacking neutrophil elastase reveal impaired host defense against gram negative bacterial sepsis. *Nature* 1998, 4:615–618.
5. Belaaouaj AA, Kim KS, Shapiro SD: Degradation of Outer Membrane Protein A in Escherichia coli Killing by Neutrophil Elastase. *Science* 2000, 289:1185–1187.
6. Standish AJ, Weiser JN: Human neutrophils kill Streptococcus pneumoniae via serine proteases. *J. Immunol.* 2009, 183:2602–2609.
7. Hahn I, Klaus A, Janze A-K, Steinwede K, Ding N, Bohling J, Brumshagen C, Serrano H, Gauthier F, Paton JC, et al.: Cathepsin G and Neutrophil Elastase play critical and nonredundant roles in lung-protective immunity against Streptococcus pneumoniae in mice. *Infect. Immun.* 2011, 79:4893–4901.
8. van der Windt D, Bootsma HJ, Burghout P, van der Gaast-de Jongh CE, Hermans PWM, van der Flier M: Nonencapsulated Streptococcus pneumoniae resists extracellular human neutrophil elastase- and cathepsin G-mediated killing. *FEMS Immunol. Med. Microbiol.* 2012, 66:445–448.
9. Gratzer W: The Wright stuff; comment on Reeves et al. (2002). *Nature* 2002, 416:275–277.
10. MacIvor DM, Shapiro SD, Pham CT, Belaaouaj A, Abraham SN, Ley TJ: Normal neutrophil function in cathepsin G-deficient mice. *Blood* 1999, 94:4282–4293.
11. Stapels DAC, Ramyar KX, Bischoff M, von Köckritz-Blickwede M, Milder FJ, Ruyken M, Eisenbeis J, McWhorter WJ, Herrmann M, van Kessel KPM, et al.: Staphylococcus aureus secretes a unique class of neutrophil serine protease inhibitors. *Proc. Natl. Acad. Sci. U. S. A.* 2014, 111:13187–13192.
12. Sørensen OE, Follin P, Johnson AH, Calafat J, Tjabringa GS, Hiemstra PS, Borregaard N: Human cathelicidin, hCAP-18, is processed to the antimicrobial peptide LL-37 by extracellular cleavage with proteinase 3. *Blood* 2001, 97:3951–3959.
13. Ong PY, Ohtake T, Brandt C, Strickland I, Boguniewicz M, Ganz T, Gallo RL, Leung DY: Endogenous antimicrobial peptides and skin infections in atopic dermatitis. *N. Engl. J. Med.* 2002, 347:1151–1160.
14. Nordahl EA, Rydengård V, Nyberg P, Nitsche DP, Mörgelin M, Malmsten M, Björck L, Schmidtchen A: Activation of the complement system generates antibacterial peptides. *Proc. Natl. Acad. Sci. U. S. A.* 2004, 101:16879–16884.
15. Papareddy P, Rydengård V, Pasupuleti M, Walse B, Mörgelin M, Chalupka A, Malmsten M, Schmidtchen A: Proteolysis of human thrombin generates novel host defense peptides. *PLoS Pathog.* 2010, 6:e1000857.
16. Papareddy P, Kalle M, Kasetty G, Mörgelin M, Rydengård V, Albiger B, Lundqvist K, Malmsten M, Schmidtchen A: C-terminal peptides of tissue factor pathway inhibitor are novel host defense molecules. *J. Biol. Chem.* 2010, 285:28387–28398.
17. Papareddy P, Kalle M, Sørensen OE, Lundqvist K, Mörgelin M, Malmsten M, Schmidtchen A: Tissue factor pathway inhibitor 2 is found in skin and its C-terminal region encodes for antibacterial activity. *PLoS One* 2012,

7:e52772.
18. Weinrauch Y, Drujan D, Shapiro SD, Weiss J, Zychlinsky A: Neutrophil elastase targets virulence factors of enterobacteria. *Nature* 2002, 417:91–94.
19. Hazenbos WLW, Kajihara KK, Vandlen R, Morisaki JH, Lehar SM, Kwakkenbos MJ, Beaumont T, Bakker AQ, Phung Q, Swem LR, et al.: Novel Staphylococcal Glycosyltransferases SdgA and SdgB Mediate Immunogenicity and Protection of Virulence-Associated Cell Wall Proteins. *PLoS Pathog.* 2013, 9:e1003653.
20. Brinkmann V, Reichard U, Goosmann C, Fauler B, Uhlemann Y, Weiss DS, Weinrauch Y, Zychlinsky A: Neutrophil extracellular traps kill bacteria. *Science* 2004, 303:1532–1535.
21. Papayannopoulos V, Metzler KD, Hakkim A, Zychlinsky A: Neutrophil elastase and myeloperoxidase regulate the formation of neutrophil extracellular traps. *J. Cell Biol.* 2010, 191:677–691.
22. Metzler KD, Goosmann C, Lubojemska A, Zychlinsky A, Papayannopoulos V: A Myeloperoxidase-Containing Complex Regulates Neutrophil Elastase Release and Actin Dynamics during NETosis. *Cell Rep.* 2014, 8:883–896.
23. Urban CF, Ermert D, Schmid M, Abu-Abed U, Goosmann C, Nacken W, Brinkmann V, Jungblut PR, Zychlinsky A: Neutrophil extracellular traps contain calprotectin, a cytosolic protein complex involved in host defense against Candida albicans. *PLoS Pathog.* 2009, 5:e1000639.
24. Papayannopoulos V, Zychlinsky A: NETs: a new strategy for using old weapons. *Trends Immunol.* 2009, 30:513–521.
25. Beiter K, Wartha F, Albiger B, Normark S, Zychlinsky A, Henriques-Normark B: An endonuclease allows Streptococcus pneumoniae to escape from neutrophil extracellular traps. *Curr. Biol.* 2006, 16:401–407.
26. Menegazzi R, Decleva E, Dri P: Killing by neutrophil extracellular traps: fact or folklore? *Blood* 2012, 119:1214–1216.
27. Dubois A V, Gauthier A, Bréa D, Varaigne F, Diot P, Gauthier F, Attucci S: Influence of DNA on the activities and inhibition of neutrophil serine proteases in cystic fibrosis sputum. *Am. J. Respir. Cell Mol. Biol.* 2012, 47:80–86.
28. Yipp BG, Kubes P: NETosis: how vital is it? *Blood* 2013, 122:2784–2794.
29. Berends ETM, Horswill AR, Haste NM, Monestier M, Nizet V, von Köckritz-Blickwede M: Nuclease expression by Staphylococcus aureus facilitates escape from neutrophil extracellular traps. *J. Innate Immun.* 2010, 2:576–586.
30. Van de Vosse E, Verhard EM, Tool AJT, de Visser AW, Kuijpers TW, Hiemstra PS, van Dissel JT: Severe congenital neutropenia in a multigenerational family with a novel neutrophil elastase (ELANE) mutation. *Ann. Hematol.* 2011, 90:151–158.
31. Bardoel BW, Kenny EF, Sollberger G, Zychlinsky A: The Balancing Act of Neutrophils. *Cell Host Microbe* 2014, 15:526–536.
32. Segal AW: How neutrophils kill microbes. *Annu. Rev. Immunol.* 2005, 23:197–223.
33. Joost I, Blass D, Burian M, Goerke C, Wolz C, Von Müller L, Becker K, Preissner K, Herrmann M, Bischoff M: Transcription analysis of the extracellular adherence protein from Staphylococcus aureus in authentic human infection and in vitro. *J. Infect. Dis.* 2009, 199:1471–1478.
34. Lappann M, Danhof S, Guenther F, Olivares-Florez S, Mordhorst IL, Vogel U: In vitro resistance mechanisms of Neisseria meningitidis against neutrophil extracellular traps. *Mol. Microbiol.* 2013, 89:433–449.
35. Palazzolo-Ballance AM, Reniere ML, Braughton KR, Sturdevant DE, Otto M, Kreiswirth BN, Skaar EP, DeLeo FR: Neutrophil Microbicides Induce a Pathogen Survival Response in Community-Associated Methicillin-Resistant Staphylococcus aureus *J. Immunol.* 2007, 180:500–509.
36. Eggers CT, Murray IA, Delmar VA, Day AG, Craik CS: The periplasmic serine protease inhibitor ecotin protects bacteria against neutrophil elastase. *Biochem. J.* 2004, 379:107–118.
37. Doan N, Gettins PGW: alpha-Macroglobulins are present in some gram-negative bacteria: characterization of the alpha2-macroglobulin from Escherichia coli. *J. Biol. Chem.* 2008, 283:28747–28756.
38. Robert-Genthon M, Casabona MG, Neves D, Couté Y, Cicéron F, Elsen S, Dessen A, Attrée I: Unique Features of a Pseudomonas aeruginosa α2-Macroglobulin Homolog. *MBio* 2013, 4:e00309–13.
39. Budd A, Blandin S, Levashina EA, Gibson TJ: Bacterial alpha2-macroglobulins: colonization factors acquired by horizontal gene transfer from the metazoan genome? *Genome Biol.* 2004, 5:R38.
40. Neves D, Estrozi LF, Job V, Gabel F, Schoehn G, Dessen A: Conformational states of a bacterial α2-macroglobulin resemble those of human complement C3. *PLoS One* 2012, 7:e35384.
41. Lee LY, Miyamoto YJ, Mcintyre BW, Höök M, Mccrea KW, Mcdevitt D, Brown EL: The Staphylococcus aureus Map protein is an immunomodulator that interferes with T cell – mediated responses. *J. Clin. Invest.*

2002, 110:1461–1471.
42. Hussain M, Haggar A, Heilmann C, Peters G, Flock J, Herrmann M: Insertional Inactivation of eap in Staphylococcus aureus Strain Newman Confers Reduced Staphylococcal Binding to Fibroblasts. *Infect. Immun.* 2002, 70:2933–2940.
43. Chavakis T, Hussain M, Kanse SM, Peters G, Bretzel RG, Flock J-I, Herrmann M, Preissner KT: Staphylococcus aureus extracellular adherence protein serves as anti-inflammatory factor by inhibiting the recruitment of host leukocytes. *Nat. Med.* 2002, 8:687–693.
44. Athanasopoulos AN, Economopoulou M, Orlova VV, Sobke A, Schneider D, Weber H, Augustin HG, Eming SA, Schubert U, Linn T, et al.: The extracellular adherence protein (Eap) of Staphylococcus aureus inhibits wound healing by interfering with host defense and repair mechanisms. *Blood* 2006, 107:2720–2727.
45. Theilgaard-Mönch K, Knudsen S, Follin P, Borregaard N: The transcriptional activation program of human neutrophils in skin lesions supports their important role in wound healing. *J. Immunol.* 2004, 172:7684–7693.
46. Lowy FD: Staphylococcus aureus infections. *N. Engl. J. Med.* 1998, 339:520–532.
47. Harding M, Kubes P: Innate immunity in the vasculature: interactions with pathogenic bacteria. *Curr. Opin. Microbiol.* 2012, 15:85–91.
48. McGavin MH, Krajewska-Pietrasik D, Rydén C, Höök M: Identification of a Staphylococcus aureus extracellular matrix-binding protein with broad specificity. *Infect. Immun.* 1993, 61:2479–2485.
49. Palma M, Haggar A, Flock J-I: Adherence of Staphylococcus aureus is enhanced by an endogenous secreted protein with broad binding activity. *J. Bacteriol.* 1999, 181:2840–2845.
50. Ying QL, Simon SR: Kinetics of the inhibition of human leukocyte elastase by elafin, a 6-kilodalton elastase-specific inhibitor from human skin. *Biochemistry* 1993, 32:1866–1874.
51. Hussain M, Haggar A, Peters G, Chhatwal GS, Herrmann M, Flock J-I, Sinha B: More than one tandem repeat domain of the extracellular adherence protein of Staphylococcus aureus is required for aggregation, adherence, and host cell invasion but not for leukocyte activation. *Infect. Immun.* 2008, 76:5615–5623.
52. Kreikemeyer B, McDevitt D, Podbielski A: The role of the map protein in Staphylococcus aureus matrix protein and eukaryotic cell adherence. *Int. J. Med. Microbiol.* 2002, 292:283–295.
53. Bur S, Preissner KT, Herrmann M, Bischoff M: The Staphylococcus aureus extracellular adherence protein promotes bacterial internalization by keratinocytes independent of fibronectin-binding proteins. *J. Invest. Dermatol.* 2013, 133:2004–2012.
54. Thompson KM, Abraham N, Jefferson KK: Staphylococcus aureus extracellular adherence protein contributes to biofilm formation in the presence of serum. *FEMS Microbiol. Lett.* 2010, 305:143–147.
55. Hansen U, Hussain M, Villone D, Herrmann M, Robenek H, Peters G, Sinha B, Bruckner P: The anchorless adhesin Eap (extracellular adherence protein) from Staphylococcus aureus selectively recognizes extracellular matrix aggregates but binds promiscuously to monomeric matrix macromolecules. *Matrix Biol.* 2006, 25:252–260.
56. Zen K, Guo Y-L, Li L-M, Bian Z, Zhang C-Y, Liu Y: Cleavage of the CD11b extracellular domain by the leukocyte serprocidins is critical for neutrophil detachment during chemotaxis. *Blood* 2011, 117:4885–4894.
57. Woehl JL, Stapels DAC, Garcia BL, Ramyar KX, Keightley A, Ruyken M, Syriga M, Sfyroera G, Weber AB, Zolkiewski M, et al.: The Extracellular Adherence Protein from Staphylococcus aureus Inhibits the Classical and Lectin Pathways of Complement by Blocking Formation of the C3 Proconvertase. *J. Immunol.* 2014, 193:6161–6171.
58. Ehrengruber MU, Geiser T, Deranleau DA: Activation of human neutrophils by C3a and C5a: Comparison of the effects on shape changes, chemotaxis, secretion, and respiratory burst. *FEBS Lett.* 1994, 346:181–184.
59. Serruto D, Rappuoli R, Scarselli M, Gros P, van Strijp JAG: Molecular mechanisms of complement evasion: learning from staphylococci and meningococci. *Nat. Rev. Microbiol.* 2010, 8:393–399.
60. Douaiher J, Succar J, Lancerotto L, Gurish MF, Orgill DP, Hamilton MJ, Krilis SA, Stevens RL: Development of mast cells and importance of their tryptase and chymase serine proteases in inflammation and wound healing. *Adv. Immunol.* 2014, 122:211–252.
61. Takato H, Yasui M, Ichikawa Y, Waseda Y, Inuzuka K, Nishizawa Y, Tagami A, Fujimura M, Nakao S: The specific chymase inhibitor TY-51469 suppresses the accumulation of neutrophils in the lung and reduces silica-induced pulmonary fibrosis in mice. *Exp. Lung Res.* 2011, 37:101–108.
62. Abel J, Goldmann O, Ziegler C, Höltje C, Smeltzer MS, Cheung AL, Bruhn D, Rohde M, Medina E: Staphylococcus aureus evades the extracellular antimicrobial activity of mast cells by promoting its own uptake. *J. Innate Immun.* 2011, 3:495–507.
63. Rönnberg E, Johnzon C-F, Calounova G, Garcia Faroldi G, Grujic M, Hartmann K, Roers A, Guss B, Lund-

equist A, Pejler G: Mast cells are activated by Staphylococcus aureus in vitro but do not influence the outcome of intraperitoneal S. aureus infection in vivo. *Immunology* 2014, 143:155–163.
64. Mantovani A, Cassatella MA, Costantini C, Jaillon S: Neutrophils in the activation and regulation of innate and adaptive immunity. *Nat. Rev. Immunol.* 2011, 11:519–531.
65. Haggar A, Shannon O, Norrby-Teglund A, Flock J-I: Dual effects of extracellular adherence protein from Staphylococcus aureus on peripheral blood mononuclear cells. *J. Infect. Dis.* 2005, 192:210–217.
66. Spaan AN, Henry T, van Rooijen WJM, Perret M, Badiou C, Aerts PC, Kemmink J, de Haas CJC, van Kessel KPM, Vandenesch F, et al.: The staphylococcal toxin Panton-Valentine Leukocidin targets human C5a receptors. *Cell Host Microbe* 2013, 13:584–594.
67. De Haas CJC, Veldkamp KE, Peschel A, Weerkamp F, van Wamel WJB, Heezius ECJM, Poppelier MJJG, van Kessel KPM, van Strijp JAG: Chemotaxis inhibitory protein of Staphylococcus aureus, a bacterial antiinflammatory agent. *J. Exp. Med.* 2004, 199:687–695.
68. Hussain M, Becker K, Von Eiff C, Peters G, Herrmann M: Analogs of Eap Protein Are Conserved and Prevalent in Clinical Staphylococcus aureus Isolates. *Clin. Diagn. Lab. Immunol.* 2001, 8:1271–1276.

ADDENDUM

Nederlandse samenvatting

Dankwoord

Curriculum vitae

List of publications

IN HET KORT

In je lichaam komen duizenden bacteriesoorten voor waar je normaal gesproken geen last van ondervindt en die zelfs nodig zijn om je lichaam goed te kunnen laten werken. Eén van die bacteriën op je huid is *Staphylococcus aureus*. Helaas kan deze, wanneer je huid beschadigd is, gemene wondinfecties veroorzaken. Waar binnengedrongen bacteriën normaal gesproken worden de opgeruimd door ons immuunsysteem, blijkt *Staphylococcus aureus* extreem goed in staat om dit immuunsysteem te ontwijken. In dit proefschrift hebben we specifiek onderzocht hoe *Staphylococcus aureus* ons aangeboren immuunsysteem, de snelst werkende tak van de menselijke afweer, ontwijkt. Twee belangrijke onderdelen van dit aangeboren immuunsysteem zijn de witte bloedcellen (onder andere neutrofielen) en een cascade van stoffen die neutrofielen helpen hun werk te doen (de complement cascade). In dit proefschrift laten we zien dat *Staphylococcus aureus* drie verschillende stoffen maakt (EAP eiwitten) die zowel functies van de neutrofiel zelf, als de complement cascade blokkeren. Op deze manier verzekert de bacterie zich ervan dat hij kan overleven in het lichaam van een patiënt. De nieuwe kennis die we hier opgedaan hebben, kunnen we later hopelijk gebruiken om medicijnen te ontwikkelen tegen *Staphylococcus aureus*. Bovendien, kunnen we hopelijk van de EAP eiwitten leren hoe we ons immuunsysteem kunnen remmen als het per ongeluk overactief is zoals in de longen van rokers, of patiënten met COPD.

NEDERLANDSE SAMENVATTING

Introductie

Ons immuunsysteem beschermt ons tegen allerlei ziekteverwekkers, waaronder bacteriën, die in eerste instantie worden afgeweerd door ons aangeboren immuunsysteem. Dit systeem herkent globale patronen op bacteriën, waardoor het snel, binnen enkele minuten, kan reageren. Belangrijke onderdelen van het aangeboren immuunsysteem zijn de complement cascade en de witte bloedcellen.

De complement cascade bestaat uit ongeveer 20 serumeiwitten die samenwerken om bacteriën te markeren en op te ruimen. Het kan worden geactiveerd via drie routes: de klassieke, lectine, en alternatieve route. Alle drie zullen ze er uiteindelijk voor zorgen dat het eiwit C3 geknipt wordt, waarbij een klein deel vrij komt (C3a) dat later immuuncellen aan kan trekken (chemotaxie), en een groter deel (C3b) dat op de bacterie afgezet wordt, zodat immuuncellen de bacterie kunnen herkennen en opnemen. Verder in de cascade wordt C5 geknipt tot C5a, dat ook chemotaxie bevordert, en C5b, dat uiteindelijk met C6-9 een porie kan vormen om bacteriën te doden. Helaas is de bacterie waar wij onderzoek naar gedaan hebben (*Staphylococcus aureus*) ongevoelig voor deze porie.

Neutrofielen zijn de meest voorkomende witte bloedcellen. Hun kracht ligt in hun aantal en de snelheid waarmee ze bij de infectie kunnen zijn, onder andere aangetrokken door het gevormde C5a. Op de plaats van infectie kunnen ze bacteriën op drie manieren onschadelijk maken: 1) opnemen en daarna doden (fagocytose); 2) de antibacteriële eiwitten uit hun intracellulaire blaasjes (granula) vrij laten komen (degranuleren); 3) netten van DNA en antibacteriële eiwitten uitgooien, waarin bacteriën gevangen kunnen worden (NET vorming). Binnen al deze processen spelen de antibacteriële eiwitten uit de neutrofiel granula een belangrijke rol, waaronder de neutrofiel serine proteases (NSPs). Deze groep enzymen kan talloze andere eiwitten afbreken en bestaat uit neutrofiel elastase (NE), cathepsine G (CG) en proteinase 3 (PR3).

De Grampositieve bacterie *Staphylococcus aureus* leeft bij 30% van de populatie achterin de neus en op de huid. Normaliter heb je hier geen last van, maar bij een wondje of een verminderde werking van je immuunsysteem kan deze bacterie nare infecties veroorzaken, zoals longontsteking, botontsteking en sepsis. Doordat *S. aureus* in vaak resistent is voor meerdere antibiotica en recente pogingen om een vaccin te maken onsuccesvol bleken, is het noodzakelijk om nieuwe medicijnen te ontwikkelen.

Eén van de redenen waardoor *S. aureus* zo goed in het menselijk lichaam kan overleven, zijn de talloze eiwitten die hij uitscheidt om ons immuunsysteem te ontwijken. Omdat NSPs zoveel functies hebben in de afweer tegen bacteriën, hebben wij onderzocht hoe *S. aureus* zich specifiek tegen deze NSPs wapent.

Dit proefschrift

In **HOOFDSTUK 2** beschrijven we dat *S. aureus* drie eiwitten uitscheidt die specifiek de activiteit van de NSPs remmen. Deze eiwitten vormen de familie van extracellulaire adherentie eiwitten (EAPs), die bestaat uit Eap (53 kDa), en twee kleinere homologen EapH1 (12 kDa) en EapH2 (13 kDa). Een kristalstructuur van EapH1 gebonden aan NE heeft laten zien dat de remming veroorzaakt wordt door non-covalente binding van EapH1 vóór het katalytische deel van NE. Omdat zowel de drie NSPs, als de drie EAPs onderling veel op elkaar lijken, gaan we er vanuit dat het mechanisme van remming voor alle mogelijke combinaties vergelijkbaar is.

In **HOOFDSTUK 3** hebben we verder ingezoomd op het mechanisme waarmee de NSPs geremd worden door de EAPs. Wonderlijk genoeg lijken de EAPs, voor zover we dit nu kunnen concluderen, elk op een verschillende manier NSPs te remmen. Verder laten we in dit hoofdstuk zien dat een ander enzym, mestcel chymase, ook geremd wordt door de EAPs, terwijl neutrofiel serine protease 4 (NSP4) alleen door Eap geremd kan worden.

In **HOOFDSTUK 4** hebben we onderzocht waarom *S. aureus* zoveel energie zou steken in het maken NSP remmers, omdat nooit onomstotelijk bewezen was dat NSPs belangrijk waren in *S. aureus* infecties. Hier laten we zien dat NSPs normaliter bacteriële virulentiefactoren afbreken, waardoor andere delen van het immuunsysteem meer kans hebben om de infectie op te ruimen. Echter, wanneer tijdens een infectie met *S. aureus* de EAPs aanwezig zijn, worden de andere virulentiefactoren beschermd tegen de NSPs, waardoor deze bacterie zijn virulentie behoudt.

In **HOOFDSTUK 5** laten we zien dat Eap nog een andere functie heeft, namelijk het remmen van complementactivatie. Doordat Eap bindt aan C4b, is het daarna onmogelijk om het C3 convertase te vormen van de klassieke en lectine activatieroutes. Hierdoor wordt er minder C3b op de bacterie afgezet, en wordt hij minder goed gedood door neutrofielen.

In **HOOFDSTUK 6** hebben we twee andere processen onderzocht waarop de EAPs zouden kunnen ingrijpen om de afweer tegen *S. aureus* zouden kunnen beïnvloeden: NET vorming en chemotaxie van neutrofielen. Beiden worden door de EAPs beïnvloed, maar op welke manier is nog niet precies bekend.

In **HOOFDSTUK 7** hebben we tenslotte vergeleken waarom en hoe andere bacteriën zich gewapend hebben tegen de NSPs (**PART I**). Vervolgens hebben we een overzicht gemaakt van alle functies die beschreven zijn voor de EAPs en beredeneerd welk effect die gehad kunnen hebben op de uitkomst van verschillende in vivo experimenten (**PART II**).

Concluderend heeft dit proefschrift laten zien dat *S. aureus* drie specifieke remmers van NSPs maakt (EAPs) en dat het zich verder wapent tegen complement activatie door de C3 convertases van de klassieke en lectine activatieroutes te remmen. Vooral het feit dat *S.*

aureus remmers maakt van de NSPs impliceert dat deze enzymen belangrijker zijn voor de afweer tegen *S. aureus* dan hiervoor gedacht werd. Hopelijk kan deze kennis in de toekomst helpen *S. aureus* infecties beter te behandelen of te voorkomen. Verder zouden deze eiwitten misschien de basis kunnen vormen voor klinische remmers van NSPs, die belangrijk zijn om ziekten te behandelen waar de NSPs overactief zijn, bijvoorbeeld bij chronische longziekten.

DANKWOORD

Zo. Dat zit erop. Meer dan vier jaar proeven doen, nadenken, schrijven. Maar gelukkig heb ik van vele kanten hulp gehad. Daarom wil ik op deze pagina tegen iedereen die geholpen heeft dit proefschrift tot stand te brengen zeggen: Duizend maal bedankt!

Daarmee is een dankwoord in de meest letterlijke zin van het woord af. Maar natuurlijk zijn er een aantal personen die bijzonder veel bijgedragen hebben en ik daarom persoonlijk wil bedanken.

Jos, NETs waren toch wel zo intrigerend dat ik direct geïnteresseerd was in het stageproject dat me je aanbood. Kort daarna hoorde ik mezelf op een borrel spontaan antwoorden dat ik na deze stage wel verder wilde in het onderzoek. Bedankt voor al je hulp op de cruciale momenten die volgden: je vertrouwen, je schema's op A3'tjes (volgens mij tekende je de layout van dit boekje twee jaar geleden al zo) en een hart onder de riem bij presentaties.

Suzan, eerst stagebegeleider en toen je Vidi binnen was copromotor. Waar dit onderzoek begon als jouw project, is het gaandeweg toch mijn project geworden. Bedankt voor alle begeleiding hierbij. Of het nu ging om het plannen van de proeven, het (voor mijn gevoel eindeloos) corrigeren van tekst, of het bedenken van wat hierna zou kunnen komen, je was altijd bereikbaar.

Kok, bij jou kon ik altijd aankloppen voor goede raad. Het uitdenken van een nieuwe proefopzet, oplossingen bedenken bij onverwachte resultaten, of een helpende hand bieden in een poging monoclonalen te maken, wat fijn dat je daar altijd beschikbaar voor was.

Another set of people has been essential for both the design of the experiments and the practical work.

Brian, thank you for the great collaboration during the past few years! Your enthusiasm is infectious and really helped the project forward. Thanks for your lengthy emails (all your hypotheses and thoughts, but also your interest in the Dutch soccer team and your stories about American winter), and your patience with my lack of knowledge of basic chemistry. Hopefully this project will not end with this thesis being finished.

Maren, vielen Dank! For all the time you invested from San Diego in the NET project and later on in the experiments in Hannover. I really enjoyed working with you and the opportunity to visit your lab. Off course also many thanks to the rest of the Hannover lab.

Sandra, du bist so süß mit den Mäusen und so gut organisiert dass zusammenarbeiten mit dir wirklich Spaß gemacht hat. **Rike**, thanks for your help in the lab and for continuing with the experiments when I left. And to all the other colleagues, hopefully we will see each other soon somewhere at a conference. I am really glad I got to know you!

Prof. Mathias Herrmann and **Dr. Markus Bischoff**, thank you for kick-starting this project by sharing your protein mutants and for the helpful discussions afterwards.

Maartje, zonder jou was dit boekje maar half zo dik geweest. De efficiëntie waarmee jij figuren bij elkaar pipetteert en je ervaring met complementproeven hebben veel toegevoegd. Maar wat was ik vooral blij toen jij je verdiepte in de problemen met de knockouts!

Annemarie, **Piet**, **Erik**, **Fin**, **Carla**, allemaal hebben jullie in het lab geholpen de eiwit-

ten, constructen, en figuren te maken die er nu liggen. Super bedankt! Studenten, **Lisette**, **Wilco**, "JB" **Aernoud**, **Angelino**, ook jullie werk is in dit boekje terecht gekomen, bedankt voor jullie enthousiasme. En mannen van de **mediaroom**, de **ICT** en het **magazijn**, super bedankt voor alle organisatie achter de schermen. **Karlijn**, naast alle dingen die jij wel even uit wilde zoeken, was het ook heerlijk om even over andere dingen bij te praten.
Evelien en **Steven**, super fijn dat jullie mijn paranimfen willen zijn! En dat met jullie eigen drukke agenda's. **Evelien**, samenwerken begon met de wekelijkse skype sessies tussen Utrecht en San Diego (voor ons bijna weekend, voor jullie bij de eerste koffie op vrijdagochtend). Bedankt voor je super gastvrije ontvangst in San Diego en voor alle gedeelde smart in de jaren als OIO. **Steven**, sinds het begin van de master op elke labbench naast elkaar: de gezelligheid tijdens incubatiestappen, veel 'muziek' op vrijdagmiddag en de enerverende discussies. Dank je wel, ik had het niet willen missen.

Natuurlijk ontstaan de beste ideeën niet door alleen achter de computer te zitten. Daarom wil ik iedereen van de MMB bedanken voor alle gezellige ontmoetingen, 's morgens wakker worden met een straffe bak, de nuttige werkbesprekingen op dinsdagochtend en natuurlijk de Koepel- en promotiefeestjes. **Maaike**, **Manouk**, **Reindert**, **Steev** en **Claudia**, super bedankt voor jullie logeerbedden, die vooral de "day after" een stuk productiever maakten!
Kamergenootjes van G04.560: Anna, Anne, Annemarie, Evelien, Maaike, Nienke, Sue, Tamara, Ron en Jasper, ondertussen is het echt geen meidenkamer meer, maar ik heb goede herinneringen aan het kaasfonduen, ons Thanksgiving dinner en alle koppen thee en chocola die er doorheen gegaan is.
Alle (oud)OIOs: bedankt voor de super sfeer! Berichtjes van de 'coffee mailing list' (die kwamen de productiviteit niet altijd ten goede), afmattende fietstochten door heel Nederland (helaas was ik er het laatste jaar niet meer zoveel bij), ICEA uitjes (alles kwam toch altijd op zijn pootjes terecht) en de vele spontane vrijdagmiddagborrels; ik kijk er met plezier op terug. En ook alle **I&I OIOs**, bedankt voor de goede discussies en feestjes bij de retraites.

Kennis van de inhoud is zeker niet altijd nodig om bij te dragen aan een project. **Denise, Elise, Rianne, Leonne**, al meer dan 10 jaar mijn beste vriendinnen. Iedereen is zijn eigen weg gegaan, maar toch weten we elkaar nog steeds te vinden. En deze zomer eindelijk weer samen op vakantie!
Pap en mam, bedankt voor alle bagage om dit project succesvol af te kunnen ronden. Ik hoop dat ik met dit boekje de gunst eindelijk terug heb kunnen doen; ik hoop dat ik jullie wat heb kunnen leren. **Simone**, **Yorick**, bedankt voor de momenten samen, hopelijk volgen er nog veel meer in jullie nieuwe huisjes.
Tinus, mijn rots in de branding. Je bent het forenzen dubbel en dwars waard en hebt het afronden van dit boekje een stuk makkelijker gemaakt. Nu op naar een nieuwe uitdaging. Ik hoop nog vele jaren lief en leed met je te mogen delen.

Daphne

CURRICULUM VITAE

Daphne Stapels was born on February 6, 1987 in Gouda, the Netherlands. She graduated from high school, Emmauscollege Rotterdam, in 2005. In the same year she started her bachelor's studies Biomedical Sciences at Utrecht University, during which she studied for five months at the University of Tromsø, Norway. Afterwards, she started the Infection and Immunity master at Utrecht University. She did her first internship in the lab of Dr. J.H.W. Leusen, under supervision of Dr. P. Boross in the department of Immunology, and her second internship in the lab of Prof. Dr. J.A.G. van Strijp, under supervision of Dr. S.H.M. Rooijakkers in the department of Medical Microbiology at the University Medical Center Utrecht. She graduated in 2010, upon which she started her PhD research in the group of Dr. S.H.M. Rooijakkers. Within this project, she was a visiting scientist in the group of Dr. M. von Köckritz-Blickwede at the Veterinary University of Hannover, Germany for two months. The research has been awarded with multiple travel grants. The results of this research have been described in this thesis and published in peer-reviewed scientific journals.

LIST OF PUBLICATIONS

Publications related to this thesis

Stapels DAC, Ramyar KX, Bischoff M, von Köckritz-Blickwede M, Milder FJ, Ruyken M, Eisenbeis J, McWhorter WJ, Herrmann M, van Kessel KPM, Geisbrecht BV, Rooijakkers SHM. Staphylococcus aureus secretes a unique class of neutrophil serine protease inhibitors. *Proc. Natl. Acad. Sci. U.S.A. (2014) 111:13187-13192.*

Woehl JL*, Stapels DAC*, Garcia BL, Ramyar KX, Keightley A, Ruyken M, Syriga M, Sfyroera G, Weber AB, Zolkiewski M, Ricklin D, Lambris JD, Rooijakkers SHM, Geisbrecht BV. The Extracellular adherence protein from Staphylococcus aureus inhibits the classical and lectin pathways of complement by blocking formation of the C3 pro-convertase. *J. Immunol. (2014) 193:6161-6171.*

Stapels DAC, Geisbrecht BV, Rooijakkers SHM. Neutrophil serine proteases in antibacterial defense. *Curr. Opin. Microbiol.(2015) 23:42-48.*

Stapels DAC*, Kuipers A*, von Köckritz-Blickwede M, Ruyken M, Tromp A, Horsburgh MJ, de Haas CJC, van Strijp JAG, van Kessel KPM, Rooijakkers SHM. Staphylococcus aureus protects its immune-evasion proteins against degradation by neutrophil serine proteases. *Under review.*

Publications not related to this thesis

Neumann A, Völlger L, Berends ETM, Molhoek EM, Stapels DAC, Midon M, Friães A, Pingoud A, Rooijakkers SHM, Gallo RL, Mörgelin M, Nizet V, Naim HY, von Köckritz-Blickwede M. Novel role of the antimicrobial peptide LL-37 in the protection of neutrophil extracellular traps against degradation by bacterial nucleases. *J. Innate Immun. (2014) 6:860-868.*

Boross P, van Montfoort N, Stapels DAC, van der Poel CE, Bertens C, Meeldijk J, Jansen M, Verbeek JS, Ossendorp F, Wubbolts R, Leusen JHW. FcRγ-chain ITAM signaling is critically required for cross-presentation of soluble antibody-antigen complexes by dendritic cells. *J. Immunol.(2014) 193:5506-5514.*

*equal contribution